

See discussions, stats, and author profiles for this publication at: <https://www.researchgate.net/publication/260482330>

# Ionic Liquids at Electrified Interfaces

ARTICLE *in* CHEMICAL REVIEWS · MARCH 2014

Impact Factor: 46.57 · DOI: 10.1021/cr400374x · Source: PubMed

---

CITATIONS

133

READS

410

## 2 AUTHORS:



Maxim V Fedorov

University of Strathclyde

98 PUBLICATIONS 2,045 CITATIONS

[SEE PROFILE](#)



A. A. Kornyshev

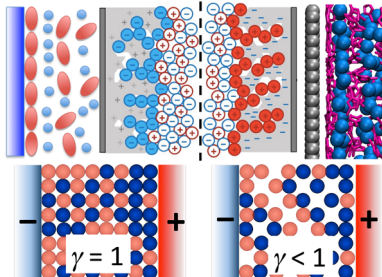
Imperial College London

261 PUBLICATIONS 7,281 CITATIONS

[SEE PROFILE](#)

## Ionic Liquids at Electrified Interfaces

 Maxim V. Fedorov<sup>\*,†</sup> and Alexei A. Kornyshev<sup>\*,‡</sup>
<sup>†</sup>Department of Physics, Scottish University Physics Alliance (SUPA), University of Strathclyde, John Anderson Bldg, 107 Rottenrow, Glasgow, G4 0NG United Kingdom

<sup>‡</sup>Department of Chemistry, Faculty of Natural Sciences, Imperial College London, C1Bldg, South Kensington Campus, London, SW7 2AZ United Kingdom


### CONTENTS

1. Introduction
2. RTILs and Some of Their Properties
  - 2.1. What Do We Imply by RTILs? Main Features and Applications
  - 2.2. A Closer Look at Some of RTILs' Properties
    - 2.2.1. Thermophysical Properties
    - 2.2.2. Transport Properties
    - 2.2.3. Dielectric Properties
    - 2.2.4. Electrochemical Stability
3. EDL before RTILs
4. Principles of the Theory of EDL in RTILs at Flat Electrodes
  - 4.1. Mean Field Theory
  - 4.2. Model Independent Result
  - 4.3. Notes on the Structure and Capacitance of the EDL in RTIL Mixtures with Neutral Solvents
  - 4.4. Beyond the Mean-Field: Direct Simulations of Ionic Liquids at Electrified Interfaces
    - 4.4.1. Course-Grained Models: Forest Behind the Trees
    - 4.4.2. Forest Is Made from Trees—From Physics to Chemistry: Fully Atomistic Models
5. Experimental Studies of EDL in RTILs at Flat Electrodes
  - 5.1. EDL Capacitance
  - 5.2. Molecular-Level Structure of the EDL
  - 5.3. Structural Transitions in the EDL: From Multilayer to Monolayer Structure
  - 5.4. EDL Properties: a Closer Look at Temperature Dependence
  - 5.5. Surface Forces, Screening, and Degree of Ion Pair Dissociation in RTILs
6. Electrode Reactions and Their Kinetics in RTILs
  - 6.1. Pros and Cons for Using RTILs As Solvents for Electrochemical Reactions

6.2. Electrochemical Reactions in RTILS: Electron Transfer Limited or Ion Transport Limited?	3006
6.2.1. Redox Current in Quantum Electrochemistry	3006
6.3. What Will Matter in RTILs?	3007
6.3.1. Reorganization Energy	3007
6.3.2. Work Terms	3008
6.3.3. Driving Force and the Potentially New Form of the Frumkin Correction	3008
6.3.4. Matrix Element of Transition (Overlap Integral)	3009
6.4. Experiments: Examples of Few Case Studies	3009
7. RTILs in Confined Geometry	3010
7.1. Electrochemical Capacitors: Targets and Challenges	3010
7.2. Superionic Effect in Narrow Nanopores: Experiments vs Theory	3011
7.3. Energy Storage in Nanoporous Electrodes: What Is the Optimal Size for the Pores?	3018
7.4. Larger Nanopores and the Capacitance Oscillations	3018
7.5. "Quantized Friction" in Confined Nanofilms of RTILs	3019
8. Examples of Other Applications of RTILs at Els	3020
8.1. Batteries	3020
8.2. Fuel Cells	3021
8.3. Solar Cells	3021
8.4. Flexible Energy Storage Devices	3021
8.5. Miniaturized Nanocarbon Based Electronics	3021
8.6. Polymer Electrolyte Composite Electroactuators	3021
9. Concluding Remarks	3022
Author Information	3023
Corresponding Authors	3023
Notes	3023
Biographies	3023
Acknowledgments	3024
Nomenclature	3024
Ionic Liquids	
Cations	3025
Anions	3025
References	3025

Received: August 6, 2013

Published: March 4, 2014



## 1. INTRODUCTION

Until recently, “room-temperature” (<100–150 °C) liquid-state electrochemistry was mostly electrochemistry of diluted electrolytes<sup>1–4</sup> where dissolved salt ions were surrounded by a considerable amount of solvent molecules. Highly concentrated liquid electrolytes were mostly considered in the narrow (albeit important) niche of high-temperature electrochemistry of molten inorganic salts<sup>5–9</sup> and in the even narrower niche of “first-generation” room temperature ionic liquids, RTILs (such as chloro-aluminates and alkylammonium nitrates).<sup>10–14</sup> The situation has changed dramatically in the 2000s after the discovery of new moisture- and temperature-stable RTILs.<sup>15,16</sup> These days, the “later generation” RTILs attracted wide attention within the electrochemical community.<sup>17–31</sup> Indeed, RTILs, as a class of compounds, possess a unique combination of properties (high charge density, electrochemical stability, low/negligible volatility, tunable polarity, etc.) that make them very attractive substances from fundamental and application points of view.<sup>32–38</sup> Most importantly, they can mix with each other in “cocktails” of one’s choice to acquire the desired properties (e.g., wider temperature range of the liquid phase<sup>39,40</sup>) and can serve as almost “universal” solvents.<sup>37,41,42</sup> It is worth noting here one of the advantages of RTILs as compared to their high-temperature molten salt (HTMS)<sup>43</sup> “sister-systems”.<sup>44</sup> In RTILs the dissolved molecules are not imbedded in a harsh high temperature environment which could be destructive for many classes of fragile (organic) molecules.

RTIL systems are far from a conventional “text-book picture” describing an electrolyte (e.g., NaCl aqueous solution) as small “roundish” ions with uniform charge density on their surface, dissolved in a large amount of solvent and interacting with each other via long-range Coulomb forces. On the contrary, there is no solvent in a neat RTIL electrolyte, unless it is deliberately added or they sorb water from the environment; the molecular RTILs ions are neither small (on an atomistic scale) nor roundish. To make things even more complicated, their molecular charge density is highly nonuniform.<sup>45–49</sup> However, it is this complexity that makes them liquid at room and in some cases even much lower temperatures.<sup>50</sup> That means that the effects of short-range ion–ion interactions, molecular shape of ions, and ion molecular charge distribution are very important for their properties both in the bulk and at interfaces. We also note that the large electrochemical window of many commercially available RTILs<sup>13,17,51</sup> allows one to achieve high electrode charge densities that are inaccessible for conventional (aqueous) electrolytes, and therefore, several interesting effects that were considered mostly as a “theoretical exotics” in the past can be found now experimentally in RTIL-based systems.<sup>52</sup> This all makes the RTILs at electrified interfaces (EIs) an important field of research (and this view is justified by the ever growing number of publications on the subject).

There is a large number of known RTIL cations and anions readily available.<sup>32,37,53,54</sup> Moreover, as mentioned, many RTILs can easily be mixed with each other and with various organic and inorganic polar solvents, giving a practically infinite number of solvent-free or solvent-enriched electrolytes with tunable properties.<sup>17,21,32,37,55</sup> That makes the task of choosing an optimum RTIL for any given application highly nontrivial. Therefore, the main goal of this article is to overview the main qualitative trends in the RTIL behavior at EIs in order to reveal

the most important factors that determine their properties and behavior there.

The fact that RTILs are far from conventional diluted electrolytes sets a number of challenges, both for theorists as well as experimentalists. To a large extent this is due to the inapplicability of standard models (e.g., Gouy–Chapman theory) for theoretical studies of these systems and interpretation of experimental results on RTILs.<sup>56</sup> Not unrelated to this, RTILs attract the attention of not only chemists and applied scientists but also theoretical physicists, based on purely fundamental grounds. Indeed, RTILs represent unique examples of highly concentrated, dense room temperature ionic plasma that exhibits strong “Coulomb correlations”,<sup>57–59</sup> the field lying at the frontier of modern statistical mechanics.<sup>60–62</sup>

At the same time, within certain constraints that will be discussed in the review, many of the classical experimental methods developed for ordinary electrolytes are still usable for the studies of RTILs (unlike HTMSs); that is, they do not require fundamental changes in the experimental protocols or data treatment, although some care has to be taken with regards to the impeded conductivity and increased viscosity of RTILs as well as their purification.<sup>63–75</sup>

Each RTIL is an overall neutral assembly of charged particles. As the majority of their applications deal with their behavior near interfaces<sup>32–38</sup> and, particularly, near EIs, understanding of the charge and electric potential distribution in RTILs at charged interfaces is crucial for understanding their performance as electrolytes.<sup>76</sup> This article is devoted to the discussion of the properties of RTILs at different EIs, in particular of the RTILs’ response to charging of the interface and how it manifests itself in a range of selected applications.

Response of an electrolyte to a charged electrode surface is described within the so-called theory of electrical double layer (EDL). We will overview the current status of the theory of EDL in RTILs, showing that the structure of EDL there is dramatically different from that of a diluted electrolyte, although having certain common features with that of HTMSs.

It is well-known that the EDL plays a crucial role in “electrodics”.<sup>2,77</sup> The potential drop across the EDL and its response to charging determines the electrical capacitance of the electrode/electrolyte interface and, thereby, the energy stored in the EDL capacitors. The potential distribution in the EDL controls electrochemical kinetics, because the voltage difference between the electrode and the point where the reactant (donor or acceptor of the electron) sits is the driving force of electrochemical reactions.<sup>2,3,76,78</sup> Since the electrochemical current depends exponentially on this driving force, even small changes in the value of the potential drop may change the current by orders of magnitude. Naturally, understanding EDL properties in RTIL systems and their dependencies on the electrode potential (that are expected to be different from what they are in ordinary electrolytes) is a primary task for electrochemistry of RTILs.

Understanding the EDL properties of RTILs is equally important for other applications. In electrowetting applications, RTILs can be used as the material of the organic droplet surrounded by aqueous electrolyte and lying at the electrode surface; how the droplet will change its shape with varying voltage of the electrode is determined by the potential distribution in the droplet.<sup>79–82</sup> In the recently discovered phenomenon of “quantized” friction between spontaneously charged solid surfaces,<sup>83</sup> the lubrication capacity of the

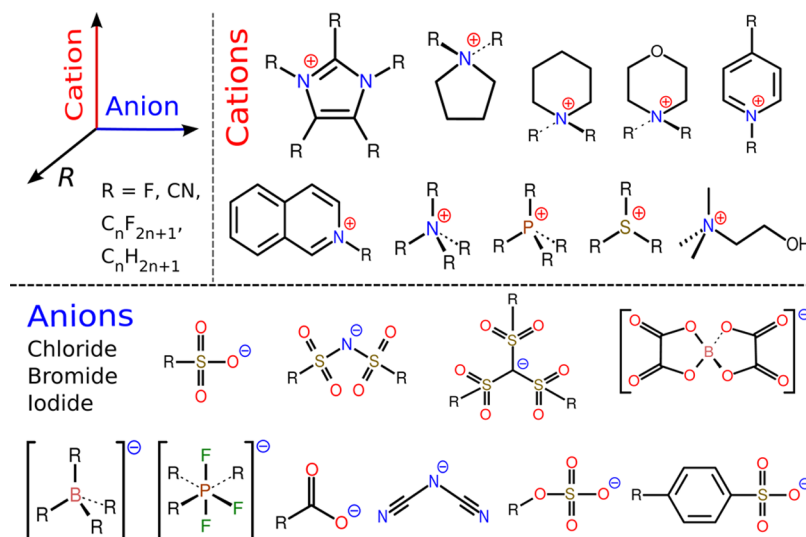


**Figure 1.** General representation of the “chemical space” of functional variations of RTILs. R states for the functional group. Most popular choice for R is the alkyl substituent  $\text{CH}_3(\text{CH}_2)_n$  ( $n = 1, 3, 5, \dots$ ); there are also many other choices available.<sup>37,97</sup> The layout of the figure was inspired by Figure 1 in ref 126.

nanolayers of RTIL is determined by the distribution of ions between them.<sup>83–88</sup> In molecular gating applications of RTILs, the current across a molecule which bridges two electrodes in a nanogap the EDL determines the ability to control independently the potentials of the two electrodes (relative to the reference electrode).<sup>184</sup> This list could be continued.

We will therefore devote a large part of this review to understanding the main properties of the EDL in RTILs. We start with the EDL at flat electrodes and then proceed to porous electrodes with enhanced surface-area-to-volume ratio with a focus on RTIL behavior in charged micro/nano pores and slits.

In many applications not only EDL equilibrium properties are important, but also the dynamics of its charging–discharging.<sup>21,24,89–92</sup> The dynamics determines the time response of the EDL capacitor, but this is not the whole story: impeded dynamics is accompanied by ohmic losses and, thereby, worsened power delivery.<sup>93</sup> This equally refers to electroactuators for artificial muscles (such a flashy name is often assigned to all electroactuators, although the whole muscle is a more complicated hierarchical construction)<sup>94</sup> as well as for sensor applications.<sup>95,96</sup> Ion transport dynamics also determine how fast the electrowetting lense will be changing its shape.<sup>55</sup> Not going into the details of this yet poorly explored territory, we only briefly discuss the main mechanisms of charge transport of ions in RTILs and some aspects of the EDL transient behavior, as there are yet more questions than answers here, and the work in this area is in progress.

The review is organized as follows. We will start with the main principles of the EDL theory in RTILs, then proceed to (molecular-scale) computer simulations of RTILs at EIs, and then discuss recent experiments that investigate the validity of theoretical/modeling predictions. Clarifying this picture as far as we can, we will then overview some manifestations of the EDL in RTILs in the properties of the selected applications, such as EDL supercapacitors, electroactuators, electrode kinetics, and quantized friction.

Trying to be as comprehensive as possible, we will nevertheless have to restrict ourselves to most recent developments, on former achievements referring the readers

to earlier surveys (see, e.g., refs 16–24 and 29). As a last note before we begin, this review is not a handbook: it overviews main principles and qualitative features rather than specific data. Some of those will be drawn in the context of ideas discussed in this review.

To set the scene, we start with a definition of RTILs and a brief overview of some of their pertinent physicochemical and electrochemical properties to which we will sporadically refer later in the review.

## 2. RTILS AND SOME OF THEIR PROPERTIES

### 2.1. What Do We Imply by RTILs? Main Features and Applications

The commonly accepted definition of RTILs these days can be formulated as follows: RTILs are materials that are composed solely from anions and cations and melt below 100–150 °C.<sup>19,32,37,54,97</sup> In the following we will use this (broad) definition, if not stated otherwise. In this section we only briefly overview some pertinent properties of RTILs because there is a number of excellent reviews on this subject already in the context of synthesis and catalysis,<sup>37,54,97</sup> industrial applications,<sup>32,35</sup> etc.<sup>38,98,99</sup> A short but comprehensive overview of the history of the subject can be found in the Wilkes’ 2002 review<sup>100</sup> (see also a recent viewpoint on the history of RTILs by Fei and Dyson<sup>101</sup>).

The first accounts of RTILs is commonly attributed to Walden, who reported in 1914 the synthesis and characterization of a new organic salt, ethylammonium nitrate, that was liquid at room temperature (mp 12 °C).<sup>102</sup> However, analysis of the literature shows that the discovery date of the first RTIL as well as the names of discoverers might be disputed.<sup>32,100</sup> For example, Gabriel and Weiner reported in 1888 a new organic salt, ethanol-ammonium nitrate with mp 52–55 °C,<sup>103</sup> (for more historical details we address the readers to refs 32 and 100). Later in 1930s and 1940s, several other RTILs were discovered<sup>104</sup> that were mixtures of alkylpyridinium-based organic salts (halides) with aluminum(III) chloride.<sup>10</sup> Since then there have been several attempts to explore this intriguing class of substances,<sup>105,106</sup> particularly by electrochemists,<sup>107</sup> that soon recognized the enormous potential of RTILs as

"electrolytes without solvent"<sup>108</sup> for applications in batteries, supercapacitors, and electrodeposition.<sup>10,11,109</sup>

In 1980s Wilkes and Hussey with co-workers discovered that alkylimidazolium halogenoaluminates<sup>110</sup> have a much larger liquid range than alkylpyridinium halogenoaluminates, and these RTILs are more stable in terms of reduction of the alkylimidazolium cation.<sup>110–118</sup> In parallel with the research on halogenoaluminate-based RTILs, several groups explored other low-temperature molten salts known by that time such as tetra-N-alkylammonium nitrates and thiocyanates.<sup>18,119</sup>

However, until the middle of the 1990s, research on RTILs was somewhat outside the mainstream of electrochemistry due to various problems with synthesis and purification of the "first-generation" RTILs that resulted in high costs of these compounds. Moreover, most of the first-generation RTILs (e.g., alkylimidazolium/alkylpyridinium halogenoaluminates) are very sensitive to moisture and have difficulties with regulation of their acidity/basicity.<sup>110,120</sup> Therefore, until recently the main focus in electrochemistry of concentrated ionic fluids (particularly from the 50s to 70s of the past century) was in high temperature ionic liquids: the molten inorganic salts (mp 300–1000 °C) and their applications in metal production processes.<sup>5,121,122</sup>

A "rediscovery" of RTILs two decades ago was mainly due to (i) discovery of RTILs with stable organic anions (such as  $[\text{PF}_6]^-$ ,  $[\text{BF}_4]^-$ , and,  $[\text{TFSA}]^-$ ) in the 1990s<sup>15,123</sup> and (ii) breakthroughs in organics synthesis of RTIL components that reduced their costs (such as, e.g., the biphasic acid scavenging utilizing ionic liquids (BASIL) process introduced by the BASF company in 2002<sup>124</sup>). This was followed by an exponential growth of interest in RTILs with thousands of papers published annually on various aspects of their chemistry and physics. For enthusiasts of metrics in science, one can draw just one illustrative figure: according to the ISI Web of Knowledge, in 2012 the overall number of papers published on the subject "ionic liquids" during only that year was around  $10^4$ . The enormous "popularity" of RTILs is related to their unique properties and the vast number of applications that are already employing RTILs or can potentially employ them in the future.<sup>32,35,38,125</sup>

Following Stark<sup>126</sup> the "chemical space" of functional variations of RTILs can be represented as a three-dimensional domain with anions, cations, and their (chemical) functional groups as (generalized) coordinates (see Figure 1).

The features of RTILs that make them special are, briefly, as follows:

- Unlike molten salts composed of small, "roundish" inorganic ions, the ions of RTIL are ordinarily large organic ions (at least one of them, usually the cation), containing a substantial amount of hydrophobic constituents<sup>37,97</sup> (see Figure 1). They often have anisotropic and asymmetric shapes. These two features, that principally distinguish them from molten inorganic salts, reduce the freezing temperature of the liquid: the Coulomb interactions are weaker in the range of their action, whereas their complicated shape does not let the RTIL ions easily acquire stable ordered crystal structures.<sup>50</sup>
- RTILs are electrolytes without solvents that stay liquid in a broad temperature interval around the room temperature.<sup>13,127</sup>

- Strongly kept together by electrostatic interactions of cations and anions, many RTILs have low or ultralow volatility.<sup>53,128–133</sup>
- Those RTILs that are composed from less reactive ions are more inert electrochemically than many standard electrolytes; that is, as solvents at electrodes they can sustain higher voltages before their electrochemical (and thermal<sup>134</sup>) decomposition.<sup>13,51,127,135–140</sup>
- Different RTILs can be mixed with each other and one can make "cocktails" of them.<sup>41,42</sup> Moreover, RTILs can be slightly diluted by adding to them organic dipolar solvents.<sup>141,142</sup> The resulting mixture can be called a designer solvent, as it can be adjusted to provide targeted functions for reactions of substances dissolved in them.<sup>37,54</sup> Since thousands of RTILs have been or can be synthesized, the discovery of RTILs caused a revolution in chemistry: one in principle can have practically an unlimited number of solvents and electrolytes, whereas in the past they all could be counted.<sup>3,143</sup>

Calling RTILs green electrolytes is more of wishful thinking<sup>144–146</sup> as many of them are not green at all,<sup>147,148</sup> some are toxic<sup>149,150</sup> and hazardous,<sup>151,152</sup> and most of them are difficult to wash away.<sup>153</sup> However, the other listed properties make them promising in various applications, as they can be used as:

- designer solvents for homogeneous and surface catalysis and synthesis<sup>37,54,154</sup>
- extraction liquids for purification of metals,<sup>155,156</sup> proteins and colloids,<sup>32</sup> and biomass conversion<sup>157,158</sup>
- media for electrochemical reactions, electrocatalysis, and electrodeposition<sup>13,17,18,21,159–163</sup>
- electrolytes for power sources and generators,<sup>164</sup> such as supercapacitors,<sup>39,40,90,91,165–168</sup> batteries,<sup>135,140,169,170</sup> solar cells,<sup>171–175</sup> and, prospectively, fuel cells (once RTILs with high proton conductance are found)<sup>176</sup>
- liquids for electrowetting based variable lenses and microfluidics applications<sup>177–179</sup>
- lubricants, from macromechanisms to micro and nanodevices<sup>83,85,88,180–182</sup>
- the organic liquid component for self-assembled nano-plasmonic devices<sup>183</sup>
- electronic gating media for single molecule devices<sup>184,185</sup> and electrolyte-gated transistors for organic and printed electronics<sup>185–189</sup> and superconductors<sup>190</sup>
- chemical and electrochemical sensing<sup>23,191,192</sup>

The list could be continued but these are those applications that are clearly seen now.

## 2.2. A Closer Look at Some of RTILs' Properties

In this section we will provide a brief (and nonextensive) overview of several main properties of RTILs focusing on those that are important for understanding their behavior at EIs. Emphasis is set on a few examples of commercially available RTILs that are frequently used in experimental and simulations studies of electrical double layer and various applications. For extensive reviews of RTIL properties we refer the readers to the following databases, books, and essays:

- A large collection of thermodynamical, thermochemical, and transport properties data of RTILs and their mixtures is given in the ILThermo online database.<sup>193</sup> There is also recent critical review by Aparicio et al.<sup>194</sup> on thermo-physical properties of new RTILs that analyses

Table 1. Typical Ranges of RTILs Properties<sup>a</sup>

property	lower limit example	typical values for most of RTILs	upper limit example
melting point/glass transition	[EMIm]Cl/AlCl <sub>3</sub> = (1:2) = -96 °C (glass transition)	0–60 °C	100–150 °C depending on RTIL
density	[HMPyr][DCA] = 0.92 g L <sup>-1</sup>	1.1–1.6 g L <sup>-1</sup> <sup>b</sup>	[EMIm]Br/AlBr <sub>3</sub> :1/2 = 2.2 g L <sup>-1</sup>
viscosity <sup>b</sup>	[EMIm]Cl/AlCl <sub>3</sub> :1/2 = 14 mPa s	40–800 mPa s	[BMIm]Cl (super-cooled) = 40.89 Pa s
thermal stability	[EMIm][OAc] = ~200 °C <sup>c</sup>	230–300 °C <sup>c</sup>	[EMIm][TFSA] = 400 °C <sup>c</sup>
surface tension	[C <sub>12</sub> MIm][PF <sub>6</sub> ] = 23.6 mN m <sup>-1</sup>	30–50 mN m <sup>-1</sup>	[MMIm][MeSO <sub>4</sub> ] <sup>-</sup> = 59.8 mN m <sup>-1</sup>
heat capacity	[BMIm][MeSO <sub>4</sub> ] = 247 J mol <sup>-1</sup> K <sup>-1</sup>	300–400 J mol <sup>-1</sup> K <sup>-1</sup>	[OMIm][TFSA] = 654 J mol <sup>-1</sup> K <sup>-1</sup>
water miscibility	[TFSA] <sup>-</sup> , [FAP] <sup>-</sup>	varies in a large range depending on hydrophobicity/hydrophilicity of RTIL ions; it is difficult to completely remove traces of water from many of commercially available RTILs	[RSO <sub>3</sub> ] <sup>-</sup> , [RSO <sub>4</sub> ] <sup>-</sup> , [R <sub>2</sub> PO <sub>4</sub> ] <sup>-</sup> , halogen anions
hydrolytic stability	[BF <sub>4</sub> ] <sup>-</sup> , [PF <sub>6</sub> ] <sup>-</sup>	heterocyclic cations can hydrolyze under extreme conditions	[TFSA] <sup>-</sup> , [TFO] <sup>-</sup> , [CH <sub>3</sub> SO <sub>3</sub> ] <sup>-</sup>
base stability	[Al <sub>2</sub> Cl <sub>7</sub> ] <sup>-</sup> , [HSO <sub>4</sub> ] <sup>-</sup>	all 1,3-dialkylimidazolium RTILs are subject to deprotonation	[PR <sub>4</sub> ] <sup>+</sup> , [OAc] <sup>-</sup>
corrosion	[TFSA] <sup>-</sup> , [TFO] <sup>-</sup>	many RTILs are corrosive versus Cu; additives to inhibit corrosion are available	Cl <sup>-</sup> , HF formed from [MF <sub>x</sub> ] <sup>-</sup> hydrolysis
toxicity	[cholinium][OAc]	toxicity often increases with increasing lipophilicity <sup>200</sup>	[EMIm][CN]
static dielectric constant	[HMIm][PF <sub>6</sub> ] = 8.9 ± 0.9 (ref 201)	10–15 (refs 202,203)	(2-hydroxyethyl)ammonium lactate = 85.6 ± 3 (ref 203)
electrical conductivity <sup>b</sup>	[BMIm][C <sub>4</sub> F <sub>9</sub> SO <sub>3</sub> ] = 0.45 mS cm <sup>-1</sup> (refs 97,204)	1–10 mS cm <sup>-1</sup> (ref 13)	[EMIm][BF <sub>4</sub> ] = 16.3 ± 1.6 mS cm <sup>-1</sup> <sup>d</sup> (ref 205)

<sup>a</sup>Large part of the table is taken from ref 35 (Table 1 there) with some extension and adaptation; the presented data are taken from the ref 35 and references therein if not specified otherwise. The abbreviations in the table are as follows (see also the list of used abbreviations at the end of this review): [EMIm], 1-ethyl-3-methylimidazolium; [HMPyr], 1-hexyl-1-methyl-pyrrolidinium; [BMIm], 1-butyl-3-methylimidazolium; [C<sub>n</sub>MIm], 1-alkyl-3-methylimidazolium; [TFSA], [(CF<sub>3</sub>SO<sub>2</sub>)<sub>2</sub>N]<sup>-</sup>; TFO, trifluoromethanesulfonate (triflate); [BMMIm], 1-butyl-2,3 dimethylimidazolium. <sup>b</sup>At room temperature. <sup>c</sup>TGA experiments at 10 K min<sup>-1</sup>. <sup>d</sup>Measured at 298.15 K.

different experimental methods for measuring thermophysical properties and possible sources of errors.

- The book of Zhang et al. “Ionic liquids: physicochemical properties”.<sup>195</sup> To the best of our knowledge this is the most extensive handbook on physicochemical properties of ionic liquids currently available<sup>196</sup> (the book was preceded by an earlier review publication by the same group of authors<sup>197</sup>). The book contains a large database of physical properties of ionic liquids including density, viscosity, phase transition temperatures, thermal decomposition temperature, polarity, and the electrochemical window.
- The 2008 review by Weingärtner<sup>198</sup> discusses in detail the molecular foundations of RTILs focusing on experimental methods that can provide molecular-level insights on structure and dynamics of RTILs.
- The 2005 compiled book “Electrochemical aspects of Ionic Liquids” edited by Ohno<sup>19</sup> provides a large amount of data on electrochemical behavior of RTILs. The book also provides good introduction to the subject and contains many innovative ideas that were later developed by the authors of the contributed chapters and other groups.
- The 2008 complied volume “Electrodeposition from ionic liquids” edited by Endres, MacFarlane, and Abbott<sup>199</sup> provides a good introduction to the electrochemistry of RTILs and contains a large amount of information on relevant electrochemical and physical-chemical properties that might be difficult to find elsewhere.

- The 2008 review by Hapiot and Langost on electrochemical reactivity in RTILs<sup>163</sup> that discusses different physical and electrochemical properties of RTIL-based systems in a view of their applications as reactive media for electrochemical reactions at interfaces. See also Chapter 4 in the review by Yoshida et al.<sup>162</sup> on modern strategies in electroorganic synthesis that also discusses applications of RTILs as reactive media for electrocatalytic reactions.

To overview the typical ranges of main properties of RTILs that are relevant to the subject of the article, we provide here (in Table 1) an updated and extended version of Table 1 from the 2010 review of RTIL applications in chemical engineering by Werner et al.<sup>35</sup> Several important properties of RTILs are also discussed in more detail below.

**2.2.1. Thermophysical Properties.** Most RTILs at normal atmospheric pressure stay in the liquid state up to temperatures as high as 200–300 °C where water and common organic solvents already evaporate.<sup>194</sup> Due to the strong ion–ion interactions, volatility of RTILs is typically very low.<sup>53</sup> Therefore, in principle, RTILs themselves could also withstand high operation temperatures in energy storage devices.<sup>164,206</sup> However, elevated temperatures<sup>207</sup> can activate undesired electrochemical reactions,<sup>134</sup> involving RTIL ions both at cathodes and anodes; that would narrow the window of electrochemical stability of RTIL (see also discussion below).

We note that at temperatures higher than 200–300 °C most RTILs start to decompose; moreover, the RTIL thermal decomposition process can generate flammable and toxic gases.<sup>38,98</sup>

Following Aparicio et al.<sup>194</sup> the melting point of ionic liquids depends on a balance between cation and anion symmetry,

flexibility of chains in the ions, and charge accessibility. Increasing the length of alkyl chains in the cations and/or increasing the anion size generally leads to a decrease in the RTIL melting points.<sup>193,194,208</sup>

We note that there are already available quite advanced procedures for predictions of melting points and thermodynamic stability of RTILs<sup>209</sup> (as well as other thermophysical parameters, see ref 210); however, their usage is still not widely applied in the field. As was pointed by Coutinho et al. in their recent review on predictive models for thermophysical and transport properties of pure RTILs,<sup>211</sup> the major problems in the development of a reliable model are that “many ILs do not have a melting point, that the boiling temperatures of the ILs are as elusive as their critical temperatures, and consequently that the uncertainties associated with those estimates are necessarily very large.”<sup>211</sup> That correlates with opinions discussed in a recent critical review by Aparicio et al. on experimental methods for measurements of thermophysical properties of RTILs.<sup>194</sup>

**2.2.2. Transport Properties.** As was mentioned in the Introduction, transport properties of RTILs directly affect the performance of RTIL-based electrochemical applications.<sup>212</sup> In fact, high viscosity and low diffusion of ions of most of the electrochemically stable RTILs are the main bottlenecks in the development of electrochemical applications of RTILs in energy storage and electrodeposition areas. Indeed, at room temperatures viscosity of RTILs varies between 20 and 40 000 cP<sup>32</sup> (compared to the viscosity of standard solvents that varies in the range of 0.2–100 cP). Even low-viscous RTILs have viscosities around 20–30 cP at room temperature;<sup>213</sup> that is one order of magnitude higher than the viscosity of water at these temperatures ( $\sim 1$  cP)<sup>32</sup> and molten inorganic salts at high temperatures (1–3 cP).<sup>59</sup>

Transport properties of RTILs are of considerable fundamental interest due to a large number of intriguing phenomena.<sup>214,215</sup> For example, the measured electrical conductivity of many RTILs significantly deviates from the Nernst–Einstein relation.<sup>205,214,216–218</sup> The phenomenon can be explained by assuming that the effective degree of ion pair dissociation in RTILs is less than 100%.<sup>214,216,217</sup> Thus, following Tokuda et al.<sup>214,216,217</sup> for many commonly used RTILs, their actual degree of ion pair dissociation at room temperature typically varies between 50 and 70%. However we note that the actual degree of ion pair association in RTILs is currently a subject of intensive debates in the literature,<sup>198,217,219–224</sup> and there have been suggested several other explanations of the deviation of electrical conductivity measurements in RTILs from the Nernst–Einstein relation (see, e.g., refs 198, 225, and 226).

Also, experimental results on ion mobility in RTILs show that small anions have a reduced mobility compared to (much larger) cations;<sup>198,214,227</sup> this interesting counterintuitive phenomenon can be explained by the stronger solvation of anions by the counterions.<sup>228</sup> Overall, many RTILs show non-Arrhenius behavior of kinetic coefficients.<sup>229</sup>

The literature analysis shows that the main factors that determine the magnitude of self-diffusion in imidazolium-based RTILs are the ion size, the geometric shape of the RTIL anion, and the charge delocalization in the anion (see, e.g., ref 230). Tsuzuki in his recent mini-review<sup>231</sup> summarized the main factors controlling the diffusion of ions in ionic liquids and their mixtures: the size and shape of ions, the magnitude of interaction between cation and anion, conformational flexibility,

molecular mass of ions, solvent additives, and the effects of formation of local nanostructures. See also the work by Okoturo and Van der Noot<sup>229</sup> that discusses several molecular-scale factors influencing the viscosity of RTILs. An overview of transport properties of common RTILs can be found in the Galinski et al.’s review on RTIL-based electrolytes.<sup>13</sup>

In general, viscosity of RTILs decreases with the increase of the size of ions and temperature.<sup>211,232</sup> Also, Krossing and co-workers observed that for a given class of RTILs the viscosity (and, consequently, the electrical conductivity) of RTILs have a strong dependence on the RTIL molecular volume.<sup>233,234</sup>

First-generation chloroaluminate-based RTILs usually show low viscosity and high ionic conductivity compared to the hydrophobic RTILs based on large hydrophobic anions (e.g., [TFSA]<sup>-</sup>);<sup>229,235</sup> therefore, chloroaluminates and halogen-based other RTILs have favorable electrochemical properties for processes like electrodeposition that stimulates researchers to continue to investigate these substances (e.g., with an eye toward developing electroplating applications)<sup>14,236,237</sup> despite several issues with stability and large hydrophilicity of chloroaluminate-based RTILs (many of them dangerously react with water especially at higher Lewis acidity).<sup>32</sup> It should be noted, however, that it is more difficult to prepare a high-purity hydrophilic RTIL than a hydrophobic RTIL.<sup>199,235</sup>

In the context of comparing viscosities of different classes of RTILs, we also would like to refer to the work by Okoturo and Van der Noot<sup>229</sup> that presents a thorough investigation of the absolute viscosity behavior of ten air/moisture-sensitive acidic chloroaluminate-based RTILs and thirteen air/moisture-tolerant RTILs. They reported that “the Arrhenius plot was not linear for the majority of the RTILs and some of these RTILs were better fitted with the Vogel–Tammann–Fulcher (VTF) equation. Those RTILs which obeyed the Arrhenius law typically contained asymmetric cations and the majority did not contain functional groups. Those RTILs which obeyed the VTF law contained small and symmetrical cations with low molar mass. Those RTILs which obeyed neither the Arrhenius nor the VTF law consisted of cations which were less symmetric, contained functional groups (e.g., OH and C–O) and had higher molar mass. The glass transition temperatures  $T_g$  (calculated from the VTF fittings) generally decreased with increasing size and molar mass of the cation and anion. The chloroaluminate RTILs containing oxygenated cations were more volatile than the corresponding de-oxygenated RTILs making them unsuitable for applications as solvents and/or electrolytes above ambient temperature.”<sup>229</sup>

We also note that slow dynamics of most RTIL systems poses a challenge to modeling transport and dynamic properties of RTILs.<sup>215,238</sup> In general, molecular simulations of RTIL systems require specific adjustments of standard molecular models and force fields;<sup>238–240</sup> otherwise, the calculated values of diffusion coefficients, viscosity, and ionic conductivity can be far from even qualitative correlations with experimental data.<sup>241,242</sup> Equally, the high viscosity and related low diffusion coefficients of most RTILs will also affect any molecules that will be dissolved in such media. This makes both experiments and computer modeling of solute transport properties in RTILs to be a challenging task. In this context we would like to refer to an interesting work by Eiden et al.<sup>243</sup> There it was shown that solvation free energies of anions and cations calculated by computational quantum chemistry methods at the DFT-level (RI-)BP86/TZVP/COSMO combined with other molecular-scale parameters (molecular radius

and the symmetry number) can be used as input parameters for high-accuracy predicting models. These describe reasonably well the temperature dependence of macroscopic transport properties of RTILs such as viscosity and electrical conductivity.

Overall, due to the high viscosity and low ion mobility, neat RTILs have low conductivity.<sup>127</sup> In spite of the high concentration of charge carriers, it is typically in the range of 0.1–18 mS cm<sup>-1</sup><sup>127</sup> at room temperature; that is much lower than the conductivity range for conventional aqueous electrolytes applied in electrochemistry that is around 200–800 mS cm<sup>-1</sup>.<sup>13</sup>

Chemical structures of RTIL anions and cations have a significant effect on their electrical conductivity, particularly at low temperatures.<sup>205,214,216–218,244–246</sup> Conductivity at the level of ~10 mS cm<sup>-1</sup> at room temperature is typical for ionic liquids based on the [EMIm]<sup>+</sup> cation.<sup>205,218</sup> RTILs based on cations such as pyrrolidinium or piperidinium show lower conductivities at room temperature that are at the level of ~1–2 mS cm<sup>-1</sup>.<sup>13</sup>

Vila and co-workers performed systematic experimental study of the electrical conductivity of nine different imidazolium-based RTILs with [BF<sub>4</sub>]<sup>-</sup> anion and its dependence on temperature.<sup>218</sup> They found that at a given temperature the conductivity decreases as the length of the cation alkyl chain increases. Careful analysis of conductivity behavior in a wide temperature range (from -35 to +195 °C) of different imidasolium-based RTILs with the same [BF<sub>4</sub>]<sup>-</sup> anion in ref 245 also shows that the electrical conductivity decreases with increase of the cation alkyl chain for a given temperature (we note that the results of refs 218 and 245 are in line with general conclusions from an earlier work on this subject by Tokuda et al.,<sup>214</sup> who studied conductivities of imidasolium-based RTILs with TFSA<sup>-</sup> anion).

Effects of anion structure on conductivity of RTILs were considered in refs 216, 218, and 246. For instance, the authors of ref 218 studied effects of anions on the conductivity of [EMIm]-based RTILs by systematically varying the anion size. They found that there is an optimum size of anion (that correspond to [BF<sub>4</sub>]<sup>-</sup>) where the conductivity reaches its maximum value (~16 mS cm<sup>-1</sup> at room temperature for [EMIm][BF<sub>4</sub>]).<sup>218</sup>

Conductivity of RTILs greatly increases with temperature;<sup>205,214,216–218,244–247</sup> for example, for [EMIm][BF<sub>4</sub>] it takes ~16 mS cm<sup>-1</sup> at 25 °C, ~70 mS cm<sup>-1</sup> at 100 °C and ~120 mS cm<sup>-1</sup> at 150 °C.<sup>218</sup> For many commonly used RTILs the temperature dependence of their conductivity can be well fit by the VFT equation.<sup>244,247</sup>

We note that dissolution of the Li<sup>+</sup> ion in neat RTILs typically increases their viscosity and lowers conductivity.<sup>127,248</sup>

As shown by Vila et al.<sup>205</sup> mixing RTILs with some amount of water (between 20 and 50 wt %) can significantly increase their conductivity at room temperature; that is, they show that the conductivity of [EMIm][BF<sub>4</sub>] mixture with ~30 wt % of water is more than 80 mS cm<sup>-1</sup> at 25 °C. However, we note that adding water to an RTIL leads to significant deterioration of its electrochemical stability<sup>249</sup> (see more discussion on this subject below in section 2.2.4).

Instead of water, in many electrochemical applications RTILs are mixed with more electrochemically stable organic solvents (mostly with acetonitrile and propylene carbonate) to decrease viscosity and increase conductivity<sup>250,251</sup> as well as to lower the operation temperature.<sup>252</sup> Thus, mixing [EMIm][BF<sub>4</sub>] with

acetonitrile at the concentration of 2 mol/dm increases the conductivity 3 times (to ~50 mS cm<sup>-1</sup> at room temperature) compared to the conductivity of neat [EMIm][BF<sub>4</sub>] at the same temperature.<sup>13</sup>

**2.2.3. Dielectric Properties.** RTILs have a high concentration of charges, and therefore, they would fully screen a static electric field that would penetrate into the liquid within the range of its short-range structure.<sup>253,254</sup> Because RTILs are conductive media, their response to electric field involves a dynamic component determined by the ionic current due to the translational motion of ions in the field.<sup>255,256</sup> However, there are many other degrees of freedom than those of the translational motion (rotational, vibrational, etc.); these degrees of freedom contribute to polarizability of the liquids at different frequencies.<sup>227</sup> Thus the term "static dielectric constant" must be used with care for RTILs, assuming that it encompasses the contribution of all of the polarization active modes, such as polarizability of atoms, vibrations of ionic pairs and decaying phonon modes, and librations and rotations of ion pairs and larger ionic clusters. Since the translational motions of ions in RTILs are strongly coupled to many of these modes, it makes the measurement of the "static dielectric constant" of RTILs challenging.<sup>202,257</sup> The most popular methods for determining the static dielectric constant values are different dielectric relaxation spectroscopy techniques.<sup>97,202,203,258</sup> We note, however, that several other parameters and techniques are used in the general context of determining RTIL polarity such as Kosower's Z values determined by the charge-transfer absorption band of 1-ethyl-4-(methoxycarbonyl)pyridinium iodide<sup>259</sup> and the Kamlet-Taft solvent parameters<sup>260</sup> (hydrogen-bond acidity ( $\alpha$ ), hydrogen-bond basicity ( $\beta$ ), and (particularly) dipolarity/polarizability  $\pi^*$ ); see the extended discussions on this subject in refs 202, 257, and 261.

According to refs 97, 202, and 203, static dielectric constants of different RTILs vary in the range of 7–85 with many widely used RTILs having a dielectric constant around 10–15. The work of Kobrak<sup>202</sup> shows interesting trends in relationships between the dielectric response of RTILs and the molecular structure of RTIL ions. Kobrak pinpoints that "if a high dipolarity/polarizability is desired for a certain task, the liquid should either (1) incorporate very small ions, or (2) incorporate ionic structures that frustrate the formation of nanoscale domains." From another side we would like to cite in this context the recent work of Choi et al.<sup>258</sup> on imidazolium acrylates and methacrylates and their ionomers. Using dielectric spectroscopy, they showed that polymerization of ionic liquids can significantly enhance their static dielectric constant (they report values as high as ~140 at room temperature). They explain this effect by synergistic dipole alignment of long polymer segments in response to the external field.<sup>258</sup>

**2.2.4. Electrochemical Stability.** For electrochemical applications of RTILs, their stability at charged interfaces is of great importance because in many modern applications (batteries, supercapacitors, electrocatalysis, electrodeposition, etc.) there is a strong need for ionic liquids that are electrochemically stable at as wide as possible potential range. Electrochemical window (EW) is often used as a measure of electrochemical stability; it is defined as the operating potential range or the difference between the maximum oxidation and reduction potentials for a given solvent-electrode system. Most of commonly used RTILs have much higher EW (up to 5–6 V but typically about 2–3 V) than aqueous electrolytes (see ref 127 and 262). We note though that the real usable potential

range becomes often lower in the presence of dissolved molecules in RTIL due to possible catalytic oxidation or reduction of the RTILs mediated by such molecules or electrochemical processes directly involving them.<sup>26,163</sup> A large collection of data on EWs of many RTILs at different electrodes can be found in refs 28, 51, 195, 199, and 263.

Lane recently overviewed main mechanisms of electro-reduction of RTIL cations.<sup>263</sup> Following this review, the best estimates of maximum cathodic stabilities for main types of RTIL cations can be arranged as pyridinium < sulfonium < 1,2-dialkylimidazolium < 1,2,3-trialkylimidazolium < morpholinium < phosphonium < quaternary ammonium (see Figure 16 in ref 263) with the cathodic limit of -2.7 V for phosphonium and quaternary ammonium cations. The comprehensive study of Hayyan et al.<sup>51</sup> summarizes the electrochemical stability of cations of as follows:  $[P_{14,666}]^+ > [N_{112,102}]^+ > [HMPyr]^+ > [EMIm]^+ > [MOEMMor]^+ = [MOPMPip]^+ > [S_{222}]^+ > [BMPy]^+$ . The oxidative limits for anions reported in this paper were found to follow the sequence of  $[TFSA]^- > [FAP]^- > [TFO]^- > [DCA]^- > [TFA]^-$ .<sup>51</sup>

The revealed trends in cathodic and anodic stability of RTIL ions can be quite useful for the first guess about an EW of a particular RTIL; however, we note that, as shown by refs 136 and 264, the size of the EW of an RTIL-based electrolyte "is affected not only by the identity of the cations and anions but also by the particular combinations of the ionic substituents."<sup>136</sup>

Fletcher et al.<sup>134</sup> reported two RTILs with EWs at the platinum electrode to be as high as 8–9 V, hexyltriethylammonium bis(trifluoromethylsulfonyl)imide ([HTEA][TFSA]) and butyltrimethylammonium bis(trifluoromethylsulfonyl)imide ([BTMA][TFSA]). The authors of the work<sup>134</sup> also discuss some observed trends in relationships between the ion geometry and their electrochemical stability and melting point. They find that increasing the chain length of the alkyl groups leads to improved chemical inertness of the RTIL ions. They also note that decreasing the symmetry of the quaternary ammonium cations lowers the melting points of the corresponding ionic liquids (see also discussions on relationships between the molecular structure of RTIL ions with their melting points and other transport and thermophysical properties in refs 37, 54, and 265). We think though that, due to their large potential importance for the field, these results need extra verification by other groups to prove that such enormous enhancement of electrochemical stability is not an artifact related to formation of passivation layers on platinum electrodes. However, if confirmed by independent tests, the results by Fletcher et al. can open new avenues toward development of RTILs of exceptional electrochemical stability.

Naturally, the EW of a particular RTIL strongly depends on the type of electrodes used.<sup>199,266,267</sup> A good summary of types of electrodes that have been used in conjunction with RTILs can be found in ref 199. Following this source as well as analysis of the literature data,<sup>28,127,195,262</sup> one may conclude that for fundamental studies of RTILs at EIs the most popular metallic electrodes are made from Au, Hg, and Pt due to their stability. Au and Pt electrodes are also used in analytical and sensor applications of RTILs.<sup>268</sup> The anodic limit at the named metals in RTILs is usually set by anion oxidation.<sup>199</sup> However, it was found that some RTILs promote oxidative dissolution of electrode material. This feature reveals new approach to the efficient recovery of noble metals through their electro-dissolution.<sup>269</sup> For less stable RTILs and more active metals, like copper, the metal dissolution is tightly linked with

oxidation of fluorinated anion through formation of  $[MeF_x]^{n-}$  complexes<sup>270</sup> (overall, it was shown that copper electrodes sufficiently decrease electrochemical stability of RTILs with fluorinated ions<sup>270</sup>).

Recent work of Lust and co-workers attracted attention to the potential use of Bi electrodes for fundamental studies on RTILs as well as applications.<sup>271</sup> Indeed, Bi electrodes have certain advantages: their costs are much less than for Au and Pt electrodes, they are less toxic than Hg electrodes, and they are stable and operationally efficient.<sup>272</sup>

Recently there has been much interest in RTIL properties at the interface with carbon-based electrodes (amorphous (glassy) carbon, graphite, carbide-derived-carbon, carbon cloth, nano-carbon composites, etc.)<sup>29,206,273–276</sup> due to the large amount of current and potential applications of these materials (see the more detailed discussion on this subject later on in this article).

For ions in aqueous solutions, surface charge densities between -40 to +80  $\mu C/cm^2$  have been reported.<sup>277</sup> To determine the actual range of experimentally accessible electrode charge densities in RTILs is a nontrivial task and such data are sparse in the literature. However, upon considering the area under an experimentally measured capacitance/potential-curve starting from the potential of zero charge, the surface charge density can be roughly estimated.<sup>278</sup> Using the experimental data reported in ref 279, one could estimate that, for the spherical ion  $[PF_6]^-$  at a Au(111) electrode, the surface charge density can be as high as  $\approx 40 \mu C/cm^2$ . In their recent work Costa et al.<sup>280</sup> reported that the surface charge densities for different imidazolium-based RTILs and their mixtures at a Hg electrode can be as high as  $\pm 25 \mu C/cm^2$  for a potential window of  $\sim 2.5$  V. Therefore, we anticipate that for RTILs with higher electrochemical windows the cathodic/anodic limits for the electrode charge density could be at least around  $-40/+50 \mu C/cm^2$ . We note that the cathodic upper values are comparable with the surface charge density on muscovite mica that has a fixed layer charge of around  $-32$  to  $-34 \mu C/cm^2$ .<sup>91,281,282</sup>

Even a small amount of impurities (such as, e.g., water, traces of alkali salts, organic solvents, etc.) may have a profound effect on electrochemical stability of RTILs at EIs.<sup>249,266,283</sup> As was shown in ref 249 for several types of RTILs, even a small water intake from the atmosphere significantly decreases their EWs. Because even hydrophobic RTILs sorb minor amounts of water from the atmosphere,<sup>249</sup> this issue becomes important both for fundamental studies of RTILs at EIs<sup>284,285</sup> and for developing applications.<sup>286,152</sup>

Other effects are related to spontaneous absorption of  $CO_2$ <sup>287–289</sup> and other gases in RTILs.<sup>290,291</sup> Generally the difficulty to prepare "clean" RTILs is another challenge of this media at least for large scale utilization without sophisticated preparation, unless RTILs are deliberately used as sorbents for such substances<sup>291–293</sup> with their subsequent treatment, including electrochemical activation.<sup>294</sup>

### 3. EDL BEFORE RTILS

The first concepts of EDL were developed a century ago in the context of ordinary inorganic electrolytic solutions.

The earliest model for EDL was suggested by Helmholtz in 1853.<sup>295</sup> In this model the EDL is described mathematically as a simple, plane dielectric capacitor, assuming that the counter charge of ions forms the second plate of the capacitor, oppositely charged with respect to the first plate (the electrode). This picture corresponds to a single layer of ions

driven to the surface by the electric field of the electrode and totally screening it. The Helmholtz model did not imply any space charge of ions behind that layer. Presumably because of the Helmholtz model, the mere term double layer (sometimes quite confusing, because the EDL is normally not one layer thick) has forever established itself in the scientific literature. In the Hemholtz model, the electrostatic potential drops linearly between the electrode and electrolyte, and the whole drop is confined between those two plates. The capacitance of such EDL is just the same as of a macroscopic capacitor, and it is given by

$$C = C_H = \frac{\epsilon^*}{4\pi d} \quad (1)$$

where  $d$  is the distance between the plates and  $\epsilon^*$  is the effective dielectric constant of the medium between them (note that throughout the paper all electrostatics related equations, will be consistently written in the Gaussian system of units<sup>296</sup>). With  $d = 0.5$  nm and  $\epsilon^* = 5$  for a water layer with “frozen” orientational polarizability with only librations allowed, one gets  $C = 8.5 = \mu\text{F}/\text{cm}^2$  which is of the order of the typically measured capacitance of inorganic electrolytes.

However, in real systems the EDL is (generally) not one layer thick because of entropy: thermal disorder does not allow all counterions to gather on a monolayer-thick plane. Instead, a space charge of ions forms at the polarized interface, which was clarified half a century later. A French physicist Gouy pioneered a theory of such space charge in 1909–1910,<sup>297,298</sup> and a British physical chemist Chapman in 1913 developed it into a form that we now call the Poisson–Boltzmann theory of diffuse EDL or the Gouy–Chapman theory (GCh theory). The distribution of counterions in the GCh theory is smeared within the so-called Gouy length,  $\lambda_G$ , the value of which is found self-consistently, and it depends on the potential drop across the EDL,  $U$ . For 1–1-electrolyte, using modern notations, this expression reads as follows:

$$\begin{aligned} \lambda_G &= \frac{\lambda_D}{\cosh(u/2)}, \quad u = \frac{eU}{k_B T}, \quad \lambda_D = \sqrt{\frac{1}{8\pi L_B c_0}}, \\ L_B &= \frac{e^2}{\epsilon k_B T} \end{aligned} \quad (2)$$

Here  $u = eU/k_B T$ ; that is, it is the potential drop across the double layer measured in the units of the so-called “thermal voltage”,  $k_B T/e$  where  $k_B$  is the Boltzmann constant,  $T$  is the absolute temperature, and  $e$  is the elementary charge; at room temperature  $k_B T/e = 0.0256$  V, usually memorized as 25 mV.  $\lambda_D$  is the Debye length expressed here through the Bjerrum length,  $L_B$  (the length at which the energy of the Coulomb interaction of two elementary charges in a dielectric medium with a macroscopic dielectric constant  $\epsilon$  is equal to the thermal energy  $k_B T$ ), and the bulk electrolyte concentration. Note that nowadays we express the Gouy length,  $\lambda_G$ , through the Debye length,  $\lambda_D$ , whereas  $\lambda_D$  itself was introduced by Debye and Hückel a decade later<sup>299</sup> with, however, a reference to the Gouy paper.

As a function of the electrode surface charge density  $\sigma$ , the Gouy length reads as

$$\lambda_G = \frac{\lambda_D}{\sqrt{1 + 4\pi^2 L_B^2 \lambda_D^2 (\sigma/e)^2}} \quad (3)$$

The Gouy length turns into the Debye length at small voltages,  $u \rightarrow 0$ ,  $\lambda_G \rightarrow \lambda_D$ ; at large voltages,  $u \gg 1$ ,  $\lambda_G \propto e^{-u/2}$ ; that is,  $\lambda_G$  becomes exponentially small with increasing electrode polarization. As a function of the electrode charge at large charges, it, however, diminishes only hyperbolically as  $\lambda_G \approx 1/(2\pi L_B \sigma/\epsilon l)$ . Hence the differential capacitance of the diffuse EDL

$$C = C_{GC} \equiv \frac{\epsilon}{4\pi \lambda_G} \quad (4)$$

as a function of voltage has a U-shape (Figure 2), growing unlimitedly with the electrode polarization regardless of its sign, in contradiction to experiments in which the capacitance always levels off at large voltages.

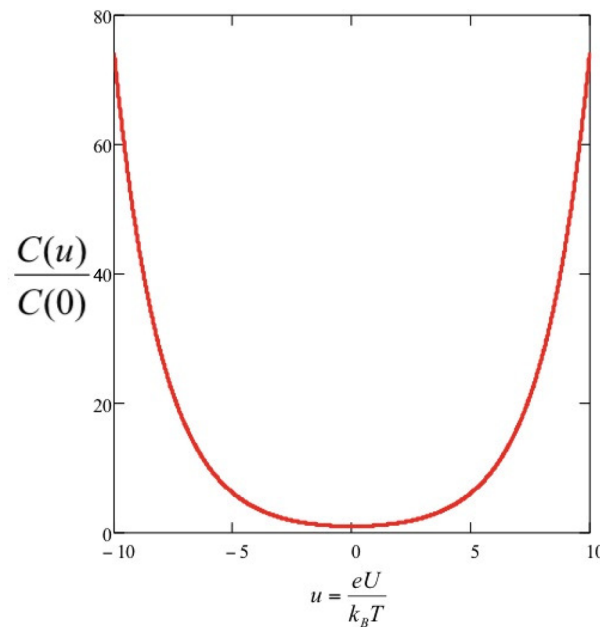


**Figure 2.** U-shape of the capacitance predicted by the Gouy–Chapman theory (eq 4).

It was clear that the GCh theory should break down at large voltages, when the estimated Gouy length approaches the diameter of the ion or even earlier. Indeed, the Gouy length diminishes unlimitedly, because there is no finite size of ions or any discreteness scale in the Gouy–Chapman theory.

An attempt to introduce such a discreteness effect was made by Stern,<sup>300</sup> motivated in the first place by that controversy. To avoid the unlimitedly large capacitances of the EDL which contradict experimental observations, he introduced a “cutoff”, having added a compact layer capacitance, the analog of the Helmholtz capacitance, in series to the Gouy–Chapman capacitance, such that

$$\frac{1}{C} = \frac{1}{C_H} + \frac{1}{C_{GC}(u(u_{tot}))} \quad (5)$$

In the Gouy–Chapman–Stern model, the potential drops down linearly within the compact layer, and then decays quasi-exponentially in the diffuse layer. Generally the overall potential drop  $u_{tot}$  splits into two parts,  $u_{tot} - u$  across the Stern layer and  $u$  across the Gouy–Chapman diffuse layer. The value of  $u_{tot}$  must be found subject to the values of  $C_H$  and  $C_{GC}$ , according to the equation

$$u = \frac{u_{\text{tot}}}{1 + \frac{K_{\text{GC}}(u)}{K_{\text{H}}}} \quad (6)$$

where the symbol  $K$  stands for the integral capacitance, defined as the ratio of the minus-charge accumulated in the compact layer (equal to the charge of the electrode) to the voltage drop across the layer minus its value at zero charge, i.e. potential of zero charge (pzc). The integral capacitance is related to the differential one as:

$$K = \frac{1}{u - u_0} \int_{u_0}^u C(u') du' = \frac{\sigma}{\int_0^\sigma \frac{1}{C} d\sigma} \quad (7)$$

where  $u_0$  is the pzc.

However, for moderate electrode polarizations (and not too high ion concentrations) the original GCh theory [eqs 2 and 4] has proved to work very well. Therefore, it became a background of many estimates not only in electrochemistry but also in colloid science and biophysics.<sup>301–306</sup> Practically every textbook in these areas starts the introduction of the principles of EDL from the GCh theory. The latter suggests that the minimum of capacitance in solution without specifically adsorbing electrolyte coincides with the pzc, at least in dilute electrolytes where the diffuse layer capacitance dominates the total one in a wide range of electrode potentials. This has offered an easy method for estimating the value of pzc for different electrode/electrolyte interfaces. More involved methods have also been developed,<sup>307,308</sup> but the early one still remains to be one of the easiest and most reliable.

For large electrode polarization (and not too dilute electrolytes), it is the compact layer that determines the capacitance. That contribution has been evaluated from experiments by drawing the so-called Parson-Zobel plots,<sup>309</sup> namely showing the experimental values of the inverse capacitance  $C_{\text{experimental}}^{-1}$  vs the calculated inverse Gouy-Chapman capacitance  $C_{\text{GC}}^{-1}$ , at varied electrolyte concentrations. If eq 5 is valid and the value of  $C_{\text{H}}$  does not depend on electrolyte concentration (the so-called “Graham ansatz”; for a review see, ref 2), one must get a straight line with the intercept in the limit of high concentrations, usually extrapolated, giving the value of  $C_{\text{H}}^{-1}$ . Such lines can be plotted for different electrode polarizations, and notably,  $C_{\text{H}}$  assessed in this way usually revealed strong dependence on the charge of the electrode voltage.<sup>2,310</sup>

Hence, many models were proposed to describe the nonlinear polarization of the compact layer; for a review, see the monographic articles.<sup>310,311</sup> These models spanned from descriptions of the monolayers of solvent molecules at the interface, adsorption–desorption of organic molecules if present in the solution, to the profiles of the electronic excess charge density at electrodes and even surface reconstruction.<sup>312</sup>

Most importantly the Graham ansatz is valid only in the absence of specific adsorption of ions. An extension of the theory that takes into account effects of the specific ion adsorption has been made first by Graham and Parsons,<sup>5,313,314</sup> and a review of further developments can be found in the Vorotnytsev's monographic chapter.<sup>315</sup>

Much effort was devoted later to develop a unified theory of EDL without distinguishing between the compact and the diffuse parts, either on a phenomenological level<sup>310,316,317</sup> or on the molecular level considering ions and solvent molecules on the same footing.<sup>4,318–320</sup> The upshot of those studies is that in

the systems without specific ionic adsorption there is a contribution to capacitance that is independent of electrolyte concentration. Therefore, the apparent compact layer contribution appears automatically upon incorporation of the structure of the solvent into the theory. We refer the reader to the corresponding reviews mentioned above; the progress along those lines for the cases when the ions adsorb specifically was also reviewed in detail.<sup>310</sup>

In the past few years we have witnessed a renaissance in developing more sophisticated statistical mechanical or extended mean-field models for the EDL within the so-called restrictive primitive model of electrolytes (charged hard spheres in a background with a constant dielectric permittivity), which we will selectively cover in sections to follow later in the review in the context of potential applications to RTILs.

For the subject of this article, we will first need to focus on one direction in this research area. Conceptually, one of the main weaknesses of the GCh theory is the neglect of the finite size of ions (that allows them to accumulate at large voltages at any concentration at the electrode). As such, the 1999 simulation work of Boda and co-workers<sup>321</sup> showed that the GCh theory fails to reproduce the qualitative behavior of the electrical double layer capacitance of high-temperature molten salts, where the effects of the finite ion size are important. However this drawback usually does not manifest itself in the theory of ordinary (diluted) electrolytic solutions. With an increase of the voltage, long before the ions will start “feeling” their excluded volume, electrochemical reactions involving these ions or solvent at the corresponding electrodes will take place. For this reason the pioneering works that were devoted to the inclusion of the excluded volume effects in the EDL theory<sup>322–326</sup> did not receive enough credit and attention in electrochemical community (as well as some follow up literature that also failed to notice those works;<sup>327–329</sup> more detailed exploration of the history of this subject and more references of this kind one can find in ref 330). All these works were rediscovered only recently in the context of such highly concentrated ionic systems as RTILs or in microfluidics, where the effects of the finite size of ions start playing an important role at voltages below the onset of electrochemical reactions. In fact, several results from these works were independently reproduced again. We will dwell on the most important of them and generally on a detailed description of the excluded volume effects in the context of the problems where they become crucial: EDL in RTILs.

Obviously, integral characteristics of the double layer are not the whole story. Whereas the capacitance is an important characteristic of energy storage devices, as a diagnostic feature it integrates out many details which one must be interested to reveal. The key characteristics are the molecular-scale distribution of ions and the whole molecular picture of the EDL. The greatest interest nowadays is in a direct assessment of the structure and chemical composition of the EDL in RTILs through X-ray<sup>331–333</sup> and neutron scattering,<sup>334,335</sup> angle-resolved and energy-resolved X-ray photoelectron spectroscopy (XPS),<sup>336–339</sup> metastable induced electron spectroscopy (MIES) scanning probe techniques,<sup>340</sup> neutral-impact-collision ion scattering spectroscopy (NICISS, that recently became popular method for investigating interfacial properties of RTILs),<sup>285,341–343</sup> or any other *in situ* methods, including STM and AFM measurements.<sup>65,344–347</sup>

As we have stressed already, the study of the highly concentrated ionic systems was very much “catalyzed” by the

interest in molten salts. In particular, pioneering theoretical works of Tosi and collaborators<sup>348–351</sup> for molten salts have discovered a spectacular phenomenon that they termed “overscreening”.<sup>351</sup> It was found there that at small electrode polarizations, the first layer of ions delivers a counter charge greater in absolute value than the one on the electrode. The next layer was on average oppositely signed, but with the absolute value of the charge larger than the absolute value of the difference between the charge of the electrode and the charge of the first layer. And off these decaying charge oscillations go over several layers before reaching electro-neutrality in the “bulk”. Torrie and Valleau were among the first who used simulation techniques (Monte Carlo) for systematical studies of EDL formation at charged interfaces in concentrated electrolytes. In their 1980 work they showed that, at high concentration of ions in an electrolyte, the charge density in the EDL starts to oscillate.<sup>352</sup> Their pioneering works on modeling EDL in concentrated electrolytes showed apparent limitations of the GCh theory.<sup>353,354</sup>

However, the physical nature of overscreening, to our knowledge has never been clearly rationalized in the literature. We will get back to this issue, when discussing the situation with RTILs, where it becomes central for small and medium electrode polarizations.

Note that the papers by Tosi et al. on molten salts did not study the effect of the voltage on the ionic distribution near the interface, having limited the analysis to the linear response.<sup>351</sup> The nonlinear response was much more difficult to handle, and here simulation has started to play a pivotal role, as we discuss later in this review. For molten salts, such a study has been performed in ref 355, albeit not for a wide set of charges of the electrode. It has, however, detected some suppression of overscreening at large electrode polarization. We will dwell on a similar phenomenon in the context of RTILs later in this review.

The detailed Monte Carlo simulation studies of overscreening by Tosi et al. were inspired by a short note by Dogonadze and Chizmadzhev.<sup>356</sup> Based on the experimental evidence (well established at that time) for the decaying oscillating structure of the bulk binary correlation function in simple liquids, Dogonadze and Chizmadzhev correctly deduced that the charge density correlation function in an ionic liquid should also have a form of decaying oscillations. They related the EDL capacitance with the features of the bulk correlation function of that charge distribution; such relationship is possible in the linear response regime neglecting the breakdown of the translational invariance of the system in the direction perpendicular to the electrode. They came to the conclusion that the capacitance is simply inversely proportional to the distance to the first peak. Their suggestion has paved the way to much later statements that the EDL in ionic liquids is effectively one layer thick. This was bold and novel at that time, but in fact appeared to be not always accurate.

Indeed, it can be shown exactly that the differential capacitance of EDL is inversely proportional to the center of mass of the excess charge distribution in the double layer

$$\begin{aligned}\lambda(\sigma) &= \lim_{\delta\sigma \rightarrow 0} \left[ \frac{\int_0^{z^*} dz \delta\rho_{\text{ion}}(\sigma, z) z}{\int_0^{z^*} dz \delta\rho_{\text{ion}}(\sigma, z)} \right] \\ &\equiv \frac{\int_0^{z^*} dz \delta\rho_{\text{ion}}(\sigma, z) z}{-\delta\sigma} \\ &= \int_0^{z^*} dz \left\{ -\frac{d\rho_{\text{ion}}(\sigma, z)}{d\sigma} \right\}_z\end{aligned}\quad (8)$$

Here  $\delta\rho_{\text{ion}}(\sigma, z) = \rho_{\text{ion}}(z)|_{\sigma+\delta\sigma} - \rho_{\text{ion}}(z)|_\sigma$  is the difference between the charge densities in the liquids at the charge of the electrode equal to  $\sigma + \delta\sigma$  and  $\sigma$  and  $z^*$  is some distance in the electroneutral bulk which may be put equal to infinity for large separation between the electrodes. Namely

$$C = \frac{\varepsilon_*}{4\pi\lambda(\sigma)} \quad (9)$$

where  $\varepsilon_*$  is the effective dielectric function of the dipole active degrees of freedom in the electrolyte, due to vibrations and rotations of ionic pairs and clusters, electronic polarizability of ions of the solute and solvent molecules, etc. In the case of solvent-free RTIL it is the polarizability of all the degrees of freedom that are faster than translational motions of the same ions of RTIL, and it redresses Coulomb interactions in RTIL. Systematic measurements show that for many RTILs  $\varepsilon_*$  is of the order of 10, cf., refs 198, 202, and 357. However, in the case of molten salts this is just due the electronic polarizability of ions, and  $\varepsilon_* \approx 2$ .

Oscillations in the potential distribution are related with the oscillations in  $\rho_{\text{ion}}(\sigma, z)$  as a function of  $z$ , because the distribution of electrostatic potential in the double layer is given by

$$\Phi_{\text{IL}}(z) = -\frac{4\pi}{\varepsilon_*} \int_0^z (z - z') \rho_{\text{ion}}(z') dz' \quad (10)$$

All in all, had the first peak in  $\delta\rho_{\text{ion}}(\sigma, z)$  been totally dominating, the Dogonadze–Chizmadzhev conjecture would have been justified. However, even in HTMSs more than one peak is seen on the density profiles (and even more in RTILs). The way how all these peaks get restructured with applied voltage is decisive for the capacitance dependence upon voltage.

Measurements of the EDL capacitance at high temperatures typical for molten salts using electrochemical impedance techniques,<sup>5,358,359</sup> are generally very difficult and are prone to all sorts of experimental artifacts (for a critical review, see ref 359). In particular, the controversy in the literature data for the temperature dependence of the EDL capacitance in molten salts (different trends reported by different authors) that challenged theorists for decades, remains unresolved (see also discussion on this subject in the following sections below).

There is one issue to be mentioned before we conclude this section. In the midlate 1980s there was a great interest in understanding the role of the electrons of the electrode in the result for EDL capacitance, specifically the effect of the spillover of the surface electron cloud into the solvent, and of the response of the surface electronic profile to charging (for reviews read refs 2, 360, and 361). Indeed, the distance to the center of mass of the excess charge distribution should be calculated not from the hypothetical “edge of the electrode”, say the edge of its ionic skeleton, but from a position of the

excess charge in the electrode. This position is determined by the distribution of electrons near the interface and the latter is affected by the net charge of the electrode. The effect on the compact layer capacitance and its dependence on the electrode potential could be substantial, the surface electronic profile of the electrode being sensitive to the electrode polarization.<sup>2</sup> How important this effect is for ionic liquids is not clear, as so far all the attention has been addressed to the double layer on the liquid side. It is, however, very important for any electrolyte, whether the electrode is an ideal metal, semiconductor, or semimetal.

From the very first steps of the electrochemistry of semiconductors, it was made clear that the potential distribution on the electrode side of the interface can be very important. Semiconductor electrode contributes a capacitance in series with the capacitance of the electrolyte side, which is due to a space charge of the electrons and holes in the semiconductor. If the concentration of charge carriers is low there, this space charge region will totally dominate the overall capacitance of the interface. Gerischer and coworkers<sup>362,363</sup> noted some 30 years ago that the measured capacitance of the semimetal graphite electrode/electrolyte solution will unlikely display any information on the EDL in the electrolyte, being totally determined by the EDL in the electrode! Indeed, the two capacitances add in series and thus the smaller one will determine the capacitance. As calculated by Gerischer et al, it appears that the dominant contribution is due to the graphite side, unless one goes to very low electrolyte concentrations. It will be worth to keep this in mind, when trying to interpret experimental data on various carbon electrodes. We note that this conclusion has not been approved by recent findings of Shklovskii et al.<sup>364</sup> Theoretical estimates reported in that work suggested that the electric field should decay to zero within the first graphite layer. However, the recent quantum density functional theory (DFT) study by Luque and Schmickler that explicitly considered the layered structure of the graphite electrode showed that “on the basal plane of graphite, an external field penetrates over a distance of a few tenth of a nm into the surface”.<sup>365</sup> Luque and Schmickler also showed that the induced charge density inside the first several layers of graphite strongly oscillates (displaying Friedel-like oscillations). That work used a combination of the quantum DFT results with the hard-sphere model for the electrolyte solution to calculate the overall capacitance of the graphite/electrolyte interface. The computational and theoretical results presented in that work were shown to be in an excellent agreement with experimental data.<sup>365</sup>

Therefore, one may conclude that, indeed, the interfacial capacity between graphite and an electrolyte solution with high ionic concentration is dominated by the electronic response of graphite. However, there are still many open questions in this area (e.g., effects of surface roughness, impurities, chemical modification of the surface and surface adsorption). Further detailed investigations of the appropriate quantum chemistry level combined with an adequate description of the liquid side are needed for various carbon materials. This is perhaps one of the most important challenges for the theory, in view of a wide use of carbon materials in supercapacitors, batteries, and other electrochemical applications.<sup>29,89,92,166,168,206,366–378</sup>

## 4. PRINCIPLES OF THE THEORY OF EDL IN RTILS AT FLAT ELECTRODES

### 4.1. Mean Field Theory

Mean field theories are usual first steps in description of complex statistical-mechanical systems. They serve as common reference bases for more sophisticated theories and computer simulations. The simplest mean field theory of EDL for RTILs at a flat interface was suggested in a 2007 feature article<sup>56,476(erata)</sup> in the context of the overall broad discussion of various new features that EDL in RTILs may exhibit in contrast to EDL in ordinary diluted electrolytes. The approach used simple principles of the lattice gas model, in which  $N_+$  cations and  $N_-$  anions, with a fixed total number  $\bar{N} = N_+ + N_-$ , are distributed over  $N$  available lattice sites. The distribution is random except for when it is influenced by electric field. The electrostatic potential  $\Phi$  of this field is self-consistently determined by the distribution of ions near the boundary with the electrode the polarization of which is taken into account through the boundary condition.

The free energy of such system may be approximated by

$$F = e\Phi(N_+ - N_-) + B_+N_+^2 + B_-N_-^2 + CN_+N_- \\ - k_B T \ln \frac{N!}{(N - N_+ - N_-)!N_+!N_-!} \quad (11)$$

Here the electrostatic potential  $\Phi$  and the distribution of ions are related via the Poisson equation, which for a system with the anisotropy axis (the one perpendicular to the surface of the flat electrode),  $z$ , reads as

$$\epsilon_* \frac{d^2\Phi}{dz^2} = 4\pi e[c_- - c_+] \quad (12)$$

with concentrations of anions  $c_- = N_-/\Omega$  and cations  $c_+ = N_+/\Omega$  where  $\Omega$  is the total volume of the system. The second, third, and fourth terms in eq 11 take into account for specific interactions between cations and anions the nontrivial consequences of which were the subject of intensive investigations in this class of models in different contexts in the past.<sup>379–381</sup> In the first approximation, however, as in ref 56, one can drop these terms out, just putting  $B_+ = B_- = C = 0$  as this is the only way to keep the algebra simple and get analytical results. Minimization of the free energy with respect to  $N_+$  and  $N_-$  gives “Fermi-like” distributions of cation and ion densities as a function of electrostatic potential:

$$c_+ = c_0 \frac{\exp\left(-\frac{e\Phi}{k_B T}\right)}{1 - \gamma + \gamma \cosh\left(\frac{e\Phi}{k_B T}\right)}, \\ c_- = c_0 \frac{\exp\left(\frac{e\Phi}{k_B T}\right)}{1 - \gamma + \gamma \cosh\left(\frac{e\Phi}{k_B T}\right)} \quad (13)$$

controlled by a single parameter of the model, the ratio of average concentration in electroneutral region (where,  $\Phi = 0$  and  $c_+ = c_- = c_0$ ) to the maximum possible local concentration

$$\gamma = \bar{N}/N = 2c_0/c_{\max} \quad (14)$$

The physical meaning of this parameter is straightforward (see Figure 3). In solvent-free ionic liquids,  $1 - \gamma$  is the portion of free volume, i.e., the portion of voids in the system that can

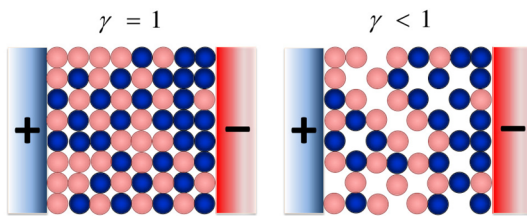


**Figure 3.** Cartoon showing an ionic liquid between two electrodes, representing the concept of the compacity parameter  $\gamma$  (red spheres standing for anions, blue spheres depict cations, and empty space in the lattice representing voids). For these 2D cartoons,  $\gamma = 1$  for the left picture and  $\gamma = 3/4$  for the right picture.

potentially accommodate extra ions (analogous to what is called porosity, with  $\gamma$  being equivalent to what is called compacity<sup>382</sup>). Some RTILs spontaneously absorb some small amount of water from the air<sup>22,32,41,152,249,285,383,384</sup> or they can be deliberately mixed with some amount of organic solvents (usually for the purpose of increasing the mobility of ions);<sup>37,54,142,252,385–388</sup>  $1 - \gamma$  will then characterize the volume portion of those molecules. The case of  $\gamma = 1$  corresponds to an ultra dense system with maximum packing density of ions and no solvent. The value of  $\gamma$  should vary for different RTILs, but for many of them is expected to lie around or above  $1/2$ ; however, in the case of an RTIL with solvent additives it can be substantially lower.

Combination of eq 12 and eq 13 gives the so-called Poisson–Fermi equation

$$\frac{d^2\Phi}{dz^2} = \frac{8\pi e c_0}{\epsilon_*} \frac{\sinh\left(\frac{e\Phi}{k_B T}\right)}{1 + 2\gamma \sinh^2\left(\frac{e\Phi}{2k_B T}\right)} \quad (15)$$

This nonlinear second order differential equation can be easily integrated subject to the corresponding two boundary conditions, and this solution will give us the distribution of potential  $\Phi(z)$ . For a single double layer at one electrode located at  $z = 0$ , one may use as the boundary conditions (i) the Gaussian law at the electrode/electrolyte interface,  $-e^*(d\Phi/dz)|_{z=0} = 4\pi\sigma$ , where  $\sigma$  is the surface charge density, and (ii) the absence of the electric field in the electroneutrality region,  $(d\Phi/dz)|_{z\rightarrow\infty} = 0$ . Setting the potential in the bulk,  $z \rightarrow \infty$ , at zero, together with the full solution for  $\Phi(x)$ , one gets the potential drop across the EDL,  $V = \Phi(0)$ , thus establishing the relationship between  $V$  and  $\sigma$ . The capacitance per unit surface area of the electrode then is obtained  $C = (d\sigma/dV)$  at any value of electrode potential.

As noted in the previous section, devoted to the introduction to EDL in ordinary electrolytes, the Poisson–Fermi equations have been earlier solved in different contexts in a number of recent and much older works<sup>322–326,328,329</sup> starting with the pioneering paper by Bickerman;<sup>322</sup> for a comprehensive review see ref 330. For details of the potential distribution  $\Phi(x)$  at the flat interface, we refer the reader to ref 56, here outlining just the main points: the absolute value of the potential decreases from  $\Phi(0)$  to zero (i) monotonously (mean-field solution!) and (ii) slower than the Gouy–Chapman solution. How much slower? This is determined by the compacity factor,  $\gamma$ . When  $\gamma = 0$  the shape of  $\Phi(z)$  is the same as in the Gouy–Chapman theory; however, when  $\gamma$  approaches 1 the shape becomes much less prolate because of the volumetric constraints on the density of counterions that accumulate in the double layer in

response to the polarization of the electrode. This effect is often called “lattice saturation” or “crowding”, and it has an important consequence on the voltage-dependence the EDL differential capacitance.<sup>52,389</sup>

The resulting expression for the latter through the overall potential drop across the double layer, written for compactness in dimensionless units,  $u = eU/k_B T$ , reads

$$C = C_D \cosh\left(\frac{u}{2}\right) \frac{1}{1 + 2\gamma \sinh^2\left(\frac{u}{2}\right)} \sqrt{\frac{2\gamma \sinh^2\left(\frac{u}{2}\right)}{\ln\left[1 + 2\gamma \sinh^2\left(\frac{u}{2}\right)\right]}} \quad (16)$$

The particular case of  $\gamma = 1$  can also be retrieved

$$C = C_D \cosh\left(\frac{u}{2}\right) \frac{\sqrt{2} |\sinh(u/2)|}{\sqrt{\ln[\cosh u]} \cosh u} \quad (17)$$

In the both expressions

$$C_D = \frac{\epsilon_*}{4\pi L_D}, \quad \lambda_D = \sqrt{\frac{1}{8\pi L_B c_0}}, \quad L_B = \frac{e^2}{\epsilon_* k_B T} \quad (18)$$

are the Debye capacitance, the Debye length, and the Bjerrum length, respectively. These three factors have the same form as in electrolytic solutions (c.f. eq 2), but they use  $\epsilon_*$ , the “high frequency dielectric constant” of the RTIL that for pure, solvent-free RTILs is determined by all dipole-active collective excitations in RTIL (see section 2.2.3 above); an addition of organic solvent molecules can affect (usually increase) that value.

The first two of the four factors in eq 16 determine the Gouy–Chapman capacitance, but the two other factors convert the result into something very different. Such, the second factor in eq 17 makes the voltage-dependence of capacitance opposite to the Gouy–Chapman one: the curve takes a bell-shape instead of the U-shape. The behavior of the more general case, 16, depends on the value of  $\gamma$ . For  $\gamma > 1/3$  it has a bell-like shape, whereas for  $\gamma < 1/3$  it has a double hump shape, called camel-shape in ref 56. In Figure 4 we reproduce plots of that paper that show qualitatively different modes of behavior.

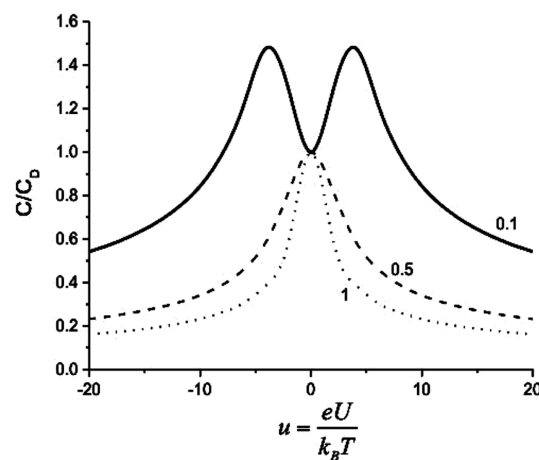


**Figure 4.** Capacitance given by the mean-field theory, eq 16, for indicated values of the compacity parameter,  $\gamma$ . The graph shows “camel” and “bell” shapes, for small and large values of  $\gamma$ , respectively. Reprinted with permission from ref 56. Copyright 2007 American Chemical Society.

The physical nature of the two different modes of behavior is clear. The crossover from the bell shape to the camel shape takes place when the density of electrolyte is diminished. The parameter  $\gamma$  is the key measure of the density of electrolyte, scaled to the maximum possible local density. For small  $\gamma$  there is some room to make the double layer more dense with the increase of voltage, filling up the voids (the free volume) in the liquid or, if instead of voids we have some space occupied by organic solvent, expelling solvent molecules out of the double layer.<sup>390</sup> This will provide the Gouy–Chapman like behavior at small/moderate voltages (see Figure 2 above). On the contrary if there are no voids or no solvent to realize the drive to compress the double layer with the increase of the voltage, the counterions will start to line up in front of the electrode and the double layer will be getting thicker and the capacitance will fall, demonstrating the bell shape.

In this mean-field theory the borderline between the two modes of behavior (bell-like and camel-like shapes) is at  $\gamma = 1/3$ . We fail to see any general law that could have dictated this; in reality the position of the demarcation line in terms of the average density of electrolyte (i.e., of parameter  $\gamma$ ) should depend on details of the studied system.<sup>52,391</sup>

Simultaneously with ref 56, which was focused entirely on RTILs, the formula eq 16 in a different physical context was reported by Kilic and co-workers;<sup>392</sup> a year later, in connection with RTILs, its particular case of  $\gamma = 1$  was reported by Oldham.<sup>393</sup> References 56 and 393 became particularly popular in the community that deals with electrochemistry of RTILs; that analysis was also subjected to various extensions.<sup>394,395</sup>

The papers<sup>56,393</sup> missed, however, an early article by Freise,<sup>326</sup> who had derived similar formula as eq 17 but in the context of the double layer in concentrated electrolytes. That early work was essentially ignored at the time of its publication (1952); we think that this happened mainly because the decreasing wings of the capacitance shape in electrochemical experiments had not been reported before RTILs. Indeed, the Freise's theory predicted them for voltages at which electrochemical reactions already turn on in common electrolytes. For this reason, electrochemists did not pay enough attention to it: in 1950s the time of the Freise's findings did not come. It was due to Bazant and his colleagues with their passion for the history of science<sup>330,392</sup> that the Freise's work has been retrieved from oblivion and began to be quoted, at least in the microfluidics community.

Note that the mean-field model can be modified to take into account the asymmetry of ion sizes. The easiest thing, as suggested in ref 56 and implemented in ref 396, is to assume that  $c_{\max}$  on the two wings of polarization will be different. If cations are larger than anions, then close to the positively polarized electrode (the anode)  $c_{\max}$  will be higher than near negatively polarized electrode (the cathode). Consequently,  $\gamma$  will be smaller for positive polarization of the electrode than for negative polarization. This can be phenomenologically implemented into the previous equations by attributing to  $\gamma$  a voltage dependence. In the spirit of refs 56 and 396, avoiding introduction of any new parameters, such dependence can be parametrized as

$$\gamma(u) = \gamma_- + (\gamma_+ - \gamma_-)/(1 + e^u) \quad (19)$$

This will immediately introduce an asymmetry in the capacitance curve around the pzc: the positive wing lying higher than the negative wing, with the maximum/maxima shifted from the pzc to positive potentials.

The temperature dependence of capacitance, the subject of controversy in experimental data, in the mean-field theory enters through the value of  $u = eU/k_B T$ , and through the expression for the Debye length, eq 2, which it enters explicitly as well as through some mild dependence of  $\epsilon_*(T)$ . Graphs, plotted in ref 397, show that the increase of temperature broadens maxima in capacitance but leaves practically unaltered the large voltage wings (cf. the next section).

#### 4.2. Model Independent Result

Reference 56 has addressed attention to an interesting fact: the behavior of the wings is likely to be universal, independent of the model. The mean-field theory formula gives it as an asymptotic law,  $C = \epsilon_*/(4\pi L_{\text{eff}}(u))$  where the effective thickness of the double layer is  $L_{\text{eff}} \approx L_D(2\gamma|u|)^{1/2}$ , so that

$$C \approx C_D \sqrt{\frac{1}{2\gamma|u|}} \quad (20)$$

As it has been shown in ref 56, this asymptotic law can indeed be derived in the so-called "de Gennes" style, i.e., without any complicated algebra or any model. It is worth to reproduce those arguments here. In the saturation regime, when ions of one sign in the double layer are densely packed,  $|o| \approx L_{\text{eff}} c_{\max}$ . Equally, using the Gauss theorem,  $|o| = (\epsilon_*/4\pi)(|\partial\Phi/\partial x|_{x=0}) | \approx (\epsilon_*/4\pi)\{[(k_B T/e)|u|]/L_{\text{eff}}\}$ . Equalizing these two expressions for  $|o|$ ,  $(\epsilon_*/4\pi)\{[(k_B T/e)|u|]/L_{\text{eff}}\} = L_{\text{eff}} c_{\max}$  we get

$$L_{\text{eff}}^2 \approx \frac{\epsilon_* (k_B T/e)|u|}{4\pi c_{\max}} = \frac{\epsilon_* k_B T}{8\pi c_0 e^2} \frac{2c_0|u|}{c_{\max}} = L_D^2 \gamma|u| \quad (21)$$

i.e.,  $L_{\text{eff}} \approx L_D(\gamma|u|)^{1/2}$ , which, to the accuracy of the factor  $\sqrt{2}$ , coincides with the limiting law of the mean field theory. In other words

$$C \propto |u|^{-1/2} \quad (22)$$

is the universal, model independent law imposed by the overall conservation of charge.

From here it follows that the capacitance at the wings must weekly depend on the temperature. Indeed

$$C \approx \frac{\epsilon_*}{4\pi L_D} \frac{1}{\sqrt{2\gamma|u|}} = \frac{\epsilon_*}{4\pi} \frac{\sqrt{\epsilon_* k_B T}}{\sqrt{8\pi c_0^2} \sqrt{\sqrt{2\gamma} e^{|\text{U}|}/k_B T}} = \sqrt{\frac{\epsilon_* c_{\max}}{8\pi|U|}} \quad (23)$$

Hence the temperature dependence can enter here only through the value of  $(\epsilon_* c_{\max})^{1/2}$ . The  $\epsilon_*$  factor may have some mild temperature dependence, but the  $c_{\max}$  factor is unlikely to have it at all, so that their product, square-rooted, will have very weak temperature dependence.

#### 4.3. Notes on the Structure and Capacitance of the EDL in RTIL Mixtures with Neutral Solvents

The above-discussed conclusions about the EDL structure of RTIL will not be valid if we deal with a highly diluted solution of organic ions in organic solvents, but they should be to a high degree relevant for the case of a minor addition of the molecules of organic solvent to RTIL, the often used trick to decrease the RTIL's viscosity.<sup>13,250,251</sup>

How will adding a small amount of neutral solvents to RTIL change the structure of the EDL and affect capacitance?<sup>398</sup> From the definition of the compacity parameter  $\gamma$ , eq 14, it follows that this would strongly affect this key parameter of the mean-field theory.<sup>56</sup> Indeed, the  $c_0$  decreases with dilution, proportionally to the volume portion of the solvent component

mixed with the ionic liquid, whereas  $c_{\max}$  remains the same. This effect should tend the capacitance to change its shape from the bell like to the camel shape. We note though that in some cases the effect of dilution may be actually more complicated than just modification of  $\gamma$  because (i) the distribution of solvent molecules near the interface can be nonhomogeneous and (ii) there can be effects of specific adsorption of solvent or RTIL to the interface.

If the RTIL and the solvent wet differently the electrode surface, phase separation near the interface may take place, coupled with electric field induced wetting/dewetting transitions. Generally the ionic liquid phase should be closer to the electrode at large electrode potentials (independently of the sign) than a neutral solvent. At low voltages it all depends on the solvent, whether it wets the surface of the electrode better than the ionic liquid or not. The phenomenon of stabilization of one phase in a film near the surface phase, with other phase moved away from the surface, and the peculiar behavior of this phase separation when the system is close to the critical point is called critical wetting. It was a subject of intensive research in theoretical physics in the 80s (for a review, see ref 399).

Phase separation may take place as a first order or a second order transition. When one of the phases is stabilized near the surface, either spontaneously or with applied electric field, the thickness of the wetting layer near the critical point of the bulk solution can jump or even diverge (as in the case of the second order transition). Correspondingly sharp changes in response functions or divergences will take place when varying the temperature or electric field. In the EDL problem in liquid electrolytes, such a response function is the differential capacitance, and it may reveal singularities.

We note that similar effects have been studied a long time ago in the context of the potential induced desorption of organic molecules, replaced by water (the effects were rationalized as competitive adsorption of water, organic molecules, and ions in a two-dimensional-like compact layer of EDL); the effect formed the basis of the famous Frumkin adsorption isotherm.<sup>400</sup> Similar problems also attracted attention in the context of the structure and properties of diffuse EDL in ordinary electrolytes.<sup>401</sup> In the context of the mixture of ionic liquids with neutral solvents, ordinarily motivated by the reduction of viscosity and facilitation of migration of ions, this problem has been revisited by Szparaga and co-workers.<sup>402</sup> Using the classical density functional theory they showed that close to the critical point of the bulk solution, there indeed may be an extraordinary increase of capacitance. The authors speculate about the possible exploitation of the predicted effect for energy storage. It will be very interesting to test this prediction experimentally. Note, however, that the stored electrical energy in the capacitor is given by  $\int_{U_{pc}}^U C(U)U \, dU$ , and just one peak at a critical value of the voltage may not change the integral dramatically. We will discuss various aspects of this problem below, in the section on optimized energy storage of supercapacitors.

#### 4.4. Beyond the Mean-Field: Direct Simulations of Ionic Liquids at Electrified Interfaces

Even the most advanced theories have serious limitations due to a number of approximations behind them. The main points of concern are (i) the correct account of multibody correlations, (ii) the correct account of the effects related with the molecular structure of ions, and (iii) geometry and chemical composition of the electrode. These phenomena can

be more easily handled by computer simulations (or sometimes only by computer simulations). In turn, simulations may not intend to consider these problems in their whole complexity at once. The cleverest way would be to increase sophistication of the model step by step, in order to reveal the role of different factors.

Therefore, since the middle of the 70s researchers actively use Monte Carlo and molecular dynamics simulation methods to study structural and thermodynamic properties of molten salts in the bulk<sup>57,121,122</sup> (these early achievements were summarized in ref 403; see also ref 358). Later on, first studies appeared on the properties of molten salts and concentrated electrolytes at electrified solid interfaces.<sup>404,405</sup>

In the early simulations of molten salts at electrified interfaces, much attention was paid to the temperature dependence of the electrical double layer capacitance. Several pioneering theoretical works (based on approximate integral equation schemes)<sup>320,348</sup> in 1980s suggested that at low temperatures the capacitance first increases and then starts to decrease with the temperature. The topic was later revisited by Boda and Henderson and their co-workers who investigated in detail several model systems of concentrated electrolytes<sup>406</sup> and molten salts as well as their mixtures.<sup>407</sup> The main messages from those early works were as follows:

- The electrode/molten salt interface has a multilayer structure with several layers that penetrate to the bulk up to several nanometers from the interface.
- The effects of ion size are important.
- Mixtures (other salts, solvent, etc.) strongly affect properties of the electrical double layer.

Despite the many achievements during this first wave of interest to simulations of molten salts at electrified interfaces, the low-temperature regimes were not sufficiently explored. Partially it was due to the fact that the investigated models operated with ion sizes in the range typical for mineral salts (like alkali halides). As a result, the systems (as well as the real alkali halides) become solid at low temperatures. Partially it was also due to the high viscosity of the ionic systems and other technical problems with simulations<sup>321</sup> (see also the discussion below).

That can explain, why the bell-shape of the electrical double layer capacitance was not seen in these simulations. As we discussed above this regime is characteristic for low-temperatures and at high temperatures the capacitance becomes flat or even U-shaped.

**General Methodological Comments on Simulations of Highly Concentrated Electrolytes/Ionic Liquids.** The first works on concentrated electrolytes/molten salts already identified several general methodological problems:

- Very accurate methods for electrostatics calculations are absolutely necessary to simulate such systems; these methods (such as Ewald summation<sup>408,409</sup>) are more computationally expensive than simple cutoff methods and they require large computational resources.
- The slab geometry pertinent for electrostatic calculations for most of the electrochemical systems demands the use of the so-called 2D Ewald summation method<sup>408</sup> that is computationally expensive and poorly parallelizable (see ref 408 and references therein).
- Strong short-range correlations between the ions lead to large viscosity in these systems, and as a result, increase

the sampling/simulation time as compared to neutral liquids.

- Due to the highly pronounced interfacial oscillations, a relatively large distance between the electrodes is necessary to achieve bulk-like regime in the middle of the simulations box, which increases the size of the simulation cell.

We also note that incorporation of the polarizability of electrodes/image forces in molecular models of electrochemical interface is nontrivial and leads to significant increase of the computational time.<sup>410–412</sup>

Overall, these problems made simulations of ionic liquids a challenging task at that time, when even the fastest supercomputers had computational power not more than several Gflops (which corresponds to a typical modern laptop computer).

It has been shown that the 3D Ewald method and other 3D electrostatic methods (like, e.g., particle mesh Ewald, PME<sup>413</sup>) that are less expensive than the 2D Ewald method can be still used for simulations of a 2D slab geometry with some corrections. As such, Torrie and Valeu suggested a so-called charged-sheet correction (CS).<sup>353,405</sup> Later on, in 1999 Yeh and Berkowitz suggested another correction method for using 3D Ewald methods in slab-like geometries, 3D-EWC.<sup>414</sup>

Effects of electrostatic boundary conditions and system size on results of simulations of interfacial properties in aqueous electrolyte systems were thoroughly investigated by Spohr. In ref 415, he showed that appropriate long-range corrections are mandatory for simulations of interfacial properties of electrolyte solutions. Indeed, the existing truncation schemes lead to unphysical electric fields in the solution, which prevent the formation of a “bulk” region in the simulation cell. Later on Henderson and co-workers investigated both CS and 3D-EWC corrections in refs 416 and 417 in a view of applications to concentrated electrolytes and molten salts. These works identified several problems associated with using CS for the approximation of long-range forces in the X and Y directions in electrolyte systems with high particle density. In turn, ref 416 showed that in 3D-EWC there is no abrupt minimum image discontinuity in the x and y directions, and therefore the system size effect gets much smaller, as compared to the CS method. Thus, ref 416 concluded that 3D-EWC is preferred over CS for use in simulations with high particle density. Overall, Spohr recommended to use the 3D-EWC correction rather than the CS despite the fact that 3D-EWC is more computationally demanding.<sup>415</sup> Till now, the 3D-EWC is the most accepted technique in this field.

Today, one can roughly classify direct simulation models for modeling ionic liquids into two main categories: simple models (also referred as “coarse grain” models or “toy models”) and molecular models (also referred as “atomistic models”).

The simple models operate with a coarse-grain representation of the ion and solvent molecular structure. The molecular models use more sophisticated atomistic description of molecular structures of the electrolyte components, sometimes in its full chemical complexity. The exact borderline between these classes of models is somewhat arbitrary. Indeed, even simple spherical models of ions can be a good quantitative approximation for monatomic molten salts systems (e.g., molten alkali halides). On the other hand, even fully atomistic models of classical molecular mechanics are “force-field”-sensitive and do not reproduce all features of the systems (e.g., charge transfer, electron distribution and polarizability,

chemical reactivity, etc.; to model these phenomena more sophisticated quantum mechanics models are necessary).

#### 4.4.1. Course-Grained Models: Forest Behind the Trees.

*Overscreening vs Crowding Physics.* The mean-field results published in ref 56 were beneficial for explanations of (somewhat puzzling) experimental capacitance curves in RTILs that do not display the Gouy–Chapman-like U-shape<sup>418–424</sup> (some of these experimental works will be discussed in details below). However, it was clearly underlined in the same paper<sup>56</sup> that the strong Coulomb correlations at the nanoscale<sup>60</sup> in such a dense “ionic plasma” as RTILs should inevitably make the mean-field unreliable at least in some range of potentials.

The questions, (i) what is this range, (ii) what are the features of the simple mean-field theory that will retain after a more sophisticated analysis, and (iii) what will be the new features coming from those Coulomb correlations, remained to be answered.

The motivation for that quest had several reasons. First, it was known from theory and computer simulation of molten salts that electrostatic potential as well as the charge density near a mildly polarized electrode oscillates, exhibiting the above-mentioned phenomenon of overscreening.<sup>321,355,355,425–428</sup> Similar effects were expected to be seen for RTILs, the more so that first molecular-scale computer simulations of interfacial behavior of RTILs have shown decaying oscillation potentials at interfaces.<sup>429–432</sup> Second, there were structural experiments for concentrated electrolytes in the bulk<sup>281,433</sup> and first-generation RTIL (ethylammonium nitrate).<sup>433</sup> They all showed oscillating structures in very concentrated electrolytic solutions. Third, oscillating potentials and charge distributions were well established in dipolar liquids (such as water),<sup>434–438</sup> plasmas, charged colloidal suspensions, and similar kinds of “Coulomb” liquids;<sup>60</sup> these oscillations caused by proximity of positive and negative charges were also to be expected for RTILs (a series of recent experiments by different surface-specific techniques have shown that, indeed, charge density distributions oscillate in RTILs at interfaces<sup>285,337,340,342,343</sup>). Last but not least, the capacitance predicted by the mean-field theory seemed to be too large at small electrode potentials as compared to the experimental values indicating that there is something missing in the mean-field theory, at least in that range of potentials.

As a result, the recent wave of interest to coarse-grained simulations of RTILs at EIs<sup>52,391,396,439–445</sup> was to our opinion triggered by several factors: (i) the increased number of applications of different RTILs demanded development of toy models that could capture main trends in the RTIL behavior at EIs; (ii) as summarized above, there was a list of fundamental questions about the behavior of RTILs at electrified interfaces that were poorly understood and required to go beyond simple theories (see also ref 56); (iii) the computational power of supercomputers increased and access to high performance computing facilities became easily available for wide circles of researchers.

Moreover, coarse-grained models of RTILs provide input for advanced theories<sup>446–452</sup> as well as classical DFT models<sup>441,453–456</sup> that recently became increasingly popular for theoretical/computational studies of RTIL behavior at flat EIs<sup>455–460</sup> as well as in porous electrodes.<sup>450,461–463</sup>

In refs 52, 391, 396, and 439 several coarse grained RTIL models of different complexity were used. The main features of these models and the main results of these works are discussed in details below. The works in refs 396 and 439 studied dense

liquid-like assemblies of spherical charged particles. The main results of these works show that

- The electrical double layer capacitance in dense ionic liquid systems has an overall bell-shaped character as a function of electrode potential, with no signs of the Gouy–Chapman behavior.
- There is substantial overscreening effect at small electrode polarizations; here the double layer in RTILs has an oscillating structure, in which counterion-rich layers alternate with co-ion-rich layers.
- Such structures are eliminated at large polarizations, replaced by the “lattice saturation” effect.

More complicated models were later used to understand the effects of nonspherical geometry of RTIL ions and the nonpolar part of the RTIL molecules.<sup>52,391</sup> The main conclusions from these works were later confirmed by more sophisticated molecular models of RTILs.<sup>254,464–468</sup>

The analysis of those effects had started first with computer simulations of a deliberately simplified system<sup>439</sup> that we briefly overview below:

Electrodes were considered as flat squares, each filled with charged spheres (spherical “atoms”) with the same intersphere distance. The partial charge of the spheres is equal in absolute value and opposite in sign on the cathode and anode, its absolute value being fixed for each simulation. By varying the partial charge of the spheres the surface charge density on the electrodes,  $\sigma$ , was varied in different simulations from 0 to 48  $\mu\text{C}/\text{cm}^2$ .

The gap distance between the electrodes was set 30 nm to avoid overlap between the EDLs of the electrodes. The substantial gap-width is necessary in such simulations to avoid the overlap of the double layers whether one expects the overscreening oscillations or the crowding regime.<sup>469</sup> Thus in a set of simulations the charge of the electrodes is controllably varied, and the potential variation across the double layers, which never overlap in such large system, as well as the overall potential drop across each of the double layers, is calculated from the simulation data.

The gap between the electrodes was filled with equal numbers of RTIL spherical particles, cations and anions, both considered as soft charged van der Waals spheres (with only the repulsive part of the Lennard-Jones potential considered) of the same radius, 0.5 nm and charge 1e for a cation and -1e for anion; partial densities of cations and anions,  $c_+$  and  $c_-$  were the same (about 0.3 ion/nm<sup>3</sup>) giving the total particle concentration around 0.6 ion/nm<sup>3</sup>. Taking into account the actual size of the ions this concentration corresponds to the value of  $\gamma$  (see eq 14) around 0.43.

The polarizability of RTIL species was implemented in this model in a crude way by scaling the charges in the model by an effective factor  $1/\sqrt{2}$ . A similar approach was later used in other works on coarse-grained<sup>278,396</sup> and nonpolarizable atomistic RTIL models<sup>240,470</sup> as an easy way to take into account the polarizability of RTIL molecules.<sup>471</sup> Simulations themselves used periodical boundary conditions in the lateral dimension and perpendicular to the electrodes with 15 nm of an empty space till the next pair of electrodes (necessary for correct use of the 3D-EWC correction<sup>414</sup>); standard molecular dynamics with Gromacs MD software<sup>472–475</sup> were used. Because such an idealistic symmetric system freezes much easier than the ionic liquids composed of real ions, the temperature in the simulation was elevated and kept at  $T = 450$ .

Such an approach ignored all the effects of the polarizability of real conducting electrodes (image forces), as well as attractive van der Waals forces between the RTIL ions (such effects have been considered in later works), but the task of this study was to reveal the effects of Coulomb correlations in its pure form, and the results<sup>439</sup> were lessening.

The potential profiles, reproduced in Figure 5, show sharp decaying oscillations with at least five visible peaks. We note

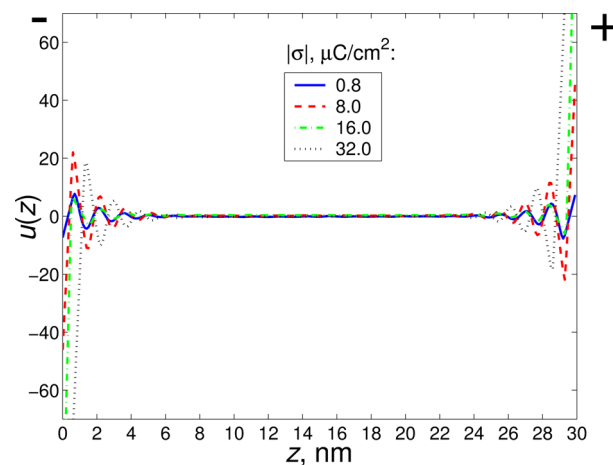


**Figure 5.** Simulated<sup>439</sup> profiles of dimensionless potential  $u(z) = eU/k_B T$  ( $z$  is the direction perpendicular to the electrode planes), between the cathode (left) and anode (right). Note that for the temperature of the simulation,  $k_B T/e = 38.8$  mV. For the symmetric systems used in that work (cations and anions distinguishable only via their charge) the profiles on the two electrodes are (anti)symmetric to each other. Reprinted with permission from ref 439. Copyright 2008, Elsevier.

that such oscillating patterns at the RTIL/EI interface, although for a smaller system with overlapping double layers, have been published earlier by Pinilla et al. for a molecular model of selected RTIL.<sup>432</sup> However, what can one learn from such figures? To answer this question the following analysis has been performed. Exploiting the symmetry of the system, the liquid slab between the electrodes was split into a set of slit “bins”, each  $i$ th bin having the same width, only slightly larger than the diameter of the ions (subject to the density of the liquid). In each bin the average charge of cations and anions per unit surface area was calculated, scaled to the absolute value of the charge of the corresponding electrode (due to the symmetry of the system the charts are mirror images of each other at the cathode and the anode). Such charts for the anode are reproduced in Figure 6.

This figure demonstrates a dramatic overscreening effects at small and medium electrode polarization. In the upper left corner (charge density of the electrode equals to 0.8  $\mu\text{C}/\text{cm}^2$ ) we see that the first bin has approximately 2.5 larger counter charge than the charge of the electrode. Increasing the charge of the electrode 10 times, upper right corner, the first bin delivers 1.4 times larger counter charge than the charge of the electrode. But then this 40% positive charge excess is overscreened in the next layer by 60% of negative charge. For even higher charge density, 16  $\mu\text{C}/\text{cm}^2$ , lower left corner, there is almost no room in the first layer to overscreen the charge of the electrode of that surface charge density. There is, perhaps, only 5% overscreening, and this excess is dramatically overscreened, as it should be, in the next layer by a 20 times larger charge than that minute charge

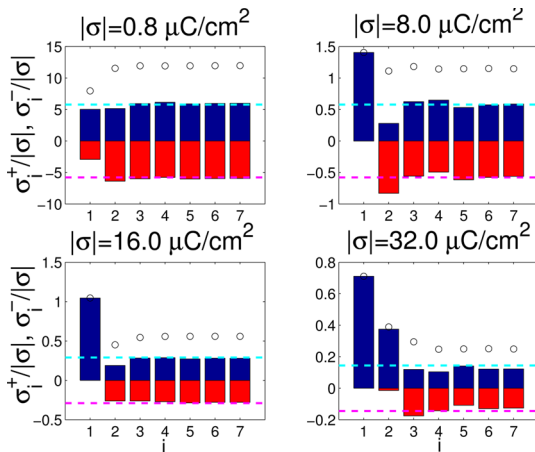


**Figure 6.** Partial charge densities per unit cross-section area in the first 7 monolayers of ionic liquid ions near the cathode, scaled to the absolute values of the surface charge density of the electrode,  $|\sigma|$  (for a reference:  $1\text{e}/\text{nm}^2 = 16 \mu\text{C}/\text{cm}^2$ ). Blue bars correspond to cations, red bars to anions. The corresponding numbers for the scaled partial charge densities per unit cross-section area in the bulk for cations (cyan) and anions (magenta) are shown by horizontal lines as a guide for the eye. The figure is reprinted with permission from ref 439. Copyright 2008, Elsevier.

difference. Only when we further increase twice the charge of the electrode (the lower right corner) we see the onset of the lattice saturation: there is room to accommodate only 70% of the net counter charge in the first layer (cations only). The next layer, however, endorses slightly more than 30% of the missing balance showing yet some overscreening. Had one plotted the results for even higher charges, one would have presumably encountered with more pronounced lattice saturation, when more successive layers would have been dominated by ions of the same sign.

We went through this analysis in such detail, first of all because the overscreening patterns is actually what distinguishes the real double layer structure in RTILs from the behavior predicted by the mean field theory. Another reason is (as we will discuss later) that the oscillating overscreening profiles may play crucial role in electrode kinetics when using RTILs as “solvents” for the reacting ions.<sup>428</sup>

The main lesson from this analysis is that at small electrode polarizations the overscreening effect is maximal. With increase of the absolute value of the electrode charge, i.e., voltage drop across the double layer, overscreening is gradually replaced by crowding of ions of the same sign (lattice saturation) described by the model-independent limiting law (see section 4.2 above); simulations reproduce the tendency to reach the limiting law, eq 22.

The EDL differential capacitance calculated from the simulation data<sup>439</sup> has a bell shape that correlates very well with the predictions by the mean-field theory<sup>56,476</sup> for the estimated value of compacity  $\gamma \approx 0.43$  for the system (that is higher than  $1/3$ ); however, due to the integral effect of overscreening a substantial reduction of the capacitance value was observed compared to the one given by the mean-field theory.

In ref 396 the same analysis has been performed for ions modeled by spheres of different size: cations twice as large as the anions. As the general arguments would suggest (cf. the consequence of eq 19, discussed in section 4.1), the curve should shift to positive potential, the positive wing lying higher

than the negative wing. This is exactly what has been observed in Figure 1 of ref 396. Because of the “proper” asymmetry of the curve that paper is somewhat more often quoted, than the, perhaps, more fundamental ref 439.

Further insight into the generic structure of the double layer in RTIL was given by a toy model of ref 391 which used the same class, “bead” type of models. There anions remained to be spherical beads of a defined size, but several cases of different cations were separately considered: (i) cations made of beads of the same size as anions, (ii) cations modeled as dumbbells in which one of the beads is charged and the other one is neutral, and (iii) cations modeled as triple-bead structures with one bead charged and two neutral. That was the way to capture the generic effects associated with anisotropy of the shape of RTIL ions and unequal intramolecular charge distribution. The neutral beads were imitating “fatty” neutral counterparts (“tails”) typical for many RTIL cations. The density of the mixture was relatively large and so was the value of the compacity,  $\gamma$ .

Using these three models of cations, a bell shape capacitance was recovered for one bead model but a camel shape for both two- and three-bead models (see Figure 8). The latter was shown to be a consequence of the following effect: the neutral beads play the role of latent voids that can be replaced by charges thereby allowing to increase the local concentration of charges providing the growth of capacitance at small and intermediate voltages. This is schematically shown in the cartoon of Figure 7; in ref 391, this picture is justified by the

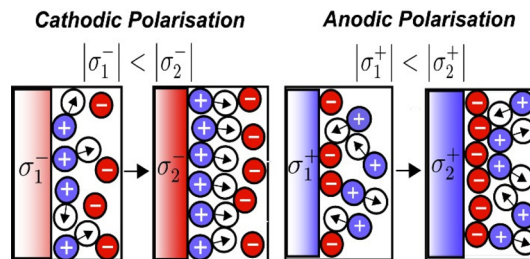


**Figure 7.** Cartoon showing how (i) increasing negative (cathodic) polarization of the electrode, the neutral tails of cations are got expelled from the electrode vicinity, in favor of the charged cation heads, and (ii) increasing positive (anodic) polarization the neutral tails are expelled in favor of anions. The figure is reproduced with permission from ref 391. Copyright 2010, Elsevier.

plots of the distribution of the neutral beads near the electrode surface as a function of the charge of the electrode. More details revealed by this model are presented in ref 52. For instance it has been shown that the onset of the lattice saturation manifested in the inverse-square-root capacitance scaling is shifted toward higher negative potentials for cations with longer tails.

It is important to emphasize that had the compacity,  $\gamma$ , been sufficiently small in these simulations this would have inevitably led to the camel shape even for the one bead model. Thus the conclusion of refs 52 and 391 must not be misinterpreted (as, e.g., it was in ref 460). In fact, the camel shape is not exclusively conditioned by the existence of neutral tails of ions. As mentioned, the latter simply play the role of latent voids, allowing for a compression of the charge even in a very dense liquid. Free voids, if in abundance, or a sufficient amount of solvent will do this even better: they will cause the capacitance to display the initial Gouy–Chapman-like at small voltages

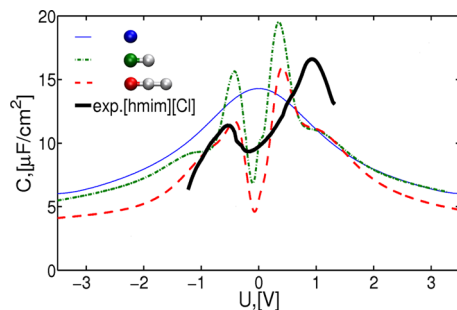


**Figure 8.** Differential capacitance simulated in ref 391 for the electroneutral mixture of charged beads, with single bead anions, and single-, double-, and triple-bead cations where only the colored beads are charged, the gray beads representing neutral tails of cations. The black solid line shows an experimental capacitance curve from ref 424. The figure is reproduced with permission from ref 391. Copyright 2010, Elsevier.

changed by the saturation wings at large voltages overall warranting the double hump camel shape (see also discussion above in section 4.3).

With an intention to build a phenomenological theory that will incorporate ion exclusion effect and strong short-range-Coulomb correlations, Bazant et al.<sup>389</sup> have constructed a phenomenological free energy functional. It reflects the latter correlations through a term providing a propensity for oscillating profiles in the charge and potential distribution near the interface (in the spirit of the work of Santangelo<sup>477</sup>). At the same time, it incorporates the exclusion-volume effect through the lattice gas type entropy (in a simplified form, as used in ref 56). The analysis of this model that could be performed to a high degree in analytical terms, has shown the interplay between overscreening and crowding, showing how the former has got destroyed by large external fields (electrode polarization) in favor of lattice saturation. The inverse square root law for capacitance was recovered only at very large electrode polarizations; interestingly an intermediate asymptotic law of slower capacitance decay, was revealed at intermediate voltages. With essentially just one fitting parameter (the correlation length standing as a coefficient in the term favoring the oscillating patterns) this theory, continuously covering both the overscreening and covering regimes, almost quantitatively reproduced the simulations of ref.<sup>439</sup> This was an unexpected success, and encouragement for developing more sophisticated theories.

Recently Demery et al.<sup>478,479</sup> reported a Coulomb gas model that has allowed them to obtain an exact solution of the problem of the double layer near the charged electrode, however, under one condition: the model is one-dimensional. That means that all the properties of each ionic layer near the surface were averaged in the plane parallel to the interface. Each layer was represented by a point on a 1D lattice, which could be occupied with a spin  $s = 1$  (cations),  $s = -1$  (anions), and  $s = 0$  (voids or neutral molecules, if the ionic liquid is not pure but has “solvent” additives.). The 1D model is an abstraction though, because it implies that that if  $s = 1$  the whole layer is composed entirely of cations,  $s = -1$  of anions and  $s = 0$  will be a layer of neutral molecules, or even worse than that: voids. However, exactly solvable models in statistical mechanics are rare and therefore are of great value, as they allow to get results free of any approximations. Coulomb interactions in 1D are  $\propto i - j$  where  $i$  and  $j$  are the indexes of the sites. No screening of

these interactions is imposed; it emerges as a result of the solution of this many-body problem.

Arsenal of modern methods of statistical physics was invoked to get an exact solution of this model. The results of refs 478 and 479 can be summarized as follows: (i) Overscreening is a typical feature for the potential and charge density distribution. (ii) The overall shape of the EDL capacitance–voltage dependence has a bell-like center-line curve for the small number of voids (large compacity/packing fraction) and the camel-like one for a large number of voids (small compacity/packing fraction); both shapes are close to those predicted by the mean-field theory. (iii) Observed systematic oscillations of the capacitance around this centerline at large values of compacity/packing fraction at low temperatures are the feature of this solution; each peak representing the voltage induced swapping of the sign of the charge of the consecutive layers. Obviously this structure, exhibiting many peaks is an artifact of the 1D model, in which each layer must be composed of identical ions. Nevertheless this solution is valuable as it is, as it rigorously proves the emergence of overscreening as a result of Coulomb correlations. We also note that while the temperature increases, the large oscillations of the exact solution in ref 478 gradually disappear and the shape of the capacitance approaches the mean-field results of ref 56 discussed in section 4.1.

All in all, both overscreening and lattice saturation in ionic systems of such density as in RTILs seem to be established facts. The physical nature of the lattice saturation is straightforward: counterions have no room to accumulate in one layer and they start to line up, forming a queue in front of the electrode, increasing the thickness of the double layer and thereby decreasing the capacitance. The nature of the overscreening is less obvious. There were many debates about it in the context of dipolar liquids such as water, where overscreening is the typical feature of the dielectric response of the liquids.<sup>434,435,437</sup> The rationale of this phenomenon is as follows. There is a strong motif for charge alternation in dense ionic (or zwitterions/dipolar) systems with a wavelength comparable with the nearest neighbor distance between oppositely charged entities. Small charge on the electrode cannot change this propensity and the charge distribution will oscillate with that wavelength. However to conserve the charge the net charge, in the double layer must be equal (with an opposite sign) to the charge on the electrode. It is a simple mathematical exercise to show that overscreening is a prerequisite for satisfying simultaneously the two requirements.

**4.4.2. Forest Is Made from Trees—From Physics to Chemistry: Fully Atomistic Models.** “There could be no theory of liquids because every liquid will have to be described by its own theory.” This sentence is often attributed to theoretical physicist Landau. We could not find documented records of this saying, propagated by a word of mouth. However, fortunately, the conservative opinion of one of the most bold and innovative theorists of the 20th century (who had published ground-breaking works not only in pure physics but also in physical chemistry and chemical physics, see ref 480) was not shared by everyone in the theoretical community. The theory of liquids had been actively developed during the last century starting from the pioneering work of Ornstein and Zernike<sup>481</sup> followed by fundamental contributions of Frenkel,<sup>482</sup> Yvon,<sup>483</sup> Bogolyubov,<sup>484</sup> Kirkwood,<sup>485,486</sup> Born and Green,<sup>487</sup> and many others (for the history of the subject see, e.g., refs 488 and 489).

The theory of liquids started systematically from the theory of simple liquids, such as liquid noble gases or liquid metals.<sup>488,489</sup> Within each of the two classes, there was no need to build for every particular substance “its own theory”. What it required, was heuristic assumptions on the closure of an infinite chain of nonlinear integro-differential Bogolyubov–Born–Green–Kirkwood–Yvon (BBGKY) equations<sup>483–485,487</sup> that could be in principle verified by comparison with computer simulations or various scattering experiments.<sup>489</sup> Taking-off from the classical works on simple liquids the theory moved to simple dipolar fluids and then to more complicated, hydrogen bonded liquids, such as water and alcohols and then even to complex fluids (for an overview see refs 488–491). Different advanced methods were developed such as the Reference Interaction Site Model (RISM) for homogeneous<sup>492–495</sup> and inhomogeneous<sup>496</sup> liquids, complex bridge closures of extension of the nonlinear integro-differential equations for the correlation functions<sup>497–500</sup> or approximations for free energy functionals<sup>501,502</sup> in the classical DFT.<sup>503–505</sup> The theories were originally targeted to describe equilibrium properties but later were expanded to describe liquid dynamics.<sup>506–508</sup> Most importantly, certain routines for building these closures or the forms of DFT were developed, linked to the molecular structure of the liquids.<sup>509,510</sup>

Is the situation with RTILs different, where we can potentially deal with an unlimited number of liquids? Must every ionic liquid have its own theory? There is not enough history of RTIL-focused research in the theory of molecular liquids to answer this question unambiguously. It is clear, however, that the main principles of building approximate bridge functions in molecular theories as well as forms of classical DFT theory can be applied to various RTILs, based on understanding of atomic/electronic structure of the ions (see, e.g., the pioneering work of Malvaldi et al. on modeling solvation effects in methyl–methylimidazolium chloride by a combination of quantum DFT with three-dimensional RISM<sup>511</sup>); however, as in the case of simpler liquids, those approximations must be checked via diffraction experiments and/or computer simulations taking into account effects of spatial heterogeneity in RTILs at the microlevel.<sup>228,512–515</sup> The situation with dynamics is less clear due to slow relaxation processes and mysterious glassy-like mesophases in RTILs,<sup>198,516</sup> posing questions, whether one can ever reach equilibrium simulating RTILs.

We note that molecular theories were successfully applied to different kinds of EIs with polar solvents and diluted electrolytes, from flat solid/liquid interfaces<sup>449,517–519</sup> to electrolyte solutions sorbed in nanoporous carbon electrodes.<sup>520,521</sup> However, somehow, in the double layer theory of RTILs the progress on developing molecular-scale theories was not that advanced. In our opinion, this is partially due to the relatively short history of the subject and partially due to an easy access to supercomputer resources these days and a number of well-developed molecular modeling packages available for researchers. Therefore, in view of the first model theories, which bypassed the level of sophistication of the description of ordinary liquids, the next step was to proceed straightforwardly to computer simulations that use sophisticated models of ions of RTIL, i.e., realistic force-fields representing interionic interactions. Indeed there are many phenomena (e.g., ion interfacial orientation) that require more detailed description of molecular structure of RTIL ions than it is provided by the coarse grain models. Generally, the response of

real RTILs to the electrostatic field of the electrode is affected by rearrangements of nonspherically shaped ions and more complex structure of force fields acting between them. Every ionic liquid is then expected to display “individual” EDL structure and capacitance features.

However, most of the generic qualitative effects discussed in the previous sections have been reproduced in those computer simulations. Furthermore, by comparing the results with the above-described “physical” toy-model simulations, those “molecular” simulations were able to reveal, which features of EDL are generic and which are specific for particular liquids.

Due to various interesting molecular-scale phenomena in RTILs at EIs and their importance for different applications there has been published a considerable number of molecular simulations works in the area during the last several years.<sup>254,431,432,465,466,522–538</sup> Molecular modeling techniques were used to study not only neat RTILs at different EIs but also behavior of RTIL mixtures with polar solvents.<sup>251,539–542</sup> We have opted to discuss here in details only some of the molecular simulation papers, most closely related to the main line of this article. For a more general and detailed overview of recent developments in this field we address our readers to the recent review article by Merlet et al.<sup>543</sup>

The role of surface chemistry has been emphasized in the study of Feng and co-workers,<sup>467</sup> who have studied the properties of [BMIm][NO<sub>3</sub>] confined between oppositely charged walls, each imitated by  $\alpha$ -quartz like slabs oriented in [100] direction. The distance between the walls was substantial, 6.63 nm for the EDLs on the opposing electrodes not to overlap, so that unlike the pioneering paper of the Belfast group<sup>522</sup> in which the ion distribution profiles of [MMIm]Cl were studied in a much narrower gap (that led to a partial overlap of the cathodic and anodic EDLs), Feng et al.<sup>467</sup> were able to study the properties of individual EDLs. They performed simulations for different fixed charges on the wall. The proximity to chemical reality in that work was not through the description of electrodes but through the force-fields-based description of the liquid.

Feng et al. showed local density of ions depicting the localization of the center of imidazolium ring for cations and the geometrical center of the anion. When increasing surface charge positively, they saw a dramatic increase of the density of [NO<sub>3</sub>]<sup>–</sup> ions near the electrodes. Simultaneously they see a significant accumulation of [BMIm]<sup>+</sup> ions in the “next” layer. However, since the cations are larger than anions, these two first layers partially overlap. Overall the authors see several layers both of cations and anions. Polarizing the electrodes negatively the two (overlapping) layers swap. With further increase of negative polarization the maxima in the cationic density profiles, move away from the first peak, at the cost of the increase of its height; the first peak for anions substantially moves away from the surface, but more distant peaks are only slightly affected. Interestingly, the first peak moving away becomes in the end higher. The analysis of overscreening (using diagrams of the kind suggested in refs 391, 396, and 439) was not performed here, but such character of the curves is typical for overscreening. In addition they have encountered with the phenomenon, already noticed in the simulations of ref 432: [BMIm]<sup>+</sup> cations are persistently adsorbed on the surface; their presence in the first layer is substantial even for mildly positive electrode polarization. The authors explain these effects by enhanced van der Waals attraction between the cation and the electrode, much less pronounced for anions. Differential

capacitance here was rather featureless, constant for cathodic polarization and growing monotonously in the anodic range.<sup>544</sup>

Lynden-Bell et al.<sup>254</sup> studied the same [MMIm][Cl] but in a wider gap and analyzing the EDL molecular structure in detail. In addition to some findings potentially important for electrode kinetics in RTILs (that we will touch later in the review), they have obtained a number of results that are similar to those of Feng et al.<sup>467</sup> Namely, they detected significant changes in the structure of the ionic profiles as a function of electrode charge. They found that with positive charging of the electrode, anions substitute cations in the first layer that at neutral polarizations are preferentially adsorbed; at negative charges the anions are expelled from the first layer to form a new second layer. The cations in the first layer at low electrode charges are oriented predominantly parallel to the electrode surface (similar observations one can find in the simulation data of Feng et al.<sup>467</sup>). However, at high negative charges they tend to orient perpendicular to the interface, maximizing the density of ions in the first layer. They found clear signatures of overscreening in their system. No capacitance data were reported in their paper to compare with those puzzling data of Feng et al.<sup>467</sup>

Vatamanu et al.<sup>466</sup> performed molecular dynamic computer simulations of EDL structure and capacitance for [PMPyr]-[TFSA] near a graphite electrode. Although the electrode was not described in the most primitive way, through a system of fixed charges (the electrode polarization was evaluated by minimizing the total electrostatic energy with respect to electrode charges, each graphite electrode consisting of three graphene layers), this approach could not incorporate the true electronic structure of a semi-infinite semimetal electrode, i.e., to involve into the simulation the EDL in the graphite. We, thus, temporarily, put away Gerischer's concerns,<sup>362,363</sup> focusing now only the findings of this team about the EDL on the RTIL side. The calculated capacitance in that work has a camel shape structure, except for very high temperatures where the two maxima essentially merge (Figure 9). Within the

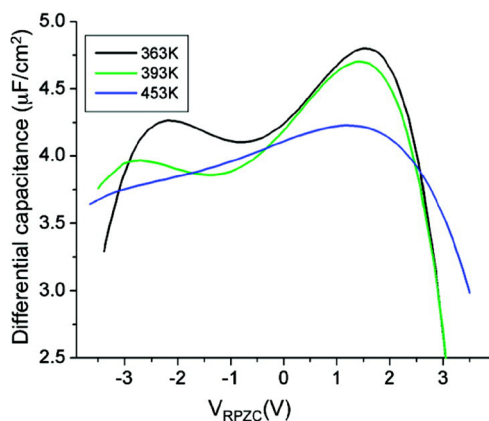


**Figure 9.** Differential capacitance of EDL in [PMPyr][TFSA] simulated in ref 466. Reprinted with permission from ref 466. Copyright 2010 American Chemical Society.

studied broad range of potentials ( $-3.5\text{V} \leftrightarrow +3.5\text{V}$ ) the lattice saturation regime, where  $C \propto |u|^{-1/2}$ , has not been reached, the capacitance was falling off steeper. A greater structure in the charge density profiles is observed at the positive electrode (the EDL is more compact, and this is reflected in the higher value of capacitance), as compared to negative electrode. The paper shows the density profiles for cations and anions as a function

of their position to the electrode at different voltages. An innermost layer is seen 4–5.3 Å away from the interface, an intermediate layer at 5.3–7.5 Å, and the third layer at 7.5–9 Å. At potentials near pzc, the cation and anion populate both the first and intermediate layers, with the majority of ion centers located in the intermediate layer. This distribution changes with increasing electrode potential, positively or negatively: the co-ion distribution in the first layer decreases and the co-ion in the intermediate layer initially increases, but only up to 1 V voltage variation (simultaneously, the counterion population in the intermediate layer decreases). At larger electrode potentials, positive or negative, the density of co-ions in the intermediate layer decreases, increasing in the third layer. These are typical signatures of overscreening, although the analysis of it in terms suggested in refs 396 and 439 has not been performed. In the next paper<sup>465</sup> the same group extended their investigation to [PMPyr][FSI] comparing their results with those of [PMPyr]-[TFSA].  $[\text{FSI}]^-$  is a more compact molecule than  $[\text{TFSA}]^-$ . Correspondingly, with electrode polarization, the density profiles of counterions showed a stronger increase of the first peak and the sharpening of their overall distribution, while the co-ions move out of innermost layer of EDL. The first peak of  $[\text{PMPyr}]^+$  moves closer to the electrode, as the potential becomes more negative, whereas the position of the first peak of the  $[\text{FSI}]^-$  does not significantly change with the increase of the positive potential. More subtle details are revealed in the paper including the distribution of orientations of ions relative to the surface as a function of electrode potential, that demonstrated substantial differences between  $[\text{FSI}]^-$  and  $[\text{TFSA}]^-$ . Remarkably, in that work the authors went to much higher electrode polarizations in order to check both for  $[\text{TFSA}]^-$  and  $[\text{FSI}]^-$  cases the existence of the “crowding law”: the inverse square root dependence for capacitance,  $C \propto |u|^{-1/2}$ . They found this regime but only for unrealistically high voltages, about 15 V (achievable in simulations but not experiments). Close below those voltages they found the crossover between overscreening and crowding. Of course, this is a purely academic investigation, because the decomposition of RTILs starts at about 3 times lower voltages. Similarly to Georgi et al.,<sup>391</sup> Vatamanu et al. found the neutral groups of ions pointing away from the surface at large potentials, but they see it at much higher potentials than in ref 52. The authors explain this difference by the need to assume a stretched tail conformation first, needed to repel neutral tails from the surface, which requires higher voltages; no estimates were given, however, how large voltage it would take, to substantiate this interpretation.

A recent paper by Paek et al.<sup>545</sup> reported MD simulations of the EDL and interfacial capacitance at the interface of [BMIm][PF<sub>6</sub>] with a graphene plane. The EDL properties on the liquid side appeared to be qualitatively similar to the conclusions of other studies of this kind as discussed above. However a dramatically new element of that work was taking into account the quantum capacitance of graphene together with the EDL capacitance of the liquid half-space. This was essentially a development of the Gerischer's ideas,<sup>362,363</sup> who related the capacitance of a semi-infinite graphite with the electronic density of states and the Fermi-distribution in graphite. In ref 545 this has been done for a two-dimensional graphene for which the dependence of the density of states on electric field is different from graphite. The quantum capacitance of graphene in the work of Paek et al.<sup>545</sup> was found to be (i) smaller than the capacitance of the EDL in the

liquid half-space and thus determining the overall capacitance of the two capacitors in series and (ii) of U-shape. Having found a clear bell-shaped capacitance for the EDL in the liquid, the authors nevertheless obtained a U-shape-like result for the total capacitance because the shape of the capacitance curve is dominated by the contribution from the graphene electrode. The results of this computational study correlate well with the recent experimental work by Uesugi et al.<sup>377</sup> where different contributions to the EDL capacitance of the graphene–RTIL ( $[\text{BMIm}][\text{PF}_6]$ ) interface were measured. We thus witness how the pioneering Gerischer's idea takes-off in the graphene era.

In continuation of that line of thought, the effect of field penetration into the carbon type electrodes was recently investigated in ref 546, where the DFT of Luque and Schmickler<sup>365</sup> for graphite electrode was combined with the mean-field theory of the double layer on the RTIL side of the contact.<sup>56,476</sup> The results have shown that at small voltages the curve should take a U-shape, independently of the value of RTIL's compacity  $\gamma$ , being dominated by the electronic double layer in carbon, as being smaller than that of the RTIL. Only with the onset of the "lattice-saturation" in RTIL when the double layer capacitance in RTIL substantially diminishes, the capacitance of the RTIL side will dominate and the wings of the overall capacitance will start decreasing. As a result, the model predicts not exactly a U-shape but rather a "seagull-wings" shape whereas the experimental data of ref 423 look more U-like.

Such crude estimates<sup>546</sup> may still capture the main trends. Indeed, in the voltage range where the mean-field theory works the worst, i.e., at small voltages (as it missed to cover there the overscreening effect), the capacitance is determined by the electronic double layer in graphite. In the range of large voltages, where the mean-field theory of the double layer in RTIL becomes more accurate, the latter determines the result. The main inaccuracy thus lies in the range of intermediate voltages. Of course, this study is only a first step, and the combination of the DFT theory with molecular dynamics simulations of RTIL (either coarse-grain or atomistic) will be the natural next step in extending the Gerischer's idea to carbon electrodes in contact with ionic liquids.

## 5. EXPERIMENTAL STUDIES OF EDL IN RTILS AT FLAT ELECTRODES

### 5.1. EDL Capacitance

Before 2000, to the authors' knowledge, the only two reports on the EDL capacitance in RTIL were two sets of curves for the salts based on a mixture of aluminum chloride with 1-butylpyridinium<sup>107</sup> and 1-ethyl-3-methyl imidazolium cation  $[\text{EMIm}]^+$  and  $[\text{TfO}^-]^- = \text{CF}_3\text{SO}_3^-$ ,  $[\text{Me}]^- = (\text{CF}_3\text{SO}_2)\text{C}^-$ ,  $[\text{Im}]^- = (\text{CF}_3\text{SO}_2)\text{N}^-$  anions<sup>418</sup> (in both studies a mercury electrode was used). Then in 2003 the group of Mao reported the capacitance curve for a nonchloroaluminate RTIL,  $[\text{BMIm}][\text{BF}_4]$ .<sup>419</sup> All capacitance curves reported in these works have little in common with Gouy–Chapman shapes but these publications, although pioneering, remained a scientific curiosity before the feature article<sup>56,476</sup> addressed attention to the fact that the EDL capacitance in RTILs should look different from that in diluted electrolytes and the concepts of bell and camel shape were suggested to the ionic liquid electrochemists. Since 2007 several experimental groups started to publish data on EDL capacitance in various

RTILs.<sup>63,71,75,420–424,547–552</sup> We cannot review all of them here but stop on few milestones.

Systematic studies were undertaken by the group of Ohsaka,<sup>420–423,547–549</sup> take alone ref 423 in which the authors compared systematically their experimental data for a set of RTILs based on combinations of cations and anions shown in Figure 10 (and few others) at different electrodes.

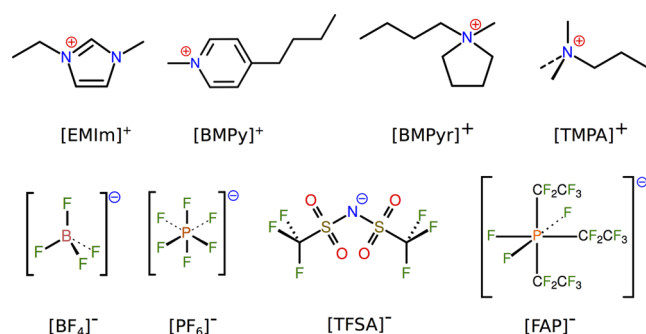


**Figure 10.** Cations and anions selected in ref 423 for capacitance studies of RTILs at different electrodes.

That work has classified different types of capacitance curves observed, most of which were either of bell or camel shape; below, we reproduce the pertinent columns of the summary in Table 2.

We note that U-like shapes were obtained on glassy carbon (GC) electrode (see Table 2). Gerischer's concerns<sup>362,363</sup> about a possibility of extracting information on the EDL in the liquid phase, whereas they in fact may refer to the electronic EDL on the electrode side, may be applicable to these measurements. However, the same glassy carbon electrode exhibited in another RTIL a camel shape. It is difficult to diagnose unambiguously, why some of the electrode/electrolyte combinations deliver a camel- and some a bell-form, because we do not know the real compacities of these RTILs. Those are difficult to estimate using the available theories due to the complex shapes of the ions (developing techniques for reliable estimation of real compacities is in progress). On the other hand the  $[\text{EMIm}]\text{Cl}$  camel shape data well corresponds to the capacitance curves of model ionic liquids with neutral tails calculated in ref 391. However, some other of the considered cation–anion pairs although also having neutral tails still bring bell shapes of the capacitance. Analysis of the data at the wings (see the inset in Figure 11) encouragingly supports the lattice saturation limiting law; however, it seems to begin "too early" compared to the theoretical and computational results discussed above: indeed, so far no theory, and the more so no simulation predicted it for such small voltages. The molecular force-field computer simulations, as discussed above, were supposed to bring more light on the reported features, but perhaps more systematic variations, i.e. within the similar sorts of ions, might still be needed. A typical bell shape drawn in ref 423 is reproduced below in Figure 11.

The group of Bing-Wei Mao performed measurements of the capacitive response simultaneously with the investigation of the structural changes of and at the interface at atomic resolution, giving new challenges for the theory. They reported capacitance data for (100) face of single crystal gold electrode<sup>553a</sup> in  $[\text{BMIm}][\text{BF}_4]$ . A distinct peak in the measured capacitance could be classified as a bell-type behavior, however in each marked sections of the curve the structure of the electrode

Table 2. Summary of the Features of the EDL Capacitance for Indicated Electrode/RTIL Combinations<sup>a</sup>

RTILs	electrodes	shape	Results Obtained From the Differential Capacitance Curves Measured at Different Electrodes in Various RTILs			
			maximum (minimum) or pzc/V <sup>b</sup>	hump/V <sup>b</sup>	C <sub>d</sub> at maximum (minimum)/μF cm <sup>-2</sup>	characteristics of the capacitance curves
[DMOA][TFSA]	Pt	bell-like	-0.2		11.4	
	Au	bell-like	-0.45	0.3	19.5	
	GC	U-like	-0.7 (minimum)		9.6	
[TMPA][TFSA]	Pt	bell-like	-0.78	-0.43	11.4	
		(camel-like)	(-0.58) (minimum)			
[BMPyr][TFSA]	Pt	bell-like	-0.87	>0	8.7	
[EMIm][BF <sub>4</sub> ]	Hg		-0.23 (minimum) <sup>c</sup>	-0.34 <sup>c</sup>	19.7	
	Au		-0.51 (minimum) <sup>c</sup>	0.45 <sup>c</sup>	12.6	
	GC	U-like	0.09 (minimum) <sup>c</sup>		12.8	
[EMIm]Cl	GC	camel-like	0.32 (minimum) <sup>d</sup>	1.0 and <0 <sup>d</sup>	23	

<sup>a</sup>Taken from ref 423 with some adaptation. C<sub>d</sub> states for differential capacitance, GC for Glassy Carbon. <sup>b</sup>Value versus Ag wire. <sup>c</sup>Value versus Ag/AgCl (solid). <sup>d</sup>Value versus Ag/Ag/RTIL.

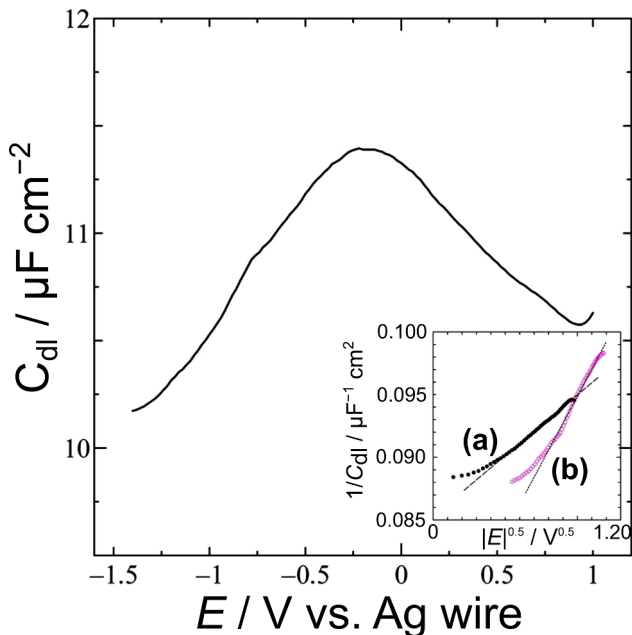


**Figure 11.** Typical capacitance–voltage curve measured at the platinum electrode in argon-saturated [DMOA][TFSA] reproduced from ref 423. C<sub>dl</sub> states for the measured double layer (differential) capacitance. Inset shows the plots of the inverse capacitance ( $\mu\text{F}^{-1}\text{cm}^2$ ) vs the square root of the absolute value of voltage drop across the EDL, in  $\text{V}^{1/2}$ , derived from the data of the (a) right and (b) left wings of the measured capacitance curve. Reprinted with permission from ref 423. Copyright 2008 American Chemical Society.

surface, studied by STM, looks different, partially related with the electric-field-induced and ion-adsorption influenced surface reconstruction of Au(100), the phenomenon intensively studied earlier in ordinary electrochemical cells with aqueous electrolytes (for a review, see ref 312). But there is in fact more to it. The work of the Mao's group revealed the richness of the structures of ions at the interface. An apparently clean bare surface of the metal is seen at -0.65 V indicating a state without specific adsorption of cations and anions. Moving the potential to -0.7 V leads to the formation of a loose layer formed by disordered adsorption of [BMIm]<sup>+</sup> cations. At higher negative potentials the latter undergoes a disorder-to-order transition, with [BMIm]<sup>+</sup> rings taking a near-parallel orientation, with a slight incline, relative to the surface.

Interestingly, ordered adsorption of [BMIm]<sup>+</sup> occurs only on Au(100) surface, but, not on Au(111). This fact reveals the necessity of some kind of structural commensurability of the surface and adsorbed [BMIm]<sup>+</sup>. The adsorption of the [BF<sub>4</sub>]<sup>-</sup> anions starts at potentials positive of -0.1 V up to 0.4 V in the form of an ordered superstructure.<sup>553a</sup> Thus, the maximum of the bell corresponds to a potential region of a crossover from anion adsorption to cation adsorption. Changes in the lateral structure of the electrode surface or layers of adsorbed ions is not something that so far was incorporated to the theory of EDL in RTILs.

Lockett and collaborators<sup>424,550</sup> systematically studied several RTILs with different size of cations and anions, at different temperatures. All curves, as measured between -1.5 and +1.5 V reveal camel shape curves, the qualitative features of which seemed to be in line with the results of refs 56 and 391. However, the temperature dependence looks different. Except at the wings the capacitance increases (quite substantially at maxima) with the temperature. No simple mean field theory predicts anything like that, neither coarse grain simulations mimic it.<sup>397</sup> The authors, however, give it an interesting interpretation. They attribute it to the presence of ion complexes in imidazolium-based ionic liquids, as was shown by time-of-flight secondary mass spectroscopy<sup>554</sup> and dielectric spectroscopy<sup>555</sup> that indicated that some 8% of all ions in the RTILs under study may be bound in contact ionic pairs. The increase of temperature may unbind such pairs, and they may additionally contribute to the capacitance response. How, however, 8% of such releases can contribute a two times increase in capacitance with temperature is yet unclear. We also note that, as mentioned above, the actual degree of ion pair association in RTILs is currently a subject of intensive debates in the literature<sup>216,219–224</sup> (see also the discussion in section 5.5 below). In this context, it might be interesting to adopt and explore pertinent ideas of the almost forgotten Gurevich and Kharkats statistical models of adsorption,<sup>379</sup> an interesting option for a future investigation.

Interesting observations of slow and fast capacitive processes taking place at the electrode-RTIL interface were recently published by Drüscher and co-workers.<sup>66,67</sup>

The list of further papers reporting the capacitance in RTILs could be continued. It is time, however, to refer to the 2011 work of Kolb and Paikossy<sup>556</sup> preceded by an earlier study.<sup>344</sup> In ref 556 they performed a detailed investigation of capacitive processes in RTILs using high resolution electrical current scale

(the  $\mu\text{A cm}^{-2}$  scale in contrast to the  $\text{mA cm}^{-2}$  used in most of the capacitance measurements with RTILs). The conclusion of their paper was that all data reported so far should be taken with care because the electrical impedance of the interface contains a remarkable constant phase element (CPE) even at atomically smooth, single crystal electrodes that they have studied, and therefore, the capacitive element of the equivalent circuit is practically impossible to extract. Kolb and Paikossy related the observed CPE to some slow relaxation dynamics in the studied RTIL (in their case, 1-butyl-3-methyl-imidazolium hexafluorophosphate). From that fact they came to conclusion that such equilibrium quantity like equilibrium capacitance for RTILs which behave more like glasses than equilibrium media,<sup>516</sup> is very difficult to achieve at realistic experimental conditions. They pointed out that earlier theories of the EDL and the double layer capacitance should be updated to take into account kinetic process in RTILs. We note that Wang and Pilon in their recent work also raised some concerns about intrinsic limitations of impedance measurements in determining electric double layer capacitances.<sup>557</sup> Understanding the importance of issues raised by the authors of refs 344, 556, and 557, we note that the capacitance itself is an equilibrium quantity, which characterizes the relationship between the charge on the electrode and the voltage across the double layer. The fact that impedance measurements cannot reliably assess equilibrium characteristics is not a problem of the EDL theory that operates with equilibrium properties, but rather a problem of experimental techniques available these days. (we also note that the conclusions from refs 344 and 557 were debated by Drüscher and Roling in their comments on these works;<sup>70,558</sup> we refer to these comments and the corresponding replies to them by Pajkossy<sup>559</sup> and Wang and Pilon<sup>560</sup> for more detailed discussion on this subject).

A different way to assess the capacitance is to extract this from the plateaus of the cyclic voltammetry curves,<sup>561,562</sup> that show the current,  $j(t)$ , vs voltage  $e$ ,  $U(t)$ . Since voltage in one sweep is varied with a constant speed:  $U(t) = vt$ , and current at the plateau is constant, then in principle  $j/v = (dQ/dt)/(dU/dt) = d\sigma/dU = C$ . This method of measuring the capacitance suffers from low accuracy, in particular if one wants to get not just rough estimate of it, but its voltage dependence. Recent investigation of EDL capacitance in [EMIm][BF<sub>4</sub>] and [BMIm][BF<sub>4</sub>] extracted from electrochemical impedance spectroscopy and from cyclic voltammograms has shown drastically different values and shapes of  $C(V)$ ,<sup>562</sup> led the authors to pessimistic conclusions about the reliability of assessing capacitance from impedance data, whereas frankly it is not clear which of the two methods gives poorer results.

With the due warning about typical artifacts in extraction of capacitance from electrochemical impedance data and a particular skepticism about the possibility of retrieving from those data reliable capacitance values, when dealing with RTILs,<sup>563,564</sup> Gnahn et al., nevertheless, presented some capacitance results.<sup>344</sup> These were estimated to be close to 6–7  $\mu\text{F/cm}^2$  and practically not varying with voltage. Roling et al. have addressed attention to several points that might help to avoid artifacts in capacitance measurements,<sup>67</sup> whereas Drüscher and Roling<sup>558</sup> expressed concerns on the data analysis pursued in ref 344 that may have affected the results presented in that work; Pajkossy replied<sup>559</sup> and the question about the best technique/analysis for RTIL capacitance measurements seems to be still on hold.

## 5.2. Molecular-Level Structure of the EDL

As we have earlier mentioned, the capacitance is not the only measure of EDL properties. Mezger et al.<sup>565,566</sup> reported high-energy X-ray reflectivity data on the structure of the distribution of cations and anions in different RTILs at spontaneously charged sapphire surface. Unfortunately the charge on that surface could not be independently varied, and thus no information could have been obtained how those profiles change with voltage. Nevertheless, the results of these studies were quite remarkable. They have unambiguously shown the oscillating over screening patterns of charge distribution in an RTIL at an EI. Note that those results were published simultaneously and independently from the simulations studies of refs 396 and 439 that revealed very similar features of the overscreening but also explored the effect of the electrode polarization. In follow up papers, Mezger et al.<sup>567</sup> as well as Nishi et al.<sup>568,569</sup> has shown the effect of layering near free surfaces of the corresponding ionic liquids.

The soil was ready for X-ray studies of the structure of ionic liquids at electrodes at varied voltages and an interesting work of this kind has been recently reported, based on X-ray reflectometry study.<sup>570</sup> That work investigated the structure of  $N,N$ -diethyl- $N$ -methyl- $N$ -(2-methoxyethyl) ammonium] [bis-(trifluoromethanesulfonyl)imide] at the single crystal Au(111) electrode. Not only was the overscreening clearly demonstrated there at low voltages but also its weakening at voltages up to  $\pm 3$  V, qualitatively in line with the simulation studies of ref 439 and predictions of ref 389. Voltages of that scale were shown to be yet not sufficient to turn on in full the crowding effects; that is perhaps due to the effect of the tails: several simulations works show that the presence of longer neutral tails of ions shifts the onset of lattice saturation to larger voltages (cf, refs 52, 391, and 466). The observed asymmetry in the ionic liquid response to the sign of the voltage was also not something surprising as the shape and size of the cations and anions used in that work is substantially different, consequently affecting the structure of the first layers at different electrodes depending on the electrode polarization.

Interesting attempt to perform neutron reflectometry studies of the structure of EDL as a function of electrode potential was recently reported in ref 335. The limited wave-vector transfer range prevented observation of cation/anion layering. Somehow, in the available Q-range only subtle differences were observed between the reflectivity data at three different applied potentials. The data analysis revealed an excess of [BMPyr]<sup>+</sup> at the interface, with the amount decreasing at increasingly positive potentials, but a cation rich interface was found even at a positively charged electrode. Seemingly some strong chemisorption prevented dramatic changes of the content of the [BMPyr]<sup>+</sup> cations on the gold electrode. However, the simultaneously measured capacitance curves showed signatures of a camel-shape behavior with strong decaying wings at large and positive and negative potentials, which if our understanding of the data is correct, must indicate crowding. A dip on the capacitance curve close to the pzc (see Figure 2 in that work) is likely to indicate the role of substantial neutral tails of [BMPyr]<sup>+</sup> cations, acting as latent voids for the local increase of the charge density and causing the initial rise of capacitance, in the spirit of the predictions of ref 391.

The exploration of the ionic structuring in RTILs in electrochemical environment, where one can change the electrode potential and trace how the structure will change has been successfully pursued using other surface-specific

experimental methods. Atkin and co-workers applied AFM for studying the “layering” behavior of ionic liquids, again not in electrochemical cells.<sup>571–573</sup> That approach has been later extended to electrochemical interfaces.<sup>65,574,575</sup> The 2011 work by Hayes et al.<sup>574</sup> studied the interface of Au(111) with two ionic liquids, [BMPy][FAP] and [EMIm][FAP], by measuring AFM force-separation profiles at different electrode potentials. Figures 1 and 2 of that article had unambiguously demonstrated the layered structures of the EDL in these RTILs, revealing typically between 4 and 7 layers (signatures of layering in the force–distance curves is consistent with the diameters of ions). It was found that negative polarizations stabilize the layered structure; positive polarization has the same but a weaker effect on layering. The authors relate these differences with the difference of the molecular structure of the cations and anions in the both liquids. But the common trend is that with polarizing the electrode (negatively or positively), both the number of ionic layers and the force needed to rupture them increases. Comparing the two RTILs studied, they found that [BMPy][FAP] delivers more rigid structures than [EMIm][FAP], attributing it to an on-one-atom localization of charge in [BMPy]<sup>+</sup>, as compared to more delocalized structure of charge in [EMIm]<sup>+</sup>. The AFM technique in combination with STM, cyclic voltammetry and electrochemical impedance spectroscopy has been also used for a very detailed study of the structure and dynamics of the interfacial layers between extremely pure [BMPy][FAP] and Au(111).<sup>65</sup> We believe that these studies<sup>65,574</sup> were among the first where the EDL structure in RTILs was probed by “touching the ionic layers in it one by one”.

Note that Perkin et al.<sup>83</sup> (who used the surface force apparatus<sup>301</sup> technique) reported similar normal-force measurements of another RTIL, [EMIm][EtSO<sub>4</sub>], confined between two spontaneously charged mica surfaces. In that work they could distinctly detect about three layers. However, their setup was not an electrochemical one, and the charge on the surfaces was not variable (Perkin’s group is currently working on modification of the surface force apparatus techniques for *in situ* measurements in electrochemical environment<sup>576</sup>).

In a later paper, Smith et al.<sup>577</sup> have studied interfacial structuring in a series of dialkylpyrrolidinium-based ionic liquids induced by confinement. They found that ionic liquids containing cations with shorter alkyl chain form alternating cation–anion monolayer structures, similar to the interfacial behavior in the liquids studied in ref 83, however in a RTIL with cations having a longer alkyl chain they observed well-pronounced bilayer structures. The crossover from monolayer to bilayer type structures occurs between chain lengths with the number of alkyl groups  $n = 8$  and 10. The bilayer structure for  $n = 10$  involves full interdigitation of the alkyl chains. Thus the structure in such liquids appeared to be very different than in “simple” imidazolium-based ionic liquids with short alkyl chains. Existence of the bilayer type structures was not unexpected though (cf. Figure 6 of ref 56); but the work of Perkin et al. provided a solid evidence of their reality.

Inspired by refs 83 and 577, one may suggest conventional notions of “simple ionic liquids” (composed of ions with short tails) and complex ionic liquids (with at least one sort of ions having long tails), which are expected to display different structural behaviors in the bulk and at interfaces.

In continuation of this topic it is worth to mention that the approach of Hayes et al.<sup>574</sup> has been extended by the group of Bing-Wei Mao<sup>578</sup> in which they have studied the structure of

gold electrode/“simple ionic liquid” interface Au(111)/[BMIm][PF<sub>6</sub>]. They showed, in particular, a graph with the dependence of the force at the first and the second interior layers on electrode potential. They note that the first layer always show reduced thickness regardless of the polarity of the electrode and indicated that the interaction between the surface and the ions of the first layer is the strongest and it promotes the most compact structure. Next, the force is higher at cathode polarizations (just like in ref 574) than at the anode polarization of the electrode, indicating that the cation-rich layers do form more rigid structures than the anion rich layers. Hayes et al.<sup>574</sup> suggested already that the cations of the innermost layer lie flat on the surface at large negative polarization, but neither that work or the work of Mao’s group<sup>578</sup> offer a molecular-scale interpretation of why this should be so. Note that in the simulations of refs 52 and 391 neutral tails of cations got expelled from the electrode with increasing negative electrode polarization. This puzzle remains to be understood.

In another paper of the Mao’s group, the structure of interfacial layers was studied using *in situ* STM.<sup>553b</sup> That work has demonstrated a complicated interplay between building micellar vs “worm-like” ordering of cations and the voltage affected structural transitions (surface reconstruction) of Au(111) and Au(100) electrodes. They established tricky correlations between the crystallography of gold surfaces and the lateral structures in the adsorption layers, visualized by STM. At the same time this study shows that with a target of rationalizing first the effect of electrode potential on the layered structure in RTIL, it might be better to stay away from gold surfaces, which themselves undergo field-induced and adsorption-affected structural transitions<sup>312</sup> that in turn affect the structure of the ionic layers.

A complex AFM, STM, and distance tunnelling spectroscopy study has been reported recently as a result of collaboration between the groups of Atkin and Endres.<sup>579</sup> One of the conclusions of this sophisticated study was that “the electrode potential dictates the extent of multilayering, as the number of layers detected and the force required to rupture these layers increases with cathodic or anodic potential”. Because the methods used in this work cannot distinguish the prevailing sign of charge accumulated in the layers, this conclusion cannot answer, do we encounter here with the onset of a crossover between overscreening and crowding (perhaps it is unlikely, as voltages had been varied here only between –2 and +2 V (vs Pt reference electrode)). It is not entirely clear that the observed multilayered structures in that work are formed due to the overscreening effect, but the above-mentioned X-ray reflectivity study pushes one to expect that this might be the case.

To summarize, the layered structures in RTILs observed in the majority of discussed works are quite distinct. Their lateral structures, as well as profiles can be complicated though and they depend on the structure of the ions, in particular the extension of their organic uncharged tails. When these tails are not too long, normal distributions demonstrate typical oscillating overscreening profiles, highlighting the critical role of charge-induced nanoscale correlations in RTILs. These observations generally confirm key aspects of predicted overscreening structures in the EDL in “simple RTILs”, while revealing more intricate structures in complex RTILs. These recent experimental achievements suggest that the existing theoretical knowledge of main principles of the EDL formation in ionic liquids provide us a good baseline for understanding

the fundamentals of nanoscale response of RTILs at charged interfaces.

### 5.3. Structural Transitions in the EDL: From Multilayer to Monolayer Structure

Although the articles discussed above report a number of experimental and molecular modeling observations of multilayered structures formed at RTIL-solid interfaces, there is no general agreement in the literature about this. Such, Baldelli in his recent perspectives article<sup>580</sup> questions the formation of multilayers at the interface in ionic liquids. He suggests that at certain conditions the structure of the EDL in RTILs might consist of a single monolayer of counterions close to the electrode surface with RTIL ions further from the electrode behaving similar to the bulk liquid phase. This opinion is based on a critical review of experimental works that studied interfacial RTIL systems by the sum frequency generation (SFG) spectroscopy technique<sup>581–584</sup> (see also an earlier review by Baldelli on the surface structure of RTILs at electrified metal interfaces<sup>585</sup>). The discussed results suggest that ions at the solid–liquid interface are organized into essentially one ion-layer, a Helmholtz-like structure in which the orientational order beyond this layer is negligible.

This view on the interfacial structure of RTILs correlates with other independent experimental findings. As such, Pan et al. reported a monolayer structure of PF<sub>6</sub><sup>-</sup> anions adsorbed at electrified Au(111) electrode surface.<sup>586</sup> This study investigated 2D phase transition of PF<sub>6</sub><sup>-</sup> adlayers at the electrified ionic liquid/Au(111) interface with [BMIm][PF<sub>6</sub>] by in situ STM. They found that at potential above -0.2 V vs Pt reference, PF<sub>6</sub><sup>-</sup> anions form a dense monolayer with Moire-like patterns, as revealed by STM images. In most of the studied cases such patterns seemed to coexist with the uncompressed structures. The same paper reports a structural transition at the interface at more negative voltages with the structural changes occur gradually with a ( $\sqrt{3} \times \sqrt{3}$ ) phase forming at approximate -0.45 V.

Recently, Castillo et al. used the solid-state NMR techniques to investigate the structure and dynamics of [BMIm][PF<sub>6</sub>] at the interface with silica (not charged) and laponite clay (negatively charged) surfaces.<sup>587</sup> They found that in the case of an uncharged amorphous support, such as silica, the ionic liquid phase behaves as an almost liquid phase but with restricted mobility. However, their results suggest that on the negatively charged layered surface of laponite clay, the ionic liquid can form two different phases, a thin solid layer (close to a monolayer) and a truly liquid phase over the first solid layer, showing that the order imposed by the clay is not transferred beyond a few monolayers of supported solid phase. We note that there are other experimental works reporting the solid-like layer formation in RTILs, see, e.g., refs 588 and 589 (these works also reported the lateral heterogeneity of the interfacial structures).

The contradiction between the different experimental observations of the EDL structure in RTILs discussed above may be (at least partially) resolved by the results of recent modeling work of Kirchner et al.<sup>278</sup> where the authors performed large-scale MD simulations of a coarse-grain model RTIL between two nonpolarizable electrodes (the same model as in ref 396). There it was found that for most charge densities studied in that work the EDL has a multilayered structure with multiple alternating layers of counter and co-ions at the electrode-RTIL interface; however,

at certain charge densities the alternating multilayer structure of the electrical double layer undergoes a structural transition to a surface-frozen monolayer of densely packed counterions (Moire-like structure). At this point the dense ordered monolayer of counterions close to the electrode surface coexists with apparently nonstructured RTIL further from the electrode. The points of the structural transitions are determined by the balance between the surface-counterion attraction and the ion–ion steric repulsion. The authors of ref 278 found that the multilayer to monolayer transition is directly correlated with the surface charge density, counterion diameter and counterion charge; thereby indicating that at the point of the structural transitions:

- There is total charge compensation of the electrode charge by the interfacial monolayer of counterions at the transition point; that is, the phenomena of overscreening and alternating layers are almost absent at this point.
- There is dense geometric ordering of the interfacial counterions in a form of a dense ordered structure (so-called Moire-like structure).

We note that ref 278 is a pilot study that used a crude model both for the RTIL and for the electrodes. Therefore, the conclusions from that work are in no way final. More theoretical and experimental studies are necessary to explore the effects of structural transitions in the EDL in RTIL-based interfacial systems.

### 5.4. EDL Properties: a Closer Look at Temperature Dependence

It should be noted that the history of debates on the temperature effect on EDL properties in HTMSs (e.g., molten alkali halides) goes to as early as 1950s with the first peak of interest to this subject in 1970s.<sup>5,356</sup> In particular, determining the character of temperature dependence of the EDL capacitance was the primary subject of a considerable number of experimental and theoretical works.<sup>5,320,406,590</sup> However, due to a number of (i) experimental problems related with electrochemical measurements in harsh conditions of HTMSs, (ii) problems with incorporating short-range ion correlation effects into atomistic-scale theories of concentrated electrolytes (see sections 3 and 4 above), and (iii) relatively short time and length scales accessible for simulations till very recently, there was no common opinion on the subject in the literature of 1970s–1990s,<sup>5,320,406,590</sup> to the best of our knowledge the question still remains these days.<sup>591</sup>

Nowadays this controversy transfers into the RTIL domain and that is reflected by a large number of new experimental<sup>69,73,75,424,550,563,564</sup> and computational<sup>397,465,466,524,538</sup> works that studied the effect of the temperature on EDL properties in RTILs (see also a brief literature analysis of the area in ref 397).

For instance, several recent experimental studies of the EDL capacitance of different RTILs at different electrodes reported observations of increased capacitance at elevated temperatures.<sup>73,75,424,563,564</sup> This view on the capacitance behavior in RTILs is supported by the simulation results of Kislenko et al.,<sup>524,538</sup> who investigated the structure and dynamics of the [BMIM][PF<sub>6</sub>] RTIL/graphite interface in the temperature range of 300–400 K; for this system they reported a positive dependency of the EDL capacitance from temperature.<sup>524,538</sup>

However, at the same time the recently published results of molecular simulations by Vatamanu et al.<sup>466</sup> led the authors of that work to a conclusion about negative dependence of the EDL capacitance from temperature. That work investigated the

differential capacitance for *N*-methyl-*N*-propylpyrrolidinium bis(trifluoromethane)-sulfonyl imide ([PMPyr][TFSA]) near a graphite electrode. The authors of<sup>466</sup> explain the negative temperature dependence of the capacitance by “melting” of the EDL in this system at elevated temperature; melting of the interfacial structure at neutral graphite interface at higher temperatures was also reported in a simulation work by Dou et al.;<sup>530</sup> this effect has been also observed in the recent experimental work of Nishi et al. (X-ray reflectivity measurements)<sup>569</sup> on the temperature dependence of multilayering at the free surface of an RTIL, (triethyltetradecylphosphonium bis(nonafluorobutanesulfonyl)amide). The authors of that paper note, however, that the effect depends on the RTIL molecular structure (e.g., their results have shown little temperature dependence of the multilayer structure for another RTIL studied in that work, trioctylmethylammonium bis(nonafluorobutanesulfonyl)amide).

Druschler et al.<sup>69</sup> recently reported a detailed experimental study of electrochemical processes at the interface between extremely pure RTIL ([BMPyr][FAP]) and an Au(111) electrode where they used different experimental techniques like electrochemical impedance spectroscopy, *in situ* STM and *in situ* AFM. Similar to the modeling work of Vatamanu et al.<sup>466</sup> and in contrast to the results obtained in refs 424, 524, 538, 563, and 564 that study has shown an overall decrease of the EDL capacitance (determined for the fast capacitive process) when the temperature in these experiments was increased from 30 to 90 °C.

Also, as we discussed above, the comparison of EDL capacitance measurements and simulations obtained with metal and carbon electrodes remains to be questionable; indeed, although carbon materials (glassy carbon, porous carbon, graphite, or graphene) might reveal some metal properties they also possess semi metal properties as well. Skinner et al. in their recent work<sup>364</sup> emphasized that the temperature-effect on the EDL capacitance at the semi metal and semiconductor electrode can be determined by the T-dependence of the Debye length in the electrode if the contribution of electronic EDL in the electrode to the total capacitance of the interface is dominating. This comes primarily from the variation of the number of charge carriers.<sup>592</sup>

To conclude, as the literature analysis in this section shows, currently there is no commonly accepted opinion about (i) should there be any general laws for temperature-dependence of the EDL differential capacitance in RTILs, or should it be both, RTIL- and electrode-specific; (ii) how much the electrode potential should affect the temperature dependence in different potential range, except for may be the discussed weak or no dependence in the lattice saturation regime. To make things worse, not always is there an agreement about the credibility of experimental data on capacitance measurement (see discussion in the corresponding section of this review and references therein).

### 5.5. Surface Forces, Screening, and Degree of Ion Pair Dissociation in RTILs

Gebbie et al.<sup>224</sup> have recently reported measurements of equilibrium force-distance curves between charged mica and gold surfaces in a popular RTIL, [BMIm][TFSA] (the original paper used another notation for this RTIL, [C<sub>4</sub>mim][NTf<sub>2</sub>]), using a surface force apparatus. The measured force-distance profiles in this work were found to be exponentially decaying, with a long (>10 nm) decay length. Interpretation of these

forces in terms of the DLVO theory<sup>301</sup> suggested a long Debye screening length, which could only be rationalized by a very low effective concentration of charge carriers.

Based on these results Gebbie et al.<sup>224</sup> concluded that this RTIL behaves as “an effectively neutral, coordinated cation–anion network that exists in equilibrium with a small fraction of effectively dissociated ions” and suggested a mechanism of the electrode charge screening in this RTIL “through the formation of both bound (Stern) and diffuse electric double layers”.

In other words, this picture of RTIL implies that its ions are bound into clusters or ion pairs and behave like a polar medium with a small impurity of mobile charge carriers. The dielectric response of the nonconductive degrees of freedom in this liquid would be dominated by vibrations and rotations of ion pairs and more complex polarization modes of the clusters. These degrees of freedom would determine the effective dielectric constant of the liquid, whereas only a minute portion of dissociated ions that are free to move will contribute to the full screening; there should be also a virtual exchange between the mobile and immobile states of ions. Analogies to this picture are known in solid state physics. Probably, the closest one would be an n-doped semiconductor with thermal population of conductance band delivering only a small number of conductance electrons if the gap between the donor level and conductance band is large. The difference is that there we deal with cations coupled with electrons, while in RTILs with cations coupled with anions. Another possible analogy are ionic conductors with Frenkel defects and defect mobility. Most of the ions there belong to the lattice (i.e., they are in a bound state), but they can be thermally excited to get into a mobile state; the concentration of mobile charge carriers in such systems should have Arrhenius dependence (and, therefore, it might be interesting to repeat the experiments in ref 224 at different temperatures).

One can imagine that such a picture could be realized in RTILs at very low temperatures, but at normal conditions (the experiments in ref 224 were done at 295 K) the estimated value of effective dissociated ion concentration of 0.003% for [BMIm][TFSA] in ref 224 seems to be at odds with the results of electrical conductivity and diffusivity measurements by Tokuda et al.<sup>214</sup> and Bulut et al.<sup>593</sup> that have shown that the effective dissociated ion concentration for this RTIL at 295 K is around 60% (see also ref 594 for general discussion on ionicity of RTILs and comparison of the effective dissociated ion concentrations for different RTILs at different temperatures).

We note that Gebbie et al. argued in their work that the technique that was used in refs 214 and 594 for estimating the effective dissociated ion concentration in RTILs (so-called “ionicity” approach) does not apply for estimation of effective dissociated ion concentration at equilibrium because “conductivity and diffusivity measurements inherently include kinetic (dynamic transport) effects, and thus are not directly related to the equilibrium (static) association and dissociation (i.e., the  $K_d$  value) of pairs of ions”.<sup>224</sup> This statement is, formally, correct; however, we note that the thermodynamic analysis done in ref 224 is based on quantum chemistry calculations of dissociation energy of [BMIm][TFSA] ion pair in the gas phase ( $E_d$ ) that gave the value of  $E_d = +315.26 \text{ kJ/mol}$ . The obtained value of  $E_d$  is indeed quite high and that led the authors of ref 224 to a conclusion that this value of  $E_d$  should correspond to a very low solubility of separate ions and, consequently, to the low value of the effective dissociated ion concentration (that was estimated in ref 224 as  $1.2 \times 10^{-4} \text{ M}$

(mol/L)). However, following the thermodynamic cycle for dissolving molecules in the liquid phase,<sup>595,596</sup> solubility in the liquid phase depends not only on the dissociation energy in the gas phase but also on the solvation Gibbs energies  $\Delta G_{\text{sol}}$  of dissociating solutes; therefore, favorable solvation contributions of individual ions can overcompensate the energy penalty for ion pair dissociation in the gas phase.<sup>253</sup> We note that  $\Delta G_{\text{sol}}$  values were not provided in ref 224, but judging by the formula 2 and an explanatory paragraph in that work, the solvation effects there were taken into account through a simple dielectric continuum model that can be rather crude approximation for ion solvation in a polar liquid (see, e.g., ref 438). Eiden et al.<sup>243</sup> estimated  $\Delta G_{\text{sol}}$  for  $[\text{BMIm}]^+$  and  $[\text{TFSA}]^-$  ions at room temperature to be  $-209.5$  and  $-219.0$  kJ/mol correspondingly. So, comparing these values with the  $E_d$  value from ref 224, one gets the overall energetic balance for dissolution of one ion pair to be around  $-113.2$  kJ/mol; the negative energetic balance for ion pair dissolution would mean rather high solubility of individual ions in  $[\text{BMIm}][\text{TFSA}]$  and, consequently, high effective ion dissociation concentration. Saying that, we note that the estimates we provide above have to be taken with great care because (i) they were done by comparison of  $E_d$  and  $\Delta G_{\text{sol}}$  values obtained by different models; (ii) rigorously speaking, the calculations of solubility and dissociation constant should be done consistently through a proper thermodynamic cycle;<sup>42,596,597</sup> (iii) in principle, such calculations should be performed with taking molecular effects of solvent into account.<sup>253,596</sup>

The results of Gebbie et al. became a subject of active discussion in the literature.<sup>598–600</sup> Perkin et al.<sup>598</sup> pointed in their follow up comment that overall conclusions in ref 224 about the structure of the interfacial layer in RTILs and low degree of effective dissociation of RTIL ions seem to contradict several other available experimental observations for similar kinds of RTILs as well as computer simulations of RTILs done by other groups (all these works were discussed earlier in this review). We address the readers to ref 598 and to the recent rebuttal of Gebbie et al. to that comment<sup>599</sup> for further details of this interesting discussion.

We note in addition, that if the actual degree of ion dissociation in RTILs would have been indeed as low as the “effective dissociation” value 0.003%, as stated in the ref 224, then all capacitances in RTILs would have had U-shapes which does not seem to be the case. For this particular RTIL, the differential capacitance have been measured in ref 550, but it does not have such shape (it has one large maximum and several lower maxima; see Figure 6 in that work). Reference 335 recently presented the measurements of differential capacitance, cyclic voltammetry and neutron reflectivity for a similar RTIL (1-butyl-1-methylpyrrolidinium bis(trifluoromethylsulfonyl)imide). The differential capacitance of this RTIL presented in that work has also a camel-like shape but not a U-shape. It would be also difficult to rationalize fast charging dynamics in RTIL-based activated graphene supercapacitors<sup>601</sup> with such low and temperature dependent concentration of mobile ions.

Overall we think that the results of ref 224 are indeed challenging and, if correct, may have important implications. However, we note that they were not directly related with measurements of dissociation constants, but with force measurements. We therefore believe that the paradigm-changing hypothesis of low portion of effectively dissociated

ion pairs in RTILs as proposed in ref 224 requires further cross-investigation by experimental and computational approaches.

## 6. ELECTRODE REACTIONS AND THEIR KINETICS IN RTILS

RTILs have attracted much of interest as “designer solvents” for chemical reactions in the bulk- for synthesis and catalysis;<sup>37,54</sup> however, they are equally interesting for electrochemical reactions at electrodes, electrosynthesis and electrocatalysis due to their electrochemical and thermal stability, non-flammability/nonvolatility, electroconductivity and ability to dissolve different classes of substances.<sup>19,21,26,37,54,199</sup> During the past decade there have been published large amount of literature on the subject, covering this vast area of research in detail, take alone extraction of metals from RTILs and electrodeposition (for reviews, see, e.g., refs 18, 25–27, 155, and 602–605). We will not even try to overview this topic in full details here, referring the reader to the literature quoted above. Instead, we will just make a few brief comments on the basic principles behind electrode processes in RTILs, and how their kinetics are related with the properties of electrified interfaces and their response to charging. Dwelling on those principles, we will highlight, as we see them now, the main avenues for the development of the theory, which is here pretty much behind the existing experiments and applications.

### 6.1. Pros and Cons for Using RTILs As Solvents for Electrochemical Reactions

First, we note that, by selecting a proper cation/anion combination, RTILs can solubilize many substances from metal salts to nonpolar organic molecules and cellulose;<sup>37,54,158</sup> therefore, RTILs (as a class of compounds) can be used for a wider range of applications than conventional solvents. However, this is not the only benefit of using RTILs as solvents for electrochemical reactions. When one chooses a solvent for electrode reaction of dissolved species of interest one wants those species to react but not the solvent. Thus each solvent has its “EW”, i.e., the range of potentials within which it is electrochemically passive. As discussed in section 2.2.4, the edges of EW in RTILs in practice are not always as large as one may want to have it; they are also different for different cations and anions that at large enough voltages can themselves become the redox-active species.<sup>18,28,127,195,262</sup> Still within those windows, however, many inorganic solutes can undergo reduction/oxidation reactions, depending on the electrode polarization, without unwanted secondary Faraday processes involving the electrochemical transformations of the ions of the “solvent” RTIL. The anodic potential edge may not vary much when dealing with the most “popular” ions such as  $[\text{BF}_4]^-$ ,  $[\text{PF}_6]^-$ , and  $[\text{TFSA}]^-$ , but the cathodic limit is more variable depending on the identity of the cation, normally increasing with its size (see also recent review by Lane<sup>263</sup> that presents the specific reduction reactions that may occur at the negative electrode in commonly used RTILs).

The possible width of 3–5 V of that window for a considerable number of known RTILs is their substantial advantage,<sup>606</sup> because the electrode polarization has an exponential effect on driving the reaction, and being able to increase the overvoltage, say twice, may result in orders-of-magnitude increase of the reaction rate. We recap on it in a more detailed discussion below.

However that advantage comes at the cost of slow migration of the reactants to the electrode. The majority of RTILs have

decent intrinsic ionic conductivity due to the high density of ions. However, the mobilities of ions in RTILs, including the reactant ions, are (approximately) inversely proportional to the viscosity that at room temperature is typically one or even two orders of magnitude higher for most RTILs compared to ordinary electrolytes.

On the other hand, in general, viscosity of RTILs decreases with the increase of temperature<sup>211,214,216,232</sup> (for more details and for an updated list of RTIL viscosities see refs 19, 97, and 607 and the ILThermo database<sup>193</sup>). Correspondingly, the mobility of ions can be greatly increased with the temperature. Due to their low vapor pressures, RTILs as solvents can be operated at elevated temperatures overcoming the viscosity problem and related transport limitations.<sup>276</sup>

## 6.2. Electrochemical Reactions in RTILS: Electron Transfer Limited or Ion Transport Limited?

If the reactions are reactant transport limited, we should observe the diffusion limiting current  $J_{\text{lim}} \approx ez_{\text{tr}}D_{\text{reac}}(c_{\text{reac}}/L_{\text{dif}})$  where  $D_{\text{reac}}$  is the diffusion coefficient of the reactant,  $c_{\text{reac}}$  is the concentration of reactants in the bulk,  $L_{\text{dif}}$  is the effective diffusion length,  $z_{\text{tr}}$  is the number of transferred electrons in each elementary act of reaction. The properties of RTIL will enter through  $D_{\text{reac}}$  and  $L_{\text{dif}}$ . From the theoretical point of view it will not be very interesting. However, using the techniques of the rotating disk electrode<sup>78,608,609</sup> one can reduce diffusion limitations and extract the parameters of the electrochemical electron transfer rate. Recently this has been shown feasible in RTILs,<sup>610</sup> although it was previously considered difficult due to their high viscosity (for the discussion of factors hindering the application of this technique in RTILs, see ref 611). We will therefore focus below on the current voltage characteristics limited by the electron transfer reaction, and particular by those with small electron tunneling probabilities in the transitional configuration of the nuclear degrees of freedom, i.e. dwell on the case described by theory of nonadiabatic transitions.

**6.2.1. Redox Current in Quantum Electrochemistry.** It will be useful to put down the most complete expression for the electrode current at a given electrode in order to illuminate the factors that may be important and specific for RTILs. In spite of generality of these expressions, they still contain a number of approximations about which one can read in ref 612. Hence

$$J = J_c - J_a \quad (24)$$

where the cathodic and anodic currents, related respectively with the electron transfer from the electrode to the oxidized acceptor of electrons and with the electron transfer from the reduced donor of electrons to the electrode, are given by

$$\begin{aligned} J_c &= ec_{\text{ox}}\Delta z \int dE \rho(E) n(E) W_c\{E; V_1(V)\}, \\ J_a &= ec_{\text{red}}\Delta z \int dE \rho(E) [1 - n(E)] W_a\{E; V_1(V)\} \end{aligned} \quad (25)$$

with  $c_{\text{ox}}$  and  $c_{\text{red}}$  being the concentrations of oxidized and reduced species on the effective reaction plane,  $\Delta z$  is the effective width of the reaction zone,  $\rho(E)$  and  $n(E)$  are, respectively, the electron density of states and the Fermi-function at the electron energy level  $E$ ,  $W_c\{E; V_1(V)\}$  and  $W_a\{E; V_1(V)\}$  are respectively the transition probabilities of the elementary acts of the cathodic and anodic processes. The latter quantities depend on the electron energy level  $E$  from which the electron is transferred to the acceptor in the cathodic transfer and to which the electron is transferred from the donor

in the anodic transfer. The both transition probabilities depend on the potential drop between the electrode and the reaction plane  $V_1(V)$  where the donor or acceptor are located, which generally may not be equal to the total potential drop between the electrode and the bulk of the solution,  $V$ . The expressions for the transition probabilities read as

$$\begin{aligned} W_c\{E; V_1(V)\} &= [T_{\text{MA}}(E, V)]^2 \exp\left(-\frac{w_{\text{ox}}(V)}{k_B T}\right) \\ &\times \sqrt{\frac{\pi}{E_r^{(c)} k_B T h^2}} \exp\left\{-\frac{[E_r^{(c)} + \Delta G_c(E, V)]^2}{4E_r^{(c)} k_B T}\right\} \end{aligned} \quad (26)$$

and

$$\begin{aligned} W_a\{E; V_1(V)\} &= [T_{\text{DM}}(E, V)]^2 \exp\left(-\frac{w_{\text{red}}(V)}{k_B T}\right) \\ &\times \sqrt{\frac{\pi}{E_r^{(a)} k_B T h^2}} \exp\left\{-\frac{[E_r^{(a)} + \Delta G_a(E, V)]^2}{4E_r^{(a)} k_B T}\right\} \end{aligned} \quad (27)$$

Here  $T_{\text{MA}}(E, V)$  and  $T_{\text{DM}}(E, V)$  are the matrix elements of transition (overlap integrals between the wave functions of the electron states of the electrode and the acceptor, and the donor and electrode, respectively). Determination of these factors is a special task of quantum chemistry. To the accuracy of the effects considered in ref.<sup>613</sup> they may be assumed, in the first approximation, to be independent of voltage. The second factor in these expressions is the Boltzmann probability for the acceptor or donor to set on the reaction plane, with  $w_{\text{ox}}$  and  $w_{\text{red}}$  being their energies, generally potentially dependent.  $E_r^{(c)}$  and  $E_r^{(a)}$  are the reorganization energies which may generally be different for the cathodic and anodic transfers (the quantities in the Marcus theory<sup>614</sup> generally denoted by the symbol  $\lambda$ ).  $\Delta G_c(E, V)$  and  $\Delta G_a(E, V)$  are the Gibbs free energy change on single electron transfer from the electron energy level  $E$  to equilibrated level of the acceptor and from the equilibrated level of donor to the electron energy level  $E$ :

$$\begin{aligned} \Delta G_c &= V_1(V) - V_1^{(0)} - (E - E_F) + w_{\text{red}}(V) - w_{\text{ox}}(V) \\ &- k_B T \ln \frac{c_{\text{ox}}}{c_{\text{red}}} \end{aligned} \quad (28)$$

$$\begin{aligned} \Delta G_a &= V_1(V) - V_1^{(0)} + (E - E_F) + w_{\text{ox}}(V) - w_{\text{red}}(V) \\ &+ k_B T \ln \frac{c_{\text{ox}}}{c_{\text{red}}} \end{aligned} \quad (29)$$

The last terms in these two equations are the Nernst term with  $c_{\text{red}}$  and  $c_{\text{ox}}$  being the concentrations of donors and acceptors.  $V_1^{(0)}$  is the equilibrium potential drop between the electrode and the reaction plane defined in such a way that ; it is easy to see that when  $V_1(V) = V_1^{(0)}$ ,  $J_c = J_a$  and  $J = 0$  (the definition of equilibrium).

Introducing the notion of overpotential, one can reduce the expression for the current to a much more compact form,<sup>612</sup> but for us it was important to keep it as it is, in order to reveal microscopic effects that the medium of reaction, in our case RTIL, can contribute. Looking at these equations we see that many terms depend here on the electrode potential, in the first place the driving force of reaction  $V_1(V)$ .

### 6.3. What Will Matter in RTILs?

The key factors here are the reorganization energy, the work terms, the driving force, and the overlap integral. Let us comment on each of them separately.

**6.3.1. Reorganization Energy.** Let us assume that for a single electron cathode and anode transfer the reorganization energies are the same.  $E_r^{(c)} = E_r^{(a)} = E_r$ . This is usually estimated using the Marcus formula,<sup>615</sup> which near the electrode with account of image forces reads

$$E_r = e^2 \left( \frac{1}{\epsilon_\infty} - \frac{1}{\epsilon} \right) \left( \frac{1}{2a} - \frac{1}{4d} \right) \quad (30)$$

where  $a$  is the effective radius of the oxidized and reduced forms of the reactant (assumed to be the same in both cases) and  $d$  is the distance to the reaction plane;  $\epsilon_\infty$  and  $\epsilon$  are respectively the high and low frequency dielectric constants of the liquid.  $\epsilon_\infty$  is due to the contribution of the polarizability of internal electrons of ions of the liquid, the quantity usually close to 2.  $\epsilon$  is the “static” dielectric constant; the latter stands in the quotes because, as emphasized earlier in this review, formally, there is no such thing as static dielectric constant of ionically conducting liquid. We mean here the measured “intermediate” dielectric constant due to vibrations and librations of ionic pairs, or more generally the strongly dissipating polar-phonon-like modes of the ionic liquid, the quantity of the order of 10 (see section 2.2.3), i.e. for an RTIL  $\epsilon = \epsilon_*$ .

This formula was the Marcus-derived<sup>616</sup> extension of the Pekar–Marcus (formula for the reorganization energy of the electron exchange between the ions of radii  $a$  in the bulk of a dielectric medium).<sup>616–618</sup>

$$E_r = e^2 \left( \frac{1}{\epsilon_\infty} - \frac{1}{\epsilon} \right) \left( \frac{1}{a} - \frac{1}{d} \right) \quad (31)$$

The reorganization energy in the bulk is larger because the electric field of ions near the electrode is image-screened by the metal. Generally both formulas are expected to give rough estimates of the corresponding reorganization energies, because they do not take into account the short-range structure of the liquid, neither the electric field penetration into the electrode. There were various attempts to take both effects into account through the spatial dispersion of dielectric permittivity of the liquid and the metal in various approximations of the latter for these two phases, done in the context of reactions in ordinary polar liquids.<sup>619–624</sup> These studies used a number of approximations; most importantly they are built on a linear response theory of the medium to the reorganizing charge of the reactant. The study in ref 438 has shown, however, that the mere presence of the solute as well as the nonlinear electrostatic effects can perturb the environment and substantially distort the nonlocal electrostatic response of the liquid washing out some of the fine structural effects that are predicted by the linear response nonlocal electrostatic theory.<sup>625,626</sup> In view of such a situation the simple formulas of Marcus type remain to be a good orientation point. How much this should be applicable for RTILs? First modelling studies for an electron transfer in the bulk<sup>627–629</sup> and at electrodes<sup>428</sup> have shown substantial deviations of the estimates due to the short-range structure, although as an “order of magnitude estimate” the Marcus formulas can still be used.

One of the sources of the deviation can be actually traced, if we go back to more general expression for the reorganization

energy,<sup>630–632</sup> which, if we do not take into account spatial dispersion of the dielectric permittivity, reads

$$E_r = e^2 \left( \frac{1}{a} - \frac{1}{d} \right) \frac{2}{\pi} \int_0^{k_B T / 4h} d\omega \frac{\text{Im } \epsilon(\omega)}{\omega |\epsilon(\omega)|^2} \quad (32)$$

where  $\epsilon(\omega)$  is the complex frequency dependent dielectric permittivity of the liquid. The exact Kramers-Kroenig (KK) relation expresses the integral over all frequencies with the static dielectric constant  $\epsilon$ , if  $\epsilon(0) = \epsilon$

$$\frac{2}{\pi} \int_0^\infty d\omega \frac{\text{Im } \epsilon(\omega)}{\omega |\epsilon(\omega)|^2} = 1 - \frac{1}{\epsilon(0)} \quad (33)$$

For the integral in eq 33 there is an approximate KK relation if the frequency  $k_B T / 4h$  lies in the transparency band between the electronic excitations in the liquid and the vibrational modes<sup>631</sup> and if  $\epsilon(\omega \rightarrow 0) = \epsilon = \text{const}$ .

$$\frac{2}{\pi} \int_0^{k_B T / 4h} d\omega \frac{\text{Im } \epsilon(\omega)}{\omega |\epsilon(\omega)|^2} = \left( \frac{1}{\epsilon_\infty} - \frac{1}{\epsilon} \right) \quad (34)$$

With this equation valid, we recover expression of eq 32 for the reorganization energy. However, in RTILs we do not know whether any of the two assumptions hold. In particular in view of the very slow relaxation in ionic liquid (low frequency tail of,  $\epsilon(\omega)$ , where should we truncate the integration in eq 34? So the best strategy would be, if we have experimental data for  $\text{Im } \epsilon(\omega) / (|\epsilon(\omega)|)^2$  to keep the integral form for the reorganization energy. Even better, had we had information not only about frequency- but also the wave-vector-dependence of the dielectric response function  $\text{Im } \epsilon(k, \omega) / (|\epsilon(k, \omega)|)^2$  (say, from computer simulations, such as, e.g., obtained for water<sup>436</sup>) we could use then even more general equations for the reorganization energy

$$E_r = e^2 \frac{2}{\pi} \int_0^\infty dk \left\{ \frac{1}{2} \left[ \frac{(\sin ka_1)^2}{(ka_1)^2} + \frac{(\sin ka_2)^2}{(ka_2)^2} \right] - \frac{\sin ka_1 \sin ka_2 \sin kd}{ka_1 ka_2 kd} \right\} \frac{2}{\pi} \int_0^{k_B T / 4h} \frac{d\omega}{\omega} \frac{\text{Im } \epsilon(k, \omega)}{|\epsilon(k, \omega)|^2} \quad (35)$$

drawn here for a single electron exchange between two “spherical ions of radii”  $a_1$  and  $a_2$ , the centers of which are separated by a distance  $d \geq (a_1 + a_2)$ . In the case of  $k$ -independent dielectric-response function

$$\frac{\text{Im } \epsilon(k, \omega)}{|\epsilon(k, \omega)|^2} \approx \frac{\text{Im } \epsilon(k = 0, \omega)}{|\epsilon(k = 0, \omega)|^2} = \frac{\text{Im } \epsilon(\omega)}{|\epsilon(\omega)|^2} \quad (36)$$

the two integrals in eq 35 are decoupled, and eq 35 reduces to eq 33 (if we put there  $a_1 = a_2 = a$ ). For RTILs such assumption in the range of wave numbers  $k \sim (2\pi/a)$ , important in the integral eq 35, will unlikely be realistic. Thus eq 35 suggests an interesting scheme for future calculation of the reorganization energy and comparison of the results with the direct simulation of the latter.<sup>628,629</sup>

This expression however would only be applicable for the electron transfer between donor and acceptor ions in the bulk. How it should look for the electrochemical electron transfer reactions at electrodes? This is generally a difficult problem, cf, refs 619–622 and 633, which is yet to be solved. Such

enterprise, however, would only make sense if such approach showed good results in the bulk; the studies in ref 438 performed for water, suggest that this may not be the case. However, a priori we do not know whether this would be the same for RTILs.

**6.3.2. Work Terms.** These tell us what will be the concentrations of oxidized (for the cathodic current) and reduced (for the anodic current) species at the reaction plane, the factors also determining the currents. The probability to find there those species will depend on their charge and the potential of the plane. The latter is very much an issue of the potential distribution near the electrode, and the effects of overscreening can contribute new interesting effects here (but see a discussion below). They may be particularly important for electrodeposition reactions with a slow adsorption stage.

**6.3.3. Driving Force and the Potentially New Form of the Frumkin Correction.** One of the functions of electrolyte in electrode kinetics is to provide the most compact localization of the electrostatic potential drop between the electrode and the reaction plane, to utilize the strongest drive for the reaction. In diluted electrolyte solution the potential drop between the electrode and the bulk will be spread over the diffuse double layer and only a small portion of this drop will be localized between the electrode and the reaction plane. Hence polarizing the electrode will be majorly wasted for the electrode kinetics. The correction to the expressions for the electrode current which takes into account this effect is known as the Frumkin correction.<sup>634,635</sup> This we symbolically incorporated in the expression for  $V_1(V)$ , with  $V_1(V) \approx V$  only if total potential drop is fully localized between the electrode and the reaction plane. With the effect of overscreening in place in RTILs, one may expect to encounter something completely new, different from the case of diluted electrolytic solutions where  $V_1(V) < V$ . Here, in the overscreening regime,  $V_1(V)$  may quite easily become substantially larger than  $V$ .

To our knowledge this opportunity was first noticed and investigated in molecular dynamic simulations of Reed et al.<sup>428</sup>. The results of that pioneering study, however, did not show any significant effect of overscreening on the driving force of reaction although overscreening itself was found (that work describes pronounced oscillations in the mean electrical potential at the electrode-HTMS interface; see e.g. Figure 2 or Figure 12 in ref 428). The authors of ref 428 concluded that the potential distribution near the electrode averaged in the lateral plane in the absence of the reactant is not what actually counts in the driving force. They write: "Rather we should be considering the potential at the ion's center due only to the other charges present in the system: this might be better called a Madelung potential." Translating that conclusion into the necessity to take into account what is in electrochemistry commonly called the effect of micropotential,<sup>636</sup> we ought to assume that such effects should be abnormally high in strong correlated Coulombic systems, such as RTILs. In other words, they can be so high that the electrochemical overpotential can become uncorrelated with the electrostatic potential profile in the electrical double layer.

Recent work<sup>254</sup> studied free energy barriers for solute ions and neutral species in RTIL across the distance to the electrode by Molecular Dynamics simulations. It has been shown that the potential actually experienced by a solute ion in RTIL is indeed substantially different from the electrostatic potential that sets in the absence of such ion. However, Figures 6–12 in that work show that the oscillating overscreening patterns still have

significant effects on the shapes of free energy profiles of charged solutes near the electrode.<sup>254</sup> Indeed the redox-relevant free every profiles of solute species at the electrode-RTIL interface calculated in that work have pronounced oscillations up to the ~2 nm distance from the electrodes (see Figure 12 in this review that is reprinted from ref 254).

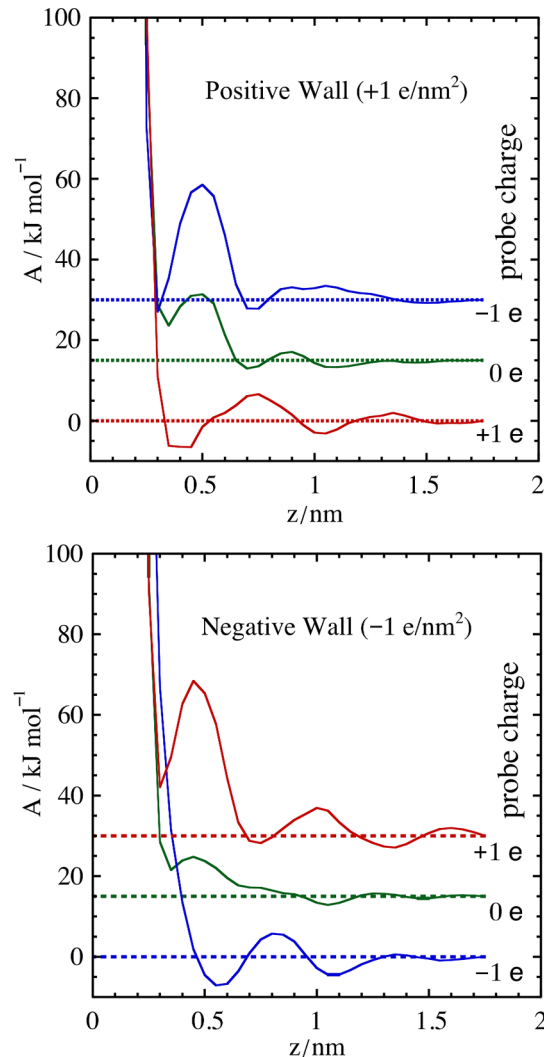


**Figure 12.** Redox-relevant free energy curves (in  $\text{kJ mol}^{-1}$ ) reproduced from ref 254. The curves are free energy profiles of charged and neutral solutes near the electrode along the perpendicular direction to the electrode plane ( $z$  direction). The relative positions of these curves have arbitrary offsets of  $15 \text{ kJ mol}^{-1}$  for the sake of clarity. The curves were calculated for negative, positive and neutral spherical probe particles in  $[\text{MMIm}][\text{Cl}]$  at charged flat graphite monolayers (graphene electrodes) with charge densities  $\pm 1.0 \text{ e nm}^{-2}$  ( $= \pm 16.0 \mu\text{C cm}^{-2}$ ). Above: Free energy profiles for probes with various charges approaching a positively charged electrode. Probe charges are: upper curve,  $-1\text{e}$ ; middle curve,  $0$ ; bottom curve,  $+1\text{e}$ . Below: corresponding curves for a negatively charged electrode. Reprinted with permission from ref 254. Copyright 2012 The Royal Society of Chemistry.

All in all, due to its fundamental and practical importance, this question requires further investigations. We need more evidence that overscreening does not affect (or only minorly affects) electrode kinetics; if such evidence was provided, it would be a challenging task for theory and simulations to fully rationalize it.

This puzzle may be related with the experimentally observed variation in the rates of different redox reactions at electrodes in RTILs; that is, why some reactions in RTILs are faster than in organic solvents<sup>637–641</sup> and some are slower,<sup>642,643</sup> as discussed below. However one must be careful here with conclusions because that variance may not be directly related with the effect of overpotential but rather with activation energies of the reactions, matrix elements and other pre-exponential factors, and even diffusion control.

Last but not least, in the regime of very large electrode polarization where the lattice saturation effects (crowding) might be expected,  $V_1(V) \propto \sqrt{V}$ .<sup>644</sup> This can result in a current–voltage law qualitatively different (cf., ref 644) from the Bulmer–Volmer's law.<sup>636</sup> This is a whole new area for future investigations, where, however, experiments should first set the scene.

#### 6.3.4. Matrix Element of Transition (Overlap Integral).

Evaluation of this quantity requires extension of modern methods of quantum chemistry with account of dense ionic environment of RTIL. In a simplified version<sup>612,613</sup> this may take a combination of electron density functional theory and molecular dynamics, in the spirit of ab initio Car–Parrinello schemes.<sup>645</sup> Will that be worth the effort? The question is, indeed, justified as it refers to the calculation of the pre-exponential factor in the expression for the electrode current, whereas so many issues are yet unclear about the exponential factors! The importance of the overlap integrals is, however, obvious when they are vanishingly small, as then they substantially affect the scale of the electrode current. They are certainly important for tuning the optimal parameters of the electrodeposition reactions. Next, if they also become voltage dependent<sup>612,613</sup> the matrix element of transition can contribute corrections to the current voltage plot. To our knowledge, for RTILs no detailed studies in this direction have yet been reported.

#### 6.4. Experiments: Examples of Few Case Studies

We did not intend to go into the review of any particular published papers on the electrode kinetics of RTILs, having focused in the previous sections of this chapter on certain general features of the most elementary electron transfer processes at electrodes, as such “quantum electrochemistry” might appear to be useful in rationalization of the simplest electrochemical reactions in RTILs. We nevertheless will briefly discuss below a very limited selection of published, predominantly experimental papers (for a more detailed review of this topic, see ref 163).

Lagrost et al.<sup>642</sup> have studied four different ionic liquids, based on 1-alkyl-3-methylimidazolium or quaternary ammonium cations as reaction media for several typical electrochemical reactions of oxidation of organic molecules (anthracene, naphthalene, durene, 1,4-dithiafulvene, and veratrole). They recover the reaction mechanisms from the analysis of cyclic voltammetry curves and determine the thermodynamic and kinetics parameters of the corresponding reactions. Based on this analysis they come to a conclusion that the uncovered mechanisms seem to be almost unchanged in ionic liquids, as compared with conventional organic media. However, the overall 1 order of magnitude decrease of the electron-transfer rates between the studied aromatic molecules and the electrode, observed for all the studied molecules, indicated at a higher solvent reorganization energy compared to ordinary organic solutions. Reorganization of dense ionic

atmospheres in RTILs can indeed be larger than the reorganization in a polar solvent, so these results are quite encouraging for application of the theory. These reactions, however, are not the simplest ones for theoretical analysis as they involve both first and second order reactions of cation radicals.

Later, studying the reduction mechanisms for a series of nitro aromatic and aliphatic compounds, the same team measured the electron transfer rate constants in two ionic liquids (1-butyl-3-methylimidazolium bis(trifluoromethylsulfonyl)imide and triethylbutylammonium bis(trifluoromethylsulfonyl)imide) and compared them with the data for the same reactions in acetonitrile.<sup>646</sup> For the reactions of the fastest redox couples (nitrobenzene derivatives) which could be classified as outer sphere ones (for which the reorganization of continuous surroundings is the major effect), the authors found that the contribution to the activation energy is the major factor controlling the electron transfer. The values of the rate constants were found to decrease in the ionic liquids by at least two orders of magnitude as compared to acetonitrile. For other reactions that could be classified as predominantly the inner-sphere ones (for which the reorganization of the modes inside the molecules and its first solvation shell is a predominant factor), such as in the case of the reduction of the 2-methyl-2-nitropropane, no major difference from the corresponding reaction in acetonitrile was found. This may indicate that the outersphere reorganization energy may indeed be substantially larger in the studied RTILs. Of course, conclusions of this kind must be taken with a pinch of salt, as they rest on simple principles of the elementary act of electron transfer reactions, the applicability of which for RTILs awaits verification. However, it shows, at least, that no “magic” enhancement of the driving force and neither overscreening-amplified Frumkin correction presumably take place in this example. This does not exclude the existence of such effects for some other reactions.

Generally, for a variety of studied RTIL systems both the diffusion coefficients and the electron transfer rates for heterogeneous electron transfer reactions of organic molecules can be smaller in RTILs than in classical organic solvents. The diffusion coefficients are smaller due to the higher viscosity of RTILs;<sup>193,195</sup> whereas the reaction rate constants may be smaller for some reactions<sup>642,643</sup> due a number of factors discussed above, reorganization energy in the first place. If that is the case for a particular reaction, the speed of production of new chemicals during the reaction would not benefit from using RTIL solvents (that are also generally more expensive than commonly used organic solvents); however, there may be still other benefits for using (some) RTILs for these reactions (e.g., low vapor pressure, wide temperature range, electrochemical stability, etc.).

Due to the high importance of the subject for potential applications, there have been many studies (both at electrochemical interfaces and in the bulk) on reaction mechanisms in RTILs that analyzed differences between reaction kinetics in RTILs and in organic solvents (see refs 18,163 for a review). Alongside with the observations of lower reaction rates in RTILs discussed above, many examples of accelerated reaction rates in RTILs were also found (see, e.g., refs 637–641). Quite often though the factors responsible for the accelerated reaction rates in RTILs were found to be related with specific molecular-scale reactant-solvent interactions that may not always be

rationalized in the simple terms described above in section 6.3.2.

Matsumiya et al.<sup>647</sup> studied electrochemical ferrocene-ferricenium electron transfer reactions in ammonium-imide RTILs, via the analysis of cyclic voltammograms over a potential range  $-0.3$  to  $+0.5$  V versus  $\text{I}^-/\text{I}_3^-$  reference electrode in a wide enough temperature range of  $298$ – $373$  K. The  $\text{Fc}/\text{Fc}^+$  reaction was found to be a single-electron transfer process (as expected) and diffusion controlled. The electron transfer rate constant and transfer coefficient have been retrieved by electroanalysis.<sup>648</sup> Both the rate constant and the diffusion coefficients for  $\text{Fc}/\text{Fc}^+$  were studied as a function of temperature, exhibiting Arrhenius dependencies.

Efforts have been invested in optimizing reference electrodes for voltammetry in RTILs.<sup>649</sup> In that work both the diffusion and the kinetics of electron transfer across the ionic liquid/electrode interface were studied using cyclic voltammetry and scanning electrochemical microscopy. In another work in this area<sup>650</sup> the authors studied the anodic oxidation of several arenes and anthracenes in RTILs. They made conclusion about substantial deviation from the outer-sphere Marcus-type behavior of these compounds in contrast to their behavior in traditional organic solvents, in terms of correlations of the rate constant with molecular size and solvent static dielectric constant. For a number of processes in a series of RTILs the electron-transfer kinetics was found to be independent of the solution viscosity.

In ref 651 ferrocene was used as a redox probe and the electrochemical properties of a series of RTILs were studied using voltammetric methods and scanning electrochemical microscopy. The effect of RTIL viscosity on mass transfer dynamics within each RTIL was studied, and their heterogeneous electron transfer rate constants were determined.

The classical example of rather complicated electron transfer reactions, the oxygen reduction reaction (ORR), has been studied in ref 652 at Pt surfaces in a protic RTIL using the method of rotating disk electrode. Water content measurements suggested that the ORR proceeded in the ionic liquid via a 4-electron reduction to water. A Tafel analysis of the rotating disk voltammetry data performed in that work revealed a change in the ORR Tafel slope which seemed to be related with the change of the exchange current density with the applied potential.

Interesting results were obtained for oxidation of dissolved hydrogen gas on platinum electrodes in different ionic liquids.<sup>653</sup> Studies of similar processes in protic ionic liquids have also been reported.<sup>654</sup>

The hydrogen evolution reaction has been explored at gold, molybdenum, nickel, titanium and platinum electrodes. Significant differences in electrochemical rate constants were observed between the different metals. Most importantly, the authors came to a conclusion that the reaction mechanism was consistent at all five metals in the studied RTIL, in contrast to the known variations in a series of these metals in aqueous systems.<sup>655</sup> Hydrogen evolution was also investigated in various RTILs in ref.<sup>656</sup> at Pt electrode. That work revealed a strong effect of the nature of anion, suggesting significant interaction between protons and anions.  $\text{H}^+$  reduction on a palladium microelectrode in RTIL was studied in ref 657 showing signatures of  $\text{Pd}/\text{H}$  layer formation under the studied conditions.

Kinetics of  $\text{Li}/\text{Li}^+$  was studied in refs 658 and 659 for a large set of RTILs.

Interesting studies of solvation effects on redox potentials of organic compounds in RTILs were done in refs 223 and 660.

That list could be continued, but all in all the experiments are far ahead of a molecular level theory (which is just to be developed), and many of the drawn examples are more complicated than the simplified one-stage processes sketched in the formalism described in this chapter above. The synergy will come after theorists will be able to formulate some striking predictions of quantum electrochemistry for experimentalists to test them. It has taken many years to get such tests done for some spectacular but elementary heterogeneous electron transfer reactions in ordinary electrolytes,<sup>635,636</sup> and it will also probably take some time for this to happen in RTILs.

## 7. RTILS IN CONFINED GEOMETRY

The electrochemical performance of an electrode-RTIL interface is generally “amplified” by its area, whether it is used for energy storage (capacitors and batteries) and generation (solar cells and fuel cells) or electrocatalysis. In this respect porous and in particular nanoporous electrodes may provide the maximal enhancement of the interfacial area, as long as the electrodes are well wetted by RTIL. This justifies the interest in understanding RTIL performance in nanoconfinement.

### 7.1. Electrochemical Capacitors: Targets and Challenges

Electrochemical capacitors have a vast range of applications for electrical energy storage and its fast delivery in the form of electrical current.<sup>91,661</sup> Their common ground is the position of supercapacitors on the so-called Ragone plot, the graph of the power vs energy stored (Figure 13). High power density, i.e.,

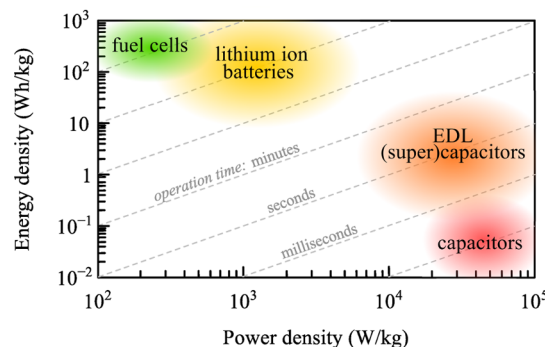


**Figure 13.** Ragone plot showing available energy of several types of energy storage devices. Characteristic operation times correspond to lines with unity slope.

high energy delivery in unit time per unit capacitor's mass or volume, is related to the ability of fast charging/discharging with minimal losses for the most compact architecture.

Looking good at the Ragone plot means to possess high energy density without sacrificing power density. The supercapacitors look better in this respect than batteries, but generally they have lower energy density and higher power density, and this determines their application niche. Scientists and engineers are interested to expand the whole band to the upper-right corner; then the supercapacitors could approach the market of applications traditionally occupied by batteries. It is wanted because EDL capacitors can be charged fast and, noninvolving any electrochemical reactions, can sustain hundreds of thousands of charging-discharging cycles. However, there are principle difficulties on the way of realization of

this target. These difficulties are inherent to the principle of the supercapacitor.

Indeed, the way to increase the energy density is to (i) maximize the double layer capacitance per unit surface area (the “specific capacitance”) and/or (ii) maximize the interfacial area per volume. The first option is about the best choice of the electrolyte and electrode material, underpinned by understanding the structure of the electrical double layer or empirical findings, the subject of studies reviewed in the previous sections. Exploring this option one may hope to increase the specific capacitance and thereby the overall capacitance of the electrodes usually by several times. The second option, however, will allow to increase the overall capacitance by orders of magnitude. Making the surface of the electrode rough is not sufficient to reach this goal. The standard strategy here is to use “volume-filling” interfaces typical for highly porous electrodes that are well wetted by the electrolyte. Therefore, engineering supercapacitors is often regarded synonymous to engineering the porous structure of the electrodes.<sup>89,91,93,370</sup> Indeed, there exist techniques for rational design of ordered mesoporous materials (e.g., they can be prepared by the template route; for a review see ref 662). Application areas of these materials are not limited only by electrochemical capacitors; they can be also effectively exploited in other electrochemical devices (e.g., electrochemical sensors).

However, using highly porous electrodes to increase capacitance automatically faces a problem. Figure 14 shows

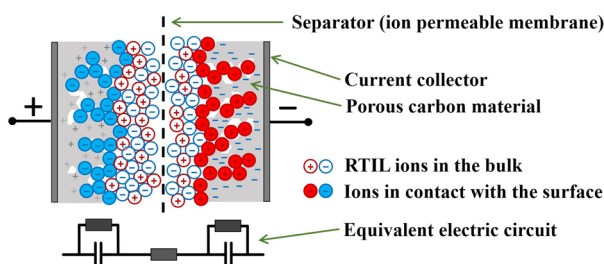


**Figure 14.** Electrochemical cell showing accumulation of RTIL ions at positively and negatively charged surfaces of porous carbon electrodes.

the cartoon of the cross-section of a supercapacitor with porous electrodes, from which the problem becomes clear. Separating charge, by charging the double layers on the opposing electrodes, means to move anions preferentially to the left electrode (anode) and cations to the right electrode (cathode). However, the higher the porosity, the longer the way for the ions to go to reach all interior parts of the volumetric surface of the electrodes. Thus, the larger the surface, the greater the

capacitance (and, consequently, the larger the stored charge for a given voltage), but simultaneously the greater the ohmic losses incurred due to the transport of ions through the long pores. The slow transport of ions into the pores causes losses in the power density, as well as it slows down the overall charging-discharging rate. Hence the trade-off between the energy density and the power density/speed of the charging cycles becomes inevitable.

Next, not only the length of the pores may be a problem but the ionic conductivity inside of them. Indeed, for wide pores the conductivity may be the same as in the bulk of electrolyte; however, for nanoscale pores, it may be different for a number of reasons. First, the ions will experience additional friction due to collision with the walls (the so-called Knudsen diffusion<sup>54</sup>). Second, the confinement may impose additional limitations on cations and anions, moving in opposite directions, bypassing each other. The third effect is the screening of the electrostatic interactions by the free electrons of the pore walls in the electrode, which can actually, be beneficial for charging the pore (see below).

The issue of the stored energy itself is not concerned with kinetic limitations, and we concentrate on it first. Note that as long as the characteristic pore radius (width) is much greater than the thickness of the electrical double layer, no new physics of the double layer and the energy stored in it will need to be invoked: the energy will just scale up with the interfacial area. This is no longer true when the two length scales become comparable. This fact was known already from the theory of mildly rough electrodes, where the modification of the double layer theory was needed.<sup>663,664</sup> For nanoporous electrodes an entirely new theory had to be developed to describe the dependence of the stored charge and energy on voltage, and this development is reviewed below.

## 7.2. Superionic Effect in Narrow Nanopores: Experiments vs Theory

Before describing the theory, we would like to highlight several interesting experimental facts that challenged our understanding of EDL properties in nanoconfinements.

The story of nanoporous electrodes for electrochemical capacitors is closely related with the new round of development of porous carbon materials for energy storage applications.<sup>92,276,370,378,665–667</sup> This is because (i) the porous structure of carbon is relatively easy to fabricate and control on industrial scale, (ii) the material is light-weighted, (iii) it is relatively cheap, (iv) it has a sufficient electronic conductivity (“current collector”) for a system in which the kinetic limitations are determined by the transport of ions, and, finally,

Material	Carbon onions	Carbon nanotubes	Graphene	Activated carbon	Carbide derived carbon	Templated carbon
Dimensionality	0-D	1-D	2-D	3-D	3-D	3-D
Conductivity	High	High	High	Low	Moderate	Low
Volumetric Capacitance	Low	Low	Moderate	High	High	Low
Cost	High	High	Moderate	Low	Moderate	High
Structure						

**Figure 15.** Different carbon material structures that are commonly used in EDL capacitors: onion-like carbon, carbon nanotubes, graphene, activated carbons, and carbide-derived carbons. Reprinted with permission from ref 276. Copyright 2013 American Chemical Society.

(v) it is electrochemically inert at higher voltages than most of the metallic electrodes.

Most popular types of porous carbon materials used as electrodes for electrochemical capacitors are: (i) activated carbon (AC), carbide-derived carbon (CDC), and templated carbon (TC); (ii) nanotube “forests”, based on single wall, double wall, or multiwall nanotubes; (iii) the structures based on graphene sheets; (iv) onion like structures, and (v) nanohorn structures (see some examples of these structures in Figure 15).<sup>92,276,370,665</sup>

It is not the task of this article to review all these structures, but we will stop on one of them which is most easy to fabricate on an industrial scale, namely CDC.<sup>668</sup> Porous carbon is produced from carbide in reactions of the following kind:  $\text{SiC(s)} + 2\text{Cl}_2\text{(g)} \rightarrow \text{SiCl}_4\text{(g)} + \text{C(s)}$ , leaving, after evaporation of the gas, structures like shown on the right in Figure 15.<sup>276,668–675</sup>

Most importantly, the average pore size can be finely tuned by controlling the derivation temperature: between 600 and 1200 °C, it monotonously grows from roughly 0.45 to 1.7 nm. Although there are debates in the literature how accurate the pore size distributions have been assessed,<sup>676,677</sup> various methods of assessing the porosity have been shown to give close results.<sup>678</sup>

With that technology in hands, a French-US team led by Simon and Gogotsi has discovered a striking effect, which they have obtained for both electrolyte solution with organic solvent<sup>679</sup> and a pure RTIL – [EMIm][TFSA] as an electrolyte.<sup>680</sup> We focus on the latter. Using several methods for assessing the surface of the open pore space, they have found that for nano and subnano sized pores the capacitance per unit surface area grows monotonously with the decrease of the pore size, reaches maximum when the average diameter of the pores becomes equal to the characteristic size of the ions, and then sharply drops down (see Figure 16).<sup>681</sup>

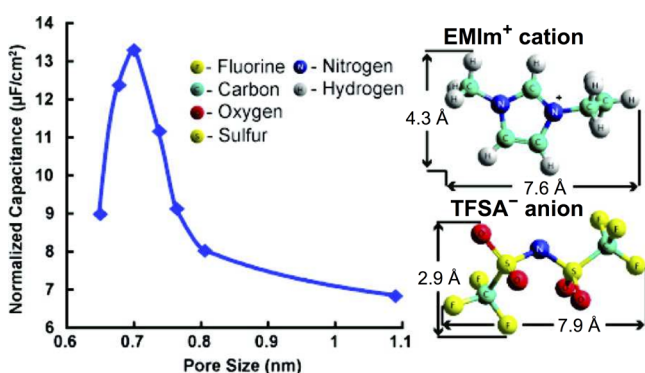


**Figure 16.** Dependence of the normalized capacitance on the pore size. Reprinted with permission from ref 680. Copyright 2008 American Chemical Society.

The drop-down itself raises no questions: the ions cannot get inside such narrow pores and the overall capacitance stops being proportional to the surface of the whole volume of the pores but only to the surface available to ions. When nevertheless scaled to the whole surface area, it becomes vanishingly small. It does not drop down to zero stepwise, as ions do not have just one size (as well as pores!): the involved ions are elongated and their diameter of rotation about the long axis is smaller than the diameter of the average pore; ions can get squeezed into the pore but this is entropically more difficult,

and the capacitance drops down. Note that it is very difficult to measure the capacitance for smaller pores, because of the inaccuracies of measurements caused by impeded transport of ions (they are definitely beyond reach for impedance measurements). However why the capacitance rises with the decrease of the pore size till the ions can still get into the pore?

This fact was first rationalized in ref 450 where the concept of a “superionic state” of ions inside nanoscale pores was suggested. The term “superionic” may sound too flashy but this is debatable. The term has been used to label a speculative phase of superionic water under extreme heat and pressure, which may be natural for giant planets.<sup>682</sup> This phase has properties of both a solid and a liquid, where the molecules break down into a structure made of hydrogen and oxygen ions, in which oxygen crystallizes but the hydrogen ions float around freely within the oxygen lattice. The term superionic is also widely familiar in a different context, as the one that describes fast ion conductivity of one sort of ions (typically cations) in solid electrolytes; in this sense superionic water is a superionic protonic conductor. In the context of electrochemical capacitors, the term reflects the idea, described in Figure 17.

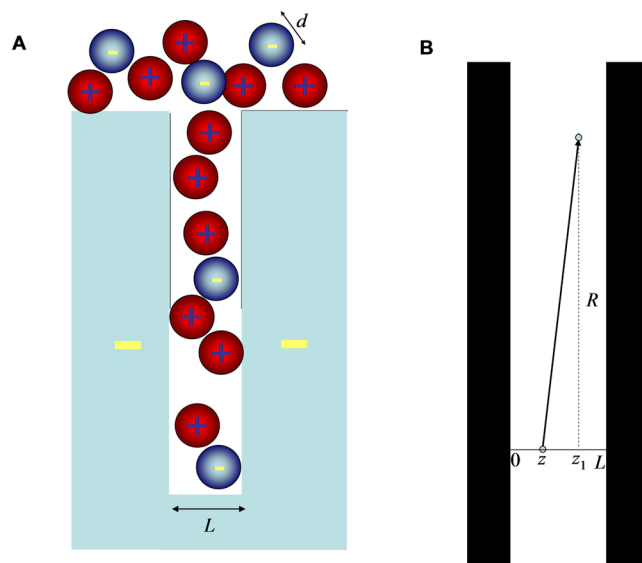


**Figure 17.** (A) Cartoon of filling a slit ionophilic pore with ions, the interaction between which is screened by conductive electrons of the electrode. (B) The geometry of two interacting point charges in a gap between two conductive plates, as described by eq 38.

When the ions get into a conductive pore, their electrostatic pair interactions are no longer given by the Coulomb's law, because they are screened by free electrons of the electrodes. The screening will be maximal in a pore of an ideal metal. For such a system, in a slit pore, electrostatic interaction energy between two elementary charges scaled to thermal energy at large distances from each other

$$R > > L/\pi \quad (37)$$

is given by the following equation:<sup>450,683</sup>

$$\frac{U(R, z, z_1)}{k_B T} = \pm 2\sqrt{2} \frac{L_B}{\sqrt{RL}} \exp\left\{-\frac{R}{L/\pi}\right\} \cdot \sin\left\{-\frac{z}{L/\pi}\right\} \sin\left\{-\frac{z_1}{L/\pi}\right\} \quad (38)$$

Here + and - signs stand for charges of the same and opposite signs, respectively,  $L_B$  is the Bjerrum length (see eq 2). The effective dielectric constant of the interior,  $\epsilon$ , should lie between the vacuum's  $\epsilon = 1$  and the optical dielectric constant of the ionic liquid, responsible for the electronic polarizability of ions,  $\epsilon \approx 2$  (if no solvent additives are involved); for the latter case  $L_B \approx 28$  nm. Applying this equation to the electrostatic interaction of ions of RTIL we must keep in mind that R cannot be smaller than the sum of ionic radii; the ion sizes also determine the smallest value for the gap width,  $L$ , for the ions to get there. For the gap just about to accommodate one layer of ions, the criterion in eq 37 is warranted even at closest separation between the ions; the interaction potential is exponentially screened with the decay length  $L/\pi$ , about three times shorter than the distance of the closest approach of ions.

Hence the ions inside the pore do interact but rather weakly. For instance, ions 0.7 nm in diameter within a pore of the same size at close contact with each other will interact within the energy of  $1.2 k_B T$ . This value will increase with increasing the size of the pore but will however similarly decrease with further increase of the distance between the ions. If the ions do interact weakly with each other, it will be much easier to pack inside the pore ions of the same sign, counterions, in response to electrode polarization, and thereby create what was called the superionic state inside the pore.<sup>450</sup> With the pore increase, the repulsion between the ions of the same sign and attraction between the ions of opposite sign becomes stronger. Hence, the wider the pore, the more difficult it will be to pack there counterions as well as unbind pairs of oppositely charged ions. The latter explains why the specific capacitance of a pore gets larger with the decrease of its size, as long as the ions can fit it.

Another consequence of the contribution of free electrons is image force attraction of ions to the conducting walls. Again assuming perfect metallic conductance, the reduction of the electrostatic energy of an ion, if it is moved from a bulk of the medium with dielectric constant  $\epsilon$  into metallic slit pore filled with the substance of the same  $\epsilon$ , is given by this equation:<sup>450</sup>

$$\frac{W_{\text{im}}}{k_B T} = -\frac{L_B}{L} (\ln 2) \chi(\delta) \quad (39)$$

where  $\delta = z/L$  is the position of the charge from the wall in the units of the total width of the gap and  $\chi(\delta)$  is a function defined as an integral

$$\chi(\delta) = \frac{1}{2 \ln 2} \int_0^\infty dt \frac{e^{2\delta t} + e^{2(1-\delta)t} - 2}{e^{2t} - 1} \quad (40)$$

when the charge is in the middle of the pore,  $\delta = 1/2$ , the integral can be exactly integrated to give  $\chi(1/2) = 1$ , otherwise it can be obtained numerically, see the graph in Figure 18.

Assuming that the center of an ion is in the middle of the pore, we can estimate the energy of transfer of the ion from hypothetic medium of dielectric constant  $\epsilon \approx 2$  into 0.7 nm wide pore at room temperature to be  $27.7 k_B T = 0.7$  eV.

However, ions get into the pore coming not from such a dielectric continuum, in the bulk they are strongly solvated by other ions. We know that the ion-ion cohesion energy as well as self-solvation free energy in RTILs must be negative (and rather large) as RTILs are nonvolatile. With the move of the ion into the pore, that free energy gain will be lost. The electrostatic contribution to the free energy of transfer can roughly be estimated as the energy of transfer of an ion from

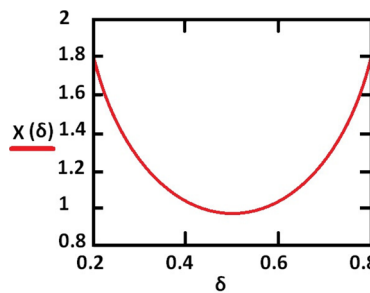


Figure 18. Function  $\chi(\delta)$ , eq 40.

the bulk of dielectric constant  $\epsilon \approx 2$  into highly concentrated electrolyte in "the solvent" of that dielectric constant,  $W_{\text{solv}} \approx -(L_B/2d)k_B T$ , where  $d$  is the ion diameter. This estimate tells us that this energy is roughly  $2 \ln 2$  times smaller than the energy of electrostatic interaction of ion with the pore walls. More sophisticated calculations, may likely give larger solvation energies but the most important issue lies elsewhere: the question whether the ions would like to go inside the pore or not would be also influenced by the entropic contribution to the free energy of transfer. Indeed, the motion of ions in the pore will be confined at least in the perpendicular direction, which would cause an unfavorable loss of entropy. How substantial is the latter term is quite difficult to assess because in the bulk of an RTIL its ions are also neither free to move (at high frequencies the ions in RTIL experience the environment similar to that of an ionic solid<sup>684</sup>). Therefore, the entropic contribution may actually be relatively small. On the other hand, ions may have additional attraction to the walls due to the van der Waals forces or in some cases even covalent interactions.

Thus a priori, we do not know if the ions have a propensity to fill the pores when the pore is not charged or they will have to climb a free energy step to get inside the pore; however, the crude estimates above suggest that they would rather be spontaneously filling the pore. Under such circumstances a wise strategy would be to keep the free energy of transfer as a free parameter of the theory waiting for accurate independent experiments that will answer this question. The answers may be different for different ions and different pore materials as the specific interaction of ions with the walls can make some ions "wall-philic" and some "wall-phobic". Thus, generally, we can speak about ionophilic or ionophobic pores.

Here we should recall again, as already mentioned above, that carbon materials are not ideally metallic. Electric field of ions will penetrate inside the pore walls. This is expected to slightly weaken the screening of interionic interactions and image attraction of ions to the walls.<sup>685,686</sup> "Ideal metal" kind estimates are the upper estimates, corresponding to the strongest screening. We will not go into further details of this question, as investigations along these lines are currently in progress.<sup>687</sup> In particular, it is interesting to know how much different will be the screening between the two sheets of graphene, as such nanotemplated structures for supercapacitors are currently under study;<sup>167,168,372,661</sup> similarly they could illuminate what will be the screening of ionic interactions in between single wall nanotubes in a carbon nanoforest electrode.

We thus now discuss the results obtained within the ideal metal approximation. The first proposed theory<sup>450</sup> which rationalized these ideas was based on an effective medium theory, in which the electrochemical potential of an ion inside

the pore was calculated with account for screened electrostatic interactions with other ions and the electrostatic potential created by the electrode, steric excluded volume effects, entropy of mixing, self-energy and entropy; for details see ref.<sup>450</sup>

Importantly, that theoretical work limited the analysis to narrow pores into which only one complete layer of ions can fit; this was needed for the quasi-two-dimensional description of the layer of ions inside the pore. The effect of the pore width was thus studied in the range from the one equal to the characteristic diameter of the ion,  $1.0 d$  to  $1.9 d$ , which is perhaps a bit too far for this approximation, but the theory can safely be applied up to  $1.5 d$  (just like in the experiments of the Gogotsi–Simon groups.<sup>680</sup> The main message from that work is seen from the two plots that we reproduced here in Figure 19.

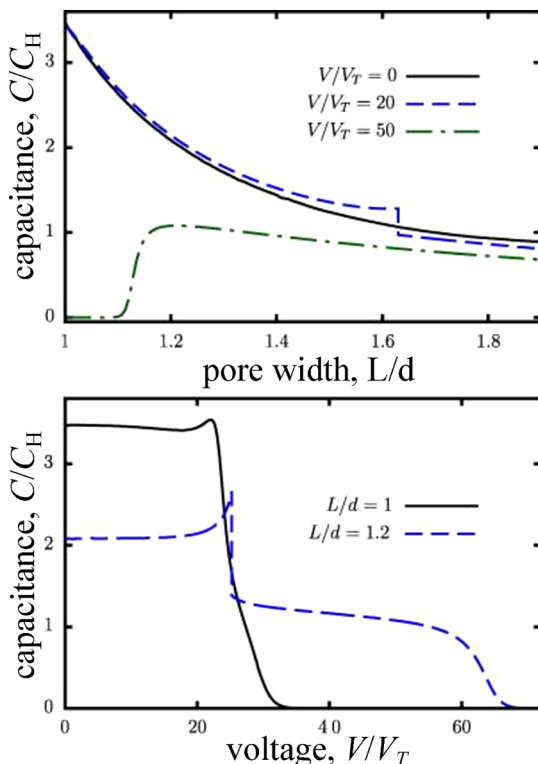


**Figure 19.** Capacitance of a slit pore scaled to Helmholtz capacitance shown as a function of pore width, scaled to the characteristic diameter of ions,  $d$ , for several values of the voltage drop between the electrode and the bulk of ionic liquids [given in the units of the thermal voltage,  $V_T = k_B T/e$ ] (the upper graph), and as a function of voltage for two different pore widths (lower graph). The figure is reproduced with permission from ref 450. Copyright 2011 The Institute of Physics.

The upper plot in Figure 19 displays the effect of pore width for fixed values of voltage. Unless for large electrode polarizations, the capacitance of the pore monotonously increases with the decrease of the pore width, approving the nature of the “Simon-Gogotsi” effect. For substantially large voltage values the capacitance vanishes at yet larger pore width than the ion diameter. This is not because the ions cannot get inside the pore; they still can, but because at such voltages the pore is already fully occupied by the counterions (here anions), and the differential capacitance response to further electrode polarization is zero.

The lower plot in Figure 19, displaying the voltage dependence of capacitance for different pore sizes, shows

three new features. This is the saturation of pores at large voltages, when no further counterions can be accommodated into the pores, mentioned in the previous paragraph. Next, in smaller pores the saturation starts at smaller voltages. Finally, for larger pores saturation takes place in two steps, preceded by a field-induced phase transition. That transition, as predicted, is responsible for an abrupt expulsion of the cations form the pore of the positively charged electrode, passing the phase poor in cations, but in which the amount of anions can still grow till the saturation, and hence the “step” preceding the complete vanishing of the capacitance. This effect is weaker for narrower pores: it practically disappears for  $L/d = 1$ , but it emerges already for  $L/d = 1.08$  (not shown above but displayed in the last figure of that paper, which investigates the possible phases and the nature of that first order transition).

All calculations in that work have been performed under an assumption that the ions have a propensity to fill in nonpolarized pores, i.e. there is a substantial reduction in free energy of individual ions when they are transferred from the bulk into the pore. Under an opposite assumption, Monte Carlo simulations have been performed by Kiyohara et al for different model electrolyte systems in porous electrodes.<sup>688–690</sup> The results of these simulations also predict a field-induced transition but of a different kind: at low voltages the pore resists to being filled by ions and the response to charging of the electrode is very minor (capacitance is close to zero); however, at some critical voltage the counterions abruptly enter the pore.

Leaving aside the question whether the pores of a nonpolarized electrode are filled by ions or not (which, as discussed, is to be answered experimentally) let us concentrate on the mere existence of the phase transition considering the situation of an initially filled pore. This issue was addressed in ref 691 generally aimed on the verification of the predictions of the effective medium theory of ref 450. This article reported grand canonical Monte Carlo simulations, performed for a restrictive primitive model of ionic liquid (charged hard spheres, 0.7 nm in diameter). The screening of electrostatic interactions between the ions by the electrons of the electrode was described exactly as in ref 450 and equal propensity was assumed for each individual cation and anion to get into the interior of a nonpolarized pore. This simulation has again shown the anomalous capacitance effect, although the enhancement of the capacitance with the decrease of the pore size was weaker than in the effective medium theory.<sup>692</sup> Typical voltage dependent capacitance curves reproduced the general character of the capacitance curves, but not all of its features. First of all, no phase transition was observed in the simulations, i.e., no jump-wise expulsion of co-ions (cations), or alike at a “critical” voltage. Consequently, no intermediate co-ion (cation)-depleted phase was detected, within which further increase of the counterion (anion) concentration would have been possible with the capacitance vanishing only at larger voltages, after the pore is completely occupied by the counterions (Figure 20). Instead, the capacitance vanishes immediately after a critical value of the voltage preceded by a peak that characterizes the voltage-induced replacement of co-ions by counterions, accompanied in the range of the peak by “electrostriction” (the increase of the overall density of the ions in the pore).<sup>450</sup>

To distinguish these fine details experimentally is not easy, due to a complicated structure of the electrodes, pore size distribution, more complicated shape of ions in reality, etc., and general difficulties of measuring the capacitance in porous systems. There, impedance measurements are highly problem-

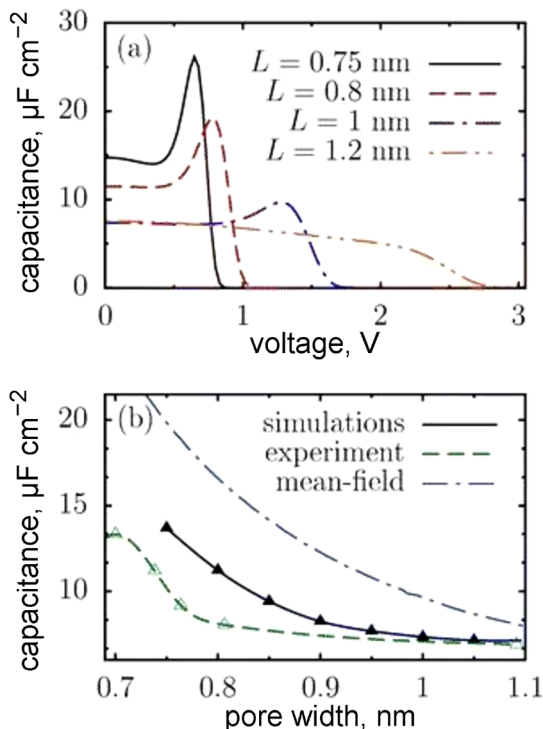


**Figure 20.** (a) Differential capacitance per surface area as a function of voltage, in volts, for a few values of the pore width, as obtained in the simulations of ref 691. (b) Differential capacitance per surface area as a function of the pore width for zero electrode polarization. The solid and the dash-dotted curves show the capacitance calculated by the simulations and the mean-field theory (in ref 450). For comparison, the experimental capacitance from ref 680 is shown by the dashed curve. For details see ref 691. Reprinted with permission from ref 691. Copyright 2011 The Royal Society of Chemistry.

atic, whereas extraction of equilibrium capacitance from cyclic voltamogram is prone to inaccuracies.<sup>693</sup> Some comparison has been made, however, in ref 694 in the context of optimization of energy storage. We underline however that under such circumstances theoretical understanding of the capacitance–voltage and capacitance–pore size dependencies may be pivotal for development of future nanoengineering strategies.

In this context it is worth dwelling on one more lessening example studied in ref 695. Let us consider a cylindrical nanopore in, again, an ideal conductor. Assume that there is a strong propensity for both cations and anions to be there, when the pore is not polarized, and what happens when it gets polarized is that the co-ions get replaced by counterions. How this occurs, kinetically, is another question; we just assume that the swapping is possible due to some degrees of freedom that we do not consider explicitly, such as phonons in the wall, fluctuations of orientations of intrinsically anisotropic ions, internal conformations of ions, etc.

Electrostatic interaction energy of two elementary charges lying on an axis of a cylindrical pore of radius  $a$  at a distance  $R$  from each other is given by an expression:<sup>683</sup>

$$\frac{eU(R)}{k_B T} = \pm 2 \frac{L_B}{a} \sum_{m=1}^{\infty} \frac{e^{-\frac{k_m R}{a}}}{k_m [J_1(k_m)]^2} \quad (41)$$

where  $k_m$  are the zeros of Bessel function of the zero order,  $J_0(k_m) = 0$ :  $k_1 = 2.4$ ,  $J_1(y_1) = 0.52$ ;  $k_2 = 5.52$ ,  $J_1(y_1) = -0.35$ , etc. However, for the purpose of describing interionic interactions,

practically for all relevant values of interionic separations,  $R$ , one may keep only the first term in the sum, using the expression

$$\frac{eU(R)}{k_B T} \approx \pm 3.082 \frac{L_B}{a} e^{-2.4R/a} \quad (42)$$

Thus, electrostatic interaction is again exponentially screened, but stronger than in a slit pore, as the decay range is roughly  $1/4.8$  of the pore diameter, whereas in a slit pore the decay range is  $1/3.14$  of the pore width. This is understandable, because in a cylindrical pore the interacting charges are surrounded by metal “from all sides”.

Assuming again the propensity of both ions to occupy a nonpolarized pore, and considering for simplicity the cations and anions to be of the same size, the Hamiltonian of such system (in the units of  $k_B T$ ) can be written<sup>695</sup> in terms of a 1-dimensional “Ising model with nearest neighbor interaction in external field”

$$\frac{H}{k_B T} = \sum_i \left\{ \frac{\alpha}{2} (S_i S_{i+1} + S_i S_{i-1}) + u S_i \right\} \quad (43)$$

where

$$\alpha = e|U(d)|/k_B T \quad (44)$$

and  $d$  is the “lattice constant”  $\approx$  diameter of the ions. In this description each site of the lattice is occupied either by the cation  $S_i = 1$  or by the anion  $S_i = -1$ . Since  $U(2d) \approx U(d) \exp\{-2.4(d/a)\}$ , and in this model  $2a < 2d$  (so that only one row of ions can fit the pore), the assumption of only the nearest neighbour interaction is justified. The first term under the sum in eq 43 favors cations to neighbor anions. The last term in that sum, in which  $u$  is the electrostatic potential drop between the electrode and the bulk of electrolyte given in the units of “thermal voltage”  $k_B T/e$ , the quantity which is constant inside the pore, favors occupation of each site by a counterion.<sup>696</sup>

Luckily, the 1D Ising model in an external field has a well-known exact solution, and no extra work is needed to obtain the result. Namely, the thermally averaged value of “spin” is given by<sup>697</sup>

$$\langle S_i \rangle = -\frac{\sinh u}{\sqrt{(\sinh u)^2 + e^{4\alpha}}} \quad (45)$$

An important response function is the derivative

$$\chi(u) = \frac{d\langle S_i \rangle}{du} \quad (46)$$

In the Ising model of magnetism the latter is proportional to magnetic susceptibility, whereas in our problem this derivative characterizes the system response to the polarization of the electrode, represented by the capacitance per unit surface area of the pore<sup>695</sup>

$$C = -\chi(u) \frac{eL_B}{2\pi ad} \quad (47)$$

Differentiating  $\langle S_i \rangle$  over  $u$  one gets a simple formula for the capacitance of a single pore<sup>695</sup>

$$\chi(u) = -e^{-2\alpha} \frac{\cosh u}{\{1 + [\sinh(u)]^2 e^{-4\alpha}\}^{3/2}} \quad (48)$$

Assuming that the capacitance of the electrode is dominated by the capacitances of its long pores, for an electrode with a system

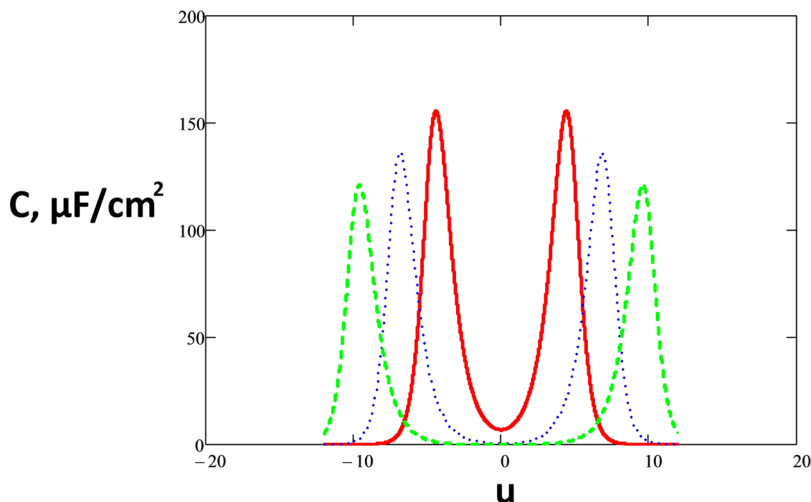


**Figure 21.** Ising model results for the capacitance–voltage dependence<sup>695</sup> (voltage given in the units of “thermal voltage”  $k_B T/e \approx \text{volt}/40$ ) – the effect of the diameter of the pore. Calculated using eqs 47 and 48 for the ions of diameter 0.7 nm. Curves:  $2a = 0.7 \text{ nm}$  [ $\alpha = 2.033$ ], red/solid; 0.8 nm [ $\alpha = 3.249$ ], blue/dotted; 0.9 nm [ $\alpha = 4.622$ ], dashed/green. Reprinted with permission from ref 695. Copyright 2013 The Royal Society of Chemistry.

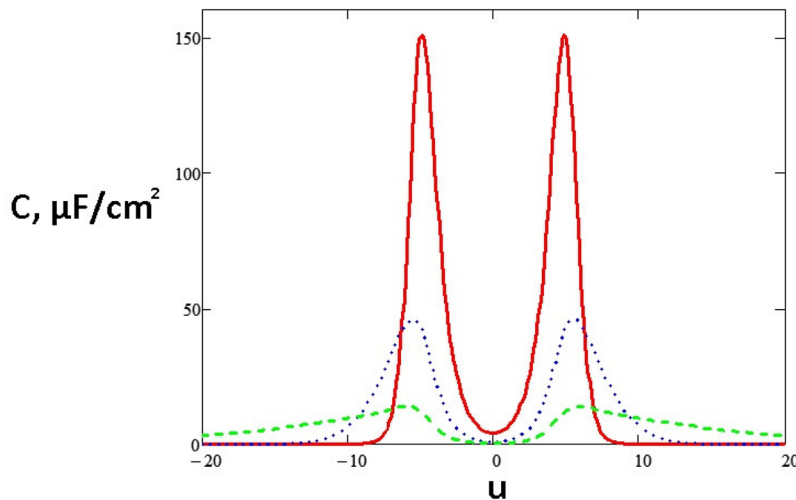


**Figure 22.** Capacitance of a narrow cylindrical pore at dense packing of ions, just about to accommodate one row of ions on its axis weighted over Gaussian pore radius distribution (for details see ref 695). Ion diameter  $d = 0.7 \text{ nm}$ , pore diameter  $2a = 7.2 \text{ nm}$ ; the curves correspond to dispersion of pore radii: 0 (red/solid), 0.05 nm (blue/dotted), and 0.2 nm (green/dashed). Reprinted with permission from ref 695. Copyright 2013 The Royal Society of Chemistry.

of identical pores, this will be the expression for the specific capacitance of the electrodes calculated per its surface area in which the internal surface area dominates.

One may also be interested in the volumetric capacitance, i.e., the capacitance per total volume of the electrodes including its pore volume with porosity  $P$

$$C_v = -\chi(u) \frac{\epsilon L_B P}{\pi a^2 d} \quad (49)$$

The capacitance per mass of the electrode is given by

$$C_m = -\chi(u) \frac{\epsilon L_B P}{\pi a^2 d \rho_m (1 - P)} \quad (50)$$

where  $\rho_m$  is the mass density of the bulk electrode material.

According to these equations, the voltage dependence of the capacitance is entirely determined by one parameter: the coupling constant  $\alpha$ . How strong is the latter? Following eqs 41 and 42, for  $d = 0.7 \text{ nm}$  and  $a = 0.35 \text{ nm}$ ,  $\alpha = 2.033$ , but when

the pore radius becomes just 0.2 nm larger,  $\alpha = 4.622$ . All in all, the interaction energy of neighboring ions in the pore is larger, but not much larger, than the thermal energy. Had it been much greater, it would have been difficult to charge the pore and the latter would have taken place only for large voltages. The graphs in Figure 21 show eq 47 and eq 48 in action: they demonstrate how the capacitance–voltage plots depend on the coupling constant affected by the increase of the pore radius at a constant packing of ions on the axis. We see that when the pore diameter is just a tiny bit larger than the diameter of an ion, the capacitance becomes almost zero for small voltages and it takes some voltage to start accepting the charge into the pore. The position of the maxima is roughly at  $u_{\max} \approx 2\alpha + \ln 2$  and after this voltage the pore admits about 70% of the counter charge, and further charging becomes increasingly difficult. The capacitance peak has a “resonance” nature. One needs to apply that much voltage that will “crash” the propensity for cations and anions to pair, i.e., the reduction of the free energy gained

by getting only counterions into the polarized pore must beat the energy of cation and anion interactions.

The effect of temperature is tricky because temperature enters both  $u$  and  $\alpha$ , we refer the reader to ref 695 for details.

However, such sharp pictures refer to the capacitance of a single pore. Even a minor dispersion of pore sizes will cause a dramatic change on the capacitance–voltage plot. This is not surprising because Figure 21 shows a very strong, resonance-kind effect even for a small variation of the pore size. Figure 22 shows the capacitance per unit surface area averaged with a Gaussian distribution of pore sizes for different dispersion of the pore sizes (note that the same averaging procedure for the volumetric capacitance or gravimetric capacitance, will lead to slightly different shape of the curves than for the specific capacitance, because of the different power of the pore radius in the denominator).

The main lesson from the results of ref 695 (some of these results we have reproduced in Figures 21 and 22) is that the voltage dependence becomes milder (peaks becomes much less sharp) with inclusion of the pore radius distribution, and the overall value of capacitance becomes smaller except for at large voltage wings. This “toy” model allows to parametrize and “visualize” these complicated effects in most simple terms.

Note that these graphs were plotted under an assumption of dense packing of cations and anions (no vacancies in the lattice, i.e., the free energies of transfer of ions from the bulk of the solution into the interior of the pore is negative and much greater in the absolute value than the thermal energy), and more specifically, for the same propensity for the cations and anions to enter the pore.

The account for the latter effect is trivial:<sup>695</sup> a difference in the free energy of transfer between cations and anions will cause a shift of the curves along the voltage axis. For instance if the absolute value of the free energy of transfer of anions into the pore is larger than for cations by the value of  $\Delta W$  (even if they are of the same size, but because of some specific interaction with the walls), this would be equivalent to subtracting half of that difference (scaled to  $k_B T$ ) from  $u$  in the expression for the Hamiltonian.<sup>37</sup> The minimum of the capacitance curves will then be shifted to  $u = e\Delta W/2k_B T$ , and the whole curve will be shifted to the right by that value.

However, when the unpolarized pores prefer to stay empty, or the free energy of transfer is not much greater than the thermal energy, the Ising model will be inapplicable. Voids in the lattice must be considered statistically and on the same footing as ions. The account for the presence of voids requires a more sophisticated, three-state model, where the new state  $S_i = 0$  means that the site is occupied by the void. Such three-state model, an analogue of the so-called Blum–Every–Griffith (BEG) model, is currently under investigation. It should show richer behavior of charging and the capacitance–voltage dependence in a situation when the competition in filling the pore is not only between cations and anions but also between ions and vacancies.

The consequences of the effects of the size of the pore and of the pore size distribution (the latter have been studied by averaging the results of Monte Carlo simulations in slit pores using pore size distributions extracted from experimental data) have been analyzed in ref 694. The results have been compared with specially performed measurements of the capacitance and the pore size distribution assessed by using established porosimetry techniques.<sup>694</sup> Most importantly, that work addressed attention to the question of the optimal size of the

pore for the maximal energy storage; we think that it is worth dwelling on the question in the next section.

Before we move to the next section we would like to overview an alternative theoretical approach to the capacitance of narrow slit pores developed in a recent work by Skinner et al.<sup>364</sup> Following ref 450, the authors of that work based their model on the idea of exponential screening of interionic interactions. Their main point, however, was that the mean-field theory is not quantitatively correct and a more “microscopic” approach should be developed. Before discussing this interesting work in details, we outline two important circumstances.

The authors of ref 450 have developed their model for what we now call ionophilic pores; that means that these pores are filled with cations and anions when the electrode is not polarized. That filling may be electroneutral if there is no preferential adsorption of one sort of ions over another into the interior of the pore. In such case, all what occurs upon charging the electrode (applying voltage relative to the bulk of the electrolyte) is that co-ions in the pore will tend to get replaced by counterions. For such systems that have a dense layer of ions present inside the pore at any voltages, the mean-field theory is expected to be (qualitatively) a good approximation; and, indeed, the validity of the theory was confirmed by Monte Carlo simulations in ref 691.

In ref 364 it was acknowledged that going beyond the mean-field in the ionophilic pore is difficult; therefore the authors of that work have chosen to treat the opposite limit, ionophobic pores (the pores that are empty at zero voltage). A simplifying circumstance here is that at a substantially unfavorable free energy of transfer of ions into the pore (free energy penalty), practically no co-ions will be in the pore but only counterions. That makes the system more convenient for theoretical treatment.

Assuming the presence of only one sort of ions in the pore (counterions) the authors of ref 364 presumed that in the ground state (i.e., at zero temperature) the ions form a two-dimensional Wigner crystal; for such lattice they have calculated the energy as a function of a given concentration of counterions in the pore. By minimizing the energy with respect to the counterion concentration they obtained the average concentration for a given voltage and, correspondingly, the capacitance at, formally,  $T = 0$ . The capacitance was obtained in a form of a parametric dependence on voltage with elegant analytical formulas for the capacitance–voltage dependence obtained in the limiting cases of small and large voltages (see eqs 9 and 10 in ref 364). At finite temperatures, however, such results may be valid only at large voltages where the concentrations of counterions in the pore are large and, therefore, the interaction of nearest neighbors at average distances between them will be larger than  $k_B T$ .

Consequently, the authors of ref 364 concluded that at room temperatures the concept of Wigner crystal should fail and they pursued instead a virial expansion approach to the calculation of the free energy since the interactions between ions are exponentially screened and are, thereby, of short-range character. They obtained the corresponding parametric result for the capacitance–voltage dependence at a finite temperature (see eqs 16 and 17 in their paper). In the following sections of ref 364, the authors extended this model for a description of a multiporous systems with ion–ion interactions across the neighboring walls and the effects of imperfect screening that we have discussed earlier in this review.

This result is complementary to the result of ref 450 that covers the case of ionophilic pores and can fill the gap in the theoretical description of capacitance in an ionophobic slit pore. As the authors of ref 364 note, the results that are based on the first virial expansion should be valid at low counterion concentrations in the pore but should fail at high concentration. However, the comparison with computer simulations performed in that work seems to show the opposite trends.<sup>364</sup> The authors of that work compared their theoretical results with Monte Carlo simulations performed at (i) a finite free energy penalty for the ions come inside the pore and (ii) zero free energy penalty (i.e., mild or no ionophobicity). In these simulations the ion diameter was taken to be equal to the pore width. The overall shape of the presented simulation curves in ref 364 shows one maximum and the saturation of the capacitance at large voltages (interestingly, the simulation results presented in that work do not show abrupt phase transitions with the variation of voltage that were obtained for a similar system by Kiyohara et al.,<sup>688</sup> who also simulated capacitive charging of ionophobic pores). The simulated capacitance curves show qualitatively similar character with the theoretical model developed in that work only in the limit of large voltages where, indeed, only counterions are present in the pore and at high ion concentrations; the discrepancy becomes quite significant at small and intermediate voltages (see Figures 4 and 5 of ref 364). The mechanisms of the observed difference at small and intermediate voltages between the theoretical and simulations results are not very clear. Perhaps, more additional comparisons with simulations performed for different free energy penalties and different ion size/pore width ratios are still needed to fully assess the overall performance of this new theoretical model.

### 7.3. Energy Storage in Nanoporous Electrodes: What Is the Optimal Size for the Pores?

Continuing the discussion of ultraporous electrodes, in which the pores can accommodate only one layer (in slit pores) or one row (in cylindrical pores) of ions, we can ask ourselves a question, what should be the optimal size of the pore for the maximal energy storage? Let us stick for definiteness to a slit pore, as was studied in ref 694; however, we note that similar analysis can be performed for cylindrical pore geometry using the equations presented above<sup>697</sup> or of any more general model, such as, e.g., the Blum–Emery–Griffith model.

The volumetric density of electrical energy stored in a sample composed from an array of slit pores of width  $L$  with the thickness of the walls,  $W$ , reads as<sup>694</sup>

$$E(V) = \int_0^V dv vC_v(v) = \frac{2}{W + L} \int_0^U dv vC(v) \quad (51)$$

In all of the curves for the differential capacitance shown above, the latter term vanishes after a certain value of voltage because the pore cannot accommodate more charge after some point. It is therefore becoming a question of finding an optimum, what should be the best pore size for the largest energy density for a given voltage, particularly because (cf. Figure 23) those capacitance curves that “survive” at larger voltages lie majorly lower than the “nonsurvivors” at smaller voltages. Integration in eq 51 and the maximization of the result for the stored energy with respect to the pore size for a given voltage gives graphs of the kind, shown in Figure 23.<sup>694</sup>

This is just a snapshot from a larger number of results of ref 694: there one can find other lessening curves as well as those

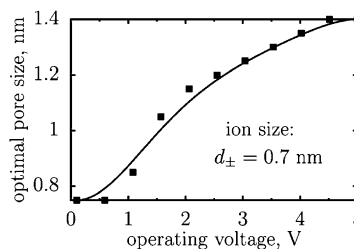


**Figure 23.** Optimal pore width of a porous supercapacitor as a function of the applied voltage. The symbols are obtained from the integration of MC simulation results for the differential capacitance, and the line using the spline curve that approximates them. The figure is reproduced with permission from ref 694. Copyright 2012 The Royal Society of Chemistry.

demonstrating the role of pore size distribution. However, the main message is that for a given operating voltage, the energy density is a nonmonotonic function of the pore width and its maximum depends on the voltage. To instruct a material engineer one needs to know the capacitance–voltage dependence which can be identified by theory, simulation<sup>443</sup> or, of course best of all, measurements. Narrowing the pore size distribution leads to the increase in the stored energy density, and a monodisperse electrode with a carefully selected pore size may be ideal for the energy storage in a nanoporous supercapacitor (cf. Figure 6b in ref 694). Note that the optimization that we were talking about so far was for “ultranarrow pores” that can accommodate just one row or one layer of ions. Larger nanopores would require different treatment.

### 7.4. Larger Nanopores and the Capacitance Oscillations

A lesson how intensive is research in this area these days is given by the following story. On 24 August 2011, two papers were received: one by *ACS Nano*<sup>531</sup> and one by *Nano Letters*,<sup>461</sup> and a month later by *The Journal of Physical Chemistry Letters*,<sup>698</sup> all published in October 2011! All three papers highlighted the phenomenon inherent to their titles: oscillatory behavior of capacitance as a function of pore size when the pore size is increasing from an ultrasmall value ( $\sim 0.7\text{--}1.0$  nm; the range where the anomalous capacitance effect is observed) to the value of several ion diameters. Although different methods as well as different levels of description of the molecular structure of RTIL ions were used in these papers (classical DFT of a restricted primitive model in ref 461, MD simulations of an assembly of charged spheres in ref 531, and fully atomistic MD simulations for model [EMIm]<sup>+</sup> and [TFSA]<sup>-</sup> ions in ref 698, all performed for model carbon slit pores), the results were qualitatively similar. The work<sup>461</sup> was later extended to the case of an RTIL-(organic)solvent mixture in a pore.<sup>462</sup>

The common conclusion of these works was that the capacitance undergoes “oscillations” with the pore size; this effect was interpreted by the layering effect. As long as only one layer of ions can fit the gap, the smaller the gap, the higher the capacitance, but when the increase of the gap will accommodate the second layer the capacitance again increases, just because more charge can be accommodated there. And off it goes, because when we further slightly increase the gap size, not yet allowing for the third layer, the capacitance will go down again due to weakening of the screening of interionic interactions, but with the accommodation of the fourth layer it will start growing again, and so on. Reference 461 has reported data for pore width up to 12 ionic diameters (it was more difficult to simulate

such large system by MD, so that refs 531 and 698 have limited their consideration by a couple of ionic diameters), with decaying oscillations extending in this ideal system up to 8 ionic diameters.

Although these predictions have not yet been experimentally verified, we believe that the effect may be real because it has clear physics behind it. According to the concept of the superionic state in a nanopore, every time when we increase the pore size we make the interaction between ions stronger and, therefore, impede the ability to charge the pore due to the increased repulsion between counterions. However, opening the possibility to fill in the next layer we double the charge and thus the capacitance per unit surface area of the pore should go up (we note that the volumetric capacitance may not; this must be specially checked for each system). The two competing trends must provide the decaying oscillations.

None of the three mentioned papers have studied the interplay of the pore width and the voltage dependence, which must be very interesting. It would be natural to expect that vanishing the differential capacitance in wider pores will take place at much larger voltages. This was predicted for narrow pores,<sup>450,691,694</sup> but in wider pores, the effects will be even more pronounced and interesting “oscillatory” dependences might appear. It will be relevant to perform investigations similar to refs 450 and 691 and in particular to ref 694 in terms of understanding the optima for energy storage for a wider scale of pore sizes.

### 7.5. “Quantized Friction” in Confined Nanofilms of RTILs

We have already discussed above some of the papers that we are going to highlight in this section in the context of layering and overscreening in RTILs. However, the results presented in these papers have also a special value for understanding the properties of RTILs as potential lubricants,<sup>181</sup> with a highly relevant (for some applications, e.g., reading computer hard disks) possibility of friction control by voltage.

Reference 83 reported high-resolution measurements of the forces between two atomically smooth surfaces across the film of the studied RTIL for film thicknesses ranging from 1 to 6 ionic diameters. Both, normal force, the so-called structural force, and a shear force were measured, using the classical surface force apparatus of mica cross cylinders,<sup>301</sup> as a function of surface-to-surface separation. For the films thinner than 2 nm, oscillatory normal forces were observed with decreasing the surface-to-surface separation, as pairs of ionic layers were squeezed out of the film. This was very much expected, as one more evidence of the layering structure of the ionic liquid between charged walls (freshly cleaved mica surfaces are spontaneously negatively charged). However, measurements of the shear force has revealed spectacular effects. Friction appeared to be 1 or 2 orders of magnitude lower than that observed for the films of nonpolar molecular liquids. Most interestingly, these studies have revealed a phenomenon of “quantized friction”. Comparing the stable thicknesses of the film with 1 layer and 3 layers (2 layers are not stable between the identically charges surfaces for obvious reasons: the net charge in the neighboring layers should alternate, and this cannot “make happy” both surfaces), the friction of a 1-layer film is an order of magnitude higher than that for a three layer film, with an abrupt jump of the friction coefficient between the two states.

These fascinating results may have far leading consequences for the application of RTILs as lubricants;<sup>87,88,181</sup> however,

qualitatively, they can be explained in a relatively straightforward way. The authors of ref 83 attributed these effects to “geometric and charge characteristics of ionic liquids”, assuming that “the irregular shapes of the ions lead to a lower shear stress, while the strong coulombic interactions between the ions and the charged confining surfaces leading to a robust film”, when the film is one layer thick. Speaking in physical terms, the whole effect should be about the interplay between the patterns of charges on mica and those in the layers of RTIL. If those can be commensurate for a thin film, the shear resistance must be strong. However, commensurate or not, the laterally oscillating patterns of electric field created by a regular pattern of charges on the mica surfaces, with periodicity length  $a$ , will decay into the bulk of the film exponentially with a decay range  $a/\pi$ . This is a “fast” decay, and the inhomogeneous component of the field crucial for shear resistance and friction will not be felt for thicker films. With that said, these phenomena certainly deserve development of a proper theory or computer simulation.

Bou-Malham and Bureau<sup>84</sup> investigated effects on surface charges on flow and molecular layering under nanoconfinement in two different RTILs that have the same organic cation,  $[\text{BMIm}]^+$ , and two different counterions ((i)  $[\text{BF}_4]^-$  and (ii)  $[\text{PF}_6]^-$ ). They also used the surface-force apparatus technique. This study has shown drastic effect of the charge surface on the layering of the RTILs in the nanoconfinement. Both ionic liquids start exhibiting strong molecular layering when confined between charge-bearing mica surfaces. The authors of ref 84 have shown that such layering dramatically affects the flow properties of the liquids: as confinement gets narrower, the viscosity increases over several orders of magnitude, until the liquids eventually get jammed and exhibited a solid-like response. However, the same liquids confined between noncharged methyl-terminated surfaces displayed no such layering and still flowed through the gap with their bulk-like viscosity, even when confined down to two monolayers in thickness.

The charge on the mica surface is fixed, so one cannot probe the effects of the voltage variation, which must obviously affect the structure of the RTIL film. Hence, very recently Sweeney et al.<sup>86</sup> went further and investigated a possibility of controlling friction by changing the voltage, using electrochemical *in situ* AFM configuration. They have studied gold electrode in RTIL measuring the friction by sliding the silica cantilever at nanoscale distance over the electrode surface. Friction force was recorded as a function of potential and applied load, varying normal loads up to 25 nN.

For all the probed potentials the shear resistance increased with the normal load, but friction was shown to depend on electrode potential: the friction coefficient was found to be always higher with positive potentials. The authors interpreted it as follows. For positive potentials the probe displaces the last cation layer for normal loads greater than 2.5 nN but never displaced the last anion layer for all other normal loads used. Correspondingly the last anion layer is displaced at negative potentials, but at no force it displaces the cation layer, kept solid at negative potentials. The authors of that very interesting paper consider various other features of the electric field effect on friction, stressing the importance of that work for a future “nanotribotronics”; a science of manipulating friction at the nanoscale, in this case by using such a handy weapon as electrode potential.

In their recent work,<sup>88</sup> Li et al. went farther in this direction and used the colloid probe AFM technique to study effects of

ion structure, surface potential and sliding velocity on RTIL lubricity. It was convincingly shown in that work that nanotribotronic tuning can be indeed performed for several different RTILs to either increase or decrease the RTIL's lubricity. Moreover, in that work as well as in ref 575, it was shown that the interfacial properties of the RTIL-electrode contact layer can be tuned by both, the surface potential as well as the RTIL ion structure (i.e., the alkyl chain length, anion type etc). These findings opened new avenues for rational interfacial design of RTIL-solid systems and we foresee many new works and applications in this direction in the nearest future.

## 8. EXAMPLES OF OTHER APPLICATIONS OF RTILS AT EIS

In this section we will briefly overview examples of other applications of RTILs at EIs such as batteries, fuel cells, solar cells and microactuators.

We note that, as mentioned in the introduction, there are many other application areas of RTILs at EIs such as electrodeposition, reactive media for electrosynthesis, electroanalytical and sensing applications etc. However, there are several good reviews and books on these subjects already and due to space limitations we would like to address interested readers to such essays, as refs 25, 64, 199, and 699 (electrodeposition), refs 162 and 163 (electrosynthesis and electrochemical reactivity), refs 19 and 30 (electroanalytical chemistry), ref 164 (energy), and refs 23 and 268 (sensors); see also refs 35, 38, 97, 98, and 602 and references therein for general information about RTIL applications.

### 8.1. Batteries

The main advantages of using RTILs in batteries are (i) large EW of some RTILs; (ii) nonvolatility; (iii) higher conductivity compared to standard polymer electrolytes used in commercial batteries; (iv) large operation range of temperatures; and (v) many of RTILs are nonflammable.

Indeed, large EW leads to higher operation voltage of the batteries and, consequently, to higher amount of energy storage per battery mass. Batteries are meant to operate for years, and, improves their shelf life.<sup>700</sup> Therefore, for years, nonvolatile polymer electrolytes were used in commercial batteries for electronic applications. However, the polymer electrolytes have one main drawback - their low ionic conductivity that leads to high ohmic losses in batteries.<sup>209,701</sup> RTILs, being also inflammable, have much higher conductivity than the polymer electrolytes. At the same time, they can operate in a large range of temperatures. Because they furthermore are nonaggressive to metals and other substances, that makes them attractive alternative electrolytes for large-scale commercial use in batteries. There is an ongoing research on the properties of new battery systems based on RTILs.<sup>135,140,169,170,388,702</sup>

Most of these studies are focused on applications of RTILs in lithium-based batteries,<sup>703</sup> although there is intensive ongoing research on replacing lithium in batteries by other metals, e.g., sodium or magnesium<sup>164</sup> (for general overview of recent developments in lithium-ion rechargeable batteries see ref 700). Recent review by Lewandowski and Swiderska-Mocek<sup>127</sup> overviews properties of RTILs as electrolytes for lithium and lithium-ion batteries. They point to the critical importance of the formation of the solid electrolyte interface (SEI) on the anode surface for correct operation of secondary lithium-ion batteries based on RTIL electrolytes. The authors conclude that

SEI layer may be formed by electrochemical transformation of (i) a molecular additive, (ii) RTIL cations, or (iii) RTIL anions. They argue that, due to the SEI formation the reference system in lithium battery-relevant electrochemical studies should be Li/SEI/Li<sup>+</sup> rather than Li/Li<sup>+</sup>.<sup>704</sup> Reference 127 also discusses such properties of RTIL electrolytes as viscosity, conductivity, vapor pressure and lithium-ion transport numbers, all from the point of view of their influence on battery performance. Recent updates on using RTILs for developing advanced battery technologies can be found in Chapter 2 of ref 164.

Primary lithium batteries that use a metal lithium electrode (Li/Li<sup>+</sup>) have higher energy densities compared to the secondary lithium batteries that use a carbon negative electrode which works as a host for Li<sup>+</sup> ions by intercalation.<sup>3,701,705</sup> However, one of the main problems with the development of rechargeable primary lithium batteries is that the metallic lithium electrode used in these batteries quickly loses its smoothness during the repeated charging/discharging cycles with consequent forming of dendritic deposits on the electrode surface.<sup>3,388,703</sup> These deposits may cause an internal electrical short-circuit between the cathode and anode that would quickly deteriorate the battery properties. The deterioration of the electrode surface is the main reason of why despite of the irreversible character of the reaction on the Li/Li<sup>+</sup> electrode, the number of battery charging/recharging cycles is limited. Another problem is safety issues related with dangerous reactions of metallic lithium and its alloys with water and other commonly used solvents.<sup>703</sup>

The high potential of RTIL-based electrolytes to overcome these complications because of their high electrochemical stability and overall chemical inertness was recognized in the early 2000s.<sup>703,706–708</sup> Howlett et al. reported high lithium metal cycling efficiency in RTILs (made from *N*-methyl-*N*-alkylpyrrolidinium cations with [TFSA]<sup>-</sup> anion).<sup>708</sup> Shin et al. suggested to incorporate of RTILs into polymer electrolytes to develop safe and stable battery electrolytes with higher conductivity than the "dry" polymer electrolytes.<sup>705</sup>

To increase conductivity, RTILs in battery applications can be mixed with organic solvents.<sup>387,709,710</sup> Schweikert et al.<sup>710</sup> investigated formation of lithium dendrites in lithium/Li<sub>4</sub>Ti<sub>5</sub>O<sub>12</sub> battery cells with different electrolytes by using a combination of different experimental techniques such as electrochemical impedance spectroscopy, scanning electron microscopy and in situ <sup>7</sup>Li nuclear magnetic resonance spectroscopy. They demonstrated that the growth of lithium dendrites is significantly correlated with the electrolyte employed. All electrolytes used in that work, based on the ionic liquid 1-ethyl-3-methylimidazolium bis(trifluoromethanesulfonyl)azanide ([EMIM][TFSA]) (either neat [EMIM][TFSA] or a mixture of [EMIM][TFSA] with ethylene carbonate or propylene carbonate), show reduced dendrite growth in comparison to the standard electrolyte for Li-ion batteries, lithium hexafluorophosphate (Li[PF<sub>6</sub>]) in ethylene carbonate/dimethyl carbonate (EC/DMC). In the same work it has also been shown that Li[PF<sub>6</sub>] in [EMIM][TFSA] and Li[PF<sub>6</sub>] in [EMIM][TFSA]/propylene carbonate efficiently suppress lithium dendrites.

Even higher energy storage than in Li-ion batteries can be achieved in Li–O<sub>2</sub> and Li–S batteries.<sup>711</sup> However, these devices currently exist only as prototypes because there are still a number of problems that need to be solved for the development of commercially viable Li–O<sub>2</sub> and Li–S batteries. These are safety, stability, cycling efficiency, formation of

insulation layers on the electrode, etc.<sup>709</sup> Use of RTILs as working electrolyte in Li–O<sub>2</sub> and Li–S batteries is discussed as one of the possible solutions to overcome these problems.<sup>712,713</sup>

In all of the battery applications understanding the nanoscale structure of RTILs at electrodes is crucial for developing theoretical concepts of their performance. It is important to achieve a microscopic level of understanding of the formation of dendrites and the elementary act of electrode kinetics, if electron transfer limited.

### 8.2. Fuel Cells

Protic ionic liquids are used as proton conducting media in fuel cells due to their high proton conductivity, low water sorption, thermal stability, and low viscosity.<sup>714,716</sup> Recently, van de Ven et al. used the ionic liquid 1-H-3-methylimidazolium bis-(trifluoromethanesulfonyl) imide ([HMIIm][TFSA]) as conductive filler in a tailor-made porous, polymeric polybenzimidazole (PBI) support as proton conductive membrane for high temperature (>100 °C) fuel cell applications.<sup>176</sup> They have shown that the fuel cell performance of this membrane clearly exceeds that of Nafion 117 at temperatures above 90 C. A power density of 0.039 Wcm<sup>-2</sup> was obtained at the intended operation temperature of 150 °C; that work proved that such PBI/RTIL membranes can be considered as serious candidates for low temperature fuel cell applications.

The role of the interface between the porous electrodes and the electrolyte is complicated here by the fact that electrolyte is imbedded into the membrane, and the interface contains usually three phase boundaries.

### 8.3. Solar Cells

RTILs has been actively used for electrolytes in dye-sensitized solar cells (DSSCs) that have attracted much attention as low-cost alternatives to conventional inorganic photovoltaic devices.<sup>171,172,174,373,715,716</sup> The highest reported photoelectric conversion efficiencies of DSSC with RTIL electrolytes are within 7–8%.<sup>716</sup> Liquid-state DSSCs with standard electrolytes have stability issues due to volatility of electrolytes; however, these drawbacks can be overcome by using nonvolatile and electrochemically stable RTILs<sup>174,175,717–719</sup> (for an overview of recent developments in this area see ref 175).

### 8.4. Flexible Energy Storage Devices

It has been shown that RTIL-nanocarbon composites can be used as soft functional materials for different applications including electronics and energy.<sup>367,373,720,721</sup> Pushparaj et al. demonstrated in their paper<sup>720</sup> the possibility of development of energy-storage devices such as supercapacitors, Li-ion batteries, and their hybrids based on flexible nanocarbon-cellulose-RTIL sheets. As they write in their paper “selfstanding flexible paper devices can result in unprecedented design ingenuity, aiding in new forms of cost-effective energy storage devices that would occupy minimum space and adapt to stringent shape and space requirements”.<sup>720</sup> Tamilarasan and Ramaprabhu in their recent paper<sup>274</sup> performed thorough analysis of several factors influencing performance of hybrid electrode materials based on carbon nanotubes-graphene-RTIL composites for high performance supercapacitors.<sup>274</sup> For an overview of nanocarbon composites for capacitive energy storage see also the recent review of Simon and Gogotsi.<sup>276</sup>

### 8.5. Miniaturized Nanocarbon Based Electronics

Due to the low volatility of RTILs they can be used on a very small scale, i.e. at very high surface to volume ratios. This makes

them very attractive as electrolytes for nanoscale electronic components such as microsupercapacitors,<sup>376</sup> electrolyte-gated field-effect-transistors,<sup>187,189</sup> and polymer semiconductors.<sup>188</sup> Understanding the structure of electrical double layer at micro and nano electrodes is crucial for understanding the operation of these devices.

### 8.6. Polymer Electrolyte Composite Electroactuators

The main principle of EDL-based electroactuators is relatively simple, and as such electroactuators are nothing else than plane capacitors with electrodes attached to bendable metallic plates.<sup>722–725</sup> Electrolyte here is impregnated into the polymer matrix, separating these plates. If the sizes of cations and anions are dramatically different, by applying voltage between two electrodes one redistributes ions between them. The region near the electrode rich in larger ions gets swollen and strained, whereas the region at the other electrode, rich in smaller ions, gets shrunk and relaxed. Correspondingly, the two plates bend in the latter direction. Changing the sign of the voltage between such electrodes will change the direction of bending. Ideally, if there is no trapping of ions and hysteresis, this process will be fully reversible (which of course rarely happens in real systems).

This principle lies in the basis of a voltage-controlled “micromuscle”. Just a few volts are typically needed to achieve substantial actuation, making such systems prime candidates in applications to smart robotics and prosthetics.<sup>95,726</sup> Equally the forced bending of such beam generates voltage, which may be used for sensing beam bending fluctuations in turbulent flows, where local pressure and fluid-velocity fluctuations will generate alternating voltage, of special importance for hydraulics and aeronautics.<sup>727,728</sup> As transducers, one can envisage their applications as motion detectors and high performance sensors in artificial organs.<sup>729–732</sup> Last but not least, engineers think about using such electroactuators for generating electricity from ocean waves, coastal surf, and river white waters.<sup>733,734</sup>

The largest effect on bending is when only ions of one sign can move (can be of several sorts); the other is attached to the side chains of the polymer. Such system is realized when exchanging protons of Nafion by as-large-as-possible ionic liquid cations, which have an ability to move, with terminal SO<sub>3</sub><sup>−</sup> groups immobile residing on the side chains.<sup>735,736</sup> In addition to the EDL-formation-induced swelling strain, there is also an “electrostatic” stress on the polymer backbone due to the Coulomb repulsion of the net local unbalanced charge in the cation-depleted regions consisting predominantly of immobile anions. Depending on the average concentration of charge carriers, the latter effect can amplify the -swelling-induced bending or compete with it.<sup>737</sup> To avoid high friction and achieve faster electroactuator response organic solvent additives are often used to “lubricate” the movement of cations.

Practically analytical theory of such systems have been recently developed which formulates the laws of equilibrium bending and bending dynamics;<sup>737,738</sup> for review of previous theories see these last works. However, that theory has been developed for electrode surfaces with a mild roughness (with the correlation length of roughness much larger than the characteristic thickness of the EDL (cf. ref 663). In reality, the trend is to maximize the surface area, in order to amplify the electroactuator’s bending response. Similar to supercapacitors, porous electrodes are used, down to nanoscale porosity, e.g., by using nanotemplated structures such as carbon nanoforest rooted into the current collector beams. There was yet no theory adapted to such more complicated confinement.

Going back to the classical flat plate geometry EDL-based electroactuators, we note that the description of the EDL here is somewhat different from the case of RTIL structures at other liquid–solid flat interfaces. First we note that here we deal with only one sort of mobile ions (cations) that rearrange upon building the EDL at the anode side consequently leaving behind almost bare anode layer at the cathode. All ions in electroactuators are imbedded in the polymer matrix with average  $\sim 1$  nm distance between the side-chain-anions, and thereby the distance between the ions is (on average) also  $\sim 1$  nm. There could be also some solvent molecules added to widen and lubricate pores of the membrane. All in all, concentrations of ions might be somewhat lower in the electroactuator membrane than in neat RTILs. For such systems the theoretical framework developed earlier for solid electrolytes with single mobile charge carriers<sup>644</sup> seems to serve its purpose as demonstrated in refs 737 and 738.

## 9. CONCLUDING REMARKS

This review discussed principles of the theory of the EDL in RTILs at flat interfaces, the characteristics of RTILs in electrified nanoconfinement, and manifestations of these properties in various experimentally observed phenomena potentially important for generation and storage of electrical energy, information transduction and sensing, electrode kinetics and metal processing, and (nano)mechanical applications of RTILs (lubrication, electroactuators, etc.). It was centered on the topics that have recently received some understanding (through the theory, reasonable models, simulations, and experiments) and those where new pressing questions that await answers could be formulated.

There is no easy way to end a review of the area where new important papers appear almost every day and the total number of publications reached (according to the ISI WoS) several thousands, with >500 published in just 2013. We, therefore, conclude it with several remarks intended to sketch a big picture.

It is now commonly accepted that the EDL structure in RTILs is principally different from that of diluted electrolytic solutions, due to the effects of ion packing and strong Coulomb correlations (“lattice saturation” vs “overscreening”). Both kinds of these effects become crucial due to high ionic densities of pure RTILs, remaining important in RTILs with minor addition of neutral organic molecules. However, the sterical effects gradually become less and less important with dilution. Theoretical methods for the description of EDL on ideally flat surfaces have been developed and the basic laws of EDL response to electrode polarization (the crossover between “overscreening” and “lattice saturation”) have been uncovered. Some progress toward understanding the effects of surface roughness have been made.

The combination of the currently developed models of EDL with more involved models of the electronic double layer in the electrode remains to be the most pressing issue for the theory development, particularly in view of using various forms of carbon for which the ideal conductor approximation may not be adequate.

The ideas about EDL in semi-infinite RTILs could not be directly transferred to the polarization of RTILs in nanoconfinement. In narrow nanopores of the electrode the role of screening of interionic interactions by the electronic polarizability of the conducting walls appears crucial, as it renormalizes the ion–ion interactions. If pores are ideally

metallic, the ions inside the pores will interact with each other via attractive/repulsive Yukawa-like short-range potentials, which will change dramatically the statistical mechanics of the ionic assembly there and its response to the electrode polarization. Within reasonable approximations these effects have been described both theoretically and through simulations. Deviation from ideal metallic screening in nanopores of carbon materials may change the character of ion–ion interactions, although the strength of the interactions will be in any case reduced and should become short-range, because these materials are electronic conductors. The investigation of these effects is in progress.

Both at flat interfaces and in nanoconfinement the new theories predict strong dependence of the electrical capacitance of the interfaces on voltage. For flat interfaces it is not a Gouy–Chapman like dependence in defined cases; in nanoconfinement completely new laws come out. These show non-monotonic voltage dependence, the shape of which is very sensitive to the pore size. Strong pore size dependence of capacitance at a given voltage was obtained explaining experimental observations. When pores get larger, interesting oscillating patterns of the capacitance pore-size-dependence were predicted theoretically and by simulations; these predictions are yet to be experimentally approved. However, in porous electrodes used for practical applications there are pores of different sizes. The pore-size distributions “average out” and suppress many of the sharp features of the capacitance voltage-dependence.

Overscreening may manifest itself in the kinetics of elementary act of heterogenous electron transfer reactions through the so-called Frumkin correction. In principle, in RTIL-based electrolytes the latter may substantially affect the driving force for the electron transfer at low and even moderate voltages. At large voltages, the lattice saturation effect may cause non-Tafel current–voltage characteristics. However, the theory and understanding of these effects are still in their infancy, and the above expectations may not be exactly confirmed, due to the perturbation of the potential distribution at the electrode/electrolyte interface by the reactant.

Overscreening may appear to be very important in electrochemical kinetics through the so-called Frumkin correction effect. In RTIL-based electrolytes this may become not a correction at all but something that fully renormalizes the driving force for electron transfer reactions at electrodes, at low and moderate voltages. At large voltages, the lattice saturation effect may cause non-Tafel current–voltage characteristics. The theory and understanding of these effects are still in their infancy.

The effects of surface roughness and chemical inhomogeneity of electrode surfaces on the overscreening and layering remain to be theoretically investigated. If the correlation length of roughness (or chemical inhomogeneity) and the mean height of roughness are of the order of the characteristic correlation lengths in RTILs, the layering and overscreening (which are some kind of resonance phenomena) can get smeared out. This will not happen, however, if the roughness/inhomogeneity scales are much larger, because for the structure of EDL the interface will locally look smooth and homogeneous.

RTILs in elastic media and the role of excluded volume effects in these systems is another interesting area for future development. Progress has been made in the theory, understanding, and experimental characterization of electroactuation with RTILs using mildly rough electrodes. In nanoporous

electrodes of supercapacitors and electroactuators, the effects of ion-induced stress and strain remain to be understood and quantitatively investigated.

Many interesting effects of ion molecular shape have been studied in the EDL at flat electrodes, but this remains to be explored in nanoconfinement.

Some first steps toward rationalizing the differences between the laws of energy storage in porous electrodes with RTILs and with ordinarily organic or aqueous solutions have been made. In the latter case the counterions, drawn by voltage, are to replace not only the co-ions, but also the solvent molecules. Theoretical analysis has revealed the differences in the energy storage capacity between the cases of ionophobic and ionophilic and solvophobic and solvophilic pores. The predictions of the theory remain to be experimentally approved. Once established, they may appear to be lessening for energy storage technologies.

One of the possible central subjects for future studies is the dynamics of the double layer charging and relaxation in RTILs. The mysteriously slow “glassy-like” relaxation of ionic liquids in the bulk is still not well understood, the more so the fast and slow dynamic components of charging/discharging at interfaces. Investigation of transport dynamics of RTILs in nanoscale pores has just started. The EDL dynamics determines time dependent phenomena in energy storage devices, and it has a direct effect on charging-discharging rates and energy losses and, thereby, power delivery of these devices. In the context of forces between solid surfaces, it is crucial for the dissipation forces and dynamic friction. These areas will likely soon become the subject of many publications.

Recall that most of the interest to RTILs, in terms of their applications, is due to their low volatility and wider electrochemical stability compared to most standard electrolytes. The low volatility makes the large surface-to-volume ratio not a problem for applications in various nanodevices. As for the electrochemical stability, not in every RTIL it is as good as one may wish it. Establishing the voltage windows within which electrochemical reactions that may cause degradation of the electrodes do not take place is a subject of many experimental studies. These have been and are being performed for various RTILs and their mixtures at various electrodes.

For a practitioner in energy storage, one of the most important requirements is that RTIL, as an electrolyte, would provide the maximal number of charging cycles without the onset of the degradation. In particular, such high-tech devices as supercapacitors are very expensive, and currently the primary target is not only their price, but also durability and a warranted and largest return on investment during its lifetime. This aspect has to be kept in mind when formulating the tasks for chemical theory and computations in RTIL electrodics. For instance, one of the important physical effects here may be the distribution of impurities near the interface. As many RTILs are generally sorbing water from the air and easily dissolving organic additives, it remains to be understood how much of these polar or polarizable molecules will get sucked into the inhomogeneous electric field of the EDL and how they will be distributed there. A legitimate question is, how rich-in-water the EDL might become (an undesirable feature in the most cases), even at negligible concentrations of water in the bulk?

To conclude, we think that despite of the vast number of known RTIL systems (and much larger number of such systems expected in the future) it is still possible to identify some general qualitative trends of their behavior at charged

interfaces. Saying that there is still a number of questions to be understood in this area and the further progress would require a systematic analysis of the large chemical space of RTILs (as well as of their mixtures with each other and other species like metal salts, organic molecules etc) and their properties at different charged interfaces. Due to the recent achievements in high-performance computing, data mining, and high-throughput measurements, such analysis can be done with modern state-of-the art cheminformatics methods combined with experimental, theoretical, and simulation approaches. We hope that such an approach would bring many interesting findings in the near future.

## AUTHOR INFORMATION

### Corresponding Authors

\*E-mail: maxim.fedorov@strath.ac.uk.

\*E-mail: a.kornyshev@imperial.ac.uk.

### Notes

The authors declare no competing financial interest.

### Biographies



Maxim V. Fedorov is an expert in computational physical chemistry and chemical physics, electrochemistry, and molecular biophysics. His research interests focus on (i) ionic liquids at electrified interfaces, (ii) ion effects on (bio)macromolecules and nanobodies, and (iii) molecular effects at solvation interfaces. He published over 70 peer-reviewed publications and presented about 70 invited talks and lectures on these subjects. In 2002 he received his Ph.D. degree in Biophysics at the Institute of Theoretical and Experimental Biophysics of the Russian Academy of Sciences, Pushchino, Russia, with Prof. S. E. Shnoll, an expert in physical biochemistry. After his Ph.D. he worked as a researcher at the same institute until the beginning of 2004 when he moved to the University College Dublin, Republic of Ireland, as a postdoc at the Department of Chemistry. In 2005 he moved to the University of Cambridge, U.K., where he spent three years working at the Department of Chemistry as a Research Associate in the Unilever Centre for Molecular Science Informatics. Since 2007 he was a Group Leader at the Max Planck Institute for Mathematics in the Sciences, in Leipzig, Germany. In 2007 he received his DSc (Doktor Nauk) degree in Physical Chemistry from the Institute of Solution Chemistry of the Russian Academy of Sciences, Ivanovo, Russia. In 2010–2011 he was also an external Privat-Dozent at the Department of Chemistry, University of Duisburg-Essen, Germany. As a visiting scientist he worked at the University of Kassel in 2003 (with Prof. Dietmar Kolb, as a DAAD scholar), at Imperial College London in 2007 (with Prof. A. A. Kornyshev), and at the University of Osaka in 2009 (with Prof. Y. Goto). In 2011 he spent a month in the University of Lille as a Visiting Professor in the group of Prof. A. Idrissi. In 2012 he received

the Helmholtz Award from the International Association of the Properties of Water and Steam (IAWPS) for his works on theoretical physical chemistry of liquids. He organized several international conferences and workshops on biomolecule solvation, chemical physics, and physical chemistry of liquids and applications of high-performance computing in natural sciences and engineering. In 2011 he joined the University of Strathclyde in Glasgow (U.K.) as a Professor of Physics and Life Sciences. Since 2012 he has been the Director of the West of Scotland Academia-Industry Supercomputer Centre (aka ARCHIE-WeST) at the University of Strathclyde. Since 2012 he has served as the Deputy Leader of Physics and Life Sciences Theme of Scottish Universities Physics Alliance (SUPA).



Alexei Kornyshev graduated in 1970 from the Moscow Institute of Engineering Physics with a master's degree in theoretical physics. He matured as a scientist at the Frumkin Institute of Electrochemistry (Acad. Sci.) in Moscow, where he did there his Ph.D. (1974) with R. R. Dogonadze in Theoretical and Mathematical Physics and DSc in Chemistry (1986), having worked there till 1991. In 1992 he was invited to Research Centre Jülich, Germany, where he then worked for 10 years leading a Theory Division in the Institute for Materials and Processes in Energy Systems of Research Centre "Juelich", Germany, a position combined later with a Professorship of Theoretical Physics at the University of Düsseldorf. In 2002 he joined Imperial College London where he holds a chair of Chemical Physics since then. His interests span widely in theoretical condensed matter chemical physics and its application to electrochemistry, nanoscience, biological physics and energy research, using methods of theoretical physics and computer simulations, and working in close collaboration with experimentalists. An author of >200 original, refereed papers published in physics and chemistry journals and ~30 monographic/feature articles and book-chapters, he is known by his works in the theory of solvation; solid–liquid and liquid–liquid electrochemical interfaces (including functionalized and electrovariable interfaces); electron and proton transfer in complex environment (including membranes and complex electrodes) and single molecules; physical theory of fuel cells; interaction, recognition, and assembly of biomolecules, DNA biophysics, and electrovariable nanoplasmatics and optics in self-assembled systems. Room temperature ionic liquids at electrified interfaces and in nanoconfinement, together with their applications to supercapacitors and electroactuators is an important direction of his current research, where since 2007 he has published a series of papers, a number of them in cooperation with Maxim Fedorov. He was the recipient of the 1991 Humboldt Prize in Physical Chemistry/Electrochemistry, 2003 Royal Society Wolfson Award, 2003 Schonbein Silver Medal ("for outstanding contributions to understanding the fundamentals of fuel cells"), 2007 Barker Electrochemistry Medal, and 2010 Interdisciplinary Prize, Medal and Lectureship of the RSC ("for his many outstanding contributions at the interfaces of chemistry with

both physics and with biology"). He is a Fellow of five learned societies: IUPAC, Institute of Physics, Royal Society of Chemistry, Society of Biology, and International Society of Electrochemistry, and a Foreign Member of the Royal Danish Academy of Science. He is a senior Editorial Panelist of Scientific Reports (Nature Publishing Group) and is a Member of Editorial Boards of Journal of Physics Condensed Matter (IOP) and ChemElectroChem (Wiley).

## ACKNOWLEDGMENTS

We are deeply thankful to our co-workers, project partners, and colleagues (M. Bazant, R. Colby, A. Frolov, N. Georgi, Y. Gogotsi, V. Ivaniščev, S. Kondrat, R. Lynden-Bell, J. McDonough, C. Perez, V. Pesser, R. Qiao, F. Stoeckli, and B. Storey) as well as undergraduate and postgraduate students (K. Kirchner, T. Kirchner, A. Lee, and C. Rochester) the joint work and many discussions with whom have influenced the views expressed in this article. We are thankful to R. Atkin, S. Baldelli, N. Borissenko, O. Borodin, O. Cabeza, K. Collins, R. Compton, M. Drüscher, F. Endres, C. Grey, W. Kunz, V. Lockett, E. Lust, P. Madden, S. Perkin, B. Roling, A. Rozhin, M. Salanee, W. Schröer, W. Shmickler, E. Spohr, M. Stukan, G. Tsirlina, M. Urbakh and L. Varela for valuable discussions. We are thankful to S. O'Connor and S. Crosthwaite for their help with preparation of the manuscript for publication. This project has been supported by the Grants EP/H004319/1, EP/K000586/1 and EP/K000195/1 of the Engineering and Physical Sciences Research Council (U.K.).

## NOMENCLATURE

- AC = activated carbon
- AFM = atomic force microscopy
- BASIL = biphasic acid scavenging utilizing ionic liquids<sup>124</sup>
- BBGKY = Bogolyubov–Born–Green–Kirkwood–Yvon (equations)
- BEG = Blum–Every–Griffith (model)
- CDC = carbide-derived carbon
- CPE = constant phase element
- CS = charged-sheet (correction)
- DFT = density functional theory
- DSSC = dye-sensitized solar cell
- EDL = electrical double layer
- EI = electrified interface
- EW = electrochemical window
- GC = glassy carbon
- GCh = Gouy–Chapman (theory)
- HTMS = high temperature molten salt
- IL = ionic liquid
- KK = Kramers–Kroenig (relation)
- MD = molecular dynamics (simulations)
- MIES = metastable induced electron spectroscopy
- MSA = mean spherical approximation
- NICISS = neutral-impact-collision ion scattering spectroscopy
- ORR = oxygen reduction reaction
- PME = particle mesh Ewald
- pzc = potential of zero charge
- RISM = reference interaction site model
- RTIL = room temperature ionic liquid
- SEI = solid electrolyte interface
- SFG = sum frequency generation (spectroscopy)
- STM = scanning tunneling microscopy
- TC = templated carbon

TGA = thermogravimetric analysis  
 VTF = Vogel–Tammann–Fulcher (equation)  
 XPS = X-ray photoelectron spectroscopy  
 3D-EWC = 3D Ewald correction (method)

## Ionic Liquids

### Cations

BMI<sup>+</sup> = 1-butyl-3-methylimidazolium  
 BMMI<sup>+</sup> = 1-butyl-2,3 dimethylimidazolium  
 BMPy<sup>+</sup> = N-butyl-3-methyl-pyridinium  
 BMPyr<sup>+</sup> = N-n-butyl-N-methylpyrrolidinium  
 BTMA<sup>+</sup> = butyltrimethylammonium  
 C<sub>n</sub>MIm<sup>+</sup> = 1-alkyl-3-methylimidazolium  
 DMOA<sup>+</sup> = N,N-diethyl-N-methyl-N-(2-methoxyethyl)-ammonium  
 EMIm<sup>+</sup> = 1-ethyl-3-methylimidazolium  
 HMIm<sup>+</sup> = 1-hexyl-3-methylimidazolium  
 HMPyr<sup>+</sup> = 1-hexyl-1-methyl-pyrrolidinium  
 HTEA<sup>+</sup> = hexyltriethylammonium  
 MOEMMor<sup>+</sup> = 4-(2-methoxyethyl)-4-methylmorpholinium  
 MOPMPip<sup>+</sup> = 1-(3-methoxypropyl)-1-methylpiperidinium  
 N<sub>112,102</sub><sup>+</sup> = N-ethyl-N,N-dimethyl-2-methoxyethylammonium  
 PMPyr<sup>+</sup> = N-methyl-N-propylpyrrolidinium  
 P<sub>14,666</sub><sup>+</sup> = trihexyl(tetradecyl) phosphonium  
 TMPA<sup>+</sup> = N,N,N-trimethyl-N-propylammonium  
 S<sub>222</sub><sup>+</sup> = triethylsulfonium

### Anions

DCA = dicyanamide  
 FAP = tris(pentafluoroethyl)-trifluorophosphate  
 FSI = bis(fluorosulfonyl)imide  
 OAc = acetate  
 TFA = trifluoroacetate  
 TfO<sup>-</sup> = trifluoromethanesulfonate (triflate), [CF<sub>3</sub>SO<sub>3</sub>]<sup>-</sup>  
 TFSA<sup>-</sup> = bis(trifluoromethanesulfonyl)azanide, [N-(CF<sub>3</sub>SO<sub>2</sub>)<sub>2</sub>]<sup>-</sup>, (this anion has ambiguous naming<sup>740</sup> and it is also named in the literature as TFSI, bis-(trifluoromethanesulfonyl)imide, bistriflamide, or bis-(trifluoromethylsulfonyl)amide, [NTf<sub>2</sub>]<sup>-</sup> or [N(Tf)<sub>2</sub>]<sup>-</sup>)  
 TFSI<sup>-</sup> = [NTf<sub>2</sub>]<sup>-</sup> = [N(Tf)<sub>2</sub>]<sup>-</sup> = bis-(trifluoromethanesulfonyl)imide<sup>740</sup> (see also the comment above and detailed discussion on appropriate notation of this compound in ref 740)

## REFERENCES

- (1) Bockris, J. O.; Khan, S. U. M. *Surface Electrochemistry: A Molecular Level Approach*; Springer: New York, 1993.
- (2) Kornyshev, A. A.; Spohr, E.; Vorotyntsev, M. A. *Electrochemical Interfaces: At the Border line*; Wiley: New York, 2002.
- (3) Iizutsu, K. *Electrochemistry in Nonaqueous Solutions*; Wiley-VCH: Weinheim, Germany, 2009.
- (4) Schmickler, W.; Santos, E. *Interfacial Electrochemistry*, 2nd ed.; Springer: New York, 2010.
- (5) Graves, A. D.; Inman, D. *J. Electroanal. Chem.* **1970**, *25*, 357.
- (6) Rovere, M.; Tosi, M. P. *Rep. Prog. Phys.* **1986**, *49*, 1001.
- (7) G. Mamantov, E. *Molten salt chemistry. An introduction and selected application.*; NATO Advance Study Institute; Kluwer/ D.Reidel Pbls.Co.: Dordrecht, The Netherlands, 1987.
- (8) Bockris, J.; Reddy, A. K. N. *Modern electrochemistry. 1*, 2nd ed.; Kluwer Academic Publishers: New York, 2002; Vol. 1.
- (9) Gaune-Escard, E. *Molten Salts. From Fundamentals to Applications*; Proceedings of the NATO Advanced Study Institute, held in Kas, Turkey, 4–14 May 2001.; Nato Science Series II; 2002; Vol. 52.
- (10) Hurley, F. H.; Wier, T. P. *J. Electrochem. Soc.* **1951**, *98*, 207.
- (11) Ford, W. T. *Anal. Chem.* **1975**, *47*, 1125.
- (12) Welch, B.; Osteryoung, R. *J. Electroanal. Chem.* **1981**, *118*, 455.
- (13) Galiński, M.; Lewandowski, A.; St epniak, I. *Electrochim. Acta* **2006**, *51*, 5567.
- (14) Liu, Q.; El Abedin, S. Z.; Endres, F. *Surf. Coat. Technol.* **2006**, *201*, 1352.
- (15) Bonhote, P.; Dias, A. P.; Papageorgiou, N.; Kalyanasundaram, K.; Gratzel, M. *Inorg. Chem.* **1996**, *35*, 1168.
- (16) Earle, M. J.; Seddon, K. R. *Pure Appl. Chem.* **2000**, *72*, 1391.
- (17) Endres, F. *ChemPhysChem* **2002**, *3*, 144.
- (18) Buzzeo, M.; Evans, R.; Compton, R. *ChemPhysChem* **2004**, *5*, 1106.
- (19) Ohno, H., Ed. *Electrochemical Aspects of Ionic Liquids*; Wiley & Sons: New York, 2005.
- (20) Silvester, D.; Compton, R. *Z. Phys. Chem.* **2006**, *220*, 1247.
- (21) MacFarlane, D. R.; Forsyth, M.; Howlett, P. C.; Pringle, J. M.; Sun, J.; Annat, G.; Neil, W.; Izgorodina, E. I. *Acc. Chem. Res.* **2007**, *40*, 1165.
- (22) El Abedin, S. Z.; Polleth, M.; Meiss, S. A.; Janek, J.; Endres, F. *Green Chem.* **2007**, *9*, 549.
- (23) Wei, D.; Ivaska, A. *Anal. Chim. Acta* **2008**, *607*, 126.
- (24) Armand, M.; Endres, F.; MacFarlane, D. R.; Ohno, H.; Scrosati, B. *Nat. Mater.* **2009**, *8*, 621.
- (25) Su, Y. Z.; Fu, Y. C.; Wei, Y. M.; Yan, J. W.; Mao, B. W. *ChemPhysChem* **2010**, *11*, 2764.
- (26) MacFarlane, D. R.; Pringle, J. M.; Howlett, P. C.; Forsyth, M. *Phys. Chem. Chem. Phys.* **2010**, *12*, 1659.
- (27) Liu, H.; Liu, Y.; Li, J. *Phys. Chem. Chem. Phys.* **2010**, *12*, 1685.
- (28) Barrosse-Antle, L. E.; Bond, A. M.; Compton, R. G.; O'Mahony, A. M.; Rogers, E. I.; Silvester, D. S. *Chem. Asian J.* **2010**, *5*, 202.
- (29) Opallo, M.; Lesniewski, A. *J. Electroanal. Chem.* **2011**, *656*, 2.
- (30) Siangproh, W.; Duangchai, W.; Chailapakul, O. In *Handbook of Ionic Liquids: Properties, Applications and Hazards*; Mun, J., Sim, H., Eds.; Nova Science Publishers, Inc.: New York, 2012; pp 79–112.
- (31) Abbott, A. P.; Frisch, G.; Ryder, K. S. *Annu. Rev. Mater. Res.* **2013**, *43*.
- (32) Plechkova, N. V.; Seddon, K. R. *Chem. Soc. Rev.* **2008**, *37*, 123.
- (33) Wishart, J. F. *Energy Environ. Sci.* **2009**, *2*, 956.
- (34) Giernoth, R. *Angew. Chem., Int. Ed.* **2010**, *49*, 2834.
- (35) Werner, S.; Haumann, M.; Wasserscheid, P. *Annu. Rev. Chem. Biomol. Eng.* **2010**, *1*, 203.
- (36) Torimoto, T.; Tsuda, T.; Okazaki, K.-i.; Kuwabata, S. *Adv. Mater.* **2010**, *22*, 1196.
- (37) Hallett, J. P.; Welton, T. *Chem. Rev.* **2011**, *111*, 3508.
- (38) Seddon, K. R.; Plechkova, N. V. *Ionic Liquids UnCOiled: Critical Expert Overviews*; John Wiley & Sons: New York, 2012.
- (39) Lin, R.; Taberna, P.-L.; Fantini, S.; Presser, V.; Pérez, C. R.; Malbosc, F.; Rupesinghe, N. L.; Teo, K. B. K.; Gogotsi, Y.; Simon, P. J. *Phys. Chem. Lett.* **2011**, *2*, 2396.
- (40) Palm, R.; Kurig, H.; Tönurist, K.; Jänes, A.; Lust, E. *Electrochim. Commun.* **2012**, *22*, 203.
- (41) Freire, M. G.; Santos, L. M.; Fernandes, A. M.; Coutinho, J. A.; Marrucho, I. M. *Fluid Phase Equilib.* **2007**, *261*, 449.
- (42) Niedermeier, H.; Hallett, J. P.; Villar-Garcia, I. J.; Hunt, P. A.; Welton, T. *Chem. Soc. Rev.* **2012**, *41*, 7780.
- (43) To avoid confusion, we will use the HTMS abbreviation or simply “molten salts” below when we discuss high temperature ionic liquids.
- (44) Gadzuric, S.; Suh, C.; Gaune-Escard, M.; Rajan, K. *Metall. Mater. Trans. A* **2006**, *37*, 3411.
- (45) Hunt, P. A.; Kirchner, B.; Welton, T. *Chem.—Eur. J.* **2006**, *12*, 6762.
- (46) Kossmann, S.; Thar, J.; Kirchner, B.; Hunt, P. A.; Welton, T. *J. Chem. Phys.* **2006**, *124*, 174506.
- (47) Lehmann, S. B. C.; Roatsch, M.; Schöppke, M.; Kirchner, B. *Phys. Chem. Chem. Phys.* **2010**, *12*, 7473.
- (48) Kurig, H.; Vestli, M.; Tönurist, K.; Jänes, A.; Lust, E. *J. Electrochim. Soc.* **2012**, *159*, A944.

- (49) Rigby, J.; Izgorodina, E. I. *Phys. Chem. Chem. Phys.* **2013**, *15*, 1632.
- (50) Krossing, I.; Slattery, J. M.; Daguenet, C.; Dyson, P. J.; Oleinikova, A.; Weingärtner, H. *J. Am. Chem. Soc.* **2006**, *128*, 13427.
- (51) Hayyan, M.; Mjalli, F. S.; Hashim, M. A.; AlNashef, I. M.; Mei, T. X. *J. Ind. Eng. Chem.* **2013**, *19*, 106.
- (52) Georgi, N.; Kornyshev, A. A.; Fedorov, M. V. *J. Electroanal. Chem.* **2010**, *649*, 261.
- (53) Earle, M. J.; Esperança, J. M. S. S.; Gilea, M. A.; Lopes, J. N. C.; Rebelo, L. P. N.; Magee, J. W.; Seddon, K. R.; Widgren, J. A. *Nature* **2006**, *439*, 831.
- (54) Welton, T. *Chem. Rev.* **1999**, *99*, 2071.
- (55) Marinescu, M.; Urbakh, M.; Barnea, T.; Kucernak, A. R.; Kornyshev, A. A. *J. Phys. Chem. C* **2010**, *114*, 22558.
- (56) Kornyshev, A. A. *J. Phys. Chem. B* **2007**, *111*, 5545.
- (57) Hansen, J. P.; McDonald, I. R. *Phys. Rev. A* **1975**, *11*, 2111.
- (58) Rosenfeld, Y. *J. Chem. Phys.* **1993**, *98*, 8126.
- (59) Freyland, W. *Coulombic fluids: bulk and interfaces*; Springer series in solid-state sciences; *168*; Springer: Berlin, 2011.
- (60) Levin, Y. *Rep. Prog. Phys.* **2002**, *65*, 1577.
- (61) Schröer, W.; Weingartner, H. *Pure Appl. Chem.* **2004**, *76*, 19.
- (62) Schröer, W. *NATO Sci. Ser. II Math.* **2005**, *206*, 143.
- (63) Siinor, L.; Lust, K.; Lust, E. *Electrochim. Commun.* **2010**, *12*, 1058.
- (64) Aal, A. A.; Al-Salman, R.; Al-Zoubi, M.; Borisenko, N.; Endres, F.; Höfft, O.; Prowald, A.; Zein El Abedin, S. *Electrochim. Acta* **2011**, *56*, 10295.
- (65) Atkin, R.; Borisenko, N.; Drüscher, M.; El Abedin, S. Z.; Endres, F.; Hayes, R.; Huber, B.; Roling, B. *Phys. Chem. Chem. Phys.* **2011**, *13*, 6849.
- (66) Drüscher, M.; Huber, B.; Roling, B. *J. Phys. Chem. C* **2011**, *115*, 6802.
- (67) Roling, B.; Drüscher, M.; Huber, B. *Faraday Discuss.* **2011**, *154*, 303.
- (68) Gnahn, M.; Kolb, D. M. *J. Electroanal. Chem.* **2011**, *651*, 250.
- (69) Drüscher, M.; Borisenko, N.; Wallauer, J.; Winter, C.; Huber, B.; Endres, F.; Roling, B. *Phys. Chem. Chem. Phys.* **2012**, *14*, 5090.
- (70) Roling, B.; Drüscher, M. *Electrochim. Acta* **2012**, *76*, 526.
- (71) Siinor, L.; Siimenson, C.; Ivaniščev, V.; Lust, K.; Lust, E. *J. Electroanal. Chem.* **2012**, *668*, 30.
- (72) Borisenko, N.; El Abedin, S. Z.; Endres, F. *ChemPhysChem* **2012**, *13*, 1736.
- (73) Ivaniščev, V.; Ruzanov, A.; Lust, K.; Lust, E. *J. Electrochim. Soc.* **2013**, *160*, H368.
- (74) Siinor, L.; Siimenson, C.; Lust, K.; Lust, E. *Electrochim. Commun.* **2013**, *35*, 5.
- (75) Siinor, L.; Arendt, R.; Lust, K.; Lust, E. *J. Electroanal. Chem.* **2013**, *689*, 51.
- (76) Endres, F.; Hofft, O.; Borisenko, N.; Gasparotto, L. H.; Prowald, A.; Al-Salman, R.; Carstens, T.; Atkin, R.; Bund, A.; El Abedin, S. Z. *Phys. Chem. Chem. Phys.* **2010**, *12*, 1724.
- (77) Bockris, J. O.; Reddy, A. K. N.; Gamboa-Aldeco, M. *Modern electrochemistry. 2A*, 2nd ed.; Kluwer Academic Publishers: New York, 2002; Vol. 2A.
- (78) Brett, C. M.; Oliveira Brett, A. In *Comprehensive Chemical Kinetics*; Bamford, C., Compton, R. G., Eds.; Elsevier B.V.: Amsterdam, 1986; Vol. 26.
- (79) Monroe, C. W.; Daikhin, L. I.; Urbakh, M.; Kornyshev, A. A. *J. Phys.: Condens. Matter* **2006**, *18*, 2837.
- (80) Monroe, C. W.; Daikhin, L. I.; Urbakh, M.; Kornyshev, A. A. *Phys. Rev. Lett.* **2006**, *97*, 136102.
- (81) Girault, H.; Kornyshev, A. A.; Monroe, C. W.; Urbakh, M. *J. Phys.: Condens. Matter* **2007**, *19*, 370301.
- (82) Monroe, C. W.; Urbakh, M.; Kornyshev, A. A. *J. Electrochim. Soc.* **2009**, *156*, P21.
- (83) Perkin, S.; Albrecht, T.; Klein, J. *Phys. Chem. Chem. Phys.* **2010**, *12*, 1243.
- (84) Bou-Malham, L.; Bureau, L. *Soft Matter* **2010**, *6*, 4062.
- (85) Perkin, S. *Phys. Chem. Chem. Phys.* **2012**, *14*, 5052.
- (86) Sweeney, J.; Hausen, F.; Hayes, R.; Webber, G. B.; Endres, F.; Rutland, M. W.; Bennewitz, R.; Atkin, R. *Phys. Rev. Lett.* **2012**, *109*, 155502.
- (87) Elbourne, A.; Sweeney, J.; Webber, G. B.; Wanless, E. J.; Warr, G. G.; Rutland, M. W.; Atkin, R. *Chem. Commun.* **2013**, *49*, 6797.
- (88) Li, H.; Rutland, M. W.; Atkin, R. *Phys. Chem. Chem. Phys.* **2013**.
- (89) Vol'fkovich, Y. M.; Serdyuk, T. M. *R. J. Electrochem.* **2002**, *38*, 935.
- (90) Mastragostino, M.; Soavi, F. *J. Power Sources* **2007**, *174*, 89.
- (91) Simon, P.; Gogotsi, Y. *Nat. Mater.* **2008**, *7*, 845.
- (92) Beguin, F.; Frackowiak, E. *Carbons for Electrochemical Energy Storage and Conversion Systems*; CRC Press: Boca Raton, FL, 2010.
- (93) Conway, B. E. *Electrochemical supercapacitors: scientific fundamentals and technological applications*; Springer: New York, 1999.
- (94) Bar-Cohen, Y. In *Compliant structures in nature and engineering*; Jenkins, C. H., Ed.; WIT: Southampton, U.K., 2005.
- (95) Bar-Cohen, Y.; Zhang, Q. *MRS Bull.* **2008**, *33*, 173.
- (96) Xiong, L.; Fletcher, A. M.; Ernst, S.; Davies, S. G.; Compton, R. G. *Analyst* **2012**, *137*, 2567.
- (97) Wasserscheid, P.; Welton, T., Eds. *Ionic Liquids in Synthesis*; Wiley-VCH: Weinheim, Germany, 2003.
- (98) Gaune-Escard, M.; Seddon, K. R. *Molten Salts and Ionic Liquids: Never the Twain?*; John Wiley and Sons: New York, 2009.
- (99) Cao, Y.; Yao, S.; Wang, X.; Peng, Q.; Song, H. In *Handbook of Ionic Liquids: Properties, Applications and Hazards*; Mun, J., Sim, H., Eds.; Nova Science Publishers, Inc.: New York, 2012; pp 145–172.
- (100) Wilkes, J. S. *Green Chem.* **2002**, *4*, 73.
- (101) Fei, Z.; Dyson, P. J. *Chem. Commun.* **2013**, *49*, 2594.
- (102) Walden, P. *Bull. Russian Acad. Sci.* **1914**, *405*.
- (103) Gabriel, S.; Weiner, J. *Chem. Ber.* **1888**, *21*, 2669.
- (104) Graenacher, C. *Cellulose Solution*. U.S. Patent 1,943,176, Jan 9, 1934.
- (105) Chum, H. L.; Koch, V. R.; Miller, L. L.; Osteryoung, R. A. *J. Am. Chem. Soc.* **1975**, *97*, 3264.
- (106) Mirnaya, T. A.; Prisyazhnyi, V. D.; Shcherbakov, V. A. *Russ. Chem. Rev.* **1989**, *58*, 821.
- (107) Gale, R. J.; Osteryoung, R. A. *Electrochim. Acta* **1980**, *25*, 1527.
- (108) We note though that in many practical applications RTILs are mixed with some amount of solvent to decrease viscosity and lower the operation temperature; see below.
- (109) Hussey, C. L.; King, L. A.; Nardi, J. C. *AlCl<sub>3</sub> /1-alkyl pyridinium chloride room temperature electrolytes*. U.S. Patent US4122245 A, Aug 19, 1978.
- (110) Wilkes, J.; Levisky, J.; Wilson, R.; Hussey, C. *Inorg. Chem.* **1982**, *21*, 1263.
- (111) Fannin, A.; King, L.; Stech, D.; Vaughn, R.; Wilkes, J.; Williams, J. *J. Electrochim. Soc.* **1982**, *129*, C122.
- (112) Wilkes, J.; Levisky, J.; Pfugl, J.; Hussey, C.; Scheffler, T. *Anal. Chem.* **1982**, *54*, 2378.
- (113) Wilkes, J.; Frye, J.; Reynolds, G. *Inorg. Chem.* **1983**, *22*, 3870.
- (114) Fannin, A.; Floreani, D.; King, L.; Landers, J.; Piersma, B.; Stech, D.; Vaughn, R.; Wilkes, J.; Williams, J. *J. Phys. Chem.* **1984**, *88*, 2614.
- (115) Hussey, C.; Scheffler, T.; Wilkes, J.; Fannin, A. *J. Electrochim. Soc.* **1986**, *133*, 1389.
- (116) Dymek, C.; Hussey, C.; Wilkes, J.; Oye, H. *J. Electrochim. Soc.* **1987**, *134*, C510.
- (117) Øye, H.; Jagtoyen, M.; Oksefjell, T.; Wilkes, J. *Mater. Sci. Forum* **1991**, *73–75*, 183.
- (118) Elias, A.; Wilkes, J. *J. Chem. Eng. Data* **1994**, *39*, 79.
- (119) Poole, C. F. *J. Chromatogr. A* **2004**, *1037*, 49.
- (120) Gale, R.; Osteryoung, R. *Inorg. Chem.* **1979**, *18*, 1603.
- (121) Price, D.; Copley, J. *Phys. Rev. A* **1975**, *11*, 2124.
- (122) Copley, J.; Rahman, A. *Phys. Rev. A* **1976**, *13*, 2276.
- (123) Wilkes, J.; Zaworotko, M. *J. Chem. Soc. Chem. Comm.* **1992**, *965*.
- (124) Maase, M.; Massonne, K. In *Ionic Liquids IIb: Fundamentals, Progress, Challenges and Opportunities: Transformations and Processes*;

- Rogers, R. D.; Seddon, K. R., Eds.; American Chemical Society: Washington, DC, 2005; Vol. 902, pp 126–132.
- (125) Tang, S.; Baker, G. A.; Zhao, H. *Chem. Soc. Rev.* **2012**, *41*, 4030.
- (126) Stark, A. *Top. Curr. Chem.* **2009**, *290*, 41.
- (127) Lewandowski, A. *J. Power Sources* **2009**, *194*, 601.
- (128) We note, however, that although the vapour pressure of most RTILs is very small, it is, nevertheless, *measurable* for most of RTILs.<sup>38,53</sup> Moreover, as it was shown in refs 53 and 129, high-vacuum and ultrahigh vacuum (UHV) distillation of ionic liquids and separation of ionic liquid mixtures are, in principle, possible; UHV distillation can be used for obtaining high purity ionic liquids for analytical applications.
- (129) Taylor, A. W.; Lovelock, K. R. J.; Deyko, A.; Licence, P.; Jones, R. G. *Phys. Chem. Chem. Phys.* **2010**, *12*, 1772.
- (130) Armstrong, J. P.; Hurst, C.; Jones, R. G.; Licence, P.; Lovelock, K. R. J.; Satterley, C. J.; Villar-Garcia, I. J. *Phys. Chem. Chem. Phys.* **2007**, *9*, 982–990.
- (131) Ludwig, R.; Kragl, U. *Angew. Chem., Int. Ed.* **2007**, *46*, 6582.
- (132) Rocha, M. A. A.; Lima, C. F. R. A. C.; Gomes, L. R.; Schröder, B.; Coutinho, J. A. P.; Marrucho, I. M.; Esperança, J. M. S. S.; Rebelo, L. P. N.; Shimizu, K.; Lopes, J. N. C.; Santos, L. M. N. B. F. *J. Phys. Chem. B* **2011**, *115*, 10919.
- (133) Zaitsau, D. H.; Fumino, K.; Emel'yanenko, V. N.; Yermalayeu, A. V.; Ludwig, R.; Verevkin, S. P. *ChemPhysChem* **2012**, *13*, 1868.
- (134) Fletcher, S.; Black, V. J.; Kirkpatrick, I.; Varley, T. S. *J. Solid State Electrochem.* **2013**, *17*, 327.
- (135) Borgel, V.; Markevich, E.; Aurbach, D.; Semrau, G.; Schmidt, M. *J. Power Sources* **2009**, *189*, 331.
- (136) Rogers, E. I.; Šljukić, B.; Hardacre, C.; Compton, R. G. *J. Chem. Eng. Data* **2009**, *54*, 2049.
- (137) Lu, X.; Burrell, G.; Separovic, F.; Zhao, C. *J. Phys. Chem. B* **2012**, *116*, 9160.
- (138) Tian, Y.-H.; Goff, G. S.; Runde, W. H.; Batista, E. R. *J. Phys. Chem. B* **2012**, *116*, 11943.
- (139) Olson, E. J.; Bühlmann, P. *J. Electrochem. Soc.* **2013**, *160*, A320.
- (140) Xiang, J.; Wu, F.; Chen, R.; Li, L.; Yu, H. *J. Power Sources* **2013**, *233*, 115.
- (141) Freire, M. G.; Carvalho, P. J.; Gardas, R. L.; Marrucho, I. M.; Santos, L. M. N. B. F.; Coutinho, J. A. P. *J. Phys. Chem. B* **2008**, *112*, 1604.
- (142) Chaban, V. V.; Prezhdo, O. V. *J. Phys. Chem. Lett.* **2011**, *2*, 2499.
- (143) Wypych, G., Ed. *Handbook of solvents*; ChemTec Publishing: Toronto, Canada, 2001.
- (144) Cho, C. W.; Pham, T. P. T.; Jeon, Y. C.; Vijayaraghavan, K.; Choe, W. S.; Yun, Y. S. *Chemosphere* **2007**, *69*, 1003.
- (145) Stephens, G.; Licence, P. *Chim. Oggi-Chem. Today* **2011**, *29*, 72.
- (146) McCrary, P. D.; Rogers, R. D. *Chem. Commun.* **2013**.
- (147) Czerwka, M.; Stolte, S.; Muller, A.; Siedlecka, E. M.; Golebiowski, M.; Kumirska, J.; Stepnowski, P. *J. Hazard. Mater.* **2009**, *171*, 478.
- (148) Ventura, S. P. M.; Gonçalves, A. M. M.; Sintra, T.; Pereira, J. L.; Gonçalves, F.; Coutinho, J. A. P. *Ecotoxicology* **2013**, *22*, 1.
- (149) Docherty, K. M.; Kulpa, C. F. *Green Chem.* **2005**, *7*, 185.
- (150) Ranke, J.; Stolte, S.; Stormann, R.; Arning, J.; Jastorff, B. *Chem. Rev.* **2007**, *107*, 2183.
- (151) Swatoski, R. P.; Holbrey, J. D.; Rogers, R. D. *Green Chem.* **2003**, *5*, 361.
- (152) Siedlecka, E. M.; Czerwka, M.; Stolte, S.; Stepnowski, P. *Curr. Org. Chem.* **2011**, *15*, 1974.
- (153) Fernandez, J. F.; Neumann, J.; Thoming, J. *Curr. Org. Chem.* **2011**, *15*, 1992.
- (154) Steinruck, H. P.; Libuda, J.; Wasserscheid, P.; Cremer, T.; Kolbeck, C.; Laurin, M.; Maier, F.; Sobota, M.; Schulz, P. S.; Stark, M. *Adv. Mater.* **2011**, *23*, 2571.
- (155) Sun, X.; Luo, H.; Dai, S. *Chem. Rev.* **2012**, *112*, 2100.
- (156) Stojanovic, A.; Keppler, B. K. *Sep. Sci. Technol.* **2012**, *47*, 189.
- (157) Kilpeläinen, I.; Xie, H.; King, A.; Granstrom, M.; Heikkinen, S.; Argyropoulos, D. S. *J. Agr. Food Chem.* **2007**, *55*, 9142.
- (158) Wang, H.; Gurau, G.; Rogers, R. D. *Chem. Soc. Rev.* **2012**, *41*, 1519.
- (159) Freyland, W.; Zell, C.; Abedin, S. E.; Endres, F. *Electrochim. Acta* **2003**, *48*, 3053.
- (160) Zhang, M. M.; Kamavaram, V.; Reddy, R. G. *JOM* **2003**, *55*, A54.
- (161) El Abedin, S. Z.; Endres, F. *ChemPhysChem* **2006**, *7*, 58.
- (162) Yoshida, J.-i.; Kataoka, K.; Horcajada, R.; Nagaki, A. *Chem. Rev.* **2008**, *108*, 2265.
- (163) Hapiot, P.; Lagrost, C. *Chem. Rev.* **2008**, *108*, 2238.
- (164) MacFarlane, D. R.; Tachikawa, N.; Forsyth, M.; Pringle, J. M.; Howlett, P. C.; Elliott, G. D.; Davis, J. H.; Watanabe, M.; Simon, P.; Angell, C. A. *Energy Environ. Sci.* **2013**.
- (165) Balducci, A.; Bardi, U.; Caporali, S.; Mastragostino, M.; Soavi, F. *Electrochim. Commun.* **2004**, *6*, 566.
- (166) Frackowiak, E. *J. Brazil. Chem. Soc.* **2006**, *17*, 1074.
- (167) Vivekchand, S. R. C.; Rout, C. S.; Subrahmanyam, K. S.; Govindaraj, A.; Rao, C. N. R. *J. Chem. Sci.* **2008**, *120*, 9.
- (168) Liu, C.; Yu, Z.; Neff, D.; Zhamu, A.; Jang, B. Z. *Nano Lett.* **2010**, *10*, 4863.
- (169) Sakaebi, H.; Matsumoto, H.; Tatsumi, K. *Electrochim. Acta* **2007**, *53*, 1048.
- (170) Quartarone, E.; Mustarelli, P. *Chem. Soc. Rev.* **2011**, *40*, 2525.
- (171) Wang, P.; Zakeeruddin, S. M.; Moser, J.-E.; Grätzel, M. *J. Phys. Chem. B* **2003**, *107*, 13280.
- (172) Li, B.; Wang, L.; Kang, B.; Wang, P.; Qiu, Y. *Sol. Energ. Mater. Sol. C.* **2006**, *90*, 549.
- (173) Zistler, M.; Wachter, P.; Schreiner, C.; Fleischmann, M.; Gerhard, D.; Wasserscheid, P.; Hinsch, A.; Gores, H. J. *J. Electrochem. Soc.* **2007**, *154*, B925.
- (174) Hagfeldt, A.; Boschloo, G.; Sun, L.; Kloo, L.; Pettersson, H. *Chem. Rev.* **2010**, *110*, 6595.
- (175) Lee, C.-P.; Ho, K.-C. In *Handbook of Ionic Liquids: Properties, Applications and Hazards*; Mun, J., Sim, H., Eds.; Nova Science Publishers, Inc.: New York, 2012; pp 173.
- (176) van de Ven, E.; Chairuna, A.; Merle, G.; Benito, S. P.; Borneman, Z.; Nijmeijer, K. *J. Power Sources* **2013**, *222*, 202.
- (177) Millefiorini, S.; Tkaczyk, A. H.; Sedev, R.; Efthimiadis, J.; Ralston, J. *J. Am. Chem. Soc.* **2006**, *128*, 3098.
- (178) Nanayakkara, Y. S.; Moon, H.; Payagala, T.; Wijeratne, A. B.; Crank, J. A.; Sharma, P. S.; Armstrong, D. W. *Anal. Chem.* **2008**, *80*, 7690.
- (179) Zhang, X.; Cai, Y. *Angew. Chem., Int. Ed.* **2013**, *125*, 2345.
- (180) Zhou, F.; Liang, Y.; Liu, W. *Chem. Soc. Rev.* **2009**, *38*, 2590.
- (181) Palacio, M.; Bhushan, B. *Tribol. Lett.* **2010**, *40*, 247.
- (182) Werzer, O.; Cranston, E. D.; Warr, G. G.; Atkin, R.; Rutland, M. W. *Phys. Chem. Chem. Phys.* **2012**, *14*, 5147.
- (183) Garcia-Etxarri, A.; Aizpurua, J.; Molina-Aldareguia, J.; Marcilla, R.; Adolfo Pomposo, J.; Mecerreyres, D. *Front. Phys. China* **2010**, *5*, 330.
- (184) Albrecht, T.; Moth-Poulsen, K.; Christensen, J. B.; Hjelm, J.; Bjørnholm, T.; Ulstrup, J. *J. Am. Chem. Soc.* **2006**, *128*, 6574.
- (185) Chen, F.; Qing, Q.; Xia, J. L.; Li, J. H.; Tao, N. J. *J. Am. Chem. Soc.* **2009**, *131*, 9908.
- (186) Xie, W.; Frisbie, C. D. *J. Phys. Chem. C* **2011**, *115*, 14360.
- (187) Thiemann, S.; Sachnov, S.; Porscha, S.; Wasserscheid, P.; Zaumseil, J. *J. Phys. Chem. C* **2012**, *116*, 13536.
- (188) Paulsen, B. D.; Frisbie, C. D. *J. Phys. Chem. C* **2012**, *116*, 3132.
- (189) Kim, S. H.; Hong, K.; Xie, W.; Lee, K. H.; Zhang, S.; Lodge, T. P.; Frisbie, C. D. *Adv. Mater.* **2013**, *25*, 1822.
- (190) Ye, J. T.; Inoue, S.; Kobayashi, K.; Kasahara, Y.; Yuan, H. T.; Shimotani, H.; Iwasa, Y. *Nat. Mater.* **2010**, *9*, 125.
- (191) Silvester, D. S. *Analyst* **2011**, *136*, 4871–4882.
- (192) Rehman, A.; Zeng, X. *Acc. Chem. Res.* **2012**, *45*, 1667.
- (193) Ionic Liquids Database - ILThermo. 2013.
- (194) Aparicio, S.; Atilhan, M.; Karadas, F. *Ind. Eng. Chem. Res.* **2010**, *49*, 9580.

- (195) Zhang, S.; Lu, X.; Zhou, Q.; Li, X.; Zhang, X.; Li, S. *Ionic Liquids: Physicochemical Properties*, 1st ed.; Elsevier Science, 2009.
- (196) A quotation from the back-cover of this book reads: "This comprehensive database on physical properties of pure ionic liquids (ILs) contains data collected from 269 peer-reviewed papers in the period from 1982 to June 2008. There are more than 9,400 data points on the 29 kinds of physicochemical properties for 1886 available ionic liquids, from which 807 kinds of cations and 185 kinds of anions were extracted. This book includes nearly all known pure ILs and their known physicochemical properties through June 2008. In addition, the authors incorporate the main applications of individual ILs and a large number of references."
- (197) Zhang, S. J.; Sun, N.; He, X. Z.; Lu, X. M.; Zhang, X. P. *J. Phys. Chem. Ref. Data* **2006**, *35*, 1475.
- (198) Weingärtner, H. *Angew. Chem., Int. Ed.* **2008**, *47*, 654.
- (199) Endres, F.; MacFarlane, D.; Abbott, A. *Electrodeposition from Ionic Liquids*; John Wiley & Sons: New York, 2008.
- (200) For a more detailed discussion of the role of the chemical structure on toxicity of RTILs, see the recent paper by Ventura et al.<sup>148</sup>
- (201) Wakai, C.; Oleinikova, A.; Ott, M.; Weingartner, H. *J. Phys. Chem. B* **2005**, *109*, 17028.
- (202) Kobrak, M. N. *Green Chem.* **2008**, *10*, 80.
- (203) Huang, M.-M.; Jiang, Y.; Sasisanker, P.; Driver, G. W.; Weingartner, H. *J. Chem. Eng. Data* **2011**, *56*, 1494.
- (204) Abbott, A. P. *Chem. Phys. Chem.* **2005**, *6*, 2502.
- (205) Vila, J.; Ginés, P.; Rilo, E.; Cabeza, O.; Varela, L. *Fluid Phase Equilib.* **2006**, *247*, 32.
- (206) Borges, R. S.; Ribeiro, H.; Lavall, R. L.; Silva, G. G. *J. Solid State Electrochem.* **2012**, *16*, 3573.
- (207) We note that in such devices like super capacitors the temperature can increase spontaneously via Joule heat; in this case such systems would need external cooling.
- (208) Holbrey, J. D.; Seddon, K. R. *J. Chem. Soc., Dalton Trans.* **1999**, 2133.
- (209) Jayaraman, S.; Maginn, E. J. *J. Chem. Phys.* **2007**, *127*, 214504.
- (210) Lei, Z. G.; Chen, B. H.; Li, C. Y.; Liu, H. *Chem. Rev.* **2008**, *108*, 1419.
- (211) Coutinho, J. A. P.; Carvalho, P. J.; Oliveira, N. M. C. *RSC Adv.* **2012**, *2*, 7322.
- (212) Sillars, F. B.; Fletcher, S. I.; Mirzaeian, M.; Hall, P. J. *Phys. Chem. Chem. Phys.* **2012**, *14*, 6094.
- (213) Sánchez, L. G.; Espel, J. R.; Onink, F.; Meindersma, G. W.; Haan, A. B. d. *J. Chem. Eng. Data* **2009**, *54*, 2803.
- (214) Tokuda, H.; Hayamizu, K.; Ishii, K.; Susan, M. A. B. H.; Watanabe, M. *J. Phys. Chem. B* **2005**, *109*, 6103.
- (215) Maginn, E. J. *Acc. Chem. Res.* **2007**, *40*, 1200.
- (216) Tokuda, H.; Hayamizu, K.; Ishii, K.; Susan, M. A. B. H.; Watanabe, M. *J. Phys. Chem. B* **2004**, *108*, 16593.
- (217) Tokuda, H.; Ishii, K.; Susan, M. A. B. H.; Tsuzuki, S.; Hayamizu, K.; Watanabe, M. *J. Phys. Chem. B* **2006**, *110*, 2833.
- (218) Vila, J.; Varela, L.; Cabeza, O. *Electrochim. Acta* **2007**, *52*, 7413.
- (219) Lopes, J. N. C.; Gomes, M. F. C.; Padua, A. A. H. *J. Phys. Chem. B* **2006**, *110*, 16816.
- (220) Spickermann, C.; Thar, J.; Lehmann, S. B. C.; Zahn, S.; Hunger, J.; Buchner, R.; Hunt, P. A.; Welton, T.; Kirchner, B. *J. Phys. Chem. Phys.* **2008**, *129*, 104505.
- (221) Fernandes, A. M.; Rocha, M. A. A.; Freire, M. G.; Marrucho, I. M.; Coutinho, J. A. P.; Santos, L. M. N. B. F. *J. Phys. Chem. B* **2011**, *115*, 4033.
- (222) Preiss, U.; Verevkin, S. P.; Koslowski, T.; Krossing, I. *Chem.—Eur. J.* **2011**, *17*, 6508.
- (223) Nikitina, V. A.; Gruber, F.; Jansen, M.; Tsirlina, G. A. *Electrochim. Acta* **2013**, *103*, 243.
- (224) Gebbie, M. A.; Valtiner, M.; Banquy, X.; Fox, E. T.; Henderson, W. A.; Israelachvili, J. N. *Proc. Natl. Acad. Sci. U.S.A.* **2013**.
- (225) Zhao, W.; Leroy, F.; Heggen, B.; Zahn, S.; Kirchner, B.; Balasubramanian, S.; Mueller-Plathe, F. *J. Am. Chem. Soc.* **2009**, *131*, 15825.
- (226) Kashyap, H. K.; Annapureddy, H. V. R.; Rainieri, F. O.; Margulis, C. J. *J. Phys. Chem. B* **2011**, *115*, 13212.
- (227) Turton, D. A.; Hunger, J.; Stoppa, A.; Heftner, G.; Thoman, A.; Walther, M.; Buchner, R.; Wynne, K. *J. Am. Chem. Soc.* **2009**, *131*, 11140.
- (228) Pádua, A. A. H.; Costa Gomes, M. F.; Canongia Lopes, J. N. A. *Acc. Chem. Res.* **2007**, *40*, 1087.
- (229) Okoturo, O.; VanderNoot, T. *J. Electroanal. Chem.* **2004**, *568*, 167.
- (230) Kowsari, M. H.; Alavi, S.; Ashrafizadeh, M.; Najafi, B. *J. Chem. Phys.* **2008**, *129*, 224508.
- (231) Tsuzuki, S. *ChemPhysChem* **2012**, *13*, 1664–1670.
- (232) Liu, Q.-S.; Yan, P.-F.; Yang, M.; Tan, Z.-C.; Li, C.-P.; Welz-Biermann, U. *Acta Phys.-Chim. Sin.* **2011**, *27*, 2762.
- (233) Krossing, I.; Slattery, J. M. *Z. Phys. Chem.* **2006**, *220*, 1343.
- (234) Slattery, J. M.; Daguenet, C.; Dyson, P. J.; Schubert, T. J. S.; Krossing, I. *Angew. Chem., Int. Ed.* **2007**, *46*, 5384.
- (235) Tsuda, T.; Imanishi, A.; Torimoto, T.; Kuwabat, S. In *Ionic Liquids: Theory, Properties, New Approaches*; Kokorin, A., Ed.; InTech, 2011.
- (236) Zheng, Y.; Dong, K.; Wang, Q.; Zhang, J.; Lu, X. *J. Chem. Eng. Data* **2013**, *58*, 32.
- (237) Salanne, M.; Siqueira, L. J. A.; Seitsonen, A. P.; Madden, P. A.; Kirchner, B. *Faraday Discuss.* **2011**, *154*, 171.
- (238) Zahn, S.; Brehm, M.; Brüssel, M.; Hollóczki, O.; Kohagen, M.; Lehmann, S.; Malberg, F.; Pensado, A. S.; Schöppke, M.; Weber, H.; Kirchner, B. *J. Mol. Liq.* **2013**, in press.
- (239) Wendler, K.; Dommert, F.; Zhao, Y. Y.; Berger, R.; Holm, C.; Site, L. D. *Faraday Discuss.* **2011**, *154*, 111.
- (240) Dommert, F.; Wendler, K.; Berger, R.; Delle Site, L.; Holm, C. *ChemPhysChem* **2012**, *13*, 1625.
- (241) Tsuzuki, S.; Tokuda, H.; Hayamizu, K.; Watanabe, M. *J. Phys. Chem. B* **2005**, *109*, 16474.
- (242) Tsuzuki, S.; Shinoda, W.; Saito, H.; Mikami, M.; Tokuda, H.; Watanabe, M. *J. Phys. Chem. B* **2009**, *113*, 10641.
- (243) Eiden, P.; Bulut, S.; Köchner, T.; Friedrich, C.; Schubert, T.; Krossing, I. *J. Phys. Chem. B* **2011**, *115*, 300.
- (244) Leys, J.; Wübbenhörst, M.; Preethy Menon, C.; Rajesh, R.; Thoen, J.; Glorieux, C.; Nockemann, P.; Thijs, B.; Binnemans, K.; Longuemart, S. *J. Chem. Phys.* **2008**, *128*, 064509.
- (245) Stoppa, A.; Zech, O.; Kunz, W.; Buchner, R. *J. Chem. Eng. Data* **2009**, *55*, 1768.
- (246) Zech, O.; Stoppa, A.; Buchner, R.; Kunz, W. *J. Chem. Eng. Data* **2010**, *55*, 1774.
- (247) Ohno, H.; Yoshizawa, M.; Mizumo, T. In *Electrochemical Aspects of Ionic Liquids*; Ohno, H., Ed.; John Wiley & Sons, Inc.: Hoboken, NJ, 2005; p 75.
- (248) Seki, S.; Ohno, Y.; Kobayashi, Y.; Miyashiro, H.; Usami, A.; Mita, Y.; Tokuda, H.; Watanabe, M.; Hayamizu, K.; Tsuzuki, S.; Hattori, M.; Terada, N. *J. Electrochem. Soc.* **2007**, *154*, A173.
- (249) O'ahony, A. M.; Silvester, D. S.; Aldous, L.; Hardacre, C.; Compton, R. G. *J. Chem. Eng. Data* **2008**, *53*, 2884.
- (250) Segalini, J.; Daffos, B.; Taberna, P. L.; Gogotsi, Y.; Simon, P. *Electrochim. Acta* **2010**, *55*, 7489.
- (251) McDonough, J. K.; Frolov, A. I.; Presser, V.; Niu, J.; Miller, C. H.; Ubieto, T.; Fedorov, M. V.; Gogotsi, Y. *Carbon* **2012**, *50*, 3298.
- (252) Coadou, E.; Timperman, L.; Jacquemin, J.; Galiano, H.; Hardacre, C.; Anouti, M. *J. Phys. Chem. C* **2013**, in press.
- (253) Lynden-Bell, R. M. *Phys. Chem. Chem. Phys.* **2010**, *12*, 1733.
- (254) Lynden-Bell, R. M.; Frolov, A. I.; Fedorov, M. V. *Phys. Chem. Chem. Phys.* **2012**, *14*, 2693.
- (255) Segalini, M.; Kantorovich, S. S.; Arnold, A.; Holm, C. *Recent Advances in Broadband Dielectric Spectroscopy*; Springer: New York, 2013; p 103.
- (256) Weingärtner, H. *J. Mol. Liq.* **2013**.
- (257) Baker, G. A.; Rachford, A. A.; Castellano, F. N.; Baker, S. N. *ChemPhysChem* **2013**, *14*, 1025.
- (258) Choi, U. H.; Mittal, A.; Price, T. L.; Gibson, H. W.; Runt, J.; Colby, R. H. *Macromolecules* **2013**, *46*, 1175.

- (259) Kosower, E. M. *J. Am. Chem. Soc.* **1958**, *80*, 3253.
- (260) Kamlet, M. J.; Abboud, J. L. M.; Abraham, M. H.; Taft, R. W. *J. Org. Chem.* **1983**, *48*, 2877.
- (261) Rani, M. A. A.; Brant, A.; Crowhurst, L.; Dolan, A.; Lui, M.; Hassan, N. H.; Hallett, J. P.; Hunt, P. A.; Niedermeyer, H.; Perez-Arlandis, J. M.; Schrems, M.; Welton, T.; Wilding, R. *Phys. Chem. Chem. Phys.* **2011**, *13*, 16831.
- (262) Matsumoto, H. In *Electrochemical Aspects of Ionic Liquids*; Ohno, H., Ed.; John Wiley & Sons, Inc.: Hoboken, NJ, 2005; pp 35–54.
- (263) Lane, G. H. *Electrochim. Acta* **2012**, *83*, 513.
- (264) Buzzo, M. C.; Hardacre, C.; Compton, R. G. *ChemPhysChem* **2006**, *7*, 176.
- (265) Bernard, U. L.; Izgorodina, E. I.; MacFarlane, D. R. *J. Phys. Chem. C* **2010**, *114*, 20472.
- (266) Zhao, C.; Burrell, G.; Torriero, A. A. J.; Separovic, F.; Dunlop, N. F.; MacFarlane, D. R.; Bond, A. M. *J. Phys. Chem. B* **2008**, *112*, 6923.
- (267) Moganty, S. S.; Baltus, R. E.; Roy, D. *Chem. Phys. Lett.* **2009**, *483*, 90.
- (268) Shiddiky, M. J.; Torriero, A. A. *Biosens. Bioelectron.* **2011**, *26*, 1775.
- (269) Huang, J.-F.; Chen, H.-Y. *Angew. Chem.* **2012**, *124*, 1716.
- (270) Ismail, A. S.; El Abedin, S. Z.; Hofft, O.; Endres, F. *Electrochim. Commun.* **2010**, *12*, 909.
- (271) Romann, T.; Oll, O.; Pikma, P.; Lust, E. *Electrochim. Commun.* **2012**, *23*, 118.
- (272) Wang, J. *Electroanal.* **2005**, *17*, 1341.
- (273) Kurig, H.; Jänes, A.; Lust, E. *J. Electrochem. Soc.* **2010**, *157*, A272.
- (274) Tamilarasan, P.; Ramaprabhu, S. *J. Phys. Chem. C* **2012**, *116*, 14179.
- (275) Wei, Y.; Liu, H.; Jin, Y.; Cai, K.; Li, H.; Liu, Y.; Kang, Z.; Zhang, Q. *New J. Chem.* **2013**, in press.
- (276) Simon, P.; Gogotsi, Y. *Acc. Chem. Res.* **2013**, *46*, 1094.
- (277) Vivek, J. P.; Burgess, I. *J. Langmuir* **2012**, *28*, 5040.
- (278) Kirchner, K.; Kirchner, T.; Ivaniščev, V.; Fedorov, M. *Electrochim. Acta* **2013**, in press.
- (279) Gnahn, M.; Müller, C.; Répánszki, R.; Pajkossy, T.; Kolb, D. *M. Phys. Chem. Chem. Phys.* **2011**, *13*, 11627.
- (280) Costa, R.; Pereira, C. M.; Silva, F. *RSC Adv.* **2013**, in press.
- (281) Schlegel, M. L.; Nagy, K. L.; Fenter, P.; Cheng, L.; Sturchio, N. C.; Jacobsen, S. D. *Geochim. Cosmochim. Act.* **2006**, *70*, 3549.
- (282) Zhou, H.; Rouha, M.; Feng, G.; Lee, S. S.; Docherty, H.; Fenter, P.; Cummings, P. T.; Fulvio, P. F.; Dai, S.; McDonough, J.; Presser, V.; Gogotsi, Y. *ACS Nano* **2012**, *6*, 9818.
- (283) Palm, R.; Kurig, H.; Tonurist, K.; Jaenes, A.; Lust, E. *Electrochim. Acta* **2012**, *85*, 139.
- (284) Zhao, C.; Bond, A. M.; Lu, X. *Anal. Chem.* **2012**, *84*, 2784.
- (285) Ridings, C.; Lockett, V.; Andersson, G. *Phys. Chem. Chem. Phys.* **2011**, *13*, 21301.
- (286) Liu, Z.; El Abedin, S. Z.; Endres, F. *Electrochim. Acta* **2013**, *89*, 635.
- (287) Cadena, C.; Anthony, J. L.; Shah, J. K.; Morrow, T. I.; Brennecke, J. F.; Maginn, E. J. *J. Am. Chem. Soc.* **2004**, *126*, 5300.
- (288) Shiflett, M. B.; Yokozeki, A. *Ind. Eng. Chem. Res.* **2005**, *44*, 4453.
- (289) Kerlé, D.; Ludwig, R.; Geiger, A.; Paschek, D. *J. Phys. Chem. B* **2009**, *113*, 12727.
- (290) Anderson, J. L.; Dixon, J. K.; Brennecke, J. F. *Acc. Chem. Res.* **2007**, *40*, 1208.
- (291) Lei, Z.; Dai, C.; Chen, B. *Chem. Rev.* **2013**, in press.
- (292) Camper, D.; Scovazzo, P.; Koval, C.; Noble, R. *Ind. Eng. Chem. Res.* **2004**, *43*, 3049.
- (293) MacDowell, N.; Florin, N.; Buchard, A.; Hallett, J.; Galindo, A.; Jackson, G.; Adjiman, C. S.; Williams, C. K.; Shah, N.; Fennell, P. *Energy Environ. Sci.* **2010**, *3*, 1645.
- (294) Yang, H.; Gu, Y.; Deng, Y.; Shi, F. *Chem. Commun. (Camb.)* **2002**, *274*.
- (295) Helmholtz, H. *Ann. Phys.* **1853**, *89* (211), 353.
- (296) Cohen, E. R.; Cvitaš, T.; Frey, J. G.; Holmström, B.; Kuchitzu, K.; Marquardt, R.; Mills, I.; Pavese, F.; Quack, M.; Stohner, J.; Strauss, H. L.; Takami, M.; Thor, A. J. *Quantities, units and symbols in physical chemistry*, 3rd ed.; International Union of Pure and Applied Chemistry, The Royal Society of Chemistry: Cambridge, U.K., 2007.
- (297) Gouy, L. G. *C. R. Hebd. Acad. Sci.* **1909**, *149*, 654.
- (298) Gouy, L. G. *J. Phys. Théor. Appl.* **1910**, *9*, 457.
- (299) Debye, P. J. W.; Hückel, E. A. *A. J. Phys. Z.* **1923**, *24*, 185.
- (300) Stern, O. Z. *Elektrochem.* **1924**, *30*, 508.
- (301) Israelachvili, J. N. *Intermolecular and Surface Forces*; Academic Press: Boston, 1992.
- (302) Price, N. C.; Dwek, R. A.; Wormald, M.; Ratcliffe, G. R. *Principles and problems in physical chemistry for biochemists*; Oxford University Press: Oxford, U.K., 2001.
- (303) Bard, A. J.; Stratmann, M.; Wilson, G. S., Eds. *Encyclopedia of Electrochemistry: Bioelectrochemistry*; Wiley VCH: Weinheim, Germany, 2002; Vol. 9.
- (304) Scholz, F. *Electroanalytical Methods: Guide to Experiments and Applications*; Springer: New York, 2002.
- (305) Neves-Petersen, M. T.; Petersen, S. B.; El-Gewely, M. R. *Protein electrostatics: A review of the equations and methods used to model electrostatic equations in biomolecules - Applications in biotechnology*; Elsevier: Amsterdam, 2003; Vol. 9, pp 315–395.
- (306) Wu, J.; Hu, Z. B. In *Encyclopedia of Nanoscience and Nanotechnology*; Schwarz, J., Contescu, C., Putyera, K., Eds.; Marcel Dekker, Inc.: New York, 2004; p 1967.
- (307) Frumkin, A. *Potencialy nulevogo zarjada*; Nauka: Moskva, 1982.
- (308) Bockris, J. O. *Comprehensive treatise of electrochemistry*; Plenum Press: New York, 1980.
- (309) Parsons, R.; Zobel, F. *J. Electroanal. Chem.* **1965**, *9*, 333.
- (310) Kornyshev, A. A., in Dogonadze, R. R., Kalman, E., Ulstrup, J., Eds. *The Chemical Physics of Solvation. Part C*; Elsevier: Amsterdam, 1988, p 77.
- (311) Fawcett, W. *Isr. J. Chem.* **1979**, *18*, 3.
- (312) Kornyshev, A.; Vilfan, I. *Electrochim. Acta* **1995**, *40*, 109.
- (313) Grahame, D. C. *J. Am. Chem. Soc.* **1958**, *80*, 4201.
- (314) Parry, J. M.; Parsons, R. *Trans. Faraday Soc.* **1963**, *59*, 241.
- (315) Vorotyntsev, M. A. In *Modern Aspects of Electrochemistry*; Bockris, J. O., Conway, B. E., White, R. E., Eds.; Modern Aspects of Electrochemistry 17; Springer: New York, 1986; pp 131–222.
- (316) Kornyshev, A. A.; Schmickler, W.; Vorotyntsev, M. A. *Phys. Rev. B* **1982**, *25*, 5244.
- (317) Kornyshev, A.; Vorotyntsev, M. *Can. J. Chem.-Rev. Can. Chim.* **1981**, *59*, 2031.
- (318) Blum, L.; Henderson, D.; Parsons, R. *J. Electroanal. Chem.* **1984**, *161*, 389.
- (319) Fawcett, W. R. *Liquids, solutions, and interfaces: from classical macroscopic descriptions to modern microscopic details*; Oxford University Press: Oxford, U.K., 2004.
- (320) Schmickler, W.; Henderson, D. *Prog. Surf. Sci.* **1986**, *22*, 323.
- (321) Boda, D.; Henderson, D.; Chan, K. Y. *J. Chem. Phys.* **1999**, *110*, 5346.
- (322) Bikerman, J. J. *Philos. Mag.* **1942**, *33*, 384.
- (323) Grimley, T.; Mott, N. *Discuss. Faraday. Soc.* **1947**, *1*, 3.
- (324) Grimley, T. *Proc. R. Soc. Lond. A* **1950**, *201*, 40.
- (325) Dutta, M.; Bagchi, S. *Indian J. Phys.* **1950**, *24*, 61.
- (326) Freise, V. Z. *Elektrochem.* **1952**, *56*, 822.
- (327) di Caprio, D.; Borkowska, Z.; Stafiej, J. *J. Electroanal. Chem.* **2003**, *540*, 17.
- (328) Borukhov, I.; Andelman, D.; Orland, H. *Phys. Rev. Lett.* **1997**, *79*, 435.
- (329) Kralj-Iglc, V.; Iglic, A. *J. Phys. II* **1996**, *6*, 477.
- (330) Bazant, M. Z.; Kilic, M. S.; Storey, B. D.; Ajdari, A. *Adv. Colloid Interfaces* **2009**, *152*, 48.
- (331) Sloutskin, E.; Ocko, B. M.; Tamam, L.; Kuzmenko, I.; Gog, T.; Deutsch, M. *J. Am. Chem. Soc.* **2005**, *127*, 7796.
- (332) Jeon, Y.; Sung, J.; Bu, W.; Vaknin, D.; Ouchi, Y.; Kim, D. J. *Phys. Chem. C* **2008**, *112*, 19649.

- (333) Sloutskin, E.; Lynden-Bell, R. M.; Balasubramanian, S.; Deutsch, M. *J. Chem. Phys.* **2006**, *125*, 174715.
- (334) Bowers, J.; Vergara-Gutierrez, M. C.; Webster, J. R. P. *Langmuir* **2004**, *20*, 309.
- (335) Lauw, Y.; Horne, M. D.; Rodopoulos, T.; Lockett, V.; Akgun, B.; Hamilton, W. A.; Nelson, A. R. *J. Langmuir* **2012**, *28*, 7374.
- (336) Kolbeck, C.; Cremer, T.; Lovelock, K. R. J.; Paape, N.; Schulz, P. S.; Wasserscheid, P.; Maier, F.; Steinrück, H.-P. *J. Phys. Chem. B* **2009**, *113*, 8682.
- (337) Lockett, V.; Sedev, R.; Harmer, S.; Ralston, J.; Horne, M.; Rodopoulos, T. *Phys. Chem. Chem. Phys.* **2010**, *12*, 13816.
- (338) Weingarth, D.; Foelske-Schmitz, A.; Wokaun, A.; Kötz, R. *Electrochim. Commun.* **2011**, *13*, 619.
- (339) Foelske-Schmitz, A.; Weingarth, D.; Wokaun, A.; Kötz, R. *ECS Electrochem. Lett.* **2013**, *2*, H13.
- (340) Iwashashi, T.; Nishi, T.; Yamane, H.; Miyamae, T.; Kanai, K.; Seki, K.; Kim, D.; Ouchi, Y. *J. Phys. Chem. C* **2009**, *113*, 19237.
- (341) Hammer, T.; Reichelt, M.; Morgner, H. *Phys. Chem. Chem. Phys.* **2010**, *12*, 11070.
- (342) Ridings, C.; Lockett, V.; Andersson, G. *Phys. Chem. Chem. Phys.* **2011**, *13*, 17177.
- (343) Ridings, C.; Lockett, V.; Andersson, G. *Colloid Surf. A* **2012**, *413*, 149.
- (344) Gnahn, M.; Pajkossy, T.; Kolb, D. *Electrochim. Acta* **2010**, *55*, 6212.
- (345) Hayes, R.; Warr, G. G.; Atkin, R. *Phys. Chem. Chem. Phys.* **2010**, *12*, 1709.
- (346) Endres, F.; Borisenko, N.; Abedin, S. Z. E.; Hayes, R.; Atkin, R. *Faraday Discuss.* **2012**, *154*, 221.
- (347) Gnahn, M.; Berger, C.; Arkhipova, M.; Kunkel, H.; Pajkossy, T.; Maas, G.; Kolb, D. M. *Phys. Chem. Chem. Phys.* **2012**, *14*, 10647.
- (348) Painter, K. R.; Ballone, P.; Tosi, M. P.; Grout, P. J.; March, N. H. *Surf. Sci.* **1983**, *133*, 89.
- (349) Ballone, P.; Pastore, G.; Tosi, M. P.; Painter, K. R.; Grout, P. J.; March, N. H. *Phys. Chem. Liq.* **1984**, *13*, 269.
- (350) Revere, M.; Tosi, M. P. *Rep. Prog. Phys.* **1999**, *49*, 1001.
- (351) Tosi, M. P. In *Condensed Matter Physics Aspects of Electrochemistry*; Tosi, M. P., Kornyshev, A. A., Eds.; World Scientific, Singapore, 1991.
- (352) Torrie, G. M.; Valneau, J. P. *J. Chem. Phys.* **1980**, *73*, 5807.
- (353) Torrie, G. M.; Valneau, J. P.; Patey, G. N. *J. Chem. Phys.* **1982**, *76*, 4615.
- (354) Torrie, G. M.; Valneau, J. P. *J. Phys. Chem.* **1982**, *86*, 3251.
- (355) Lanning, O. J.; Madden, P. A. *J. Phys. Chem. B* **2004**, *108*, 11069.
- (356) Dogonadze, R.; Chizmadzhev, Y. *Dokl. Akad. Nauk. SSSR* **1964**, *157*, 944.
- (357) Weingartner, H. *Z. Phys. Chem.* **2006**, *220*, 1395.
- (358) Parsons, R. *Chem. Rev.* **1990**, *90*, 813.
- (359) Kisza, A. *J. Electroanal. Chem.* **2002**, *534*, 99–106.
- (360) Amokrane, S.; Badiali, J. In *Modern Aspects of Electrochemistry*; Bockris, J. O., Conway, B. E., White, R., Eds.; Plenum: New York, 1992; Vol. 22.
- (361) Kornyshev, A. A. *Electrochim. Acta* **1989**, *34*, 1829.
- (362) Gerischer, H. *J. Phys. Chem.* **1985**, *89*, 4249.
- (363) Gerischer, H.; McIntyre, R.; Scherson, D.; Storck, W. *J. Phys. Chem.* **1987**, *91*, 1930.
- (364) Skinner, B.; Chen, T.; Loth, M. S.; Shklovskii, B. I. *Phys. Rev. E* **2011**, *83*, 056102.
- (365) Luque, N.; Schmickler, W. *Electrochim. Acta* **2012**, *71*, 82.
- (366) Liu, H.; He, P.; Li, Z.; Sun, C.; Shi, L.; Liu, Y.; Zhu, G.; Li, J. *Electrochim. Commun.* **2005**, *7*, 1357.
- (367) Fukushima, T.; Aida, T. *Chem.—Eur. J.* **2007**, *13*, 5048.
- (368) Pauliukaite, R.; Murnaghan, K. D.; Doherty, A. P.; Brett, C. M. A. *J. Electroanal. Chem.* **2009**, *633*, 106.
- (369) Faribod, F.; Ganjali, M. R.; Pirali-Hamedani, M.; Norouzi, P. *Int. J. Electrochem. Sci.* **2010**, *5*, 1103.
- (370) Gogotsi, Y.; Presser, V. *Carbon Nanomaterials*; CRC Press: Boca Raton, FL, 2010.
- (371) Salimi, A.; Lasghari, S.; Noorbakhsh, A. *Electroanal.* **2010**, *22*, 1707.
- (372) Miller, J. R.; Outlaw, R. A.; Holloway, B. C. *Science* **2010**, *329*, 1637.
- (373) Brennan, L. J.; Byrne, M. T.; Bari, M.; Gun'ko, Y. K. *Adv. Energy Mater.* **2011**, *1*, 472.
- (374) Zhang, Q.; Wu, S.; Zhang, L.; Lu, J.; Verproot, F.; Liu, Y.; Xing, Z.; Li, J.; Song, X.-M. *Biosens. Bioelectron.* **2011**, *26*, 2632.
- (375) Luo, J.; Jang, H. D.; Huang, J. *ACS Nano* **2013**, in press.
- (376) Lin, J.; Zhang, C.; Yan, Z.; Zhu, Y.; Peng, Z.; Hauge, R. H.; Natelson, D.; Tour, J. M. *Nano Lett.* **2013**, *13*, 72.
- (377) Uesugi, E.; Goto, H.; Eguchi, R.; Fujiwara, A.; Kubozono, Y. *Sci. Rep.* **2013**, *3*, 1595.
- (378) Zhang, L.; Yang, X.; Zhang, F.; Long, G.; Zhang, T.; Leng, K.; Zhang, Y.; Huang, Y.; Ma, Y.; Zhang, M.; Chen, Y. *J. Am. Chem. Soc.* **2013**, *135*, 5921.
- (379) Gurevich, Y.; Kharkats, Y. *J. Electroanal. Chem.* **1978**, *86*, 245.
- (380) Gurevich, Y.; Kharkats, Y. *J. Phys. Chem. Solids* **1978**, *39*, 751.
- (381) Gurevich, Y.; Kharkats, Y. *Uspekhi. Fiz. Nauk* **1982**, *136*, 693.
- (382) Scheidegger, A. E. *The physics of flow through porous media*; University of Toronto Press: Toronto, 1974.
- (383) Seddon, K. R.; Stark, A.; Torres, M. J. *Pure Appl. Chem.* **2000**, *72*, 2275.
- (384) Huddleston, J. G.; Visser, A. E.; Reichert, W. M.; Willauer, H. D.; Broker, G. A.; Rogers, R. D. *Green Chem.* **2001**, *3*, 156.
- (385) Rausch, M. H.; Lehmann, J.; Leipertz, A.; Froba, A. P. *Phys. Chem. Chem. Phys.* **2011**, *13*, 9525.
- (386) Couadou, E.; Jacquemin, J.; Galiano, H.; Hardacre, C.; Anouti, M. *J. Phys. Chem. B* **2013**, *117*, 1389.
- (387) Lombardo, L.; Brutt, S.; Navarra, M. A.; Panero, S.; Reale, P. J. *Power Sources* **2013**, *227*, 8.
- (388) Wang, M.; Shan, Z.; Tian, J.; Yang, K.; Liu, X.; Liu, H.; Zhu, K. *Electrochim. Acta* **2013**, *95*, 301.
- (389) Bazant, M. Z.; Storey, B. D.; Kornyshev, A. A. *Phys. Rev. Lett.* **2011**, *106*, 046102.
- (390) We note that flexible nonpolar functional groups of RTIL ions (e.g., alkyl chains) can also act as voids, see refs 52 and 391.
- (391) Fedorov, M. V.; Georgi, N.; Kornyshev, A. A. *Electrochim. Commun.* **2010**, *12*, 296.
- (392) Kilic, M. S.; Bazant, M. Z.; Ajdari, A. *Phys. Rev. E* **2007**, *75*, 021503.
- (393) Oldham, K. B. *J. Electroanal. Chem.* **2008**, *613*, 131.
- (394) Fawcett, W. R.; Ryan, P. J. *Collect. Czech. Chem. Commun.* **2009**, *74*, 1665.
- (395) Fawcett, W. R.; Ryan, P. J. *Phys. Chem. Chem. Phys.* **2010**, *12*, 9816.
- (396) Fedorov, M. V.; Kornyshev, A. A. *J. Phys. Chem. B* **2008**, *112*, 11868.
- (397) Kirchner, K. A simulation study of simple ionic liquids near charged walls: The melting of the electric double layer and structural transitions at the interface. Doctoral thesis, University of Strathclyde, Glasgow, 2013.
- (398) We note that the addition of solvent can also affect the electrochemical stability of the system, see, e.g., ref 249. However, for the sake of clarity we do not discuss this effect in this section.
- (399) Binder, K. In *Phase Transitions and Critical Phenomena*; Domb, C., Lebowitz, J. L., Eds.; Academic Press: New York, 2000.
- (400) Damaskos, B. B.; Petrii, O. A.; Batrakov, V. V.; Uvarov, E. B.; Parsons, R.; Barradas, R. G. *J. Electrochim. Soc.* **1972**, *119*, 279C.
- (401) Nabutovskii, V.; Nemov, N. *J. Colloid Interface Sci.* **1986**, *114*, 208.
- (402) Szparaga, R.; Woodward, C. E.; Forsman, J. *J. Phys. Chem. C* **2012**, *116*, 15946.
- (403) Sangster, M. J. L.; Dixon, M. *Adv. Phys.* **1976**, *25*, 247.
- (404) Heyes, D. M.; Clarke, J. H. *J. Chem. Soc. Faraday Trans. 2* **1981**, *77*, 1089.
- (405) Torrie, G.; Valneau, J. *Chem. Phys. Lett.* **1979**, *65*, 343.
- (406) Boda, D.; Henderson, D.; Chan, K. Y.; Wasan, D. T. *Chem. Phys. Lett.* **1999**, *308*, 473.

- (407) Boda, D.; Henderson, D. *J. Chem. Phys.* **2000**, *112*, 8934.  
 (408) Toukmaji, A. Y.; Board, J. A. *Comput. Phys. Commun.* **1996**, *95*, 73.  
 (409) Board, J. A.; Humphres, C. W.; Lambert, C. G.; Rankin, W. T.; Toukmaji, A. Y. Ewald and Multipole Methods for Periodic N-Body Problems; Conference on Parallel Processing for Scientific Computing; Minneapolis, MN, 1997.  
 (410) Spohr, E. *J. Electroanal. Chem.* **1998**, *450*, 327.  
 (411) Spohr, E. *Electrochim. Acta* **2003**, *49*, 23.  
 (412) Kornyshev, A. A.; Spohr, E.; Vorotyntsev, M. A. *Encyclopedia of Electrochemistry*; Wiley-VCH: Weinheim, Germany, 2007.  
 (413) Darden, T.; York, D.; Pedersen, L. *J. Chem. Phys.* **1993**, *98*, 10089.  
 (414) Yeh, I.-C.; Berkowitz, M. L. *J. Chem. Phys.* **1999**, *111*, 3155.  
 (415) Spohr, E. *J. Chem. Phys.* **1997**, *107*, 6342.  
 (416) Crozier, P. S.; Rowley, R. L.; Henderson, D.; Boda, D. *Chem. Phys. Lett.* **2000**, *325*, 675.  
 (417) Crozier, P. S.; Rowley, R. L.; Spohr, E.; Henderson, D. *J. Chem. Phys.* **2000**, *112*, 9253.  
 (418) Nanjundiah, C.; McDevitt, S. F.; Koch, V. R. *J. Electrochem. Soc.* **1997**, *144*, 3392.  
 (419) Lin, L.; Wang, Y.; Yan, J.; Yuan, Y.; Xiang, J.; Mao, B. *Electrochem. Commun.* **2003**, *5*, 995.  
 (420) Alam, M.; Islam, M.; Okajima, T.; Ohsaka, T. *Electrochem. Commun.* **2007**, *9*, 2370.  
 (421) Alam, M. T.; Islam, M. M.; Okajima, T.; Ohsaka, T. *J. Phys. Chem. C* **2007**, *111*, 18326.  
 (422) Alam, M. T.; Islam, M. M.; Okajima, T.; Ohsaka, T. *J. Phys. Chem. C* **2008**, *112*, 16600.  
 (423) Islam, M. M.; Alam, M. T.; Ohsaka, T. *J. Phys. Chem. C* **2008**, *112*, 16568.  
 (424) Lockett, V.; Sedev, R.; Ralston, J.; Horne, M.; Rodopoulos, T. *J. Phys. Chem. C* **2008**, *112*, 7486.  
 (425) Booth, M. J.; Haymet, A. D. *J. Mol. Phys.* **2001**, *99*, 1817.  
 (426) Lanning, O. J.; Shellswell, S.; Madden, P. A. *Mol. Phys.* **2004**, *102*, 839.  
 (427) Reed, S. K.; Lanning, O. J.; Madden, P. A. *J. Chem. Phys.* **2007**, *126*, 084704.  
 (428) Reed, S. K.; Madden, P. A.; Papadopoulos, A. *J. Chem. Phys.* **2008**, *128*, 124701.  
 (429) Lynden-Bell, R. M. *Mol. Phys.* **2003**, *101*, 2625.  
 (430) Lynden-Bell, R. M.; Kohanoff, J.; Del Popolo, M. G. *Faraday Discuss.* **2005**, *129*, 57.  
 (431) Lynden-Bell, R. M.; Del Pópolo, M. G.; Youngs, T. G. A.; Kohanoff, J.; Hanke, C. G.; Harper, J. B.; Pinilla, C. C. *Acc. Chem. Res.* **2007**, *40*, 1138.  
 (432) Pinilla, C.; Del Pópolo, M.; Kohanoff, J.; Lynden-Bell, R. *J. Phys. Chem. B* **2007**, *111*, 4877.  
 (433) Horn, R. G.; Evans, D. F.; Ninham, B. W. *J. Phys. Chem.* **1988**, *92*, 3531.  
 (434) Lowen, H.; Hansen, J. P.; Madden, P. A. *J. Chem. Phys.* **1993**, *98*, 3275.  
 (435) Bopp, P. A.; Kornyshev, A. A.; Sutmann, G. *Phys. Rev. Lett.* **1996**, *76*, 1280.  
 (436) Bopp, P. A.; Kornyshev, A. A.; Sutmann, G. *J. Chem. Phys.* **1998**, *109*, 1939.  
 (437) Cheng, L.; Fenter, P.; Nagy, K. L.; Schlegel, M. L.; Sturchio, N. *C. Phys. Rev. Lett.* **2001**, *87*, 156103.  
 (438) Fedorov, M. V.; Kornyshev, A. A. *Mol. Phys.* **2007**, *105*, 1.  
 (439) Fedorov, M. V.; Kornyshev, A. A. *Electrochim. Acta* **2008**, *53*, 6835.  
 (440) Merlet, C.; Salanne, M.; Rotenberg, B.; Madden, P. A. *J. Phys. Chem. C* **2011**, *115*, 16613.  
 (441) Bhuiyan, L. B.; Lamperski, S.; Wu, J.; Henderson, D. *J. Phys. Chem. B* **2012**, *116*, 10364.  
 (442) Merlet, C.; Salanne, M.; Rotenberg, B. *J. Phys. Chem. C* **2012**, *116*, 7687.  
 (443) Merlet, C.; Rotenberg, B.; Madden, P. A.; Taberna, P.-L.; Simon, P.; Gogotsi, Y.; Salanne, M. *Nat. Mater.* **2012**, *11*, 306.  
 (444) Ji, Y.; Shi, R.; Wang, Y.; Saielli, G. *J. Phys. Chem. B* **2013**, *117*, 1104.  
 (445) Merlet, C.; Salanne, M.; Rotenberg, B.; Madden, P. A. *Electrochim. Acta* **2013**, *101*, 262.  
 (446) Lauw, Y.; Horne, M. D.; Rodopoulos, T.; Leermakers, F. A. M. *Phys. Rev. Lett.* **2009**, *103*, 117801.  
 (447) Lamperski, S.; Outhwaite, C. W.; Bhuiyan, L. B. *J. Phys. Chem. B* **2009**, *113*, 8925.  
 (448) Trulsson, M.; Algottsson, J.; Forsman, J.; Woodward, C. E. *J. Phys. Chem. Lett.* **2010**, *1*, 1191.  
 (449) Luque, N.; Woelki, S.; Henderson, D.; Schmickler, W. *Electrochim. Acta* **2011**, *56*, 7298.  
 (450) Kondrat, S.; Kornyshev, A. *J. Phys.: Condens. Matter* **2011**, *23*, 022201.  
 (451) Henderson, D.; Lamperski, S. *J. Chem. Eng. Data* **2011**, *56*, 1204.  
 (452) Aoki, K. *Electrochim. Acta* **2012**, *67*, 216.  
 (453) Reszko-Zygmunt, J.; Sokołowski, S.; Henderson, D.; Boda, D. *J. Chem. Phys.* **2005**, *122*, 084504.  
 (454) Wu, J.; Jiang, T.; Jiang, D.-e.; Jin, Z.; Henderson, D. *Soft Mater.* **2011**, *7*, 11222.  
 (455) Forsman, J.; Woodward, C. E.; Trulsson, M. *J. Phys. Chem. B* **2011**, *115*, 4606.  
 (456) Jiang, D.-e.; Meng, D.; Wu, J. *Chem. Phys. Lett.* **2011**, *504*, 153.  
 (457) Lauw, Y.; Horne, M. D.; Rodopoulos, T.; Nelson, A.; Leermakers, F. A. M. *J. Phys. Chem. B* **2010**, *114*, 11149.  
 (458) Henderson, D.; Lamperski, S.; Jin, Z.; Wu, J. *J. Phys. Chem. B* **2011**, *115*, 12911.  
 (459) Henderson, D.; Wu, J. *J. Phys. Chem. B* **2012**, *116*, 2520.  
 (460) Henderson, D.; Lamperski, S.; Bari Bhuiyan, L.; Wu, J. *J. Chem. Phys.* **2013**, *138*, 144704.  
 (461) Jiang, D.-e.; Jin, Z.; Wu, J. *Nano Lett.* **2011**, *11*, 5373.  
 (462) Jiang, D.-e.; Jin, Z.; Henderson, D.; Wu, J. *J. Phys. Chem. Lett.* **2012**, *3*, 1727.  
 (463) Szparaga, R.; Woodward, C. E.; Forsman, J. *J. Phys. Chem. C* **2013**, *117*, 1728.  
 (464) Vatamanu, J.; Borodin, O.; Bedrov, D.; Smith, G. D. *J. Phys. Chem. C* **2012**, *116*, 7940.  
 (465) Vatamanu, J.; Borodin, O.; Smith, G. D. *J. Phys. Chem. B* **2011**, *115*, 3073.  
 (466) Vatamanu, J.; Borodin, O.; Smith, G. D. *J. Am. Chem. Soc.* **2010**, *132*, 14825.  
 (467) Feng, G.; Zhang, J. S.; Qiao, R. *J. Phys. Chem. C* **2009**, *113*, 4549.  
 (468) Vatamanu, J.; Borodin, O.; Smith, G. D. *Phys. Chem. Chem. Phys.* **2010**, *12*, 170.  
 (469) Figure 5 shows that the oscillations of the electrostatic potential at the RTIL-electrode decay to zero only at a distance 5–6 nm from the electrodes. A number of other experimental and simulations studies on interfacial behaviour of RTILs also reported oscillations of the molecular and charge density in the interfacial layer that propagate to distances as far as 3–7 nm from the electrode depending on the system and the electrode charge density (see, e.g., refs 85, 278, 282, 439, 465, 466, 545, and 574). Therefore, to avoid overlap between the double layers at the left and right electrodes in such simulations and to achieve overall electroneutrality in the centre of the simulations box we would recommend to use the simulation box size at least 10–15 nm in the Z direction (the direction perpendicular to the electrode). The box size should be extended even more for simulations of the high charge densities (higher than  $16 \mu\text{C}/\text{cm}^2$  ( $= 1 \text{e}/\text{nm}^2$ )).  
 (470) Schmidt, J.; Krekeler, C.; Dommert, F.; Zhao, Y.; Berger, R.; Site, L. D.; Holm, C. *J. Phys. Chem. B* **2010**, *114*, 6150.  
 (471) We note that the recent ab initio Car–Parrinello Molecular Dynamics simulations of RTILs by<sup>741</sup> provided more fundamental explanations of why the rescaling of ion charges in a classical force-field model could be a good first-order approximation of electronic polarisability effects in RTILs.

- (472) Berendsen, H. J. C.; van der Spoel, D.; van Drunen, R. *Comput. Phys. Commun.* **1995**, *91*, 43.
- (473) Lindahl, E.; Hess, B.; van der Spoel, D. *J. Mol. Model.* **2001**, *7*, 306.
- (474) van der Spoel, D.; Lindahl, E.; Hess, B.; Groenhof, G.; Mark, A. E.; Berendsen, H. J. C. *J. Comput. Chem.* **2005**, *26*, 1701.
- (475) Hess, B.; Kutzner, C.; van der Spoel, D.; Lindahl, E. *J. Chem. Theory Comput.* **2008**, *4*, 435.
- (476) Kornyshev, A. A. *J. Phys. Chem. B* **2013**, *117*, 13946.
- (477) Santangelo, C. D. *Phys. Rev. E* **2006**, *73*, 041512.
- (478) Démery, V.; Dean, D. S.; Hammant, T. C.; Horgan, R. R.; Podgornik, R. *EPL* **2012**, *97*, 28004.
- (479) Démery, V.; Dean, D. S.; Hammant, T. C.; Horgan, R. R.; Podgornik, R. *J. Chem. Phys.* **2012**, *137*, 064901.
- (480) Landau, L. D. *Collected papers of L.D. Landau*; Pergamon Press: New York, 1965.
- (481) Ornstein, L. S.; Zernike, F. P. K. *Akad. Wet-Amsterd.* **1914**, *17*, 793.
- (482) Frenkel, I. I. *Kinetic Theory of Liquids*; Dover Publications: Mineola, New York, 1955.
- (483) Yvon, J. *La théorie statistique des fluides et l'équation d'état*; Hermann & cie, 1935.
- (484) Bogoliubov, N. J. *Phys. (USSR)* **1946**, *10*, 265.
- (485) Kirkwood, J. G. *J. Chem. Phys.* **1935**, *3*, 300.
- (486) Kirkwood, J. G. *J. Chem. Phys.* **1946**, *14*, 180.
- (487) Born, M.; Green, H. S. *Proc. R. Soc. London A* **1946**, *188*, 10.
- (488) Hansen, J.-P.; McDonald, I. R. *Theory of Simple Liquids*, 4th ed; Elsevier Academic Press: Amsterdam, The Netherlands, 2000.
- (489) Barrat, J.-L.; Hansen, J.-P. *Basic concepts for simple and complex liquids*; Cambridge University Press: New York, 2003.
- (490) Monson, P. A.; Morriss, G. P. *Adv. Chem. Phys.* **1990**, *77*, 451.
- (491) Hirata, F., Ed. *Molecular theory of solvation*; Kluwer Academic Publishers: Dordrecht, Netherlands, 2003.
- (492) Chandler, D.; Andersen, H. C. *J. Chem. Phys.* **1972**, *57*, 1930.
- (493) Chandler, D.; Silbey, R.; Ladanyi, B. *Mol. Phys.* **1982**, *46*, 1335.
- (494) Beglov, D.; Roux, B. *J. Phys. Chem.* **1997**, *101*, 7821.
- (495) Kovalenko, A.; Ten-No, S.; Hirata, F. *J. Comput. Chem.* **1999**, *20*, 928.
- (496) Ishizuka, R.; Chong, S. H.; Hirata, F. *J. Chem. Phys.* **2008**, *128*, 034504.
- (497) Chandler, D.; McCoy, J. D.; Singer, S. J. *J. Chem. Phys.* **1986**, *85*, 5971.
- (498) Ichiye, T.; Haymet, A. D. *J. J. Chem. Phys.* **1990**, *93*, 8954.
- (499) Perkyns, J. S.; Pettitt, B. M. *Chem. Phys. Lett.* **1992**, *190*, 626.
- (500) Raineri, F. O.; Stell, G. *J. Phys. Chem. B* **2001**, *105*, 11880.
- (501) Singer, S. J.; Chandler, D. *Mol. Phys.* **1985**, *55*, 621.
- (502) Ten-no, S.; Jung, J.; Chuman, H.; Kawashima, Y. *Mol. Phys.* **2010**, *108*, 327.
- (503) Kierlik, E.; Rosinberg, M. L. *Phys. Rev. A* **1991**, *44*, 5025.
- (504) Gendre, L.; Ramirez, R.; Borgis, D. *Chem. Phys. Lett.* **2009**, *474*, 366.
- (505) Patra, C. N. *J. Chem. Phys.* **1999**, *111*, 9832.
- (506) Wu, J. Z.; Li, Z. D. *Annu. Rev. Phys. Chem.* **2007**, *58*, 85.
- (507) Miyata, T.; Hirata, F. *J. Comput. Chem.* **2008**, *29*, 871.
- (508) Nishiyama, K.; Yamaguchi, T.; Hirata, F. *J. Phys. Chem. B* **2009**, *113*, 2800.
- (509) Llanorestre, M.; Chapman, W. G. *Int. J. Therm. Sci.* **1995**, *16*, 319.
- (510) Choudhury, N.; Ghosh, S. K. *Phys. Rev. E* **2002**, *66*, 021206.
- (511) Malvaldi, M.; Bruzzone, S.; Chiappe, C.; Gusarov, S.; Kovalenko, A. *J. Phys. Chem. B* **2009**, *113*, 3536.
- (512) Wang, Y. T.; Voth, G. A. *J. Am. Chem. Soc.* **2005**, *127*, 12192.
- (513) Canongia Lopes, J. N. A.; Pádua, A. A. H. *J. Phys. Chem. B* **2006**, *110*, 3330.
- (514) Kashyap, H. K.; Santos, C. S.; Annapureddy, H. V. R.; Murthy, N. S.; Margulis, C. J.; Castner, E. W. *Faraday Discuss.* **2012**, *154*, 133.
- (515) Greaves, T. L.; Drummond, C. J. *Chem. Soc. Rev.* **2013**, *42*, 1096.
- (516) Taylor, A. W.; Licence, P.; Abbott, A. P. *Phys. Chem. Chem. Phys.* **2011**, *13*, 10147.
- (517) Kovalenko, A.; Hirata, F. *J. Chem. Phys.* **1999**, *110*, 10095.
- (518) Woelki, S.; Kohler, H.-H.; Krienke, H. *J. Phys. Chem. B* **2008**, *112*, 3365.
- (519) Howard, J. J.; Perkyns, J. S.; Pettitt, B. M. *J. Phys. Chem. B* **2010**, *114*, 6074.
- (520) Tanimura, A.; Kovalenko, A.; Hirata, F. *Chem. Phys. Lett.* **2003**, *378*, 638.
- (521) Tanimura, A.; Kovalenko, A.; Hirata, F. *Langmuir* **2007**, *23*, 1507.
- (522) Pinilla, C.; Del Pópolo, M. G.; Lynden-Bell, R. M.; Kohanoff, J. *J. Phys. Chem. B* **2005**, *109*, 17922.
- (523) Kislenko, S. A.; Samoylov, I. S.; Amirov, R. H. *Phys. Chem. Chem. Phys.* **2009**, *11*, 5584.
- (524) Kislenko, S. A.; Amirov, R. H.; Samoylov, I. S. *Phys. Chem. Chem. Phys.* **2010**, *12*, 11245.
- (525) Sha, M. L.; Wu, G. Z.; Dou, Q. A.; Tang, Z. F.; Fang, H. P. *Langmuir* **2010**, *26*, 12667.
- (526) Wang, S.; Li, S.; Cao, Z.; Yan, T. Y. *J. Phys. Chem. C* **2010**, *114*, 990.
- (527) Shim, Y.; Kim, H. J. *ACS Nano* **2010**, *4*, 2345.
- (528) Feng, G.; Huang, J. S.; Sumpter, B. G.; Meunier, V.; Qiao, R. *Phys. Chem. Chem. Phys.* **2010**, *12*, 5468.
- (529) Vatamanu, J.; Cao, L.; Borodin, O.; Bedrov, D.; Smith, G. D. J. *Phys. Chem. Lett.* **2011**, *2*, 2267.
- (530) Dou, Q.; Sha, M. L.; Fu, H. Y.; Wu, G. Z. *J. Phys.: Condens. Matter* **2011**, *23*, 175001.
- (531) Wu, P.; Huang, J. S.; Meunier, V.; Sumpter, B. G.; Qiao, R. *ACS Nano* **2011**, *5*, 9044.
- (532) Ong, S. P.; Andreussi, O.; Wu, Y.; Marzari, N.; Ceder, G. *Chem. Mater.* **2011**, *23*, 2979.
- (533) Feng, G.; Qiao, R.; Huang, J.; Dai, S.; Sumpter, B. G.; Meunier, V. *Phys. Chem. Chem. Phys.* **2011**, *13*, 1152.
- (534) Feng, G.; Jiang, D.-e.; Cummings, P. T. *J. Chem. Theory Comput.* **2012**, *8*, 1058.
- (535) Xing, L.; Vatamanu, J.; Smith, G. D.; Bedrov, D. *J. Phys. Chem. Lett.* **2012**, *3*, 1124.
- (536) Si, X.; Li, S.; Wang, Y.; Ye, S.; Yan, T.; Si, X.; Li, S.; Wang, Y.; Ye, S.; Yan, T. *ChemPhysChem* **2012**, *13*, 1671.
- (537) Xing, L.; Vatamanu, J.; Borodin, O.; Bedrov, D. *J. Phys. Chem. Lett.* **2013**, *4*, 132.
- (538) Kislenko, S. A.; Amirov, R. H.; Samoylov, I. S. *J. Phys.: Conf. Ser.* **2013**, *418*, 012021.
- (539) Yang, L.; Fishbine, B. H.; Migliori, A.; Pratt, L. R. *J. Am. Chem. Soc.* **2009**, *131*, 12373.
- (540) Feng, G.; Huang, J.; Sumpter, B. G.; Meunier, V.; Qiao, R. *Phys. Chem. Chem. Phys.* **2011**, *13*, 14723.
- (541) Rodriguez, J.; Elola, M. D.; Laria, D. *J. Phys. Chem. C* **2012**, *116*, 5394.
- (542) Frolov, A. I.; Kirchner, K.; Kirchner, T.; Fedorov, M. V. *Faraday Discuss.* **2012**, *154*, 235.
- (543) Merlet, C.; Rotenberg, B.; Madden, P. A.; Salanne, M. *Phys. Chem. Chem. Phys.* **2013**, *15*, 15781.
- (544) A technical note: similarly to ref 468, Feng et al. displayed a picture for an “effective” capacitance  $C_{\text{eff}}$  by dividing the net charge in the EDL by the overall voltage drop across the double layer. Such an “effective” capacitance shows divergence and negative values. This is caused by the fact that, unless  $U_{\text{pzc}} = 0$  (which is usually not true, particularly in the case of preferential adsorption of one sort of ions),  $Q = 0$  at the pzc., equally means  $Q \neq 0$  at  $U = 0$ . Hence the divergence! Both groups clarified the limitation of such an effective capacitance in their papers, and were careful not to term it as the integral capacitance,  $C_{\text{int}} = Q/(U - U_{\text{pzc}})$ . To avoid confusion, as these groups have already done in their later works,<sup>528,531</sup> we suggest that a proper definition of  $C_{\text{int}}$  to be used in future studies to characterize EDLs, when referring to and plotting the integral capacitance.
- (545) Paek, E.; Pak, A. J.; Hwang, G. S. *J. Electrochem. Soc.* **2013**, *160*, A1.

- (546) Kornyshev, A. A.; Luque, N.; Schmickler, W. *J. Solid State Electrochem.* **2013**, DOI: 10.1007/s10008-013-2316-8.
- (547) Islam, M. M.; Alam, M. T.; Okajima, T.; Ohsaka, T. *J. Phys. Chem. C* **2009**, *113*, 3386.
- (548) Alam, M. T.; Islam, M. M.; Okajima, T.; Ohsaka, T. *J. Phys. Chem. C* **2009**, *113*, 6596.
- (549) Alam, M. T.; Masud, J.; Islam, M. M.; Okajima, T.; Ohsaka, T. *J. Phys. Chem. C* **2011**, *115*, 19797.
- (550) Lockett, V.; Horne, M.; Sedev, R.; Rodopoulos, T.; Ralston, J. *Phys. Chem. Chem. Phys.* **2010**, *12*, 12499.
- (551) Gore, T. R.; Bond, T.; Zhang, W.; Scott, R. W.; Burgess, I. J. *Electrochim. Commun.* **2010**, *12*, 1340.
- (552) Siinor, L.; Lust, K.; Lust, E. *J. Electrochem. Soc.* **2010**, *157*, F83.
- (553) (a) Su, Y. Z.; Fu, Y. C.; Yan, J. W.; Chen, Z. B.; Mao, B. W. *Angew. Chem. Int. Edit.* **2009**, *48*, 5148. (b) Su, Y.-Z.; Yan, J.-W.; Li, M.-G.; Xie, Z.-X.; Mao, B.-W.; Tian, Z.-Q. *Z. Phys. Chem.* **2012**, *226*, 979.
- (554) Weingärtner, H.; Knocks, A.; Schrader, W.; Kaatze, U. *J. Phys. Chem. A* **2001**, *105*, 8646.
- (555) Smith, E. F.; Rutten, F. J. M.; Villar-Garcia, I. J.; Briggs, D.; Licence, P. *Langmuir* **2006**, *22*, 9386.
- (556) Pajkossy, T.; Kolb, D. M. *Electrochim. Commun.* **2011**, *13*, 284.
- (557) Wang, H.; Pilon, L. *Electrochim. Acta* **2012**, *63*, 55.
- (558) Druschler, M.; Roling, B. *Electrochim. Acta* **2011**, *56*, 7243.
- (559) Pajkossy, T. *Electrochim. Acta* **2011**, *56*, 7246.
- (560) Wang, H.; Pilon, L. *Electrochim. Acta* **2012**, *76*, 529.
- (561) Zheng, J.; Goonetilleke, P.; Pettit, C.; Roy, D. *Talanta* **2010**, *81*, 1045.
- (562) Zheng, J. P.; Moganty, S. S.; Goonetilleke, P. C.; Baltus, R. E.; Roy, D. *J. Phys. Chem. C* **2011**, *115*, 7527.
- (563) Silva, F.; Gomes, C.; Figueiredo, M.; Costa, R.; Martins, A.; Pereira, C. M. *J. Electroanal. Chem.* **2008**, *622*, 153.
- (564) Costa, R.; Pereira, C. M.; Silva, F. *Phys. Chem. Chem. Phys.* **2010**, *12*, 11125.
- (565) Mezger, M.; Schröder, H.; Reichert, H.; Schramm, S.; Okasinski, J. S.; Schöder, S.; Honkimäki, V.; Deutsch, M.; Ocko, B. M.; Ralston, J.; Rohwerder, M.; Stratmann, M.; Dosch, H. *Science* **2008**, *322*, 424.
- (566) Mezger, M.; Schramm, S.; Schröder, H.; Reichert, H.; Deutsch, M.; De Souza, E. J.; Okasinski, J. S.; Ocko, B. M.; Honkimäki, V.; Dosch, H. *J. Chem. Phys.* **2009**, *131*, 094701.
- (567) Mezger, M.; Ocko, B. M.; Reichert, H.; Deutsch, M. *Proc. Natl. Acad. Sci. U.S.A.* **2013**, *110*, 3733.
- (568) Nishi, N.; Yasui, Y.; Uruga, T.; Tanida, H.; Yamada, T.; Nakayama, S.-i.; Matsuoka, H.; Kakiuchi, T. *J. Chem. Phys.* **2010**, *132*, 164705.
- (569) Nishi, N.; Uruga, T.; Tanida, H.; Kakiuchi, T. *Langmuir* **2011**, *27*, 7531.
- (570) Yamamoto, R.; Morisaki, H.; Sakata, O.; Shimotani, H.; Yuan, H.; Iwasa, Y.; Kimura, T.; Wakabayashi, Y. *Appl. Phys. Lett.* **2012**, *101*, 053122.
- (571) Atkin, R.; Warr, G. G. *J. Phys. Chem. C* **2007**, *111*, 5162.
- (572) Wakeham, D.; Hayes, R.; Warr, G. G.; Atkin, R. *J. Phys. Chem. B* **2009**, *113*, 5961.
- (573) Hayes, R.; El Abedin, S. Z.; Atkin, R. *J. Phys. Chem. B* **2009**, *113*, 7049.
- (574) Hayes, R.; Borisenko, N.; Tam, M. K.; Howlett, P. C.; Endres, F.; Atkin, R. *J. Phys. Chem. C* **2011**, *115*, 6855.
- (575) Li, H.; Endres, F.; Atkin, R. *Phys. Chem. Chem. Phys.* **2013**, in press.
- (576) Perkin, S.; Cousen, N. Personal communication. 2013.
- (577) Smith, A. M.; Lovelock, K. R. J.; Gosvami, N. N.; Licence, P.; Dolan, A.; Welton, T.; Perkin, S. *J. Phys. Chem. Lett.* **2013**, 378.
- (578) Zhang, X.; Zhong, Y.-X.; Yan, J.-W.; Su, Y.-Z.; Zhang, M.; Mao, B.-W. *Chem. Commun.* **2012**, *48*, 582.
- (579) Carstens, T.; Hayes, R.; Abedin, S. Z. E.; Corr, B.; Webber, G. B.; Borisenko, N.; Atkin, R.; Endres, F. *Electrochim. Acta* **2012**, *82*, 48.
- (580) Baldelli, S. *J. Phys. Chem. Lett.* **2013**, *4*, 244.
- (581) Santos, C. S.; Baldelli, S. *J. Phys. Chem. B* **2009**, *113*, 923.
- (582) Martinez, I. S.; Baldelli, S. *J. Phys. Chem. C* **2010**, *114*, 11564.
- (583) Baldelli, S.; Bao, J.; Wu, W.; Pei, S.-s. *Chem. Phys. Lett.* **2011**, *516*, 171.
- (584) Peñalber, C. Y.; Baldelli, S. *J. Phys. Chem. Lett.* **2012**, *3*, 844.
- (585) Baldelli, S. *Acc. Chem. Res.* **2008**, *41*, 421.
- (586) Pan, G.-B.; Freyland, W. *Chem. Phys. Lett.* **2006**, *427*, 96.
- (587) Castillo, M. R.; Fraile, J. M.; Mayoral, J. A. *Langmuir* **2012**, *28*, 11364.
- (588) Liu, Y.; Zhang, Y.; Wu, G.; Hu, J. *J. Am. Chem. Soc.* **2006**, *128*, 7456.
- (589) Yokota, Y.; Harada, T.; Fukui, K.-i. *Chem. Commun.* **2010**, *46*, 8627.
- (590) Henderson, J. R.; Sabeur, Z. A. *J. Chem. Phys.* **1992**, *97*, 6750.
- (591) Tsirlina, G., personal communication.
- (592) We note that, in fact, this effect was known a while ago in electrochemistry of semiconductors.<sup>742</sup>
- (593) Bulut, S.; Eiden, P.; Beichel, W.; Slattery, J. M.; Beyersdorff, T. F.; Schubert, T. J. S.; Krossing, I. *ChemPhysChem* **2011**, *12*, 2296.
- (594) Tokuda, H.; Tsuzuki, S.; Susan, M. A. B. H.; Hayamizu, K.; Watanabe, M. *J. Phys. Chem. B* **2006**, *110*, 19593.
- (595) Palmer, D. S.; Llinás, A.; Morao, I.; Day, G. M.; Goodman, J. M.; Glen, R. C.; Mitchell, J. B. O. *Mol. Pharmaceutics* **2008**, *5*, 266.
- (596) Palmer, D. S.; McDonagh, J. L.; Mitchell, J. B. O.; van Mourik, T.; Fedorov, M. V. *J. Chem. Theory Comput.* **2012**, *8*, 3322.
- (597) Lui, M. Y.; Crowhurst, L.; Hallett, J. P.; Hunt, P. A.; Niedermeyer, H.; Welton, T. *Chem. Sci.* **2011**, *2*, 1491.
- (598) Perkin, S.; Salanne, M.; Madden, P.; Lynden-Bell, R. *Proc. Natl. Acad. Sci. U.S.A.* **2013**, 201314188.
- (599) Gebbie, M. A.; Valtiner, M.; Banquy, X.; Henderson, W. A.; Israelachvili, J. N. *Proc. Natl. Acad. Sci. U.S.A.* **2013**, 201315608.
- (600) Richey, F. W.; Dyatkin, B.; Gogotsi, Y.; Elabd, Y. A. *J. Am. Chem. Soc.* **2013**, *135*, 12818.
- (601) Tsai, W.-Y.; Lin, R.; Murali, S.; Zhang, L. L.; McDonough, J. K.; Ruoff, R. S.; Taberna, P.-L.; Gogotsi, Y.; Simon, P. *Nano Energy* **2013**, *2*, 403.
- (602) Endres, F.; El Abedin, S. *Z. Phys. Chem. Chem. Phys.* **2006**, *8*, 2101.
- (603) Abbott, A. P.; McKenzie, K. *J. Phys. Chem. Chem. Phys.* **2006**, *8*, 4265.
- (604) Abbott, A. P.; Frisch, G.; Hartley, J.; Ryder, K. S. *Green Chem.* **2011**, *13*, 471.
- (605) Endres, F. *Chem.-Ing.-Tech.* **2011**, *83*, 1485–1492.
- (606) As discussed above and in section 2.2.4 these estimations of the EW width for RTILs should be taken with some care, and, overall should be considered as *optimistic* estimations because even a small amount of impurity such as e.g. water significantly decreases electrochemical stability of RTILs.<sup>249</sup>
- (607) Hagiwara, R.; Ito, Y. *J. Fluorine Chem.* **2000**, *105*, 221.
- (608) Levich, V. G. *Physicochemical hydrodynamics*; Prentice-Hall: Upper Saddle River, NJ, 1962.
- (609) Bard, A.; Faulkner, L. R. *Electrochemical Methods. Fundamentals and Applications*; John Wiley & Sons: New York, 2001.
- (610) Lloyd, D.; Vainikka, T.; Schmachtel, S.; Murtomäki, L.; Kontturi, K. *Electrochim. Acta* **2012**, *69*, 139.
- (611) Boxall, D. L.; O'Dea, J. J.; Osteryoung, R. A. *J. Electrochem. Soc.* **2002**, *149*, E468.
- (612) Kuznetsov, A.; Ulstrup, J. *Electron transfer in chemistry and biology: an introduction to the theory*; Wiley: Chichester, U.K., 1999.
- (613) Kornyshev, A. A.; Kuznetsov, A. M.; Ulstrup, J. *J. Phys. Chem.* **1993**, *98*, 3832.
- (614) Marcus, R. A. *Annu. Rev. Phys. Chem.* **1964**, *15*, 155.
- (615) Marcus, R. A. *J. Chem. Phys.* **1965**, *43*, 679.
- (616) Marcus, R. A. *Rev. Mod. Phys.* **1993**, *65*, 599.
- (617) Marcus, R. A. *J. Chem. Phys.* **1956**, *24*, 966.
- (618) Pekar, S. *Untersuchungen über die Elektronentheorie der Kristalle*; Akademie-Verlag: Berlin, 1954.
- (619) Phelps, D. K.; Kornyshev, A. A.; Weaver, M. J. *J. Phys. Chem.* **1990**, *94*, 1454.

- (620) Dzhavakhidze, P.; Kornyshev, A.; Krishtalik, L. *J. Electroanal. Chem.* **1987**, *228*, 329.
- (621) Kuznetsov, A. M.; Medvedev, I. G. *J. Phys. Chem.* **1996**, *100*, 5721.
- (622) Medvedev, I. *J. Electroanal. Chem.* **2000**, *481*, 215.
- (623) Kornyshev, A.; Ulstrup, J. *Chem. Phys. Lett.* **1986**, *126*, 74.
- (624) Kornyshev, A. A.; Sutmann, G. *Electrochim. Acta* **1997**, *42*, 2801.
- (625) Kornyshev, A. A. In *The Chemical Physics of Solvation. Part A*; Elsevier: Amsterdam, 1985, p 77.
- (626) Kornyshev, A. A. *Electrochim. Acta* **1981**, *26*, 1.
- (627) Lynden-Bell, R. M. *J. Phys. Chem. B* **2007**, *111*, 10800.
- (628) Lynden-Bell, R. *Electrochem. Commun.* **2007**, *9*, 1857.
- (629) Shim, Y.; Kim, H. *J. Phys. Chem. B* **2007**, *111*, 4510.
- (630) Dogonadze, R. R.; Kuznetsov, A. M.; Vorotyntsev, M. A. *Phys. Status Solidi B* **1972**, *54*, 125–134.
- (631) Vorotyntsev, M.; Dogonadze, R. R.; Kuznetsov, A. *Dokl. Akad. Nauk. SSSR* **1970**, *195* (5), 1135.
- (632) Kornyshev, A. A.; Kuznetsov, A. M.; Phelps, D. K.; Weaver, M. *J. Chem. Phys.* **1989**, *91*, 7159.
- (633) Medvedev, I. *J. Electroanal. Chem.* **2001**, *517*, 1.
- (634) Frumkin, A. Z. *Phys. Chem.* **1933**, *A164*, 121.
- (635) Krishtalik, L. In *Comprehensive treatise of electrochemistry*; Conway, B. E., Ed.; Plenum Press: New York, 1983.
- (636) Krishtalik, L. I. *Charge transfer reactions in electrochemical and chemical processes*; Consultant's Bureau: New York, 1986.
- (637) Lagrost, C.; Gmouh, S.; Vaultier, M.; Hapiot, P. *J. Phys. Chem. A* **2004**, *108*, 6175.
- (638) Choi, D. S.; Kim, D. H.; Shin, U. S.; Deshmukh, R. R.; Lee, S.-g.; Song, C. E. *Chem. Commun.* **2007**, 3467.
- (639) Takahashi, K.; Sakai, S.; Tezuka, H.; Hiejima, Y.; Katsumura, Y.; Watanabe, M. *J. Phys. Chem. B* **2007**, *111*, 4807.
- (640) Takahashi, K.; Tezuka, H.; Satoh, T.; Katsumura, Y.; Watanabe, M.; Crowell, R. A.; Wishart, J. F. *2009*, *38*, 236.
- (641) André, F.; Hapiot, P.; Lagrost, C. *Phys. Chem. Chem. Phys.* **2010**, *12*, 7506.
- (642) Lagrost, C.; Carrié; Vaultier, M.; Hapiot, P. *J. Phys. Chem. A* **2003**, *107*, 745.
- (643) Fietkau, N.; Clegg, A. D.; Evans, R. G.; Villagran, C.; Hardacre, C.; Compton, R. G. *ChemPhysChem* **2006**, *7*, 1041.
- (644) Kornyshev, A. A.; Vorotyntsev, M. A. *Electrochim. Acta* **1981**, *26*, 303.
- (645) Marx, D.; Hutter, J. *Mod. Methods Algorithms Quantum Chem.* **2000**, *1*, 301.
- (646) Lagrost, C.; Preda, L.; Volanschi, E.; Hapiot, P. *J. Electroanal. Chem.* **2005**, *585*, 1.
- (647) Matsumiya, M.; Terazono, M.; Tokuraku, K. *Electrochim. Acta* **2006**, *51*, 1178.
- (648) Bard, A. J.; Stratmann, M.; Calvo, E. J., Eds. *Encyclopedia of Electrochemistry: Interfacial Kinetics and Mass Transport*; Wiley VCH: Weinheim, Germany, 2003; Vol. 2.
- (649) Taylor, A. W.; Qiu, F.; Hu, J.; Licence, P.; Walsh, D. A. *J. Phys. Chem. B* **2008**, *112*, 13292.
- (650) Belding, S. R.; Rees, N. V.; Aldous, L.; Hardacre, C.; Compton, R. G. *J. Phys. Chem. C* **2008**, *112*, 1650.
- (651) Lovelock, K. R. J.; Cowling, F. N.; Taylor, A. W.; Licence, P.; Walsh, D. A. *J. Phys. Chem. B* **2010**, *114*, 4442.
- (652) Walsh, D. A.; Ejigu, A.; Smith, J.; Licence, P. *Phys. Chem. Chem. Phys.* **2013**, *15*, 7548.
- (653) Silvester, D. S.; Aldous, L.; Hardacre, C.; Compton, R. G. *J. Phys. Chem. B* **2007**, *111*, 5000.
- (654) Bautista-Martinez, J. A.; Tang, L.; Belieres, J.-P.; Zeller, R.; Angell, C. A.; Friesen, C. *J. Phys. Chem. C* **2009**, *113*, 12586.
- (655) Meng, Y.; Aldous, L.; Belding, S. R.; Compton, R. G. *Phys. Chem. Chem. Phys.* **2012**, *14*, 5222.
- (656) Meng, Y.; Aldous, L.; Belding, S. R.; Compton, R. G. *Chem. Commun.* **2012**, *48*, 5572.
- (657) Martindale, B. C. M.; Menshykau, D.; Ernst, S.; Compton, R. G. *Phys. Chem. Chem. Phys.* **2013**, *15*, 1188.
- (658) Wibowo, R.; Ward Jones, S. E.; Compton, R. G. *J. Phys. Chem. B* **2009**, *113*, 12293.
- (659) Wibowo, R.; Jones, S. E. W.; Compton, R. G. *J. Chem. Eng. Data* **2010**, *55*, 1374.
- (660) Nikitina, V. A.; Nazmutdinov, R. R.; Tsirlina, G. A. *J. Phys. Chem. B* **2011**, *115*, 668.
- (661) Miller, J. R.; Simon, P. *Science* **2008**, *321*, 651.
- (662) Walcarius, A. *Chem. Soc. Rev.* **2013**, *42*, 4098–4140.
- (663) Daikhin, L. I.; Kornyshev, A. A.; Urbakh, M. *Phys. Rev. E* **1996**, *53*, 6192.
- (664) Daikhin, L. I.; Kornyshev, A. A.; Urbakh, M. *J. Chem. Phys.* **1998**, *108*, 1715.
- (665) Simon, P.; Gogotsi, Y. *Phil. Trans. R. Soc. A* **2010**, *368*, 3457.
- (666) Daffos, B.; Taberna, P. L.; Gogotsi, Y.; Simon, P. *Fuel Cells* **2010**, *10*, 819–824.
- (667) Pech, D.; Brunet, M.; Durou, H.; Huang, P.; Mochalin, V.; Gogotsi, Y.; Taberna, P.-L.; Simon, P. *Nat. Nanotechnol.* **2010**, *5*, 651.
- (668) Presser, V.; Heon, M.; Gogotsi, Y. *Adv. Funct. Mater.* **2011**, *21*, 810.
- (669) Hutchins, O. U.S. Patent 1271713, July 9, 1918.
- (670) Mohun, W. A. Mineral Active Carbon and Process for Producing Same. U.S. Patent 3066099, Nov 27, 1962.
- (671) Shipton, G. Improvements in and relating to mineral active carbons and to a process for their preparation. U.K. Patent GB971943 (A), Oct 7, 1964.
- (672) Gordeev, S.; Vartanova, A. *J. Appl. Chem.* **1991**, *64*, 1040.
- (673) Gogotsi, Y. G.; Yoshimura, M. *Nature* **1994**, *367*, 628.
- (674) Gogotsi, Y.; Welz, S.; Ersoy, D. A.; McNallan, M. *J. Nature* **2001**, *411*, 283.
- (675) Leis, J.; Perkson, A.; Arulepp, M.; Käärik, M.; Svensson, G. *Carbon* **2001**, *39*, 2043.
- (676) Centeno, T. A.; Sereda, O.; Stoeckli, F. *Phys. Chem. Chem. Phys.* **2011**, *13*, 12403.
- (677) Stoeckli, F.; Centeno, T. A. *Phys. Chem. Chem. Phys.* **2012**, *14*, 11589.
- (678) Laudisio, G.; Dash, R. K.; Singer, J. P.; Yushin, G.; Gogotsi, Y.; Fischer, J. E. *Langmuir* **2006**, *22*, 8945.
- (679) Chmiola, J.; Largeot, C.; Taberna, P.-L.; Simon, P.; Gogotsi, Y. *Science* **2010**, *328*, 480.
- (680) Largeot, C.; Portet, C.; Chmiola, J.; Taberna, P.-L.; Gogotsi, Y.; Simon, P. *J. Am. Chem. Soc.* **2008**, *130*, 2730.
- (681) Stoeckli and Centeno<sup>677</sup> debated these findings claiming that the internal surface area of accessible pore space, the quantity critical for the conclusions about the value of the specific capacitance, is not the one assessed in Simon–Gogotsi experiments. However, we note that the latter groups have used several independent methods of evaluation of the true surface area of the carbide-derived carbon electrodes, and in the absence of other counter-evidence we will refrain from dismissing the Simon-Gogotsi “anomalous capacitance” as an artifact.
- (682) Cavazzoni, C.; Chiarotti, G. L.; Scandolo, S.; Tosatti, E.; Bernasconi, M.; Parrinello, M. *Science* **1999**, *283*, 44.
- (683) Panofsky, W. K. H.; Phillips, M. *Classical Electricity and Magnetism: Second ed.*; Dover Publications: Mineola, New York, 2012.
- (684) Vekilov, P. G., personal communication, 2011.
- (685) Vorotyntsev, M.; Kornyshev, A. *Zh. Eksp. Teor. Fiz.* **1980**, *78*, 1008.
- (686) Kornyshev, A. A.; Rubinshtein, A. I.; Vorotyntsev, M. A. *Phys. Status Solidi B* **1977**, *84*, 125.
- (687) Carbon materials are typically semimetallic due to lower concentration of charge carriers. For equilibrium properties it will not matter how much this factor will affect the electronic conductivity, neither will it be important for kinetics, as long as the electronic conductivity of the electrode is much higher than the ionic conductivity of the electrolyte. However, what will be important is the finite electronic screening length in these materials. Its value will depend on doping: the higher is the concentration of charge carriers, the shorter is the screening length, approaching the zero limit for an ideal metal; for instance for graphite it is typically about a couple of

$\text{\AA}$ .<sup>449</sup> As suggested by Skinner et al.,<sup>364</sup> the finite screening length will renormalize the effective thickness of the pore in the law for the exponentially screened interionic interactions inside the pore, making the pore effectively wider by roughly two screening lengths. This conjecture has been recently verified by a detailed calculation of Rochester et al.<sup>743</sup> Hence, due to this effect the interactions between the ions in a nanopore will be slightly less screened, than in the case when the walls are ideally metallic, although the screening will still be exponential. Any enhancement of the interaction between the ions will decrease the capacitance of the pore, as it will be more difficult to pack ions of the same sign and uncouple ions of the opposite sign (see models further discussed in this section). There will also be one more effect of finite electronic screening: weaker image attraction of ions to the walls. The effect will contribute to lower propensity of ions to enter the pore. However, as long as the pore walls are sufficiently thick, these effects will only slightly quantitatively change the results. However, very often the pore walls in nanostructured electrodes are comparable or may be even smaller than the pore dimension. In that case the mode of screening may be changed. There are first results in this direction, see the quoted paper by Skinner et al.<sup>364</sup> and somewhat different results of the quoted work of Rochester et al.,<sup>743</sup> but this question certainly requires further investigation. Moreover, with thin walls, interactions between the ions in neighbouring pores, may not be negligible, invalidating, strictly speaking, the application of 2d (for slit pores) and 1d (for cylindrical pores) models.

(688) Kiyohara, K.; Sugino, T.; Asaka, K. *J. Chem. Phys.* **2011**, *134*, 154710.

(689) Kiyohara, K.; Shioyama, H.; Sugino, T.; Asaka, K. *J. Chem. Phys.* **2012**, *136*, 4701.

(690) Kiyohara, K.; Shioyama, H.; Sugino, T.; Asaka, K.; Soneda, Y.; Imoto, K.; Kodama, M. *J. Chem. Phys.* **2013**, *138*, 234704.

(691) Kondrat, S.; Georgi, N.; Fedorov, M. V.; Kornyshev, A. A. *Phys. Chem. Chem. Phys.* **2011**, *13*, 11359.

(692) Typical experimental values lie in between these two results. However, real experimental systems can not be literally compared with the idealized models, such as treated in refs 450 and 688–690. One should therefore focus only on qualitative correspondence between the theoretical/computational results and available experimental data.

(693) There is a discussion what capacitance has been reported by Gogotsi-Simon group: integral or differential. Assessing it from  $dq/dt \Delta V/dt = dq/dV$  of cyclic voltammograms one gets differential capacitance, but in the voltage region where the capacitance seems to be practically constant, the difference would be unnoticeable.

(694) Kondrat, S.; Pérez, C. R.; Presser, V.; Gogotsi, Y.; Kornyshev, A. A. *Energy Environ. Sci.* **2012**, *5*, 6474.

(695) Kornyshev, A. *Faraday Discuss.* **2013**, *164*, 117.

(696) In the theory of magnetism,  $a$  is the so-called coupling parameter that characterises the interactions of real spins (with positive  $a >$  causing propensity for antiferromagnetic order) and the last term describing interaction of spins with the external magnetic field.

(697) Baxter, R. J. *Exactly solved models in statistical mechanics*; Academic Press: New York, 1982.

(698) Feng, G.; Cummings, P. T. *J. Phys. Chem. Lett.* **2011**, *2*, 2859.

(699) Katayama, Y. In *Electrochemical Aspects of Ionic Liquids*; Ohno, H., Ed.; John Wiley & Sons, Inc.: Hoboken, NJ, 2005; pp 111–131.

(700) Goodenough, J. B.; Park, K.-S. *J. Am. Chem. Soc.* **2013**, *135*, 1167.

(701) Linden, D.; Reddy, T. B. *Handbook of batteries*; McGraw-Hill: New York, 2002.

(702) Madria, N.; Arunkumar, T.; Nair, N. G.; Vadapalli, A.; Huang, Y.-W.; Jones, S. C.; Reddy, V. P. *J. Power Sources* **2013**, *234*, 277.

(703) Scrosati, B.; Garche, J. *J. Power Sources* **2010**, *195*, 2419.

(704) Currently lithium-metal serves usually as a counter electrode and as a commonly accepted Li/Li<sup>+</sup> reference electrode in test cells (see ref 127).

(705) Shin, J.-H.; Henderson, W. A.; Passerini, S. *Electrochim. Commun.* **2003**, *5*, 1016.

(706) Sakaebe, H.; Matsumoto, H. *Electrochim. Commun.* **2003**, *5*, 594.

(707) Garcia, B.; Lavallée, S.; Perron, G.; Michot, C.; Armand, M. *Electrochim. Acta* **2004**, *49*, 4583.

(708) Howlett, P. C.; MacFarlane, D. R.; Hollenkamp, A. F. *Electrochim. Solid-State Lett.* **2004**, *7*, A97.

(709) Nakagawa, H.; Fujino, Y.; Kozono, S.; Katayama, Y.; Nukuda, T.; Sakaebe, H.; Matsumoto, H.; Tatsumi, K. *J. Power Sources* **2007**, *174*, 1021.

(710) Schweikert, N.; Hofmann, A.; Schulz, M.; Scheuermann, M.; Boles, S. T.; Hanemann, T.; Hahn, H.; Indris, S. *J. Power Sources* **2013**, *228*, 237.

(711) Bruce, P. G.; Freunberger, S. A.; Hardwick, L. J.; Tarascon, J.-M. *Nat. Mater.* **2012**, *11*, 19.

(712) Schaefer, J.; Lu, Y.; Moganty, S.; Agarwal, P.; Jayaprakash, N.; Archer, L. *Appl. Nanosci.* **2012**, *2*, 91.

(713) Li, F.; Zhang, T.; Zhou, H. *Energy Environ. Sci.* **2013**, *6*, 1125.

(714) Eguizábal, A.; Lemus, J.; Pina, M. *J. Power Sources* **2013**, *222*, 483.

(715) Gorlov, M.; Kloof, L. *Dalton Trans.* **2008**, 2655.

(716) Lee, S. H.; Lim, Y. D.; Seo, D. W.; Hossain, M. A.; Jang, H. H.; Lee, H. C.; Kim, W. G. *J. Ind. Eng. Chem.* **2013**, *19*, 322.

(717) Jhong, H.-R.; Wong, D. S.-H.; Wan, C.-C.; Wang, Y.-Y.; Wei, T.-C. *Electrochim. Commun.* **2009**, *11*, 209.

(718) Guo, L.; Pan, X.; Wang, M.; Zhang, C.; Fang, X.; Chen, S.; Dai, S. *Sol. Energy* **2011**, *85*, 7.

(719) Wang, G.; Wang, L.; Zhuo, S.; Fang, S.; Lin, Y. *Chem. Commun.* **2011**, *47*, 2700.

(720) Pushparaj, V. L.; Shaijumon, M. M.; Kumar, A.; Murugesan, S.; Ci, L.; Vajtai, R.; Linhardt, R. J.; Nalamasu, O.; Ajayan, P. M. *Proc. Natl. Acad. Sci. U.S.A.* **2007**, *104*, 13574.

(721) Wei, D.; Wakeham, S. J.; Ng, T. W.; Thwaites, M. J.; Brown, H.; Beecher, P. *Electrochim. Commun.* **2009**, *11*, 2285.

(722) Shahinpoor, M.; Kim, K. J. *Smart Mater. Struct.* **2001**, *10*, 819.

(723) Kim, K. J.; Shahinpoor, M. *Smart Mater. Struct.* **2003**, *12*, 65.

(724) Shahinpoor, M.; Kim, K. J. *Smart Mater. Struct.* **2004**, *13*, 1362.

(725) Shahinpoor, M.; Kim, K. J. *Smart Mater. Struct.* **2005**, *14*, 197.

(726) Shahinpoor, M.; Bar-Cohen, Y.; Simpson, J. O.; Smith, J. *Smart Mater. Struct.* **1998**, *7*, R15.

(727) Löfdahl, L.; Gad-el Hak, M. *The MEMS Handbook*; CRC Press: Boca Raton, FL, 2005.

(728) Tan, X. *Mar. Technol. Soc. J.* **2011**, *45*, 31.

(729) Keshavarzi, A.; Shahinpoor, M.; Kim, K. J.; Lantz, J. W. *Proc. SPIE Smart Mater. Struct. Conf.* **1999**, 369.

(730) Ferrara, L.; Shahinpoor, M.; Kim, K. J.; Schreyer, H. B.; Keshavarzi, A.; Benzel, E.; Lantz, J. W. *Proc. SPIE* **1999**, 394.

(731) Etebari, A.; Bennett, M. D.; Leo, D. J.; Vlachos, P. P. *A dynamic wall shear stress sensor based on ionic polymers*; American Society of Mechanical Engineers: New York, 2005.

(732) Biddiss, E.; Chau, T. *Med. Eng. Phys.* **2006**, *28*, 568.

(733) Aureli, M.; Prince, C.; Porfiri, M.; Peterson, S. D. *Smart Mater. Struct.* **2010**, *19*, 015003.

(734) Giacomello, A.; Porfiri, M. *J. Appl. Phys.* **2011**, *109*, 084903.

(735) Davidson, J. D.; Goulbourne, N. C. *J. Appl. Phys.* **2011**, *109*, 084901.

(736) Davidson, J. D.; Goulbourne, N. C. *Int. J. Appl. Mech.* **2011**, *03*, 365.

(737) Lee, A. A.; Colby, R. H.; Kornyshev, A. A. *Soft Matter* **2013**, *9*, 3767.

(738) Lee, A. A.; Colby, R. H.; Kornyshev, A. A. *J. Phys.: Condens. Matter* **2013**, *25*, 082203.

(739) Kondrat, S.; Kornyshev, A. *J. Phys. Chem. C* **2013**, *117*, 12399.

(740) Wilson, G.; Hollenkamp, A. F.; Pandolfo, A. *Chem. Int.* **2007**, *29*.

(741) Wendler, K.; Zahn, S.; Dommergut, F.; Berger, R.; Holm, C.; Kirchner, B.; Delle Site, L. *J. Chem. Theory Comput.* **2011**, *7*, 3040.

(742) Myamlin, V. A.; Pleskov, Y. V. *Electrochemistry of semiconductors*; Plenum: New York, 1967.

(743) Rochester, C.; Lee, A. A.; Pruessner, G.; Kornyshev, A. A.  
*ChemPhysChem* **2013**, *14*, 4121.